University of Alberta

Generating bio-organic metal surfaces with altered surface properties using the type IV pilus of *Pseudomonas aeruginosa*

by

Elisabeth M. Davis

A thesis submitted to the Faculty of Graduate Studies and Research
in partial fulfillment of the requirements for the degree of

Doctor of Philosophy
in
Bacteriology

Medical Microbiology and Immunology

Spring 1013
Edmonton, Alberta

Abstract

Pseudomonas aeruginosa is an ubiquitiously distributed organism that functions as an aggressive opportunistic pathogen that has evolved to survive in many hosts in the plant and animal kingdoms and constitutes an important causative agent of nosocomial infections in terms of human health and serves as a major source of biofouling of surfaces in our environment. An important factor in the success of *P. aeruginosa* as a pathogen is its ability to colonize and move across various biotic and abiotic surfaces using its Type IV pilus (T4P). Binding is mediated by the receptor binding domain (RBD) and synthetic forms of the RBD irreversibly bind to stainless steel with high affinity in the absence of hydrophobic interactions.

It was determined that the high affinity of the RBD for metal surfaces is mediated by electron sharing between the peptide and the metal surface electrons. Electron sharing results in the formation of a novel organo-metallic state of matter and creates new bio-organic metals that have altered surface properties (electron work function, adhesive force, corrosion, friction, propensity for biofilm formation) compared to unaltered metal. Chiral variants of the RBD peptide interact differentially with metal surfaces, suggesting that metal surfaces have chiral structural elements that are differentially recognized by the peptides. The addition of a PEG molecule to the RBD generates a facile, single-step versatile surface coating that increases the hardness of metals (304 stainless steel, titanium, A2024 aluminum) while decreasing corrosion, friction, and the propensity for colonization by bacteria.

It was also demonstrated that the T4P of *P. aeruginosa* is an insulated molecular nanowire that facilitates electron removal from metal surfaces and can sustain the flow of high currents of up to several milliamps. The T4P also acts as a sensor, modulating

current flow in response to external stimuli such as *Pseudomonas* autoinducers and ultra-violet light, and switches between conformations that permit or restricts electron transfer.

The results in this study present attractive possibilities in industry for the facile generation of versatile surface engineering approaches for metals using non-toxic materials. The novel nanowire and environmental sensor aspects of T4P function have important implications in the pathogenesis of *P. aeruginosa* and further demonstrate the complexity and multifunctionality of the T4P.

Acknowledgements

To my family Charles, Paule, and Jean-Philippe Davis for all of your love, support, and encouragement throughout the years. To my second family Stephen and Mary Ann Power, thank you for always making me feel like a part of the family. To Keith Power thank you for standing by my side and for providing so much love, encouragement, and laughter along the way. I could not have done this without you.

I would like to thank my supervisor Randy Irvin for helping me grow as a scientist, always challenging me with new ideas, and showing me that thinking beyond the established dogma leads to some very cool science. To my supervisory committee Bart Hazes and Dongyang Li, thank you for your support, advice, and helpful discussions. Thank you to all the members of Dr. Li's lab, especially Bin Yu and Xinhu Tang, for training on equipment and for research materials. To Reinaldo Chung, thank you for some very helpful discussions about engineering theory and experiments, and for your friendship. Thanks to Stefan Pukatzki for letting me be an honorary member of your lab, it was always a joy to come visit such a fun and positive place.

To Sarah Miyata, Chad Irwin, Joel Pearson, Branawan Gowrishankar, Daniel Unterweger, Verena Bachmann, Jason Lee, Selena Wang, and all of the members of the old first floor, thank you for your friendship throughout the years. I will always have very happy memories of our snack days, sock murder planning, costume extravanganzas, volleyball games, sushi outings, and all of the other random adventures we went on during grad school.

I would also like to thank Kirsten Horn, Karenn Chan, Neil Abraham, and Reem Rostom for their friendship throughout the years and for wonderful times that provided a refreshing break from science.

List of Chapters

1. Introduction **1**

1. 1. *Pseudomonas aeruginosa* **2**

1. 1. 1. Type IV pili 2

1. 1. 2. Structure of T4P 3

1. 1. 3. The Receptor Binding Domain (RBD) of *P. aeruginosa* 7

1. 1. 4. Twitching motility mediated by T4P 10

1. 2. Metal surfaces **13**

1. 2. 1. Bacterial colonization of metal surfaces 16

1. 2. 2. Surface free energy 18

1. 2. 3. Methods for surface modification 18

1. 2. 3. 1. Altering alloying elements in metals 19

1. 2. 3. 1. Nanostructuring metal surfaces 19

1. 2. 3. 3. Surface coatings 20

1. 3. Molecular basis for interaction of the RBD with steel **21**

1. 3. 1. Interaction of the RBD with steel surfaces 21

1. 3. 2. Release of the T4P from metal surfaces 23

1. 3. 2. 1. Role of the PilT ATPase in twitching motility 24

1. 3. 3. Preferential binding of *P. aeruginosa* to metal grain boundaries 24

1. 4. Electron transfer through biosystems **25**

1. 4. 1. T4P function as bacterial nanowires 26

1. 4. 2. Charge transfer through T4P 26

1. 5. Objectives **29**

1. 5. 1. Investigating T4P release from stainless steel surfaces 29

1. 5. 2. Characterizing the RBD-steel interaction 29

1. 5. 3. Determining if the T4P of *P. aeruginosa* is a bacterial nanowire 29

1. 5. 4. Using the RBD to modify metal surface properties 30

2. Materials and methods **31**

2. 1. Bacterial Strains and Growth Conditions **32**

2. 2. Purification and biotinylation of PAK pili and RBD peptides **32**

2. 3. Coating stainless steel samples with peptides, pili, and monomer **33**

2. 3. 1. Coating metal surfaces with PEG-D-amino peptide 35
2. 4. *P. aeruginosa* stainless steel adsorption and desorbtion assays 35
2. 5. *P. aeruginosa* release and challenge study following initial colonization of steel 37
2. 6. Bacterial adherence studies on D-borgSS, RI-borgSS, and D+RI-borgSS 37
2. 7. *P. aeruginosa* adherence to D-borgTi and RI-borgTi 38
2. 8. Bacterial adhesion to PEG-D-borgSS and PEG-D-borgTi 38
2. 9. Peptide and pili dissociation/release studies 39
2. 10. Pili binding studies 39
2. 11. Imaging biotinylated peptides on steel 39
2. 12. Electron work function 40
2. 13. Adhesive force 40
2. 14. Nanoindentation 40
2. 15. Microindentation 41
2. 16. Friction 41
2. 17. Corrosion 41
2. 17. 1. Corrosion using live *P. aeruginosa* 42
2. 18. Potentiostatic measurements 42
2. 19. X-ray photoelectron spectroscopy of borg-K122SS 43
2. 20. Auger-SEM of borg-K122SS 43
2. 21. Trypsinization studies of borg-K122SS, D-borgSS, and RI-borgSS 43
2. 22. Statistical analysis 44

3. Twitching Motility: Evidence for Catch and Release of the T4P of *P. aeruginosa* 45

3. 1. Brief introduction 46
3. 2. Results 46
3. 2. 1. Release or desorption of *P. aeruginosa* from stainless steel surfaces 46
3. 2. 2. Initial colonization of stainless steel surfaces by *P. aeruginosa* 49
3. 2. 3. *P. aeruginosa* releases (desorbs) completely from steel surfaces 52
3. 2. 4. T4P release is not mediated by proteases 53
3. 2. 5. Release or desorption of the pilus from the surface is controlled by *P. aeruginosa* 53

3. 4. Conclusions **56**

4. Description and characterization of a novel peptide-steel bond: using the receptor binding domain of *P. aeruginosa* to generate a new bio-organic steel **57**

4. 1. Brief introduction **58**

4. 2. Results **58**

4. 2. 1. Characterization of the surface properties of RBD peptide bound to steel 58

4. 2. 2. X-ray photoelectron spectroscopy analysis of borg-K122SS 63

4. 2. 3. Auger scanning electron microscopy of borg-K122SS 66

4. 3. Conclusions **66**

5. The *Pseudomonas aeruginosa* Type IV Pilus is a High Current Conducting Nanowire Which Can Function as a Variable Resistance Sensor **70**

5. 1. Brief Introduction **71**

5. 2. Results **71**

5. 2. 1. Physical properties of steel modified with RBD, T4P, and pilin monomer 71

5. 2. 2. Electrochemical behavior of modified stainless steel 72

5. 2. 3. Surface-bound *P. aeruginosa* enhances corrosion of steel 72

5. 2. 4. T4P can conduct microamps of current 75

5. 2. 5. *Pseudomonas* autoinducers interact with T4P 78

5. 2. 6. T4P modulate current flow in response to environmental stimuli 79

5. 3. Conclusions **82**

6. Stereospecific modification of physicochemical surface properties of stainless steel: Evidence that bacterial adherence mechanisms exploit unanticipated chiral structural complexity for surface colonization **83**

6. 1. Brief introduction **84**

6. 2. Results **84**

6. 2. 1. Physical properties of modified 304 stainless steel 84

6. 2. 2. Electrochemical behaviour 89

6. 2. 3. Resistance to surface colonization 89

6. 2. 4. Evidence of stereospecific interactions of chiral peptides on steel surfaces 94

6. 3. Conclusions 96

7. Surface modification of metals: Improvements in hardness, friction, and resistance to bacterial colonization 97

7. 1. Brief introduction 98

7. 2. Results 98

7. 2. 1. Surface modification and physical changes of peptide-modified titanium 98

7. 2. 1. 1. The RBD-titanium interaction leads to stabilization of surface electrons 98

7. 2. 1. 2. Surface hardness of D-borgTi, RI-borgTi, and D+RI-borgTi 100

7. 2. 1. 3. Surface coefficient of friction of modified titanium surfaces 102

7. 2. 1. 4. Modified titanium is less susceptible to colonization by *P. aeruginosa* 102

7. 2. 2 PEG-ylation of steel, titanium, and aluminum alloy surfaces for biofilm control 102

7. 2. 2. 1. Surface hardness of PEG-D-borg metal surfaces 105

7. 2. 2. 2. Electrochemical behaviour of PEG-D-borgSS and PEG-D-borgTi 108

7. 2. 2. 3. Surface coefficient of friction of PEG-D-borg surfaces 108

7. 2. 2. 4. Resistance to bacterial adhesion 112

7. 3. Conclusions 115

8. Discussion 116

8. 1. The T4P catches and releases from stainless steel surfaces 117

8. 1. 1. *P. aeruginosa* release from steel is coupled to pilus retraction 117

8. 1. 2. Proteases are not required for the complete release of T4P from the surface 118

8. 1. 3. T4P release from steel requires viable bacteria 119

8. 2. The RBD of *P. aeruginosa* forms a novel peptide-steel covalent-type bond with metal surface electrons 120

8. 2. 1. Physicochemical characterization of borg-K122SS 121

8. 2. 2. Borg-K122SS is a chemically distinct material 122
8. 2. 3. Formation of borg-K122SS requires the disulfide bond of the RBD 123
8. 3. The T4P of *P. aeruginosa* is a variable resistance nanowire 125
8. 3. 1. The T4P facilitates electron removal from the steel surface 125
8. 3. 3. The T4P is a sensor that modulates current flow in response to extracellular stimuli 126
8. 3. 4. Proposed model for electron transfer in T4P 128
8. 4. Evidence of chiral features in metals 130
8. 4. 1. Enantiomers of the RBD have differential effects on surface properties 131
8. 4. 2. Bacteria employ different adherence mechanism to colonize different sites on steel surfaces 132
8. 4. 3. The RBD displays stereospecific interaction with steel surfaces 132
8. 5. Modifications of metal surfaces for improved performance 135
8. 5. 1. RBD stabilizes surface electrons of titanium to generate new materials 135
8. 5. 2. PEG-ylation of metal surfaces improves physical properties of the surface 136
8. 6. Future applications 137

Bibliography 139

Appendix A 164

List of Tables

Table 1. Synthetic peptides derived from the RBD of *P. aeruginosa*. 34

Table 2. Nomenclature of new materials generated using the RBD of *P. aeruginosa*. 36

List of Figures

Chapter 1.

Figure 1-1. Superimposed ribbon structures of pilin subunits from *P. aeruginosa* strain K (PAK), *Neisseria gonorrhoeae* and *Vibrio cholerae*. 5

Figure 1-2. Superimposition of *P. aeruginosa* truncated PilA pilins and receptor binding domains. 6

Figure 1-3. Assembly model of T4P from *P. aeruginosa*. 8

Figure 1-4. Amino acid sequence of the RBD of five strains of *P. aeruginosa*. 9

Figure 1-5. Twitching motility mediated by T4P. 11

Figure 1-6. Visualization of grains and grain boundaries of stainless steel by atomic force microscope. 14

Figure 1-7. Simplified representation of metallic boding in metals and their alloys. 15

Figure 1-8. Simplified schematic of the relationship between EWF, adhesive force, hardness, and surface electron reactivity. 17

Figure 1-9. Sequence comparison of *Geobacter sulfurreducens* GSU1496 PilA with N-terminal PilA sequence of *Pseudomonas aeruginosa* strains. 27

Chapter 3.

Figure. 3-1. Release of *P. aeruginosa* from stainless steel. 47

Figure 3-2. *P. aerugonisa* release from steel. 48

Figure 3-3. Early colonization of *P. aeruginosa* on stainless steel. 50

Figure 3-4. Early colonization of steel by *P. aeruginosa*. 51

Figure 3-5. *P. aeruginosa* pilus releases completely and in a protease-independent manner from steel. 53

Figure 3-6. PAK pili and peptide cannot be displaced from steel surface by exogenous pili or PAK(128-144)ox peptide. 55

Chapter 4.

Figure 4-1. Changes in surface electron reactivity, adhesive force and hardness of borg-K122SS steel compared with 304 stainless steel and aluminum with and without K122-4 (128-144)ox peptide. 59

Figure 4-2. Adhesive force measurements. 61

Figure 4-3. Force-displacement plots and high load nanoindentation of borg-PAKSS. 62

Figure 4-4. Analysis of XPS spectra of the elemental composition of borg-K122SS and 304 stainless steel. 64

Figure 4-5. XPS spectra analysis of elemental composition of borg-K122SS and 304 stainless steel. 65

Figure 4-6. Auger SEM scan of distribution of elements on the surface of borg-K122SS. 67

Figure 4-7. Borg-K122SS is sensitive to trypsinization. 68

Chapter 5.

Figure 5-1. Electron work function of 304 stainless steel reacted with PAK(128-144)ox peptide, full-length PAK T4P, and monomeric PAK pilin. 73

Figure 5-2. Electrochemical behaviour of borg-PAKss and stainless steel bound with T4P. 74

Figure 5-3. *P. aeruginosa* increases the corrosion rate of steel. 76

Figure 5-4. The T4P of *P. aeruginosa* conducts microamps of current. 77

Figure 5-5. PAI-2 interacts with PAK pili to modulate current flow through the pilus. 80

Figure 5-6. The T4P modulates current flow in response to UV light. 81

Chapter 6.

Figure 6-1. Structure of native pilin protein and structure of RBD within cognate protein. 85

Figure 6-2. Physical characterization of peptide-modified steel surfaces. 87

Figure 6-3. RI-borgSS is resistance to protease treatment 88

Figure 6-4. Electrochemical behaviour of 304 stainless steel modified with synthetic peptides. 90

Figure 6-5. Adherence of *Listeria monocytogenes* and *Listeria innocua* to 304 stainless steel modified with D-amino, retro-inverso D-amino, and both D-amino and retro-inverso peptides relative to unmodified stainless steel. 91

Figure 6-6. Adherence of *Staphylococcus aureus* and *Staphylococcus epidermidis* to 304 stainless steel modified D-amino, retro-inverso D-amino, and both D-amino and retro-inverso peptides relative to unmodified stainless steel. 93

Figure 6-7. Distribution of biotinylated RBD peptides on 304 stainless steel surfaces. 95

Chapter 7.

Figure 7-1. Electron work function measurements of modified titanium surfaces. 99

Figure 7-2. Nanoindentation characteristics of modified titanium surfaces. 101

Figure 7-3. Coefficient of friction of modified titanium surfaces. 103

Figure 7-4. D-borgTi and RI-borgTi are less susceptible to colonization by *P. aeruginosa*. 104

Figure 7-5. Nanoindentation characteristics of PEG-D-amino-modified surfaces of 304 stainless steel, titanium, and 2024 aluminum compared to unaltered surfaces. 107

Figure 7-6. Electrochemical behaviour of 304 stainless steel reacted with PEG-D-amino. 109

Figure 7-7. Electrochemical behaviour of titanium reacted with PEG-D-amino. 110

Figure 7-8. Coefficient of friction of PED-D-amino-modified surfaces. 111

Figure 7-9. Adhesive force of titanium with PEG-D-amino bound to the surface. 113

Figure 7-10. Adherence of *Pseudomonas aeruginosa* and *Staphyloccus aureus* to 304 stainless steel and titanium surfaces modified with PEG-D-amino. 114

Appendix A

Figure A-1. Autoinducer promotes *P. aeruginosa* colonization of stainless steel.

Figure A-2. *P. aeruginosa* and pili binding to stainless steel is influenced by PAI-2 concentration.

Figure A-3. PAI-1 and PAI-2 concentrations influence binding of pili.

List of Abbreviations

3-D	3-dimensional
ABTS	2,2'-Azino-bis(3-ethylbenzthiazoline-6-sulfonic acid) diammonium salt
AFM	Atomic force microscope
Borg	Bio-organic
CFU	Colony forming units
COF	Coefficient of friction
CPS	Counts per second
DMRB	Dissimilatory metal-reducing bacteria
ET	Electron transfer
EWF	Electron work function
FOV	Field of view
HCCI	High chromium cast irons
HRP	Horseradish peroxidase
MFC	Microbial fuel cell
OCP	Open circuit potential
OD	Optical density
PA	*Pseudomonas aeruginosa*
PAI	*Pseudomonas* autoinducer
PAI-1	*N*-3-oxododecanoyl-homoserine lactone
PAI-2	*N*-butryl-homoserine lactone
PBS	Phosphate buffered saline
PEG	Poly-ethylene glycol
RBD	Receptor binding domain
RGD	Arginine-glycine-aspartate motif
SEM	Scanning electron microscopy
SPD	Severe plastic deformation
T4P	Type IV pili
WT	Wild type
XPS	X-ray photoelectron spectroscopy
UV	Ultraviolet

Chapter 1

Introduction

1. Introduction

1.1. *Pseudomonas aeruginosa*

Pseudomonas aeruginosa is a motile, non-fermenting aerobic Gram-negative bacterium of the *Pseudomonadaceae* family (Sedlak-Weinstein *et al*., 2005) that is found ubiquitously in soil and water. An opportunistic pathogen, *P. aeruginosa* primarily infects individuals with compromised host defenses, causing infections in the respiratory tract, urinary tract, and digestive tract, as well as skin, bone, and joint infections, but possess the unique ability to also infect a diverse array of hosts in the plant and animal kingdoms (D'argenio *et al*., 2001; Green *et al*., 1974; Pellett *et al*., 1983; Plotnikova *et al*., 2000). Within the hospital environment, *P. aeruginosa* primarily colonizes medical devices but has been found in tap water and cleaning solutions (Engelhart *et al*., 2002; Ferroni *et al*., 1998). Burn victims are especially vulnerable to bacteremia and sepsis caused by *P. aeruginosa* infection of wounds (Giltner *et al*., 2006; Pruitt *et al*., 1998), whereas catheterized patients experience urinary tract infections and the majority of cystic fibrosis patients will succumb from chronic lung infections (Bagshaw & Laupland, 2006; Hoiby *et al*., 2005; Sadikot *et al*., 2005). Additionally, patients will suffer from ventilator-associated pneumonia associated with *P. aeruginosa* (Chastre & Fagon, 2002). *P. aeruginosa* is primarily a nosocomial pathogen (Lyczak *et al*., 2000; Stover *et al*., 2000) but mild, self-limiting infections in various organs including the eyes and skin can occur in healthy individuals (Fleiszig & Evans, 2002; Gustafson *et al*., 1983).

P. aeruginosa possesses a number of virulence factors important for its pathogenesis. The bacterial genome encodes a number of efflux pumps that contribute to high levels of innate and acquired antibiotic resistance in *P. aeruginosa* (Obritsch *et al*., 2005; Stover *et al*., 2000). Additional virulence factors include lipopolysaccharide (LPS), extracellular proteases, alginate, exoenzymes, outer memberane proteins, and exotoxins necessary for tissue invasion, cellular damage, and resistance to host-mediated defenses (Azghani *et al*., 2002; Baker *et al*., 1991; Doig *et al*., 1987; Gupta *et al*., 1994; Moller *et al*., 1994). *P. aeruginosa* expresses flagella and surface adhesins such as pili required for motility and surface colonization (Doig *et al*., 1988; Feldman *et al*., 1998). *P. aeruginosa* pili have been well studied due to their important role in mediating adhesion in the initial stages of pathogenesis (Beachey, 1981; Bodey *et al*., 1983).

1.1.1. Type IV pili

P. aeruginosa possesses type IV pili (T4P) that play a crucial role in mediating *P. aeruginosa* virulence. T4P pili are polar surface appendages produced by a large number of Gram-negative bacteria, ranging from pathogens such as *P. aeruginosa, Neisseriae meningitidis,*

and *Vibrio cholerae* (Swanson, 1973; Taylor *et al*., 1987; Weiss, 1971) to some environmental bacteria such as *Myxococcus*, *Geobacter*, and *Shewanella* species. Extending from the cell, T4P are thin (~ 5.4 nm diameter), flexible, long but of variable length (~2-10 μm, average length 2500 μm), linear, and retractable (Bradley, 1972; Folkhard *et al*., 1981; Paranchych *et al*., 1986; Weiss, 1971). T4P are stable, resisting depolymerization and disassembly *in vitro* except under denaturing conditions (Craig *et al*., 2003; Yu *et al*., 1996) but in nature T4P rapidly dissociate, assemble, and disassemble to efficiently carry out their multitude of functions (Bradley, 1972; Mattick, 2002; Merz & Forest, 2002; Skerker & Berg, 2001).

T4P are multi-functional virulence factors, can serve as phage receptors (Roncero *et al*., 1990), and are involved in bacterial conjugation (Horiuchi & Komano, 1998), DNA binding (van Schaik *et al*., 2005), natural transformation (Fussenegger *et al*., 1997), virulence towards other pathogens (Falkow *et al*., 1992), and induction of host cell responses (Kallstrom *et al*., 1998). T4P are important mediators of adherence (Falkow *et al*., 1992) and bind to a wide variety of biotic and abiotic surfaces. T4P bind to eukaryotic cells, including respiratory epithelial cells, via the GalNacβ1-4 Gal moiety found on asiao-GM1 and -GM2 glycosphingolipids (Saiman *et al*., 1990; Sheth *et al*., 1994). In addition, *P. aeruginosa* expresses a type III secretion system (T3SS) that is a major virulence determinant and is involved in the secretion of bacterial toxins directly into the host cell. This secretion system is dependent on bacterial-epithelial contact mediated by the T4P and in the absence of T4P the toxins cannot be injected into the host cell by the T3SS (Feldman *et al*., 1998; Hauser & Engel, 1999).

T4P mediate a form of bacterial surface motility known as twitching motility (Mattick, 2002; Merz & Forest, 2002) that is involved in microcolony formation (Kirn *et al*., 2000) and biofilm formation and development (Chiang & Burrows, 2003; O'Toole & Kolter, 1998). T4P not only mediate adhesion to surfaces but also affect the location of the bacteria within the biofilm. Piliated bacteria detach and migrate to the top of the biofilm to help maintain biofilm morphology (Chiang & Burrows, 2003; Klausen *et al*., 2003; O'Toole *et al*., 1999).

1. 1. 2. Structure of T4P

T4P are composed of a single structural subunit that has been well characterized. In *P. aeruginosa* the pilin protein, termed PilA, as well as the synthesis, export, and assembly of the pilin protein into the T4P, has been well characterized (Campbell *et al*., 1995; Campbell *et al*., 1997; Mattick, 2002; McInnes *et al*., 1994). PilA is a small 15-23 kDa protein with an average length of 150 amino acids and consists of an extended N-terminal hydrophobic α-helical region that is highly conserved among bacterial pilins (Craig *et al*., 2003; Craig *et al*., 2004; Craig *et al*.,

2006; Hazes *et al*., 2000; Parge *et al*., 1995). Lying on top of the N-terminal region is a 4 stranded, anti-parallel β-sheet-containing globular domain located in the C-terminus (**Fig. 1-1**) (Craig *et al*., 2003; Hazes *et al*., 2000; Mattick, 2002; Parge *et al*., 1995). There is little sequence conservation in the globular domain of the pilin proteins and very little sequence identity can be found between the PilA subunits of *P. aeruginosa* strains (Audette *et al*., 2004) but superimposition of the structures of the globular heads of the pilins highlights the strong structural homology despite the lack of sequence similarity (**Fig. 1-2 A**). The β-sheets pack around the α-helices with the globular domain forming a pie-shaped wedge that assembles around the α-helices to form a fiber structure. The assembled pilus consists of an outer surface composed of the anti-parallel β-sheet wrapped around a central core formed by the α-helices (Craig *et al*., 2003; Craig *et al*., 2004; Craig *et al*., 2006; Hazes *et al*., 2000; Parge *et al*., 1995). The N-terminal and C-terminal domains are connected by a structure that varies between *Pseudomonas* strains, with a small β-sheet connecting the domains in the PAK pilin (Craig *et al*., 2003; Hazes *et al*., 2000) whereas a loop connects the K122-4 pilin domains. A disulfide-bonded loop (DSL) that is structurally conserved among *P. aeruginosa* strains (**Fig. 1-2 B**) and variable in size depending on the pilin alleles is found at the C-terminal end of the protein (Hazes *et al*., 2000; Kus *et al*., 2004).

Prior to assembly, the PilA subunits may be retained in the membrane by their extended N-terminal domain to allow for processing by PilD, a peptidase-N-methylase, and for post-translational modifications (Castric, 1995; Nunn & Lory, 1991; Strom *et al*., 1993). Several other minor pilin proteins (PilE, PilV, PilW, PilX. FimT, and Fim U) are involved in pilus assembly (Alm & Mattick, 1995; Alm *et al*., 1996; Russell & Darzins, 1994; Winther-Larsen *et al*., 2005). Their exact functions have yet to be determined but they may have roles in pilus extension, retraction, or control of pilus length.

Despite the structure of the PilA subunit being known (Hazes *et al*., 2000) and the ability to visualize the pilus fibers by electron microscopy, the details governing T4P assembly remain unknown and as a result several different models have been proposed to describe the final structure of the assembled pilus. Early models suggested that the pilins assembled as a left-handed helix with a single start per helix but the exact number of PilA subunits per turn was unclear, with one model suggesting five subunits per turn (Hazes *et al*., 2000; Parge *et al*., 1995). In this model the α-helices were buried in the central core of the pilus, oligomerizing to form a coiled-coil bundle, and the β-sheets formed the outer sheath of the pilus structure (Parge *et al*., 1995). Another proposed model inverts the polarity of the pilus such that the α-helices are no

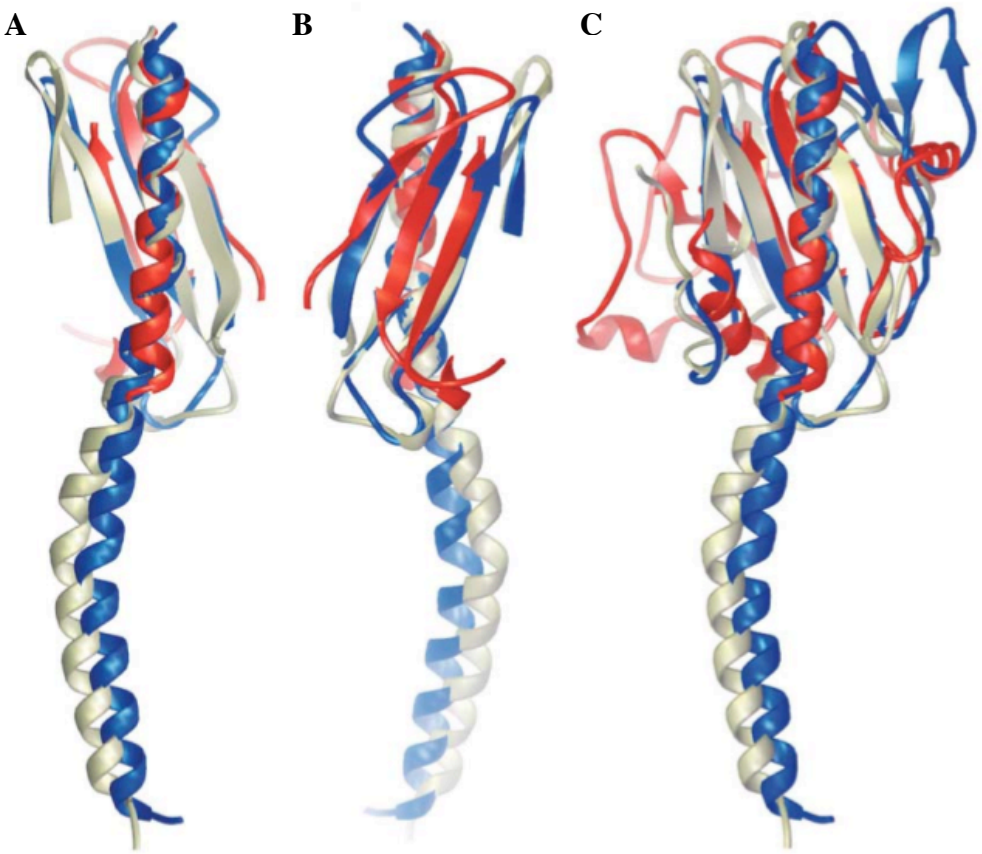

Figure 1-1. Superimposed ribbon structures of pilin subunits from *P. aeruginosa* strain K (PAK), *Neisseria gonorrhoeae*, and *Vibrio cholerae*. Front (**A**) and back (**B**) views of the conserved structural core of PilA of *P. aeruginosa* (blue), GC pilin of *N. gonorrhoeae* (white), and TcpA of *V. cholerae* (red). The α1-C region and the first three β-sheets of each pilin are shown. The variable αβ-loop and D-region have been cut away. **C.** The structure of PAK (blue), GC (white), and TcpA (red) pilins are shown. The αβ-loop and D-region have been included. This figure is adapted from Craig *et al*. (2004)(Craig *et al*., 2004) and was published in *Nature Reviews Microbiology*.

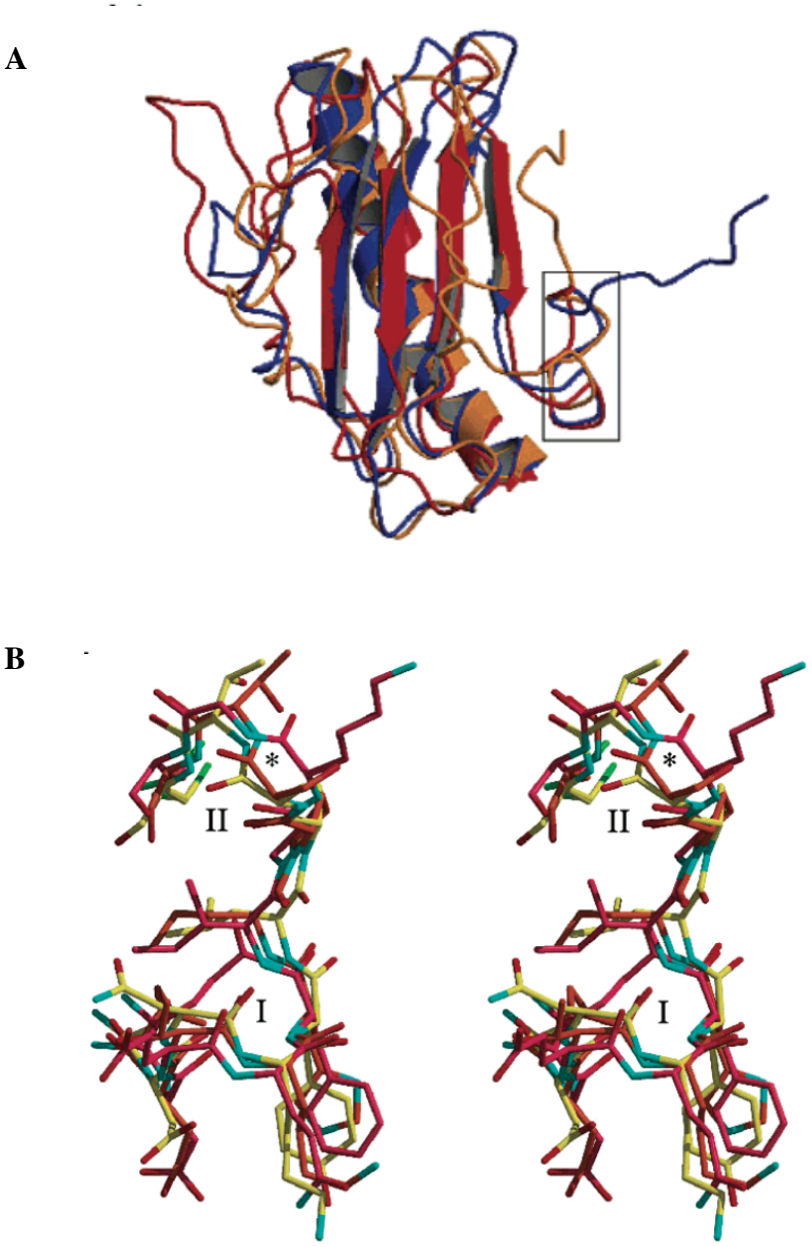

Figure 1-2. Superimposition of *P. aeruginosa* truncated PilA pilins and receptor binding domains. A. The structure of truncated PilA proteins (amino acids 1-28 have been deleted) of *P. aeruginosa* strain K (ΔPAK, red), K122-4 (ΔK122-4, blue), and MS11 (ΔMS11, orange) are superimposed to demonstrate that structural homology is conserved among the *Pseudomonas* pilins. The conserved RBD is boxed. **B.** Superimposed stereo images of the backbone atoms of the RBD of ΔPAK (red), ΔK122-4 (yellow), and ΔMS11 (orange) highlight the conserved structural homology between the RBDs. The figure was adapted from Audette *et al.* (2004)(Audette *et al.*, 2004) and was originally published in *Biochemistry*.

longer buried in the bacterial membrane but are exposed at the tip of the pilus. In agreement with previous models, the C-terminal receptor binding domain remains obscured along the length of the pilus and is exposed at the tip of the pilus (Hazes *et al*., 2000; Lee *et al*., 1994). A more recent model proposed by Craig *et al*. (2004) suggests that there may only be four subunits per turn and a total of three starts per helix.

All models predict that the pilus subunits assemble so that the core of the pilus fiber is composed of the conserved hydrophobic α-helices located in the N-terminus of the subunit while the C-terminal domains are exposed on the surface (**Fig. 1-3**). The positioning of the α-helices within the core of the pilus is believed to stabilize the pilus. Mutations in the conserved regions of the N-terminal α-helix abolished pili formation (Pasloske *et al*., 1989) and deletion of the N-terminus of PilA results in the formation of soluble pilin monomers (Audette *et al*., 2004; Hazes *et al*., 2000; Keizer *et al*., 2001), suggesting that the N-terminal α-helices of PilA are important for polymerization of PilA into full-length pili (Craig *et al*., 2004; Parge *et al*., 1995).

1. 1. 3. The Receptor Binding Domain (RBD) of *P. aeruginosa*

T4P binding is mediated by interactions with the receptor binding domain (RBD), a region containing the DSL that is encoded within residues 128-144 located in the C-terminus of the pilin monomer (Giltner *et al*., 2006; Lee *et al*., 1994). This domain mediates binding to both biotic and abiotic surfaces. Pilus-mediated adhesion can be blocked by the addition of antibodies specific to the RBD (Lee *et al*., 1994; Sheth *et al*., 1995) and synthetic peptides encompassing this region can competitively inhibit binding to epithelial cells (Lee *et al*., 1994), suggesting that PilA functions both as an adhesin and as a structural subunit for T4P. The RBD region is solvent exposed and, depending on the model, three RBDs cluster together at the tip of the pilus, thereby increasing the strength of the attachment to the surface by increasing the overall valency (Hazes *et al*., 2000).

The RBDs from different *P. aeruginosa* strains differ significantly in their amino acid sequence and yet all bind to a common receptor, although with varying binding kinetics (Sheth *et al*., 1995). Among the 17 amino acids found within residues 128 to 144, six of the twelve amino acid positions in the DSL vary greatly whereas the other six are more conserved (**Fig. 1-4**). Highly conserved residues include the proline at position 139 and the two conserved cysteine residues that are required for the formation of the intramolecular disulfide bridge. Other positions are semi-conserved and show conservative substitutions between bacterial strains (Kao *et al*., 2007). The disulfide loop encompassed in the RBD contains two β-turn motifs that increase

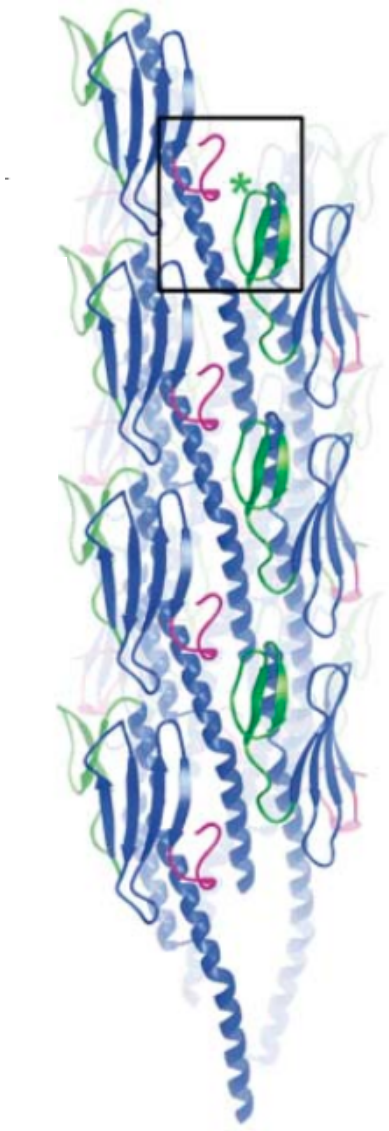

Figure 1-3. Assembly model of T4P from *P. aeruginosa*. A ribbon model of PilA subunits assembling to form the T4P. The N-terminal α-helices (closed arrow) form the core of the pilus and the C-terminal β-sheets (open arrow) pack around the helices to form the outer core. The RBD is obscured along the length of the pilus but is exposed at the tip of pilus (boxed region). This figure was adapted from Craig *et al*. (2004)(Craig *et al*., 2004) and was originally published in *Nature Reviews Microbiology*.

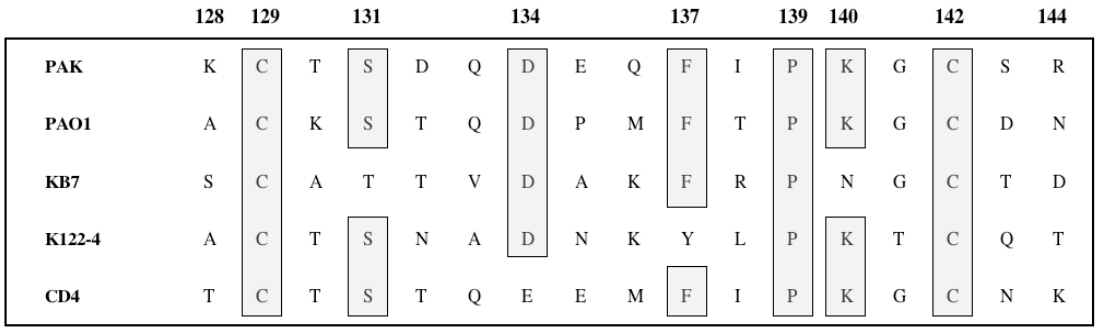

Figure 1-4. Amino acid sequence of the RBD of five strains of *P. aeruginosa*. The amino acid sequences of the RBDs of *P. aeruginosa* strains PAK, PAO1, KB7, K122-4, and CD4 are aligned and residues that are fully or partially conserved in the sequence are shaded.

structural stability (Campbell *et al*., 1997; McInnes *et al*., 1993). A synthetic peptide spanning residues 128-144 of the RBD of PilA adopts a structure that is similar but not identical to the RBD structure when it is located in the C-terminal region of PilA (Audette *et al*., 2004; Hazes *et al*., 2000). The synthetic peptides appear to lack β-structures (Campbell *et al*., 1995). The synthetic peptide was also shown to exist as a major and minor species in solution, with evidence of c*is-trans* isomeration between the central isoleucine and proline peptide bond being observed during NMR resonance studies (Campbell *et al*., 2000; McInnes *et al*., 1994). Both the isoleucine and proline residues are located in a hydrophobic pocket that is flanked by a β-turn on either side. The *trans:cis* frequency occurs at a ratio of 4:1, with the *trans* isomer being the major species. The *trans* isomer adopts two turns in solution, a type I β-turn and a type II β-turn whereas the *cis* isomer only adopts a type II β-turn, although there is evidence of a second, less-ordered turn. Immunization with the synthetic peptide elicited a polyclonal response and generated antibodies against both conformers (Campbell *et al*., 2003). The DSL also appears to have a large range of dynamic motion that suggests the existence of multiple structural conformations of the C-terminal region *in vivo* (Keizer *et al*., 2001; Suh *et al*., 2001). It is unclear how the various conformations of the RBD and DSL may affect T4P binding to biological receptors and abiotic surfaces.

1. 1. 4. Twitching motility mediated by T4P

T4P play a key role in mediating a flagellum-independent type of surface translocation termed twitching motility (or social gliding) (Bradley, 1980). Twitching motility is a highly dynamic, ATP-dependent process where T4P extend from the bacterium to initiate contact with a surface, attach, and retract to pull the bacterium closer to the point of contact (Mattick, 2002). Cells exhibiting twitching motility are chemotactic (Kearns *et al*., 2001) and twitching motility is required for biofilm formation (O'Toole & Kolter, 1998). *P. aeruginosa* mutants lacking the T4P do not exhibit twitching motility. It has been hypothesized that *P. aeruginosa* uses twitching motility during infections to spread on body surfaces or medical devices (Henricksen *et al*., 1983). Piliated bacteria lacking twitching motility were as efficient as wild-type bacteria in their ability to colonize murine airways but could not disseminate to other organs (Comolli *et al*., 1999).

Twitching motility is characterized by repeated cycles of assembly, or polymerization, and disassembly, or depolymerization, of the pilin monomers from the pilus base (**Fig. 1-5**) and the processes are driven primarily by two pilus-associated ATPases termed PilB (extension) and PilT (retraction). The function of a third ATPase, termed PilU, remains unknown.

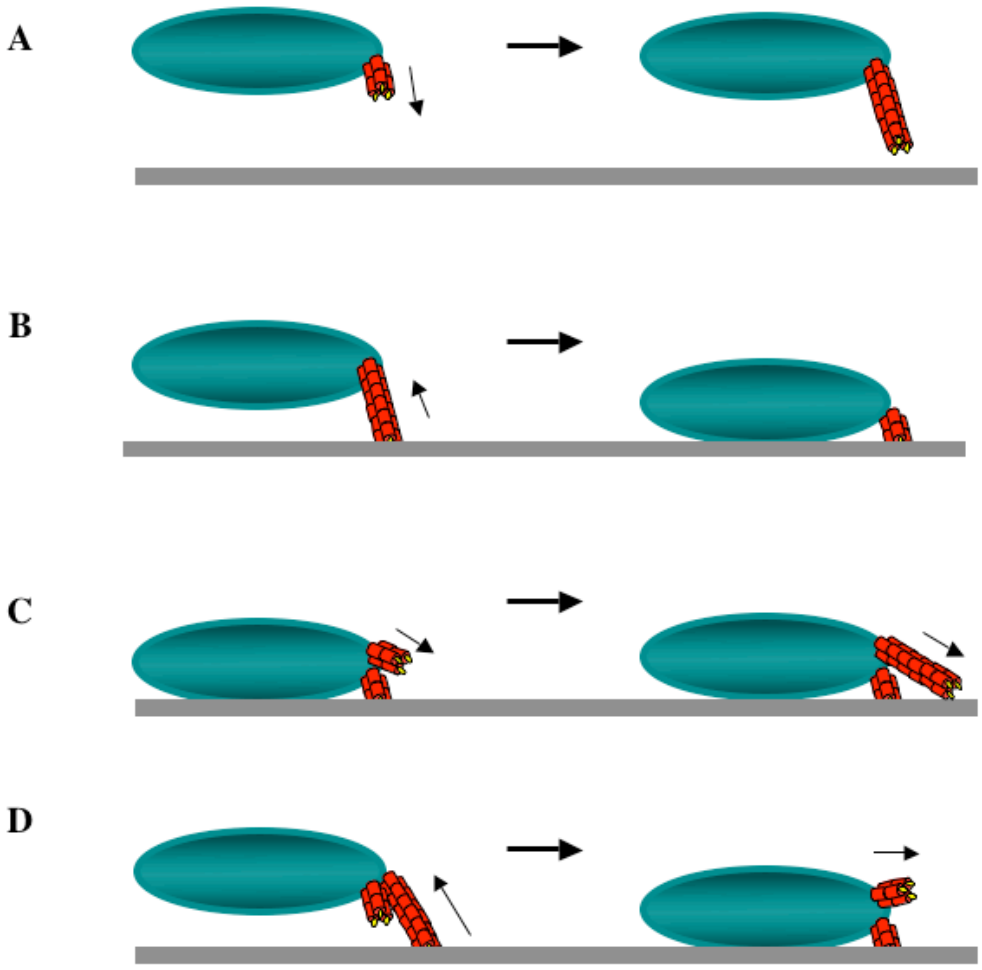

Figure 1-5. **Twitching motility mediated by T4P. A.** PilA pilin subunits polimerize (red) and the T4P extends towards to surface. **B.** Contact is made with the surface and the three receptor binding domains exposed at the tip of the pilus (yellow) bind to the surface. Retraction begins, with the T4P depolimerizing, and the bacterium comes into close contact with the surface. **C.** A second T4P extends from the surface. **D.** The second T4P comes into contact with the surface and retraction begins. The first T4P releases from the surface and the bacterium moves forward. Once the second T4P is retracted another pilus begins to extend from the bacterium and steps **A-D** repeat.

Unlike other types of fimbriae and pili, the T4P of *P. aeruginosa* and other Gram-negative bacteria have the unique ability to retract into the bacterial cell though the cell wall while still remaining attached to a surface. Retraction of the *P. aeruginosa* T4P into the bacterial cell was first described by Bradley *et al.* (1972)(Bradley, 1972). Bradley *et al.* further demonstrated that pilus retraction was prevented in the presence of bound pilus-specific bacteriophage or anti-pilin antibodies and was the first to propose that pilus retraction may play an important role in bacterial cell motility (Bradley, 1980). Real time visualization of the retraction of the T4P was later observed by Skerker and Berg (2001)(Skerker & Berg, 2001). Retraction of the pilus allows for a close interaction between the bacterial cell body and the surface. This close interaction is especially important for the contact-dependent functions of the type III secretion system and was supported by the observation that *P. aeruginosa* mutants lacking a T4P were non-cytotoxic (Kang *et al.*, 1997).

Following pilus retraction, a second pilus is then extended to attach to the surface and forward movement is achieved when the first pilus detaches and the second pilus retracts (Merz & Forest, 2002; Skerker & Berg, 2001). Thus, attachment and release must occur in a coordinated fashion for the bacteria to move rapidly and efficiently across surfaces.

Pilus retraction exerts a force that is estimated to be as great as 140 picoNewtons (pN) (Maier *et al.*, 2002). During the retraction phase of twitching motility mechanical forces are generated through a PilT-dependent depolymerization of the pilus. In *Neisseria gonorrohoeae*, the retraction of a single T4P powered by just one PilT motor generates between 50-100 pN of force on the surface, making this the strongest nanomotor to date (Maier *et al.*, 2002). Laser tweezer experiments estimated that pilus retraction occurs at approximately 0.5 μm/s and that a bacterium could move across a surface at a speed of 1 μm/s (Skerker & Berg, 2001), making pilus extension and retraction a rapid and efficient process. The pili were seen quickly extending and then retracting into both stationary cells and cells anchored to a surface by the pili, clearly demonstrating that twitching motility is driven by retraction of the T4P.

In *N. gonorrohoeae* infection models, retraction of T4P has been shown to induce changes in epithelial cells in a PilT-dependent manner (Howie *et al.*, 2005; Merz *et al.*, 1999), suggesting that this high force may be altering host cells. While the roles of the PilB and PilT ATPases have been extensively studied (Chiang & Burrows, 2003; Chiang *et al.*, 2008; Mattick, 2002; Turner *et al.*, 1993; Whitchurch *et al.*, 1991b; Whitchurch & Mattick, 1994), the role of the third ATPase, PilU, is unclear. Previous studies have shown that *pilU* mutants were unable to twitch, but showed phage sensitivity, suggesting that a small degree of pilus retraction was able to occur in these mutants (Whitchurch & Mattick, 1994). Further localization studies of PilU in *P.*

aeruginosa found that unlike the other ATPases, which where located at the cell poles, PilU was only found at the piliated pole, suggesting that PilU has a role in directionality of movement (Chiang *et al*., 2005; Chiang *et al*., 2008).

1. 2. Metal surfaces

Bacteria interact extensively with their environment, establishing bacterial communities on available surfaces including abiotic surfaces such as plastics, ceramics, glass, and metals. Metals are used ubiquitously in every aspect of modern life, serve a multitude of functions, and both pure metals and alloys cannot be ignored as important surfaces susceptible to the wear, corrosion, strain, and bacterial colonization often encountered during everyday usage that significantly limit the service life and potential future applications of the material.

Metals are composed of grains, or crystals, varying in size from 1 μm to 1 mm. The interface where two grains join is known as the grain boundary (**Fig. 1-6**). The grain boundary often contains significant crystal misalignments and various dislocation defects that occur when two grains join imperfectly resulting in areas where metal surface properties at the grain boundary differ from properties found within the grain. These areas of imperfection and weakness in the overall metal structure at the grain boundary are often the starting sites for wear, strain, corrosion, and bacterial colonization (Fionova & Artemyev, 1993; Song, 1990).

Metal atoms pack together tightly to form the crystalline structure of the metals. Despite being solid, a key feature of metals is that the bonds holding the metal atoms together must be strong enough to withstand strain and shattering while being flexible enough to allow the movement of atoms, otherwise metals would lose their malleability. Metal atoms have low electronegativities and, despite packing closely together, do not strongly attract their valence electrons. These valence electrons can be viewed as not belonging to any particular atom core but instead as shared between all of the atoms. Essentially, metals are composed of closely packed positive ion cores surrounded a sea, or cloud, of negative electrons that form delocalized bonds throughout the structure (**Fig. 1-7**). This differs greatly from traditional covalent or ionic bonds where electrons remain associated with only one or two atoms. Instead, electrons in the electron cloud are very mobile, creating a strong metallic bond that can still account for the heat and electrical transfer observed in most metals while allowing for flexibility without loss of bond strength (Louthan, 1987; McCabe & Bauer, 1964).

Due to the mobile nature of electrons in the electron cloud and the imperfection in the crystal structure at the grain boundary, electrons in these regions are at higher energy levels, rendering the grain boundary more reactive and more capable of interacting with other materials

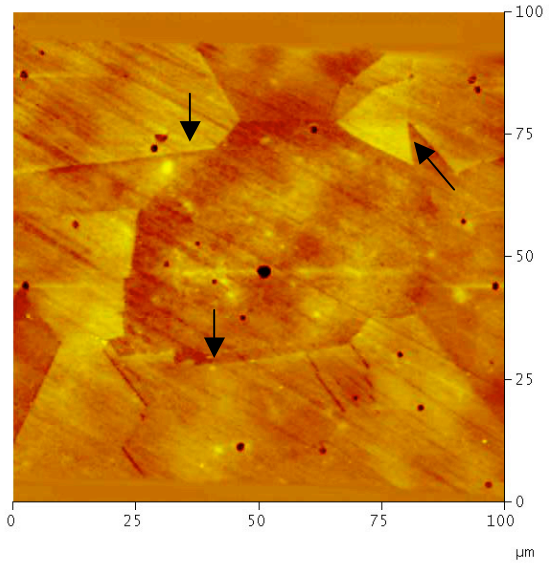

Figure 1-6. Visualization of grains and grain boundaries of stainless steel by atomic force microscope. Grains and grain boundaries (black arrow) of a 304 stainless steel. The surface was imaged at 100 µm using an AFM in contact mode.

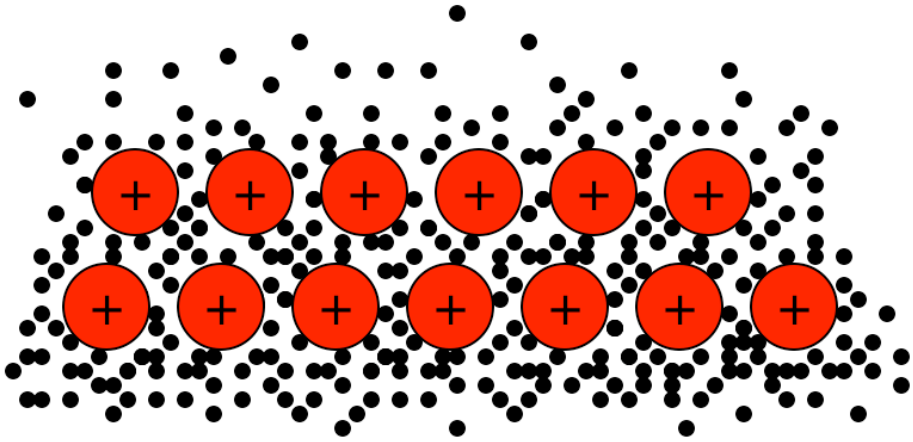

Figure 1-7. Simplified representation of metallic boding in metals and their alloys. The positive atom cores (red) are surrounded by delocalized electrons (black). The electron cloud is formed when metal atoms give up their valence electrons and form positively charged ions. The ions are held together by the surrounding electrons.

beyond the metal (Tao & Li, 2008b). As a result, common physicochemical properties that correlate to overall levels of surface electron activity are affected at grain boundaries, including the electron work function (EWF), adhesive force, and hardness. The electron work function is defined as the amount of energy in electron volts (eV) required to remove an electron from the Fermi level of the metal to a point just beyond the metal surface, with the electron possessing no kinetic energy once it is beyond the surface (Ashcroft & Mernim, 1976). Reactive surfaces have lower EWFs (**Fig. 1-8**)(Li & Li, 2005; Li & Li, 2004). The adhesive force describes the ability of the metal surface electrons to interact with exogenous materials and can be viewed as the general "stickiness" of a surface. At the nanoscale, the adhesive force is measured by determining the amount of force required to break the interaction between a standard atomic force microscope (AFM) tip and the metal surface. Surfaces with low EWF, and therefore more reactive surface electrons, have higher adhesive forces (**Fig. 1-8**)(Guan *et al*., 2005). Surface hardness, also referred to as the stiffness of a surface when measured at the microscale and nanoscale, describes the ability of a material to resist deformation in response to an applied force (Baumgart, 2000). The atomic bond strength of a metal will influence the hardness of the material and electron behavior affects bond strength. Reactive electrons reflect weaker bonds and decreased hardness and the EWF of a material correlates with surface hardness (**Fig. 1-8**)(Hua & Li, 2012).

1. 2. 1. Bacterial colonization of metal surfaces

Metal surfaces are susceptible to bacterial colonization and to the formation of bacterial communities, known as biofilms, which result when bacteria come into contact with virtually any natural or synthetic surface (Fletcher, 1994; Hall-Stoodley *et al*., 2004). Biofilms create significant financial and health issues as they are a significant source of biofouling which leads to corrosion and degradation of structural metals (LeChevallier *et al*., 1988), contamination of food products (Costerton, 1984), nosocomial infections due to colonized medical equipment and implants (Passerini *et al*., 1992), and biomaterial-centered infections, commonly described as foreign body infections, that greatly limit the use and longevity of biomaterials (Gristina, 1987) and lead to the surgical removal of implants.

It is well recognized that *P. aeruginosa* readily colonizes metal surfaces and forms biofilms on surgical implants, water storage systems, and milk distribution pipelines. Stainless steel is often the material of choice because of its resistance to staining, low corrosion propensity, relative low cost, and minimal maintenance requirements, making it an ideal metal for a wide

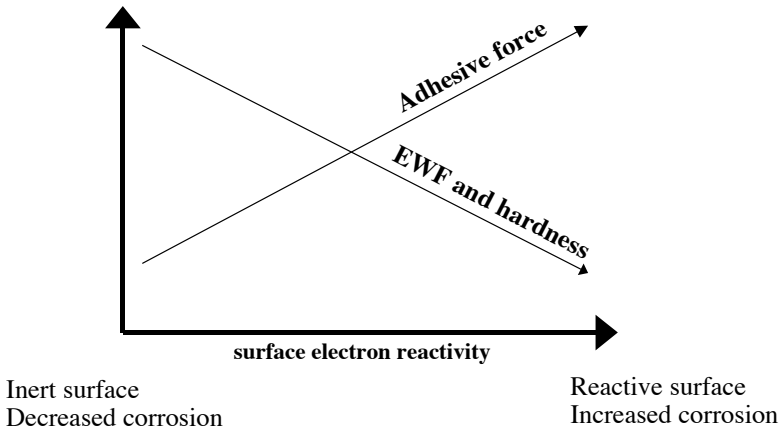

Figure 1-8. Simplified schematic of the relationship between EWF, adhesive force, hardness, and surface electron reactivity. As the reactivity of the surface electrons increase, the EWF and the hardness will decrease. The adhesive force will increase with increased electron surface reactivity. Surfaces with reactive electrons have higher rates of corrosion compared to inert surfaces.

range of applications. Efficient eradication of established biofilms is necessary in order to prevent infections but challenging because *P. aeruginosa* is innately resistant to antibiotics, host immune systems, and other biocides (Costerton *et al*., 1987; Costerton *et al*., 1999). In addition, bacteria in biofilms are more resistant than planktonic or free-floating bacteria and much higher concentrations of bacteriocidal agents are required for efficient killing (LeChevallier *et al*., 1988).

1. 2. 2. Surface free energy

The first step of biofilm formation is bacterial adherence to the surface. Although bacterial adhesion mechanisms such as the T4P in *P. aeruginosa* play a crucial role in mediating attachment and biofilm formation, the important role of the chemical and physical properties of the surface in influencing the ability of bacteria to attach to a surface and establish biofilms cannot be ignored and must be taken into account to fully understand the mechanisms underlying bacterial colonization of surfaces. These solid surface properties have been classically described in terms of surface charge and surface free energy (Zisman, 1964), with bacteria preferentially colonizing hydrophobic (low energy) versus hydrophilic (high energy) surfaces. Fletcher and Loeb (1979)(Fletcher & Loeb, 1979) found a strong positive correlation between surface hydrophobicity, quantified by water contact angle measurements, and the total number of attached bacteria on a variety of surfaces, suggesting that binding is mediated by hydrophobic interactions.

Aditionally, the majority of bacteria possess a negative surface charge and positively charged surfaces are more attractive for colonization compared to negatively charged surfaces (Harden & Harris, 1953) and bacteria with hydrophobic cell walls adhered more readily than hydrophilic bacteria (van Loosdrecht *et al*., 1987). The adsorption of macromolecules onto the surface also influences bacterial adhesion by altering the surface free energy of the surface (Fletcher & Marshall, 1982). High energy, hydrophilic surfaces adsorb macromolecules more readily and are more easily hydrated compared to low energy surfaces, leading to an increased propensity for high energy surfaces to be colonized by bacteria (Pringle & Fletcher, 1986).

1. 2. 3. Methods for surface modification

The surface free energy of a material can be modified by altering the properties of the metal surface. Altering the metal, including the surface, will affect other material properties including the EWF, adhesive force, hardness, friction, and corrosion rate. Changing the surface properties of a metal can generate multi-purpose surfaces that show improved performance not only in controlling biofilm formation but also in decreasing the reactivity of surface electrons

(including the EWF, adhesive force, and friction), decreasing corrosion propensity, and increasing surface hardness to limit wear.

1. 2. 3. 1. Altering alloying elements in metals

There are three main approaches to limiting material corrosion, wear, friction, and bacterial adhesion to surfaces. Firstly, the inherent composition of the metal alloy can be modified by the addition of additional elements into the metal alloy or altering the concentration of an element within the alloy. High chromium cast irons (HCCIs) are commonly used in processes where high resistance to wear and corrosion are required, such as in the oil sands industry for slurry pumping systems, in mining, and in milling industries (Jones & Llewellyn, 2009). Increasing the percent content of chromium and carbon in HCCIs greatly enhances their wear and corrosion resistance although casting issues leading to high rejection rates still present limitations for industrial applications (Llewellyn *et al*., 2004; Tang *et al*., 2011; Tian *et al*., 2009). Addition of tantalum (Ta) and tin (Sn) into titanium generates alloys with increased corrosion resistance and strength while retaining biocompatibility, making these alloys attractive materials for biomedical implants (Guo *et al*., 2012; Sumner *et al*., 1998; Zhou *et al*., 2004). Increased corrosion resistance is necessary because colonization by microorganisms contributes significantly to corrosion of metals in industry (Lechevallier *et al*., 1993). The major advantage is that the bulk of the material is modified. Changes in the properties of the metal are present throughout the material and are not limited to the surface.

1. 2. 3. 2. Nanostructuring metal surfaces

Secondly, the physical properties of the surface, most commonly the structure, may be modified. This method is advantageous when the bulk of the material performs adequately but the surface requires additional protection to limit susceptibility to bacterial adhesion, wear, and corrosion. Nanostructuring surfaces of both pure metals and alloys, including aluminum, brass, copper, carbon steel, aluminized steel and stainless steel, to generate grains in the nanometer versus micrometer size reduces the adhesive force, surface free energy, and enhances surface stability, resistance to mechanical wear, corrosion, and decreases colonization by bacteria (Chen *et al*., 2009a; Chen *et al*., 2009b; Chen *et al*., 2009c; Mao *et al*., 2010; Tao & Li, 2008a). Nanostructured stainless steel surfaces are less susceptible to colonization by *P. aeruginosa* (Yu *et al*., 2008; Yu *et al*., 2010; Yu *et al*., 2011).

Nanostructuring is achieved through severe plastic deformation (SPD) achieved by rounds of sandblasting or physical punching following by recovery through heat annealing

(Valiev *et al*., 1993), ball-milling (Koch *et al*., 1993), electrodeposition (Erb, 1995), the consolidation of ultrafine powder (Gleiter, 1989), or the crystallization of amorphous solids (Lu, 1996). These methods are often multi-step processes that can be time consuming, costly, and, for some of the simpler techniques such as SPD, problematic to generate on a large scale or on hard metals and alloys (Iwahashi *et al*., 1998; Wetscher *et al*., 2005).

1. 2. 3. 3. Surface coatings

Finally, surface properties can be modified by coating the surface with a metal, ceramic or organic layer. Aluminum diffused into the surface of various metals produces a passive film that is insoluble, harder, and improves the corrosion resistance (Liu *et al*., 2008; Su *et al*., 2008; Zhang *et al*., 2008). Epoxy, graphene, and diamond-like carbon coatings are used to reduce friction by decreasing surface roughness to increase flow efficiency in gas pipelines (Robertson, 1992; Sandoz-Rosado *et al*., 2012; Yang *et al*., 2005). Surface roughness correlates with higher bacterial colonization, and decreasing surface roughness not only reduces friction but also decreases a surface's propensity for biofilm formation (Costerton *et al*., 1987; Devicente *et al*., 1986; Dunsmore, 1983; Lewis *et al*., 1984). Electropolishing significantly decreases *P. aeruginosa* binding to stainless steel but cannot completely eliminate surface colonization. Adherence still occurs rapidly and can be observed within 30 seconds of inoculation with bacteria (Vanhaecke *et al*., 1990).

Coating steel surfaces with a thin layer of silver, a metal with intrinsic antimicrobial properties, has been shown to successfully limit biofilm formation on metals, although overcoming the toxicity of silver towards the human host has been problematic (Leung *et al*., 1992; Riley *et al*., 1995; Stickler *et al*., 1996). *In vivo* murine studies revealed that silver-coated orthopedic pins were much more resistant to bacterial colonization (Collinge *et al*., 1994), including colonization by *P. aeruginosa* (Wassall *et al*., 1997).

Research on organic coatings has focused on the development of very thin, or nanolayer organic coatings, for medical (biofilm reduction) and bioengineering applications (biosensor and microarray manufacturing). Coating with hydrated polymers forms a steric barrier that limits non-specific interactions between the surface and bacteria (Kingshott & Griesser, 1999). Polyethylene glycol (PEG) thin brush coatings prevent nonspecific adsorption of proteins and cells onto surfaces (Amiji & Park, 1994; Lee *et al*., 1995) and significantly reduce bacterial adhesion but do not completely eliminate the attachment of bacteria (Ista *et al*., 1996; Lee *et al*., 1995). PEG-based coatings present many advantages, including being non-toxic, non-immunogenic, inert, and can prevent the nonspecific adsorption of proteins and cells (Amiji &

Park, 1994; Lee *et al*., 1995). Traditional methods of PEG-ylating surfaces involve attaching the polymer chains through one or several anchor points on the surface by adsorption, electrodeposition or chemical coupling of the PEG to the surface. To covalently modify the surface, the polymer is either grafted to the surface via a preformed functional group on the polymer or using *in situ* polymerization using an initiator immobilized on the surface (Pyun *et al*., 2003; Sirard *et al*., 2003). PEG that is covalently coupled to the surface is more effective at preventing bacterial adhesion compared to PEG that is physically adsorbed onto the surface (Kingshott *et al*., 2003). Stainless steel with PEG covalently immobilized on the surface is resistant to protein adsorption but not to *P. aeruginosa* adhesion (Kingshott *et al*., 2003). In addition, sterilization of the surface remains problematic and highly stringent cleaning conditions cause the PEG coating to lift from the surface, highlighting that despite advances in surface coating technology obstacles must still be overcome.

1. 3. Molecular basis for interaction of the RBD with steel

There is a great need for the development of simple, versatile methods to deliver coatings onto surfaces that modify the surface for improved performance. Given that the efficient colonization of surfaces by bacteria is influenced by both the bacterial adherence mechanisms and the physicochemical properties of the surface, it is necessary to understand the mechanisms utilized by bacteria to colonize metals surface and how the physical and chemical properties of the surface affect colonization.

1. 3. 1. Interaction of the RBD with steel surfaces

Twitching motility mediated by T4P is essential for surface colonization and biofilm formation by *P. aeruginosa*. Substantial mechanical forces are generated during pilus retraction and for efficient motility to occur the interaction between the T4P and the surface must be capable of withstanding these forces while still being stable enough to allow for significant pilus retraction before release from the surface occurs. In *P. aeruginosa*, binding to biotic and abiotic surfaces is mediated by the RBD of PilA (Giltner *et al*., 2006; Lee *et al*., 1994) and the RBD retains its binding properties as a synthetic peptide. The addition of RBD-specific antibodies and synthetic peptides encompassing this region can competitively inhibit pilus-mediated adhesion to epithelial cells (Giltner *et al*., 2006; Lee *et al*., 1994; Sheth *et al*., 1995). Based on various models of pilus assembly, the RBD appears fully exposed only at the tip of the pilus, reinforcing its role as an adhesin, and a total of three RBDs may be exposed at the tip as the pilus fiber

consists of three intertwined filaments (Craig *et al*., 2006), thereby increasing the binding strength and binding avidity by tripling the valency.

P. aeruginosa binds strongly to stainless steel through the RBD. The RBD has a very high affinity for stainless steel, as exemplified by a $Ki_{apparent}$ of 0.2 nM (Giltner *et al*., 2006; Stanley, 1983), given that previously reported binding affinities of metal binding peptides fall in the mM range (Zuo *et al*., 2005). Recently a titanium-binding peptide with a reasonably high affinity (116 nM) was obtained by phage display (Khoo *et al*., 2010) although the affinity of this peptide for titanium is still significantly lower than the affinity of the RBD for stainless steel.

Traditionally, the interaction between ligands or a ligand and its receptor (in this case the metal surface) occurs in the presence of a conditioning film, where the presence of bulk solvents affects the interaction between ligands. Binding affinity and stability are influenced by hydrophobic interactions, where most of the energy required for binding is derived from the exclusion of bulk solvent such as water molecules (Li & Logan, 2004; Morra & Cassinelli, 1997; Pereni *et al*., 2006). Direct force measurements utilizing a *de novo* designed coil-coil, where silicon nitride AFM tips were derivatized to display the 17 amino acids of the RBD, were used to measure the strength of the RBD-steel interaction. Measurements revealed that there was an ~2.7 fold increase in the adhesive force between the peptide-derivatized AFM tip and the standard tip, indicating that the RBD bound with higher affinity to the steel than the control tip. The strength of the molecular interaction between the RBD and steel was estimated to range between 26-55 pN, results that are consistent with existing biological data (Yu *et al*., 2007). A force of 70-120 pN is capable of rupturing a T4P fiber attached to a surface (Touhami *et al*., 2006) and the pilus is under approximately 10 pN of stress during retraction (Li & Logan, 2004).
The RBD interacts directly and with high affinity with stainless steel surfaces in the absence of a conditioning film and the RBD-steel interaction is strong enough to withstand the force generated by the retracting pilus (Yu *et al*., 2007; Yu *et al*., 2008).

Additionally, this interaction does not appear to be mediated by hydrophobic interactions (Yu *et al*., 2007) as experiments were performed in "dry" conditions where the presence of a conditioning film was minimized by polishing, etching, and washing the steel to remove the majority of solvents that may have helped stabilize the interaction between the RBD and the steel and account for the high affinity of the peptide for steel. Given that the RBD interaction with epithelial cells is of considerably lower affinity (~200,000 times lower) and the interaction with the minimal receptor of GalNAc-Gal appears to be mediated largely through hydrophobic interactions (Schweizer & Po, 1996), the data suggests that the interaction between the RBD and stainless steel is a novel interaction.

1. 3. 2. Release of the T4P from metal surfaces

During twitching motility rapid adherence and release from the surface is required for forward movement (**Fig. 1-5**). Given the high affinity of the RBD for steel, it is unclear how the RBD, and therefore the pilus, releases from the steel surface. Initially, the tip of the pilus must be firmly attached to the surface and the RBD-surface interaction must be strong enough to withstand the force exerted during retraction for movement to occur. If the tensile strength is too great and the RBD-surface interaction is not strong enough then the pilus will detach before the pilus has retracted and motility will not occur. Following retraction, however, the pilus must detach from the surface in order for the bacterium to move forward.

In theory the rate of dissociation of the RBD from the surface would be too slow to allow the pilus to be released from the surface for efficient movement to occur and the bacterium would essentially remain trapped in one position, unable to release from the surface and unable to move forward. If the pilus cannot release then *P. aeruginosa* is presented with two alternate options to ensure motility. Release from the surface could be accomplished by shedding the intact pilus from the bacterial surface following pilus retraction, leaving the pilus bound to the surface. Alternatively, the RBD could be selectively cleaved from the PilA protein by proteases, releasing the tip from the surface without leaving behind the entire pilus. Although feasible, both options would require additional energy to be expended to synthesize new PilA subunits to replace those left behind during detachment. Twitching motility is already an energetically expensive process that requires the continuous hydrolysis of ATP to power pilus extension and retraction. It is believed that pilin monomers will dissociate from the pilus base during retraction and are stored in a pilin subunit pool that was observed in the cytoplasmic membrane (Morand *et al*., 2004). These subunits could then be recycled during pilin extension. If the pilus or the tip dissociates in order to release from the surface, this pool would need to be replenished with newly-synthesized proteins.

A more energetically favorable hypothesis is that binding of the RBD to steel is a reversible interaction somehow controlled by the bacterium and release is a tightly regulated event that occurs following pilus retraction. The tip could alternate between two binding conformations, one promoting adhesion to the surface and the other promoting release, although this hypothesis raises many questions, including whether a specific signal mediates conformational change, what such a signal would be, and how the signal might be transmitted. One possibility is that the force generated during the retraction phase serves as a signal for release, promoting a conformational change in the tip. The RBD can exist in a *trans* and a *cis* conformation around the central proline in its hydrophobic pocket (Campbell *et al*., 2003). This

change in conformation could have an important role in determining binding and release from the surface.

1. 3. 2. 1. Role of the PilT ATPase in twitching motility

Retraction is an important aspect of twitching motility and, if the bacterium is to move efficiently along a surface, must occur prior to pilus release from the surface. PilT is a hexameric ATP-ase that is required for pilus retraction. Although the exact role of PilT in twitching motility and retraction is still unclear, PilT is important for twitching motility and may play an important role in release of the pilus from the surface. *P. aeruginosa pilT* mutants are deficient in twitching motility and although capable of binding to surfaces they were hyperpiliated and unable to release from the surface (Mattick, 2002; Merz *et al*., 2000; Whitchurch *et al*., 1991b). *P. aeruginosa pilT* mutants formed very thick unstructured biofilms once bound to a surface (Burrows, 2005; Chiang *et al*., 2005).

PilT may help dissociate pilin subunits from the base of the pilus and place them in the pilin pool (Morand *et al*., 2004). Alternatively, PilT could reverse the direction of PilB, the ATP-ase motor responsible for subunit assembly and pilus extension (Turner *et al*., 1993), although evidence in *E. coli* suggests that PilT and PilB do not interact (Crowther *et al*., 2004; Morand *et al*., 2004) and Morand *et al*. (2004)(Morand *et al*., 2004) demonstrated that the control of extension and retraction of the pilus in *Neisseriae* can be separated, making this second hypothesis less likely. A third option is that PilT controls pilus depolymerization and the force generated during retraction by PilT during pilus retraction mediates a conformational change in the pilus tip required for release of the surface.

1. 3. 3. Preferential binding of *P. aeruginosa* to metal grain boundaries

During colonization of stainless steel, *P. aeruginosa* preferentially binds at grain boundaries instead of within grains (Giltner *et al*., 2006; Stanley, 1983). Adhesive force measurements using an AFM tip derivatized with the RBD of *P. aeruginosa* found that the synthetic RBD bound to the grain boundary with adhesive forces that were 2-fold greater than those measured within grains (Yu *et al*., 2007), suggesting that surface electron activity and/or the differential material composition of the grain associated with the grain boundary may contribute to the interaction and that the T4P may have higher affinity for the grain boundary compared to the interior of the grain. Further investigation using nanostructured stainless steel demonstrated that the strength of the RBD-steel interaction is directly proportional to the surface electron

activity (Yu *et al*., 2010), with the strongest RBD-steel interactions occurring in regions of high electron activity (grain boundary) and low EWF, suggesting that the high affinity binding between the RBD and the steel is the result of a sharing of reactive surface electron, similar to the covalent bonding that occurs between atoms, on the steel with the RBD. In areas where the EWF is much higher, such as in the grains, this sharing would require more energy, whereas less energy would be required for sharing electrons at grain boundaries where the EWF is lower, potentially explaining why *P. aerugniosa* preferentially adheres to grain boundaries on stainless steel surface.

1. 4. Electron transfer through biosystems

Proteins and peptides have long been recognized as important mediators of electron transfer (Cretich *et al*., 2006; Dawson *et al*., 2006; Ligler & Erickson, 2006) and the ability to extract and transfer electrons is a fundamental aspect of all biology, most notably in redox reactions ranging from photosynthesis to aerobic respiration. Bacteria have evolved diverse mechanisms to capture and divert electrons to exploit redox reactions as biological energy sources. Classical methods of electron transfer (ET) frequently employ oxygen and nitrate as terminal electron acceptors (essentially driving the continual transfer of electrons from the initial substrate to the final electron acceptor) as they are abundant and are readily accessible to cellular enzymes. However, some environmental bacteria, namely dissimilatory metal-reducing bacteria (DMRB), have evolved additional electron transfer methods to overcome the challenges associated with the low accessibility of their terminal electron acceptors (solid phase Fe(III) and Mn(IV) oxides). These organisms utilize soluble mediators as extracellular electron acceptors to shuttle electrons as well as cytoplasmic or outer membrane localized multiheme cytochromes to directly transfer electrons to the insoluble electron acceptors that are available in their environmental niches (Lovley & Phillips, 1988; Myers & Nealson, 1988). Intriguingly, these bacteria transfer their electrons to the insoluble acceptors in discrete steps associated with a clearly recognizable cycle where the bacterium binds to and interacts with the surface to effect electron transfer for a limited time frame, which is then followed by the dissociation of the bacterium from the surface when electron transfer ceases with the cycle being repeated until the insoluble electron acceptor is completely solubilized or biofilm formation begins.

1. 4. 1. T4P function as bacterial nanowires

The discovery that bacterial Type IV pili (T4P) can function as molecular “nanowires” revealed a novel method for electron transfer in biological systems, namely the ability to directly

transfer electrons from the bacterium to inanimate and primarily conductive extracellular surfaces via T4P nanowires (El-Naggar *et al*., 2010; Reguera *et al*., 2005; Reguera *et al*., 2006). *Geobacter* and *Shewanella* species possess T4P that are highly conductive and are capable of transferring electrons, obtained through the oxidation of organic compounds, to insoluble extracellular electron receptors such as Fe(III) and Mn(IV) oxides. A *pilA*$^{-}$ mutant of *Geobacter sulfurreducens* could not produce pili, was minimally able to reduce Fe(III) oxides, and pili were conductive across their diameter (Reguera *et al*., 2005). Electron conductivity was demonstrated to occur across *G. sulfureduscens* pili networks, where air dried pili carried current between electrodes spaced centimeters apart. Similar current rates were observed in live biofilm, strongly suggesting that pili conductivity can occur in physiologically relevant conditions (Malvankar *et al*., 2011). Finally, when a low voltage (<1V) was applied to purified pili, a current flow rate of up to 10^{10} electrons per second associated with the length of the pilus of *Shewanella oneidensis* was observed. No current was observed when proteins that were not pili were used or when the c-type cytochromes normally associated with the pili were absent (El-Naggar *et al*., 2010; Gorby *et al*., 2006; Reguera *et al*., 2005).

Interestingly, conductive AFM studies performed by Reguera *et al*. (Reguera *et al*., 2005) could not demonstrate conductivity of T4P isolated from *P. aeruginosa*, despite strong sequence and structural similarities between the N-terminal hydrophobic helix of PilA (**Fig. 1-9**) and the type IV pilin subunits of *G. sulfurreducens* and *S. oneidensis*. Unlike PilA, the pilin subunits of *G. sulfurreducens* and *S. oneidensis* appear to consist solely of a fairly hydrophobic α-helix and lack the hydrophilic C-terminal globular domain that encompasses the RBD of *P. aeruginosa*.

1. 4. 2. Charge transfer through T4P

Despite strong experimental evidence of electron transport through T4P, the mechanism governing transfer remains unknown. Compared to other models of ET through peptides, T4P are significantly larger and longer, and electrons are required to travel much longer distances (>0.5 microns vs an average of 30 Angstroms) through the protein, challenging the conventional view of charge flow in biological systems. The current models of protein-mediated ET propose that the protein facilitates ET between redox cofactors and electrons move by quantum mechanical electron tunneling, passing through portions of the protein that are viewed as energetically inaccessible (Bendall, 1996; Gray, 1997; Holm & Solomon, 1996) in what is viewed as direct electron transfer or via the movement of what are termed electron holes (Petrov & Hanggi, 2001; Petrov *et al*., 2003; Sheu & Yang, 2001). In these models, the electron moves, or "hops", in a

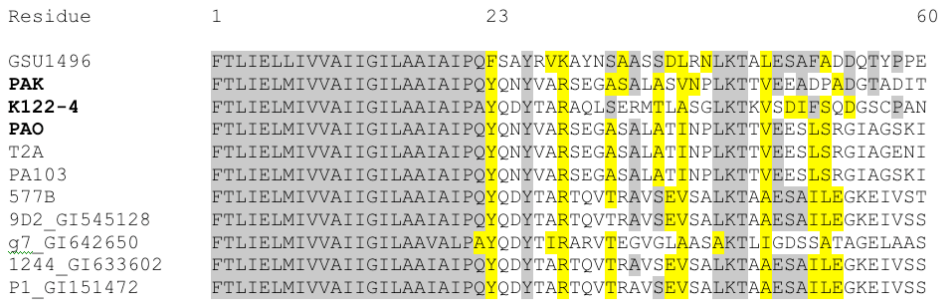

Figure 1-9. Sequence comparison of *Geobacter sulfurreducens* GSU1496 PilA with N-terminal PilA sequence of *Pseudomonas aeruginosa* strains. Strong sequence similarities can be observed between the major pilin protein of *G. sulfurreducens*, an environmental Gram-negative bacterium known to possess a conductive Type IV pilus, and the N-terminal portion of PilA, the major pilin protein of *P. aeruginosa* (*PA*). In structure prediction models, the N-terminal portion of PilA would be buried within the pilus, forming a potentially conductive core. Bolded *PA* strains represent those used in this study and from which synthetic RBD peptides were derived.

stepwise fashion between discrete resting places within the protein. The resting sites in proteins, while unknown, provide sites that are energetically accessible along the path followed by the electron and it has been suggested that electrons stop in covalent and hydrogen bonds and within amide groups or, alternatively, hop between amino acids capable of accommodating charges, such as arginines, tyrosines, and tryptophans (Long *et al*., 2005). One or several of the amino acids of the RBD of *PA*, including the positively charged arginine, lysine, aspartic acid, and glutamic acid, in addition to the disulfide loop, could serve as electron resting places. Additional arginine residues in the N-terminal helix and the two tryptophan residues found in PilA, particularly a strictly conserved tryptophan located just outside the RBD at residue 127, could also accommodate an electron.

The electron tunneling pathway model also predicts that the ET rate is influenced by the secondary structure of the protein (Scott, 1997). Extensive experiments using ruthenium-modified cytochromes and azurins suggested that the maximum ET rate was higher in β-strands compared to α-helices. Electrons tunneling through α-helices would pass through both covalent and hydrogen bonds while adopting a more circular trajectory as compared to electrons tunneling exclusively through β-strands containing only covalent bonds (DiBilio *et al*., 1997; Gray & Winkler, 1996; Skov *et al*., 1998). More recent work suggests that helical secondary structures, such as those of the N-terminus of PilA and other pilin proteins, can result in rapid electron transfer (Sek *et al*., 2006). Unfortunately conclusions cannot be generalized as multiple factors including the presence of hydrogen bonds (Antonello *et al*., 2003), amino acid sequence and length (Malak *et al*., 2004; Polo *et al*., 2005; Sek *et al*., 2005; Watanabe *et al*., 2005), and secondary structure (Antonello *et al*., 2003; Kraatz *et al*., 2004; Sasaki *et al*., 2001; Shin *et al*., 2003b; Sisido *et al*., 2001) all contribute to electron transfer rates.

Based on models of *PA* pilus assembly, the N-terminal α-helical hydrophobic domain of PilA is located in the internal core of the pilus whereas the C-terminal domain surrounds the internal core (Craig *et al*., 2006), placing the arginine residues, or any residue within the RBD, approximately 30 Angstroms apart from a matching residue in an adjacent RBD and providing a very reasonable distance for electrons to hop from one RBD to another along the length of the pilus at the ET rates observed in T4P. Theoretical analysis of the observed charge flow rate in T4P performed by Polizzi (Polizzi *et al*., 2011) emphasized the necessity of a multi-step hopping mechanism with closely packed electron resting sites, separated by less than 1 nm, to account for the rapid movement of charge across the pilus length.

Given all of the currently available information concerning electron transfer within proteins, there is both theoretical and experimental evidence to strongly suggests that the T4P of

PA may be an insulated molecular nanowire, with the N-terminal region (which shares sequence homology with the pilin proteins of Gram-negative bacteria possessing conductive T4P acting as a central conducting core and the C-terminal region creating an insulating protein cover. This theory becomes even more attractive when one considers that the RBD may be sharing electrons with stainless steel surfaces, essentially forming an electrical connection between the metal and the RBD.

1. 5. Objectives

1. 5. 1. Investigating T4P release from stainless steel surfaces

The first aim of this study was to investigate the release of the T4P from *P. aeruginosa* from stainless steel surfaces and determine whether the pilus, or a portion of the pilus, was shed during twitching motility by examining if a previously colonized surface could be as easily colonized by *P. aeruginosa* as a naïve surface. We hypothesized that pilus release would be as energetically favorable as possible, occurring in an energy and retraction-associated manner, and would not result in pilus shedding or proteolysis following a period of pilus retraction. We also hypothesized that release would be a process controlled by the bacteria. To rule out the possibility that the pilus spontaneously dissociates from the surface we investigated the ability of purified pili and synthetic RBD peptide to displace previously bound pili and RBD peptide from the surface and to desorb from the surface.

1. 5. 2. Characterizing the RBD-steel interaction

The second aim was to investigate the molecular basis of the RBD-steel interaction. The affinity of the RBD for steel is extremely high (Giltner *et al*., 2006) and is beyond what would be anticipated for a flexible peptide binding to a solid surface. Given that the RBD-steel interaction does not require a conditioning film (Yu *et al*., 2007) and the strength of interaction is directly proportional to surface electron activity or surface free energy we hypothesized that the RBD may form a novel organo-metallic state of matter with the stainless steel surface and that the RBD-steel interaction might be due to the de-localization of surface electrons through the RBD.

1. 5. 3. Determining if the T4P of *P. aeruginosa* is a bacterial nanowire

The T4P of environmental bacteria such as *G. sulfurreducens* and *S. oneidensis* function as molecular nanowires that transfer electrons from the bacterium to extracellular electron receptors (Gorby *et al*., 2006; Reguera *et al*., 2005). The N-terminal region of PilA of *P. aeruginosa* (**Fig. 1-9**) shares sequence homology with the pilin subunits of environmental

bacteria but when probed by conductive AFM no current was observed flowing through the T4P of *P. aeruginosa* (Reguera *et al*., 2005). We hypothesize that the T4P of *P. aeruginosa* may exist as an insulated nanowire. Differences between the structures of the T4P of *P. aeruginosa* and *G. sulfurreducens*, namely the presence of a C-terminal globular domain in the PilA structure of *P. aeruginosa* that is absent from PilA of *G. sulfurreducens*, suggest that the T4P of *P. aeruginosa* forms a nanowire possessing a conductive, three-stranded α-helical hydrophobic central core surrounded by an insulating sheath composed of the globular C-terminal domains. We sought to demonstrate, using alternative means to measure current flow through proteins, that the T4P of *P. aeruginosa* functions as a molecular nanowire and can transfer electrons between the bacterium and its external environment.

1. 5. 4. Using the RBD to modify metal surface properties

Finally, we hypothesized that the irreversible and high affinity binding of the RBD to stainless steel could be used to develop versatile coatings to selectively modify the properties of metal surfaces. We tested the ability of variants of the native L-amino peptide to modify the EWF, adhesive force, hardness, friction, and corrosion rate of metals, including stainless steel and titanium, as well as investigated whether these surface modifications could reduce surface colonization by bacteria.

The work in this study describes a novel peptide-metal bond that forms as a result of electron sharing between the RBD and the surface electrons of metals to generate a new material that has altered surface properties. New materials generated using variants of the RBD peptide showed differential surface properties with regards to EWF, adhesive force, hardness, coefficients of friction, and susceptibility to biofilm formation. In addition, this study demonstrates that the T4P of *P. aeruginosa* is an insulated bacterial nanowire capable of sustaining high currents.

Chapter 2

Materials and Methods

2. 1. Bacterial Strains and Growth Conditions

The *Pseudomonas aerugin*osa strains used in this study were PAK WT, PAK R364 (Whitchurch *et al*., 1991b), and PAK S34 (Whitchurch & Mattick, 1994). The PAK R364 and PAK S34 strains have a transposon insertion in the *pil*T and *pil*U genes respectively (Beatson *et al*., 2002b; Whitchurch *et al*., 1991b; Whitchurch & Mattick, 1994). Bacteria were routinely grown at 37°C in Luria-Bertani (LB) broth or LB supplemented with 50 mg/mL of tetracycline (Sigma) for PAK R364 and PAK S34 in order to positively select for the transposon and stably maintain the mutation.

Three strains of *Staphylococcus aureus* and one strain of *Staphylococcus epidermidis* were obtained from the Department of Medical Microbiology and Immunology teaching culture collection. Three strains of *Listeria monocytogenes* and an environmental isolate of *Listeria innocua* were originally obtained from Diversified Research Inc. (Toronto, Ontario). All bacterial strains were maintained as frozen stock cultures at -80 C and were recovered by culturing on LB plates at 37 C. Overnight cultures on LB agar were utilized as the source of a single colony for inoculation of LB broth which was cultured overnight at 37 C. These broth cultures were then employed directly for bacterial adherence studies.

2. 2. Purification and biotinylation of PAK pili and RBD peptides

PAK pili were isolated from the hyper-piliated mutant *P. aeruginosa* strain PAK/2Pfs as previously described (Paranchych *et al*., 1979). Purity was confirmed by sodium dodecyl surfate (SDS)-15% (wt/vol) polyacrylamide gel electrophoresis (PAGE), electron microscopy, and functional analysis of binding characteristics (Giltner *et al*., 2006; van Schaik *et al*., 2005)

PAK(128-144)ox, PAO(128-144)ox, PAO K130I(128-144)ox, K122-4(128-144)ox, D-amino K122-4(128-144)ox, and retro-inverso D-amino k122-4(128-144)ox peptides were all synthesized by solid phase peptide synthesis and purified by reversed-phase high-performance liquid chromatography (HPLC) as described by Wong *et al* (Wong *et al*., 1992; Wong *et al*., 1995). The disulphide bridge form of the peptide used in this study was generated by air-oxidization (Campbell *et al*., 1995). Purity of all peptides was verified by HPLC analysis and mass spectroscopy. All peptides utilized were >95% pure.

The D-amino acid enantiomeric form of the K122-4(128-144)ox peptide was synthesized as previously described. The oxidized peptide was coupled to monodisperse polyethylene glycol (PEG) via the free N-terminus of the peptide to generate D-PEG which was purified by reversed phase HPLC to yield a product that was >95% pure (based on HPLC analysis) and which displayed a MW of 2,955. The synthesis of all peptides was performed on a fee for service basis,

by the Peptide and Protein Chemistry Core Facility at the University of Colorado Health Sciences Centre at Fitzsimons.

Biotinylation of pili and peptides was performed as previously described by Yu *et al*. (Yu *et al*., 1996). The ability of biotinylated pili and peptide to bind to stainless steel was demonstrated by Giltner *et al*. (Giltner *et al*., 2006).

A list of all peptides and their sequences used in this study are listed in **Table 1**.

2. 3. Coating stainless steel samples with peptides, pili, and monomer

304 grade 2B finish stainless steel coupons 1 mm thick and approximately 1 cm by 1cm were annealed at 1040°C for 1 hr to release stress and then cooled at room temperature before further preparation. The stainless steel surface was polished to uniformity by sequentially employing sandpaper from 120# to 1200# grit size (MetTech Inc, Calgary) and then polished with an aqueous slurry of 0.05 μm colloidal silica. Coupons were then manually washed with detergent, rinsed with distilled water, immersed in 95 %(v/v) ethanol for 15 min with gentle agitation, rinsed with distilled water, washed with 15 mL of acetone for 1 min, rinsed with distilled water and then air dried. Polished coupons were then placed in sterile 30 mL borosilicate glass beakers (1 coupon per beaker) and incubated with 3 mL of sterile 10 mM phosphate buffered saline (PBS)(pH 7.4) containing 10 μg/mL of the appropriate peptide solution (PAK, PAO, PAO K130I, K122-4, K122-4 D-amino, K122-4 retro-inverso or a mixture of D-amino and retro-inverso both at a concentration of 10 μg/mL), incubated at room temperature for 1 hr with gentle agitation, washed 6 times with distilled water and allowed to air dry before subsequent use.

Aluminum (5mm thick) used for experiments in Chapter 4 was obtained from Bin Yu (Chemical and Materials Engineering, University of Alberta) and was cut into 1cm by 1cm samples. Aluminum samples were cleaned, polished, and coated with K122-4(128-148)ox peptide as previously described.

Titanium plate 3.175 mm thick and 99.5% pure (Alfa Aesar, Ward Hill, MA) was cut into coupons 1 cm x 1cm. The surface of titanium was polished uniformity by sequentially employing sandpaper from 120# to 600# grit and coated with peptide as described.

2024 aluminum plate was obtained from commercial sources and cut into 1 cm by 1 cm coupons. The sample was cleaned and coated with peptide as described.

***Pseudomonas aeruginosa* strains**	**Synthetic RBD peptide derived from *P. aeruginosa* strain**	**Peptide sequence**
PAK	L-amino PAK(128-144)ox	Ac-K-C-T-S-D-Q-D-E-Q-F-I-P-K-G-C-S-K-amide
		Biotin-G-G-G-K-C-T-S-D-Q-D-E-Q-F-I-P-K-G-C-S-K-amide
K122-4	L-amino K122-4(128-144)ox	Ac-A-C-T-S-N-A-D-N-K-Y-L-P-K-T-C-Q-T-amide
		Biotin-G-G-G-A-C-T-S-N-A-D-N-K-Y-L-P-K-T-C-Q-T-amide
	D-amino K122-4	Ac-ᴅA-ᴅC-ᴅT-ᴅS-ᴅN-ᴅA-ᴅD-ᴅN-ᴅK-ᴅY-ᴅL-ᴅP-ᴅK-ᴅT-ᴅC-ᴅQ-ᴅT-amide
		Biotin-G-G-G-ᴅA-ᴅC-ᴅT-ᴅS-ᴅN-ᴅA-ᴅD-ᴅN-ᴅK-ᴅY-ᴅL-ᴅP-ᴅK-ᴅT-ᴅC-ᴅQ-ᴅT-amide
	Retro-inverso D-amino K122-4	Ac-ᴅT-ᴅQ-ᴅC-ᴅT-ᴅK-ᴅP-ᴅL-ᴅY-ᴅK-ᴅN-ᴅD-ᴅA-ᴅN-ᴅS-ᴅT-ᴅC-ᴅA-amide
		Biotin-G-G-G- ᴅT-ᴅQ-ᴅC-ᴅT-ᴅK-ᴅP-ᴅL-ᴅY-ᴅK-ᴅN-ᴅD-ᴅA-ᴅN-ᴅS-ᴅT-ᴅC-ᴅA-amide
	PEG-D-amino K122-4	PEG-G-G-G- ᴅA-ᴅC-ᴅT-ᴅS-ᴅN-ᴅA-ᴅD-ᴅN-ᴅK-ᴅY-ᴅL-ᴅP-ᴅK-ᴅT-ᴅC-ᴅQ-ᴅT-amide
PAO1	L-amino PAO(128-144)ox	Ac-A-C-K-S-T-Q-D-P-M-F-T-P-K-G-C-D-N-carboxyl
	L-amino PAO K130I	Ac-A-C-**I**-S-T-Q-D-P-M-F-T-P-K-G-C-D-N-carboxyl

Table 1. Synthetic peptides derived from the RBD of *P. aeruginosa*.

For corrosion and potentiostatic testing, steel coupons were annealed as described and encased in epoxy (LECO Corporation, Mississauga) prior to polishing to a final polish of #600. Titanium samples were similarly encased in epoxy and the titanium surface was polished to a final polish of #400 grit. Once polished, samples were cleaned and coated as described.

2. 3. 1. Coating metal surfaces with PEG-D-amino peptide

The surface of the stainless steel and titanium coupons were polished to uniformity using sandpaper of increasing grit size (MetTech Inc, Calgary), from #240 to #400. All coupons were washed with dish detergent, rinsed 6x with tap water, and immersed in 95% (v/v) ethanol for 10 min with gentle agitation. Coupons were immediately immersed in 20 mL acetone for 1 min and rinsed thoroughly with distilled water. Samples were placed in sterile 50 mL glass beakers and covered with 4mL of sterile phosphate buffered saline (PBS)(ph 7.4) containing 10 μg/mL of PEG-D-amino peptide. Samples were incubated for 1hr at room temperature with gentle agitation, washed 6x with distilled water, and allowed to air dry. For the bacterial adhesion studies coupons were polished and cleaned as described and 1 μL of PEG-D-amino peptide diluted in dH_20 to 10 μg/mL was dotted onto the surface and allowed to air dry.

A list of all surfaces generated in this study can be found in **Table 2**.

2. 4. *P. aeruginosa* stainless steel adsorption and desorption assays

Grade 304 stainless steel 2B finish plates (1 mm thick, 20 gauge steel) were cut into 1 cm x 1 cm coupons and annealed at 1040°C for 1 hr. The surface was polished to uniformity using sandpaper of increasing grit size (MetTech Inc, Calgary), from 120# to 600# grit. Coupons were washed with dish detergent, thoroughly rinsed with distilled water and immersed in 95 %(v/v) ethanol for 15 min with gentle agitation. Coupons were then rinsed with distilled water, washed with 15 mL of acetone for 1 min, and rinsed with distilled water. They were placed in 6-well (1 coupon per well) tissue culture plates (Corning) and covered with 2.5 mL of sterile PBS. *P. aeruginosa* overnight cultures were subcultured into 20 mL of fresh LB and grown to early log phase to an OD_{600} ~0.25. Four mL of culture was centrifuged, washed twice with PBS, and resuspended in 1 mL of PBS. Approximately 1 x 10^6 CFU of bacteria were added to the stainless steel coupons for the release (desorption) assay. The samples were incubated at room temperature with gentle agitation.

Synthetic RBD peptide derived from *P. aeruginosa* strain	Material name	Metal
L-amino PAK(128-144)ox	Borg-PAKSS	304 stainless steel
L-amino K122-4(128-144(ox)	Borg-K122SS	304 stainless steel
D-amino K122-4	D-borgSS D-borgTi	304 stainless steel Titanium
D-amino retro-inverso K122-4	RI-borgSS RI-borgTi	304 stainless steel Titanium
PEG-D-amino K122-4	PEG-D-borgSS PEG-D-borgTi PEG-D-borgAl	304 stainless steel Titanium 2024 aluminum
PEG-D-amino K122-4		
L-amino PAO K130I		304 stainless steel Titanium

Table 2. Nomenclature of new materials generated using the RBD of *P. aeruginosa*.

Bacterial numbers were verified by plate counts. For the bacterial release assays, the coupons were incubated in bacterial cell suspensions for one hr at room temperature with gentle agitation. Bacterial suspensions were removed and all coupons were washed 6 times in sterile distilled water and allowed to air dry. The coupon for the first time point (Time 0) was allowed to air dry and all other coupons were incubated in 3 mL PBS at room temperature with gentle agitation until the subsequent time point, where all coupons were washed again, one coupon was allowed to air dry, and the remainder were incubated with PBS until the next time point. This was repeated for all time points. Samples were then incubated in 3 mL of 1 mM acridine orange stain for 3 min and rinsed three times with distilled water. Coupons were air dried and visualized using a Leitz Laborlux K microscope equipped with a Canon EOS Rebel digital camera and a 40x Neoflour lens with epifluorescent illumination. For each coupon, 25-100 digital images were taken using the 25x objective and bacteria per 25x field of view were enumerated from the digital images.

2. 5. *P. aeruginosa* release and challenge study following initial colonization of steel

Stainless steel coupons were polished and cleaned as previously described for the adsorption and desorption assays. Aliquots of 5 x 10^7 CFU of PAK WT were incubated with steel coupons at room temperature for 1 hr with gentle agitation. Coupons were washed six times with sterile distilled water, 5 x 10^7 CFU/mL PAK R364in PBS was added and samples were incubated for an hour at room temperature with agitation. Coupons were washed and allowed to air dry prior to staining with acridine orange and visualization by epifluorescent illumination as described in section **2. 4**.

When testing the effect of protease inhibitors on bacterial binding, experiments were performed as described above with the following modifications. Protease inhibitors were added at concentrations of 1 mM for PMSF, 10 mM for EDTA, and were added singly or in combination with PAK WT during the 1 hr incubation step. All coupons were stained and visualized as described in section **2.4**.

2. 6. Bacterial adherence studies on D-borgSS, RI-borgSS, and D+RI-borgSS

Broth cultures of overnight static cultures of *L. monocytogenes*, *L. innocua*, *S. aureus*, and *S. epidermid* were diluted with 10 mM PBS pH 7.4 to an OD_{650} of 0.1. Cultures were then applied to D-borgSS, RI-borgSS, and D+RI-borgSS coupons (duplicate samples) in 6-well (1 coupon per well) tissue culture plates (Corning) and incubated with 3 mL of bacteria in 10 mM PBS pH 7.4 and incubated at room temperature for 1 hour with gentle agitation. Coupons with attached bacteria were then washed 5 X with 3 mL of 10 mM PBS pH 7.4 to remove unattached

bacteria, rinsed with dH_2O and then stained with 1 mM acridine orange for 1 min at room temperature, washed 5 times with 3 mL dH_2O and air dried. Samples were then examined by epi-fluorescence microscopy with blue excitation with a Lietz laborlux K microscope with a Neofluor 25X objective lens and equipped with a Cannon camera. Bacteria bound to the surface was determined by capturing 30 25 X objective images (15 images/coupon, randomly selected across the coupon surface) and the number of bound bacteria determined utilizing NIH Image J software. Effectiveness of the image analysis was verified for each image by verifying that cell counts coincided with stained bacteria.

2. 7. *P. aeruginosa* adherence to D-borgTi and RI-borgTi

Titanium samples were polished, cleaned, and coated as previously described. Aliquots of 1 x 10^7 CFU of PAK WT were incubated with D-borgTi and RI-borgTi at room temperature for 1 hr with gentle agitation. Coupons were washed 6 times with sterile distilled water and were stained and visualized as described in section **2. 4**.

2. 8. Bacterial adhesion to PEG-D-borgSS and PEG-D-borgTi

The strain of *S. aureus* used in this study was obtained from the Department of Medical Microbiology and Immunology teaching culture collection. The *P. aeruginosa* strain used in this study was PAK R364 (Whitchurch *et al*., 1991a). The PAK R364 strain has a transposon insertion in the pilT gene (Beatson *et al*., 2002a). All bacterial strains were maintained as frozen stock cultures at -80 °C. Bacteria were recovered by culturing at 37°C on Luria-Bertani (LB) plates or LB plates supplemented with 50 mg/mL of tetracycline (Sigma) for PAK R364 in order to positively select for the transposon and stably maintain the mutation. Overnight lawn cultures of the bacteria derived from a single colony were scraped from LB plates and diluted in 3 mL PBS (pH 7.4). Bacterial cultures were applied to PEG-D-amino-dotted stainless steel and titanium coupons in 6-well (1 coupon per well) tissue culture plates (Corning) and incubated with 150 μL of bacteria in 3mL of PBS (pH 7.4). Following incubation at room temperature for 1 hour with gentle agitation coupons were washed 6 X with dH_2O to remove unattached bacteria and stained with 1 mM acridine orange for 3 min at room temperature. Coupons were rinsed 3 times with 3 mL dH_2O, allowed to air dry, and were examined by epi-fluorescence microscopy with blue excitation with a Lietz laborlux K microscope with a Neofluor 25X objective lens and equipped with a Cannon camera. Bacteria bound to the surface was determined by capturing 10 objective images (10 images/coupon).

2. 9. Peptide and pili dissociation/release studies

Grade 304 stainless steel 2B finish plates (20 gauge, 1 mm thick) were cleaned as described previously (Giltner *et al*., 2006) and assembled into a Schleicher and Schuell MinifoldTM System (Mandel Scientific). Biotinylated purified PAK pili or synthetic biotinylated PAK(128-144)ox peptide were added at a concentration of 10 μg/mL (50 μL per well in replicates of five) to the stainless steel manifold and incubated at room temperature for 1 hr with gentle agitation. The manifold was washed six times with 250 mL per well of phosphate buffered saline (PBS, pH 7.4). To test whether PAK pili or peptide could displace bound pili and peptide, varying concentrations of unbiotinylated PAK pili or PAK(128-144)ox peptide (0-1.0 μg/mL, 100 μL per well) were added and the manifold was incubated for 1 hr at room temperature with gentle agitation.

The manifold was washed six times with PBS and remaining bound biotinylated pili or peptide was assessed using streptavidin-horseradish peroxidase (HRP, Sigma) diluted 1:5000 in PBS. Following a 1 hr incubation at room temperature, the manifold was washed with PBS and substrate buffer (0.01 M sodium citrate, pH 4.2 containing 1mM 2,2'-Azino-bis-(3-ethylbenzthiazoline-6-sulfonic acid) diammonium salt (ABTS) (Sigma) and 0.03% (v/v) hydrogen peroxide) was added (125 mL per well). The manifold was incubated for 10 min at room temperature with gentle agitation. One hundred μL per well of the reaction solution were transferred to a 96-well flat bottom microtiter plate (Corning) and absorbance at 405 nm was determined using a FluoStar Optima plate reader.

2. 10. Pili binding studies

The effect of *P. aeruginosa* autoinducer-2 and ethanol exposure on binding of *P. aeruginosa* whole cells and purified pili was accomplished as previously described (Giltner *et al*., 2006). PAI-2 was chemically synthesized and purified by HPLC, purity and identity was confirmed by MALDI-ToF (generously provided by Dr. Dan Hassett, University of Cincinnati).

2. 11. Imaging biotinylated peptides on borg steel

Stainless steel coupons were polished and coated with biotinylated peptides as described. Presence of peptide on the surface was probed by immersing the coupons in Streptavidin conjugated with the fluorescent probe Cy3 (Sigma) diluted to 1:5000 in PBS and incubated at room temperature for one hour with mild agitation. Samples were washed 5x in PBS solution containing 0.5% (V/V) Tween 20. Following air drying samples were imaged using an Olympus CKX41 widefield microscope at 40x magnification with excitation and emission wavelengths of

550 nm and 570 nm respectively. Samples were stored in the dark overnight and re-imaged 24 hour later under the same conditions. Images were analyzed using Infinity software (Lumenera Corp).

2. 12. Electron work function

The electron work function (EWF) was measured using a scanning Kelvin probe (SKP, KP Techonology Ltd, UK) fitted with an Au tip with a 1mm diameter (Baikie, 1998). The probe was composed of three sub-systems controlled by a computer, including a digital oscillator, data acquisition, and sample translation. A three-axis microstep positioner allowed for precise position of the tip on the sample and controlled scanning steps of 0.4 μM per step. The oscillation frequency of the Kelvin probe was 173 Hz. Three separate areas of 0.5 mm by 0.5 mm were scanned on borg-K122SS to determine the electron activity, with a total of 100 reading per area scan. For all other samples an area of1 mm by 1 mm were scanned on each sample to determine the electron activity, with a total of 400 reading per area scan.

2. 13. Adhesive force

Adhesive force was measured using an atomic force microscope (AFM)(Hysitron, Minneapolis, USA) equipped with a silicon nitride tip with a spring constant of 0.06 N/m (Veeco, CA). The AFM was used in "contact" mode to slowly approach the tip until contact was made. The laser beam then measured the total amount of deflection of the cantilever that occurred when the tip was pulled away from the surface. Deflection reflected the adhesive force, which was quantitatively determined using the spring constant of the tip. For each experiment, between 15 and 50 adhesive force measurements were obtained per sample.

2. 14. Nanoindentation

Measurements were performed using a triboscope (Hysitron, Minneapolis, USA), a combination of a nanomechanical probe attachment and an AFM, equipped with a probe. The probe, a diamond pyramidal Vickers indenter, had a nominal radius of 150 nm with a force sensitivity of 100 nN and a displacement resolution of 0.2 nm. A force-depth curve was obtained during each nanoindentation and the total depth displacement of the tip into the surface of the sample was obtained from this curve. Nanoindentation tests were performed using forces ranging from 50 to 1000 μN, and a minimum of five force-depth curves were obtained for each force load.

For the PEG-D-borgSS, PEG-D-borgTi, and PED-D-borgAl surfaces the total depth displacement of the tip into the surface of the sample at the maximal load was used to calculate the hardness (H), using the built-in analysis software and the following formula: $H = P_{max}/A_r$ where H is the hardness in GPa, P_{max} is the maximal load applied to the sample in μN, and A_r is the residual indentation area calculated based on the geometry of the tip.

2. 15. Microindentation

Microhardness was measured using a microindenter probe (Fisher Technology Ltd, Winsor, CT) equipped with a diamond tip. A force-depth curve was obtained during each nanoindentation and the total depth displacement of the tip into the surface of the sample was obtained from this curve. Microindentation tests were performed using forces ranging from 10 to 100 mN, and a minimum of five force-depth curves were obtained for each force load.

2. 16. Friction

Friction was measured using a triboscope (Hysitron, Minneapolis, USA), a combination of a nanomechanical probe attachment and an AFM, equipped with a conical diamond tip with a radius of approximately 450 nm. Nanoscratch tests were performed under a constant load of 500 μN over a travel distance of 5 μm. Both the normal force and lateral force were recorded during the scratch test and the coefficient of friction plot over time was generated using the built-in analysis software. The coefficient of friction was calculated by dividing the normal force by the lateral force. Tests were performed in an unlubricated environment under ambient environmental conditions.

2. 17. Corrosion

Electrochemical tests were performed using a computerized scanning potentiostat (Model PC4-750, Gamry). A saturated calomel electrode (SCE) and a platinum (Pt) foil were used as the counter and reference electrodes for all corrosion experiments. The electrolyte solution used was 15mM NaCl solution (pH 7.4) and all experiments were performed at room temperature. All samples were equilibrated in 15 mM NaCl for 30 min prior to testing. At least three separate linear polarization corrosion tests were performed to measure the polarization resistance R_p, starting at 0.02V below the open circuit potential (OCP) and ending 0.02V above the OCP and using a scanning rate of 0.125 mV/s. A minimum of three Tafel plot corrosion tests were also performed. A scanning rate of 1 mV/s was used and scans began from 0.25V below the OCP and

ended 0.25V above the OCP. The corrosion rate and the polarization resistance were obtained using the Stern-Geary equation.

2. 17. 1. Corrosion using live *P. aeruginosa*

For corrosion using live bacteria, stainless steel samples encased in epoxy were incubated for one hour at room temperature in 15mM NaCl solution containing 1.0 x 10^7 CFU of PAK R364. Samples were rinsed 6 times with 15mM NaCl to remove excess bacteria before running polarization resistance and Tafel plot corrosion tests.

2. 18. Potentiostatic measurements

Samples were prepared as described for corrosion testing and were equilibrated for 30 minutes in 15mM NaCl prior to being exposed to a constant potential of +150 mV for 30 minutes. To test the effects of autoinducer, samples were incubated in 3.8μM PAI2 autoinducer or 0.095% ethanol in 15mM NaCl for 1 hour at room temperature with gentle agitation, rinsed 3x with 15mM NaCl, and exposed to a constant potential of +150 mV for 30 minutes. To test the effects of UV light, samples were equilibrated and then exposed to a constant potential of +500 mV for 1 hour. A 312 nm wavelength UV bulb was mounted above the sample to illuminate the sample and electrochemical setup. The light was turned on and allowed to warm up for 1 minute prior to all potentiostatic tests and remained on until the completion of the test.

2. 19 X-ray photoelectron spectroscopy

The measurements were performed on an AXIS-165 spectrometer (Kratos Analytical). The base pressure in the analytical chamber was lower than 3 x 10-8 Pa. Monochromatic Al Kα source ($h\nu$ = 1486.6 eV) was used at a power of 210 W. The analysis spot was 400 x 700 μm. The resolution of the instrument is 0.55 eV for Ag 3d and 0.70 eV for Au 4f peaks. Survey scans were collected for binding energy from 1100 eV to 0 with analyzer pass energy of 160 eV and a step of 0.35 eV. For the high-resolution spectra the pass-energy was 20 eV with a step between 0.1 and 0.15 eV. No charge neutralization was required. In order to increase the surface sensitivity the samples were tilted so that the angle between the sample surface and the analyzer was 30 degree. No sample etching was performed prior to analysis. Data analysis was done using Casa XPS software, version 2.3.13.

2. 20. Auger-SEM

SEM and Auger data were collected with a field-emission Auger microprobe JAMP-9500F (JEOL). The primary electron beam energy was 10 kV, and the probing beam current was 7 nA. The lateral resolutions for SEM and AES are 3.0 and 8 nm, respectively. The sample was tilted 30 degree away from the primary beam toward the axis of the electron analyzer. The SEM images were used to locate positions for collecting the Auger energy spectra, line profiles, and images. Auto probe tracking was in effect during the imaging to eliminate the drifting due to instabilities in power, temperature, etc. The intensity in the image and line profile distributions was calculated as (P-B)/B to remove edge effects, P being the peak intensity and B being the background intensity. The images are presented in a thermal scale, the brighter area corresponding to the highest intensity.

2. 21. Trypsinization studies of borg-K122SS, D-borgSS, and RI-borgSS

Grade 304 stainless steel 2B finish plates (20 gauge, 1 mm thick) were cleaned as described previously (Giltner *et al*., 2006) and assembled into a Schleicher and Schuell MinifoldTM System (Mandel Scientific). Synthetic biotinylated PAK(128-144)ox peptide were added at a concentration of 10 μg/mL (50 μL per well in replicates of five) to the stainless steel manifold and incubated at room temperature for 1 hr with gentle agitation. The manifold was washed six times with 250 mL per well of phosphate buffered saline (PBS, pH 7.4). To test whether the peptide was sensitive to trypsin, 1 μg/mL of trypsin (100 μL per well, 5 wells) was added and the manifold was incubated for 1 hr at 37°C with gentle agitation. The manifold was washed six times with PBS and remaining bound peptide was assessed using streptavidin-horseradish peroxidase (HRP, Sigma) diluted 1:5000 in PBS. Following a 1 hr incubation at room temperature, the manifold was washed with PBS and substrate buffer (0.01 M sodium citrate, pH 4.2 containing 1mM 2,2'-Azino-bis-(3-ethylbenzthiazoline-6-sulfonic acid) diammonium salt (ABTS) (Sigma) and 0.03% (v/v) hydrogen peroxide) was added (125 mL per well). The manifold was incubated for 10 min at room temperature with gentle agitation. One hundred μL per well of the reaction solution were transferred to a 96-well flat bottom microtiter plate (Corning) and absorbance at 405 nm was determined using a FluoStar Optima plate reader.

To measure the EWF of the samples following trypsin treatment, steel coupons were polished, cleaned, and coated with K122-4(128-144)ox peptide as described previously and were in 1 μg/mL trypsin for forty-five minutes at 37°C. Samples were washed six times with distilled water and allowed to air dry before testing the EWF.

2. 22. Statistical analysis

Data were analyzed using the statistics program Prism 5.0 (GraphPad Sofware). All data was analyzed to determine if the data distribution was parametric or non-parametric in nature to select the most appropriate statistical test. A significance cut-off of at least 0.05 was employed for all tests.

Chapter 3

Twitching Motility: Evidence for Catch and Release of the T4P of *P. aeruginosa*

3. 1. Brief introduction

P. aeruginosa readily colonizes and forms biofilms on stainless steel surfaces and surface roughness has been shown to be an important factor in influencing colonization. Rough and uneven surfaces are colonized more readily than smooth, highly polished surfaces and *P. aeruginosa* will preferentially bind to rougher areas, such as scratches, on steel (Arnold *et al*., 2004; Characklis & James, 2009; Lomander *et al*., 2004; Vanhaecke *et al*., 1990). Rougher surfaces have a lower EWF and high electron surface activity was demonstrated to increase a surface's propensity for bacterial colonization and biofilm formation (Yu *et al*., 2007; Yu *et al*., 2008). Once bound, bacteria engage in twitching motility, characterized by cycles of pilus extension and retraction coupled with pilus releasing from the surface. Pilus release must be closely coordinated with pilus retraction to achieve efficient twitching motility on steel and other surfaces. The mechanism governing T4P release from steel surfaces is unknown.

3. 2. Results

3. 2. 1. Release or desorption of *P. aeruginosa* from stainless steel surfaces

In order to more closely examine the relationship between pilus retraction and release, two *P. aeruginosa* strains with non-functional ATPases involved with pilus retraction were compared with wild-type PAK in their ability to release from stainless steel. PAK R364 has a transposon insertion in the *pilT* gene whereas PAK S34 has an insertion in the *pilU* gene, resulting in a non-functional ATPase, PilT or PilU respectively, in these strains. The function of the PilT and PilU ATPases remains unknown but both are hypothesized to be involved in pilus retraction. All three strains bound to steel immediately following incubation (Time 0 min), with PAK R364 binding with an average of 100 bacteria/field of view (FOV)(**Fig. 3-1 C**) compared to 40 bacteria/FOV for PAK WT (**Fig. 3-1 A**) and 11 for PAK S34 (**Fig. 3-1 B**). PAK WT were observed to release or desorb rapidly from steel and little or no bacteria could be seen 15 minutes after the initial binding (**Fig. 3-1 A and 3-2**). Similarly, PAK S34 desorbed rapidly, with some bacteria being evident at 15 minutes and few to no bacteria being observed at 30 and 45 minutes post-colonization (**Fig. 3-1 B and 3-2**). In contrast, the retraction deficient PAK R364 mutant was unable to release or desorb from the surface and total amounts of PAK R364 bacteria bound to the surface remained stable and no significant differences between numbers of cells remaining bound at the 15, 30, and 45 minute time points was observed (**Fig. 3-1 C and 3-2**). Although the bacterial counts immediately following colonization at 0 minutes for PAK R364 are statistically higher than those observed for later time points, the increased numbers are likely due to residual

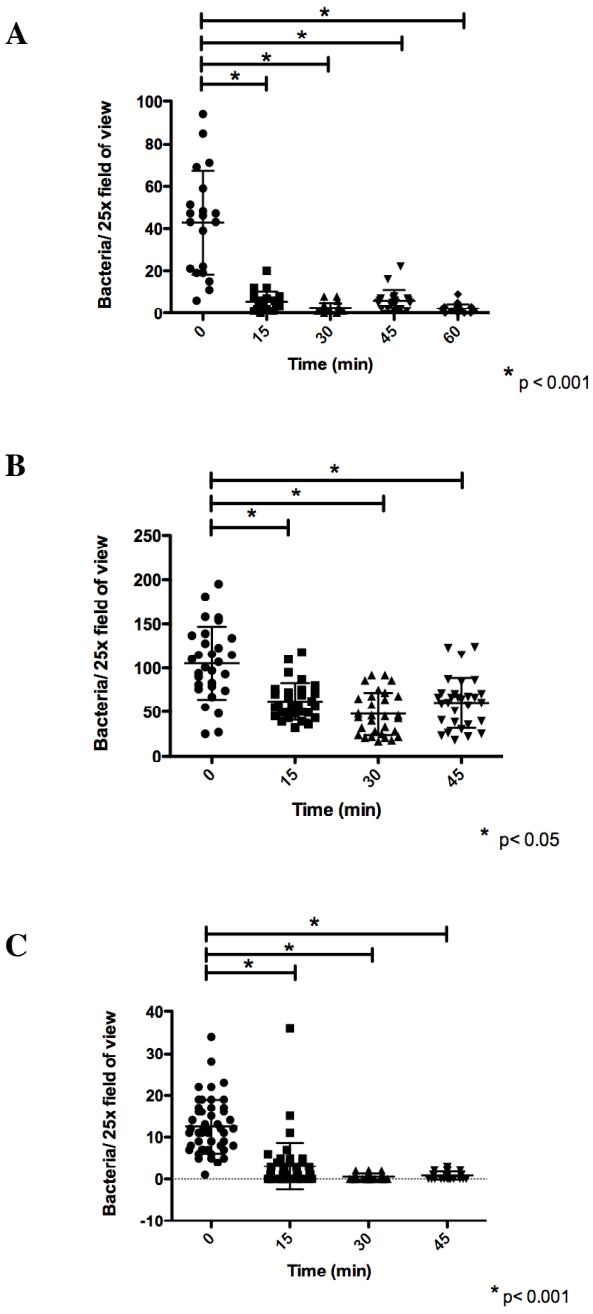

Figure. 3-1. Release of *P. aeruginosa* from stainless steel. Polished 304 stainless steel coupons colonized with 1 x 10^6 CFU with PAK WT (**A**), R364 (**B**), and S34 (**C**) were stained with acridine orange and viewed by epifluorescent microscopy. Bound bacteria were enumerated at time points of 0, 15, 30, and 45 minutes following an initial colonization time of one hour and results were expressed as total bacteria enumerated per 25x field of view. Twenty-five to fifty fields of view were counted per experiment.

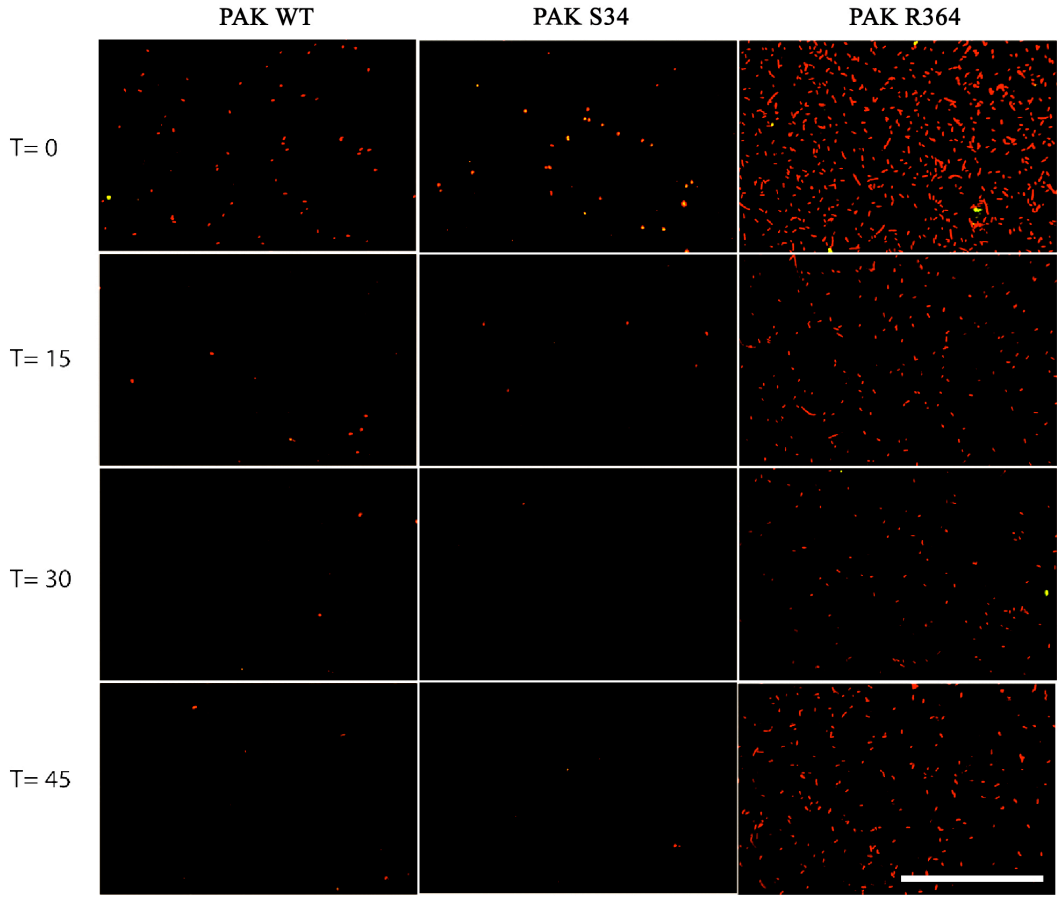

Figure 3-2. *P. aerugonisa* release from steel. Polished stainless steel coupons colonized with PAK WT, PAK-S34, and PAK-R364 were stained with acridine orange and viewed by epifluorescent microscopy using the 25x objective. Representative images at time points of 0, 15, 30, and 45 minutes following an initial colonization time of one hour are shown. Bacterial cells fluoresce orange and stainless steel fluoresces green due to non-specific background staining. The scale bar represents 100 μm.

unbound bacteria that were not completely removed by the washing step (essentially carryover of free bacteria not released by the initial wash) or represent the release of new daughter cells during the course of the experiment. The decreased bacterial numbers on the surface at later time points relative to the earlier time points do not appear to be the result of bacteria releasing from the steel over time as viable counts of PAK R364 in the wash buffer became undetectable after a limited series of washes.

3. 2. 2. Initial colonization of stainless steel surfaces by *P. aeruginosa*

Although equivalent amounts of PAK WT, PAK S34 and PAK R364 bacteria were added to the steel coupons, we noted that lower numbers of PAK WT and PAK S34 bacteria had colonized the steel after the one hour incubation relative to PAK R364. The colonization rate of all three bacterial strains was investigated during the first hour of steel colonization. Clean, polished steel coupons were incubated with bacteria for various times and bound bacteria were stained and enumerated at 15, 30, 45, and 60 minutes following addition of bacteria. PAK WT had the least amount of bound bacteria at 15 minutes, with little or none bound during the early phases but with numbers increasing and remaining stable at 30, 45, and 60 minutes (**Fig. 3-3 A and 3-4**). There was no significant difference between the 30, 45, and 60 minute time point. In some cases, however, more bacteria/FOV were enumerated from the 30 and 45 minute time points compared to the 60 minute time point, where bacteria/FOV numbers appear to cluster, suggesting that some dissociation is occurring even during the initial colonization step. The PAK S34 mutant had an average of 50 bacterial/FOV at 15 minutes incubation, and these numbers remained steady at 30 and 45 minutes, with no significant difference between 15, 30, and 45 minutes (**Fig. 3-3 C and 3-4**). A significant decrease in bacteria/FOV was observed at 60 minutes where numbers of bound bacteria dropped significantly, suggesting dissociation of bacteria from the steel. The PAK R364 mutant bound in high numbers on the steel and numbers remained steady at all time points, with maximal binding occurring at 30 minutes with approximately 750 bacteria/FOV (**Fig. 3- 3 B and 3-4**). Thus, binding assay results for strains PAK WT and PAK S34 bacteria likely reflect a dynamic situation where multiple binding/release events occur and where the relative ratio of binding to release is somewhat dependent upon the time of exposure to the stainless steel surface while the binding assay results for strain PAK R364 appear to reflect only binding events.

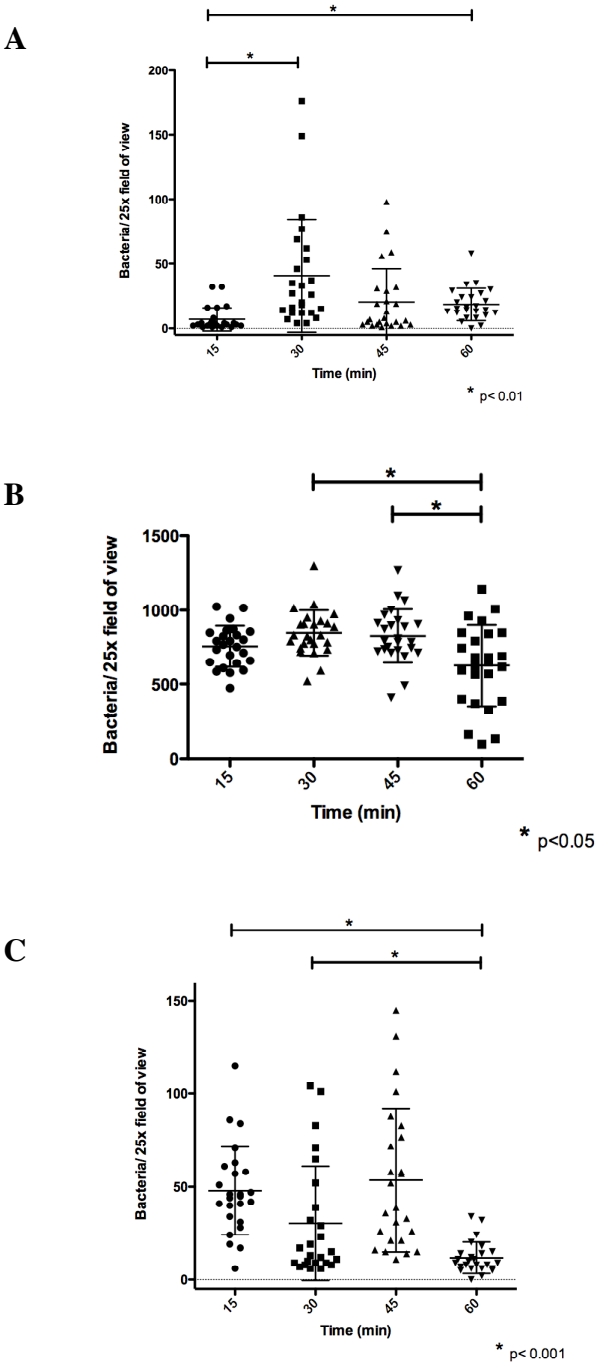

Figure 3-3. Early colonization of *P. aeruginosa* on stainless steel. Polished 304 stainless steel coupons colonized with 5 x 10^7 CFU of PAK WT (A), PAK R364 (B), and PAK S34 (C) were stained with acridine orange and viewed by epifluorescent microscopy. Bound bacteria were enumerated at time points of 15, 30, 45, and 60 minutes following addition of bacteria to the steel and results were expressed as total bacteria enumerated per 25x field of view. Twenty-five to fifty fields of view were counted per experiment.

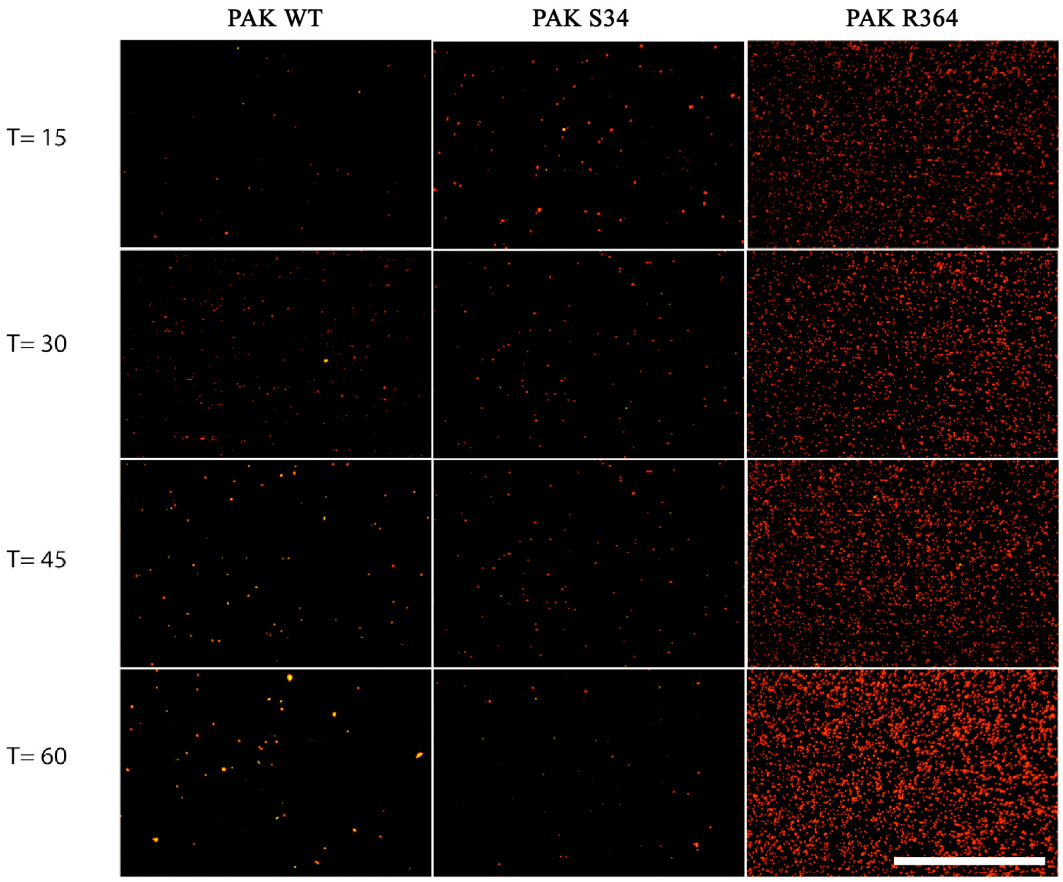

Figure 3-4. Early colonization of steel by *P. aeruginosa*. Polished stainless steel coupons colonized with PAK WT, S34, and R364 were stained with acridine orange and viewed by fluorescent microscopy using the 25x objective. Representative images at time points of 15, 30, 45, and 60 minutes following addition of bacteria to the steel are shown. Bacterial cells fluoresce orange. Stainless steel fluoresces green due to non-specific background staining. The scale bar represents 100 μm.

3. 2. 3. *P. aeruginosa* releases (desorbs) completely from steel surfaces

The mechanism of type IV pilus release from steel surfaces is unknown and several possibilities exist. The pilus, or a portion including the tip, may be severed off of the bacterial surface to elicit bacterial release. Replacement pilus components would then have to be generated during twitching motility for every binding/release event. Although a possibility, this would result in twitching motility becoming a much more energetically expensive process because, in addition to the ATP required for pilus extension and retraction, additional energy must be expended to replace the pilus components left behind during release from the surface. A more energetically favorable option is that binding of the pilus RBD to steel is a reversible interaction that is controlled by the bacterium. In this case, the pilus releases completely, leaving no pilus components behind, effectively leaving the surface "clean" and free for additional binding events to occur. Previous work demonstrated that the presence of bound purified PAK pili or the synthetic RBD peptide PAK(128-144)ox will inhibit *P. aeruginosa* whole cell binding to steel (Giltner *et al*., 2006). If full-length, partial length, or the tip of the pilus remains bound during bacterial desorption, then subsequent colonization of the surface by *P. aeruginosa* should be inhibited by the presence of the bound T4P. To test whether *P. aeruginosa* desorbs completely from steel surfaces, PAK WT were incubated with steel coupons for 1 hour to allow for multiple binding and desorption events. Unbound bacteria were removed with PBS washes and the surface was challenged with the release-deficient mutant PAK R364. As observed in the binding and release studies (**Fig. 3-1 A, 3-2, 3-3 A, and 3-4**), PAK WT bacteria began to release or desorb from the stainless steel surface within 30-45 minutes of initial exposure and binding events **(Fig. 3-3 A)**, even when excess unbound bacteria were present. After one hour of incubation, low amounts of PAK WT were bound to the surface (**Fig. 3-1A**) and incubation for an hour allowed for multiple bacterial binding and release. Following addition of PAK R364 cells and incubation for an hour, total amounts of PAK R364 bound to steel following WT adsorption and desorption was determined. There was no significant difference between the total number of bound PAK R364 on steel samples that had been previously exposed to PAK WT as compared to steel samples that were incubated only with PBS (**Fig. 3-5 A**). These results suggest that PAK WT may desorb completely from the stainless steel surface. Any portion of the T4P remaining bound on the steel following desorption would have resulted in a decrease in the total number of PAK R364 bacteria capable of adsorbing onto the steel due to binding inhibition by any remaining bound pili. *P. aeruginosa* adherence and release from steel surface appears to be a clean process that leaves no pilus components bound to the steel and leaves the steel surface unchanged.

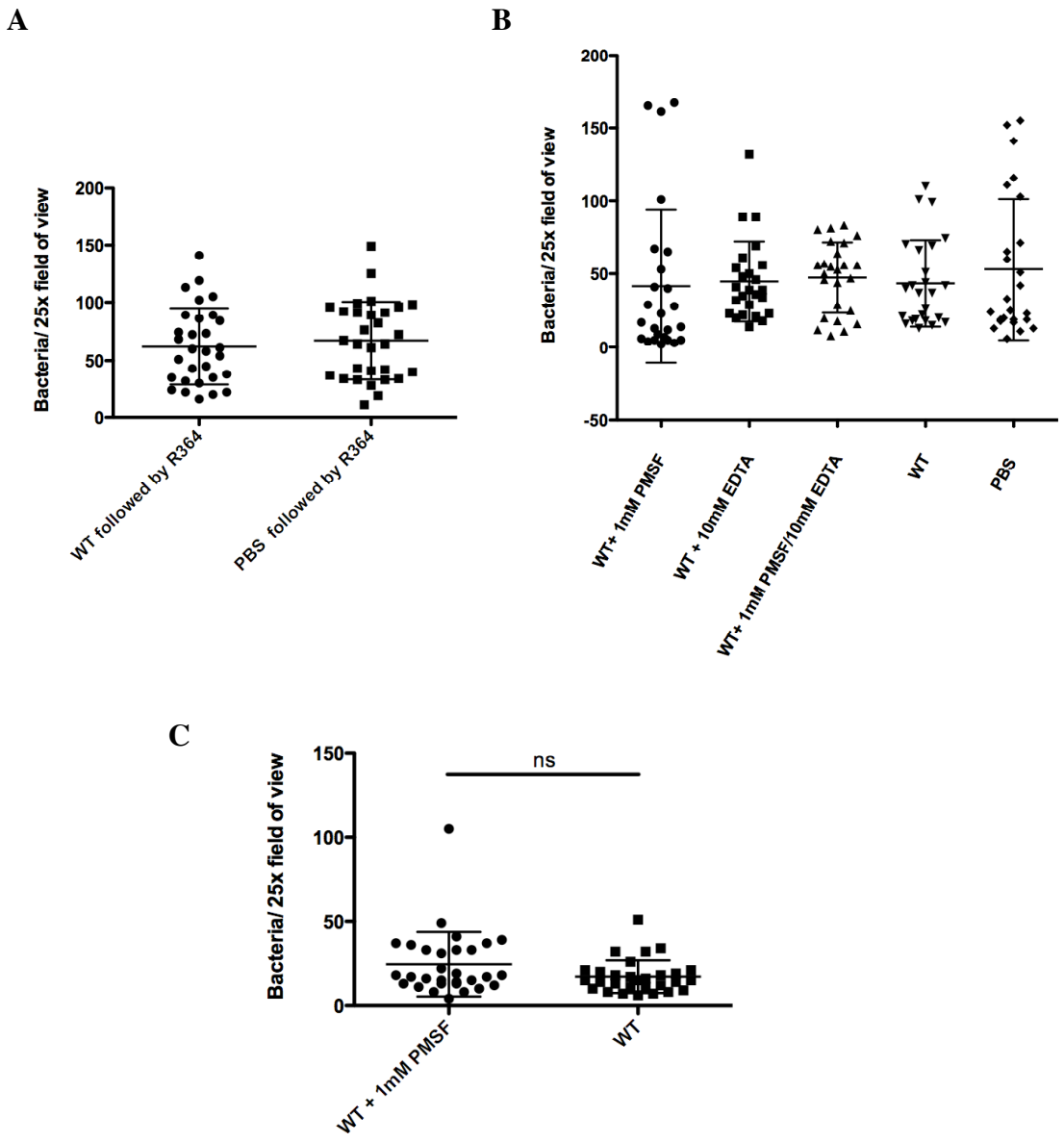

Figure 3-5 *P. aeruginosa* pilus releases completely and in a protease-independent manner from steel. A. Polished 304 stainless steel coupons colonized with 1 x 10^6 CFU with PAK WT (A) for one hour, washed, and challenged with 1 x 10^6 CFU of PAK-R364. **B.** PAK WT in the presence of protease inhibitors (1mM PMSF, 10mM EDTA, or both) were incubated with steel coupons for one hour and were then challenged with PAK-R364 for one hour. **C**. Steel coupons were incubated with 1 x 10^6 CFU PAK WT in the presence or absence of 1mM PMSF. All steel coupons were stained with acridine orange and viewed by epifluorescent microscopy. Bound bacteria were enumerated and results were expressed as total bacteria enumerated per 25x field of view. Thirty fields of view were counted per experiment.

3. 2. 4. T4P release is not mediated by proteases

To rule out the possibility that release from the steel was not due to cleavage and proteolysis of any pilus component remaining bound on the surface, and that *P. aeruginosa* did not rely on any proteases produced by the bacterium to mediate release, the PAK R364 mutant challenge experiments were repeated in the presence of serine and metallo-protease inhibitors. PAK WT bacteria were incubated with steel coupons in the presence of the serine protease inhibitor PMSF, the metal ion chelator EDTA for inhibition of metalloproteases, or a combination of both inhibitors. The steel surface was then challenged with the PAK R364 mutant and total bound bacteria were enumerated by direct counting. Equivalent numbers of PAK R364 bacteria bound to steel surfaces that were incubated with PAK WT bacteria in the presence of 1 mM PMSF compared to steel surfaces that were incubated with WT bacteria in the absence of inhibitors (**Fig. 3-5 B**). Similarly, the presence of 10 mM EDTA or a combination of PMSF and EDTA did not affect the ability of PAK R364mutant bacteria to bind as equivalent number of bacteria bound regardless of whether PAK WT bacteria were incubated in the presence or absence of protease inhibitors (**Fig. 3-5 B**). The presence of the protease inhibitors did not affect the adsorption of PAK WT on steel (**Fig. 3-5 C and D**). Therefore, our results suggest that release of the pilus from the surface and bacterial desorption are not protease-dependent. *P. aeruginosa* releases from or desorbs cleanly from the stainless steel and no pilus components are left bound to the surface upon bacterial release.

3. 2. 5. Release or desorption of the pilus from the surface is controlled by *P. aeruginosa*

P. aeruginosa bound pili may be released or displaced from the surface via an equilibrium process or exogenous ligands (such as unbound pili), resulting in a clean, complete release. Such a release would allow unbound bacteria to bind to the surface without inhibition. To test whether bound pili can easily be displaced from steel surfaces, 10 mg/mL of biotinylated purified PAK pili or 10 mg/mL of biotinylated synthetic PAK(128-144)ox peptide were coated onto clean naïve stainless steel plates. Unlabeled PAK pili or PAK(128-144)ox peptide were added at concentrations of 0.1-1.0 mg/mL and the plates were incubated for an hour. Unbound pili and peptide were removed with PBS washes and any biotinylated pili and peptide remaining bound to the surface was detected using streptavidin-HRP. Bound PAK(128-144)ox peptide could not be displaced by the addition of up to 1 mg/mL (0.5 μM of free peptide that has an $Ki_{apparent}$ 4 nM for inhibition of PAK pili and 0.2 nM for inhibition of peptide binding to steel (Giltner *et al*., 2006)) of exogenous PAK(128-144)ox peptide (**Fig. 3-6 A**).

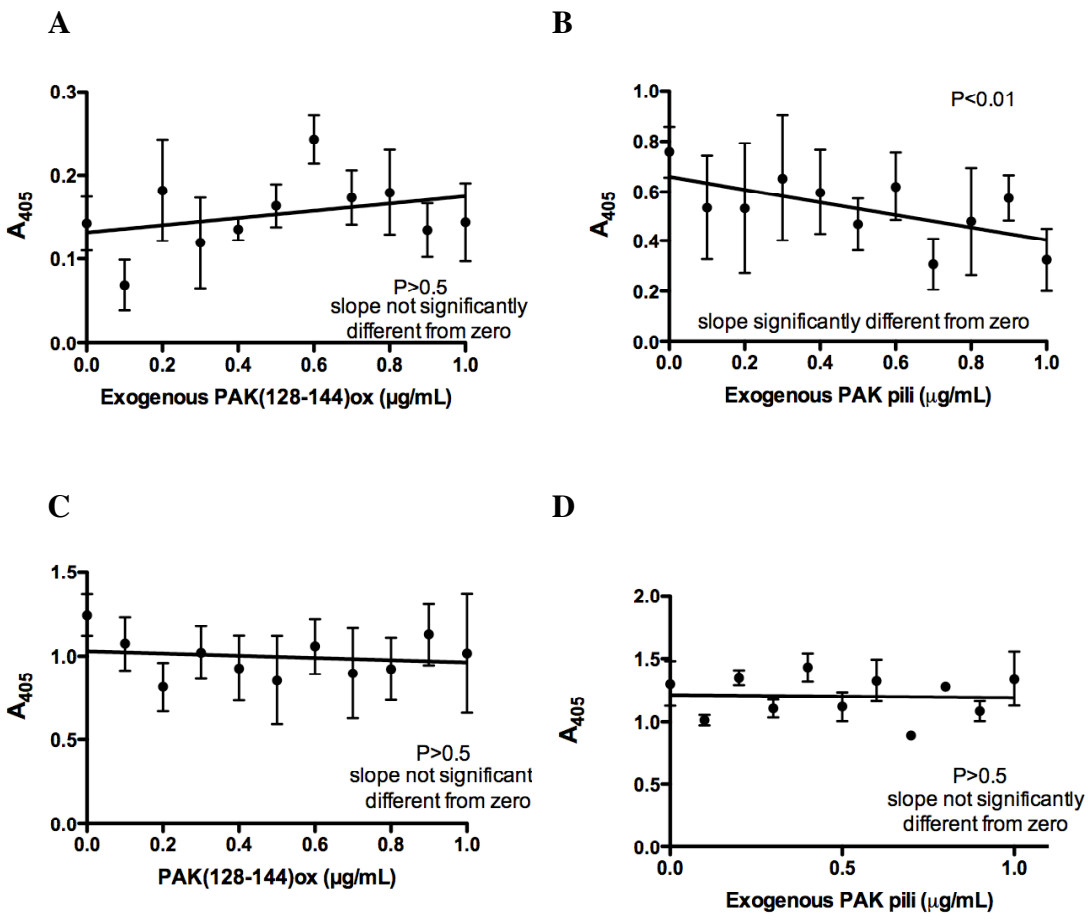

Figure 3-6 PAK pili and peptide cannot be displaced from steel surface by exogenous pili or PAK(128-144)ox peptide. Biotinylated and unlabeled PAK pili or synthetic PAK(128-144)ox peptide were resuspended in sterile water. **A and B**. Stainless steel plates were coated with 10µg/mL of biotinylated PAK(128-144)ox. 0-1µg/mL unlabeled PAK(128-144)ox (**A**) or purified PAK pili (**B**) were added and remaining bound peptide was detected. **C and D**. Stainless steel plates were coated with 10µg/mL of biotinylated PAK pili. 0-1µg/mL unlabeled PAK(128-144)ox (**C**) or PAK pili (**D**) were added and remaining bound pili was detected. Binding of biotinylated pili and peptide was quantified spectrophotometrically using streptavidin-HRP. The data are the means and standard deviations of five replicates per concentration. Experiments were repeated independently a minimum of three times and representative experiments are shown.

Given that pili display 3 binding domains at their tip (Yu *et al*., 2007), these results demonstrate that once the pilus has bound to the surface it will not desorb readily, even when exposed to vast excess amounts of exogenous unbound pili where only limited dissociation or displacement from the surface occurs suggestive of what is observed in chemical reactions where there is a large change in the initial concentrations of substrate or products that yields an equilibrium shift, but there is no evidence for a dynamic equilibrium in binding on a scale that allows for the rapid detachment required for functional twitching motility. These results suggest that release from the surface is a process that is functionally and actively (given that a deficient in an ATP dependent enzyme effectively inhibits pilus release) controlled by the bacteria.

3. 3. Conclusions

Substantial forces (50-100 pN) are generated on the surface during the retraction phase of twitching motility (Maier *et al*., 2002) and the interaction between the T4P and the surface must be able to withstand such mechanical forces without uncontrolled dissociation from the surface. Stability of the interaction is also important, as the pilus must remain bound to the surface long enough for the pilus to retract significantly before it releases. However, in order for efficient twitching motility to occur, the T4P *P. aeruginosa* must rapidly bind and release from the surface. The strong binding and high affinity of the RBD for stainless steel, as exemplified by a $Ki_{apparent}$ of 0.2 nM (Giltner *et al*., 2006; Stanley, 1983), allows it to withstand the retractional force but it remains unclear how the RBD then releases from the surface. The results in this chapter, combined with earlier observations that the strength of the RBD-steel interaction cannot not be explained by typical receptor-ligand interactions, led us to further investigate the nature of the RBD-steel interaction in order to understand the mechanism used by the RBD to bind to stainless steel with such high affinity.

Chapter 4

Description and characterization of a novel peptide-steel bond: using the receptor binding domain of *P. aeruginosa* to generate a new bio-organic steel

A portion of this chapter was published in *Biomaterials*

Davis, E. M., Li, D. Y. & Irvin, R. T. (2011). A peptide-stainless steel reaction that yields a new bioorganic-metal state of matter. *Biomaterials* **32**:5311-5319.

4. 1. Brief introduction

To elucidate the nature of the interaction between stainless steel and the RBD of the T4P of *P. aeruginosa*, the K122-4(128-144)ox synthetic peptide of the RBD (**Table 1**) was reacted with stainless steel surfaces to create a new bio-organic steel surface. This new material was termed borg-K122SS and was examined changes in the mechanical, chemical, and physical properties of its surface resulting from the K122-4 peptide binding to the metal. We hypothesized that the strength of the peptide-steel interaction, which could not be explained by typical receptor-ligand interactions, was derived from the RBD forming a novel organo-metallic state of matter by directly interacting with the surface electrons of stainless steel and that these interactions would alter electrons surface reactivity of the metal surface and result in measurable changes in the surface properties of the stainless steel.

4. 2. Results

4. 2. 1. Characterization of the surface properties of RBD peptide bound to steel

The electron work function (EWF) is used to describe the activity of metal surface electrons by measuring the minimum amount of energy required to move an electron from the Fermi level to just beyond the surface of the metal. Gold is the standard from which all other EWFs are compared and possesses an EWF of 5.1 eVolts (Ashcroft & Mernim, 1976; Bhushan & ViGoldade, 2000). In metal surfaces, the middle of grains are of low reactivity and possess high EWF values to reflect the more stable and inert properties of the surface electrons whereas less stable, more reactive regions, such as grain boundaries, have lower EWFs because they possess more reactive surface electrons. Borg-K122SS had a significantly higher EWF compared to modified steel, with the presence of K122-4(128-144)ox peptide on the surface increasing the EWF from 4.5 to 5.0 eV **($P<0.001$)(Fig. 4-1 A)**. This increase in EWF suggested that binding of the peptide on the steel surface stabilized the steel surface electrons. Interestingly, adding the peptide to the surface of a second metal, aluminum, did not increase the EWF significantly compared to uncoated aluminum **(Fig. 4-1 B)**, suggesting that even when added or dried on the surface the peptide is unable to react with and stabilize the aluminum surface electrons in the same manner as on stainless steel surfaces. Given the complex structure of stainless steel, these results further suggest that the peptide-steel interaction occurs between the peptide and one or more specific components within the steel which are absent in the aluminum.

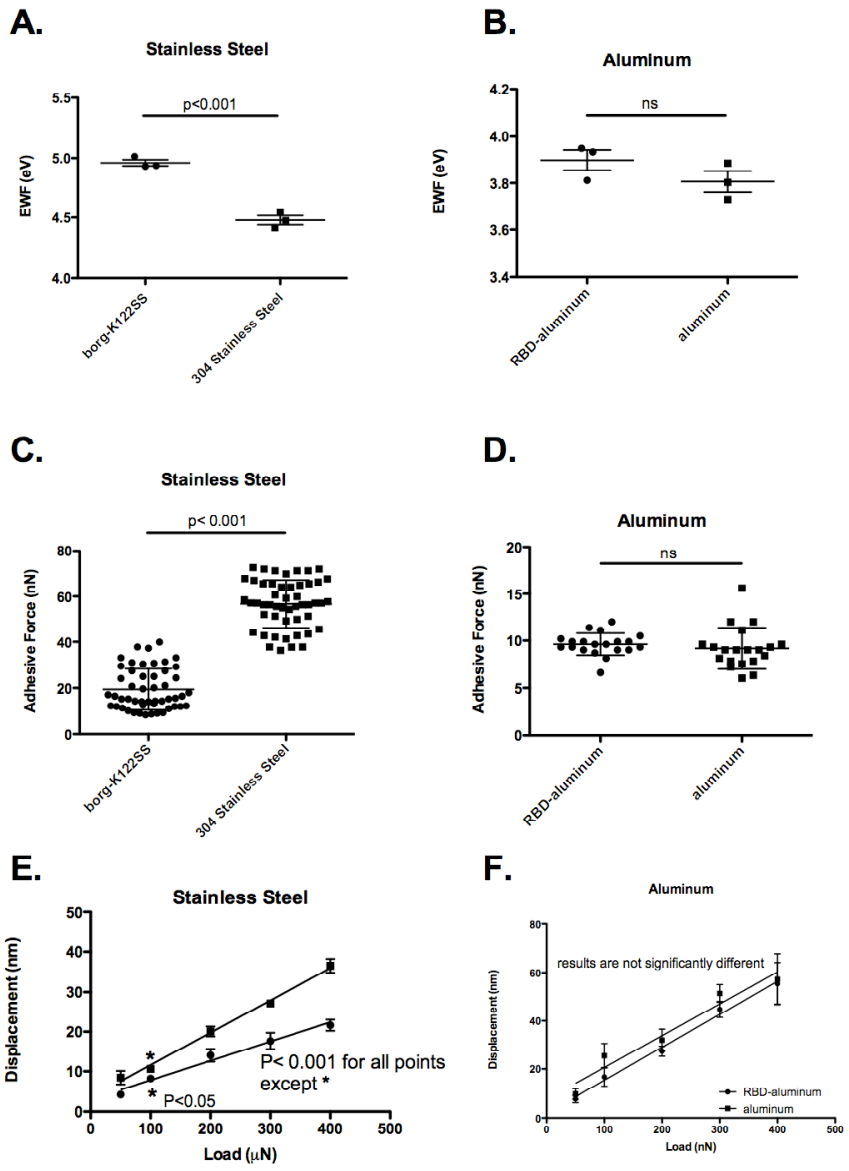

Figure 4-1. Changes in surface electron reactivity, adhesive force and hardness of borg-K122SS steel compared with 304 stainless steel and aluminum with and without K122-4 (128-144)ox peptide. A. Electron work function measurements of borg-K122SS and 304 steel performed using a Kelvin probe. Three areas (1μm x 1μm) were scanned. A total of 100 measurements were taken per area scanned and means were plotted. **B.** Electron work function measurements of aluminum with and without exposure to K122-4 (128-144)ox peptide. **C.** Adhesive force measurements on borg-K122SS and 304 stainless steel performed with an atomic force microscope (AFM) equipped with a non-conductive silicon nitride cantilever. Fifty force measurements were taken per sample. **D**. Adhesive force measurements on aluminum with and without exposure to K122-4 (128-144)ox peptide. **E.** Nanoindentation measurements of borg-K122SS and 304 steel. Five displacement measurements were taken per load. F.) Nanoindentation measurements of aluminum with and without exposure to K122-4 (128-144)ox peptide.

We subsequently tested the adhesive force, another important physical property of metal surfaces. The adhesive force describes the ability of the electrons of a metal surface to "stick to" and interact with other surfaces and is often measured as the amount of force required to break the interaction between the tip of an AFM silicon nitride cantilever and surface electrons **(Fig. 4-2 A)**(Chawick & Smith, 1979; McLean, 1957). Surfaces with reactive surface electrons interact more readily with the tip and a greater force is necessary to break the interaction. The adhesive force is increased at grain boundaries and corresponds to areas where surface electrons are more reactive and the EWF is decreased (Li & Li, 2005). The RBD was shown to bind with higher adhesive force to grain boundaries compared to regions within grains (Yu *et al*., 2008). Borg-K122SS had a lower adhesive force compared to untreated stainless steel **(P< 0.001) (Fig. 4-2 B, C)(Fig. 4-1 C)**, with borg-K122SS possessing an observed adhesive force of 19.4±8.8 nanoNewtons (nN) compared to 56.7±10.5 nN for untreated 304 steel. Given that the AFM silicon nitride tip did not interact as strongly with borg-K122SS, these results suggest that the surface of borg-K122SS is less reactive than 304 stainless steel and that the surface electrons of borg-K122SS interact less strongly with the AFM tip. There was no significant difference in adhesive force when unaltered aluminum was compared to aluminum with peptide dried on the surface **(Fig. 4-1 D)**.

Finally, we tested hardness, another important surface property. To compare the relative hardness of borg-K122SS to 304 steel at the nanoscale, an AFM equipped with a triboscope was used to obtain nanoindentation load-displacement plots. Different loads, ranging from 50 to 400 μN, were applied to the surfaces of borg-K122SS and 304 steel using a diamond indenter tip and the total displacement of the tip into the surface was measured **(Fig. 4-3 A, B)**. At all applied loads, a greater relative displacement was observed for 304 steel compared to borg-K122SS **(Fig. 4-1 E)**. Even at the highest load of 400 μN, total displacement into borg-K122SS was 20 nm compared to 35 nm for 304 steel **(P<0.0001)**. No marked difference in displacement was observed between aluminum with applied peptide and untreated aluminum **(Fig. 4-1 F)**, further suggesting that the peptide interacts with specific components in steel and that, in the presence of bound peptide, a harder material is created as a result of changes in the physical and mechanical properties of the steel when it interacts with the organic peptide.

A

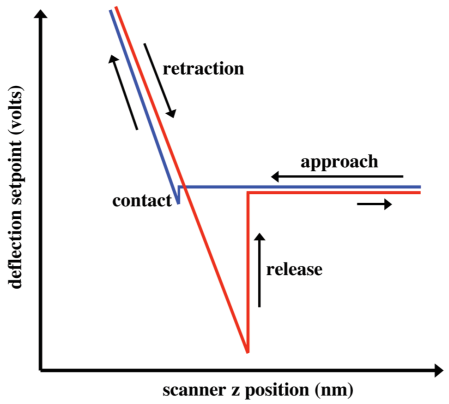

B

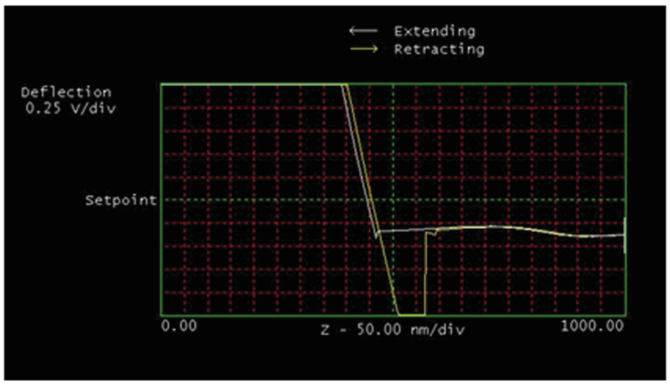

C

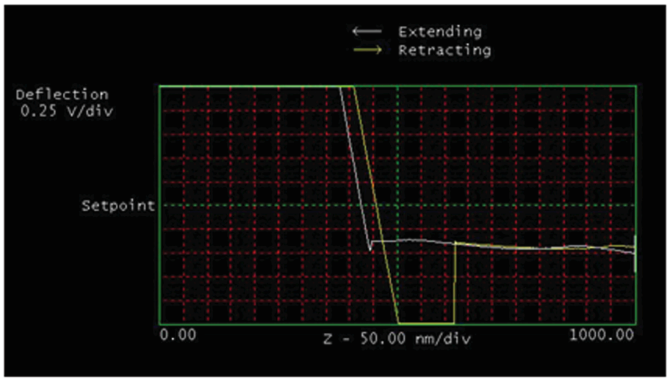

Figure 4-2. Adhesive force measurements. A. Schematic of a curve of deflection versus displacement (Z) of the cantilever approaching, contacting, and releasing from a surface during adhesive force measurement. Typical cantilever deflection plot for calculating adhesive force for **B)** borg-K122SS and **C)** 304 stainless steel.

A

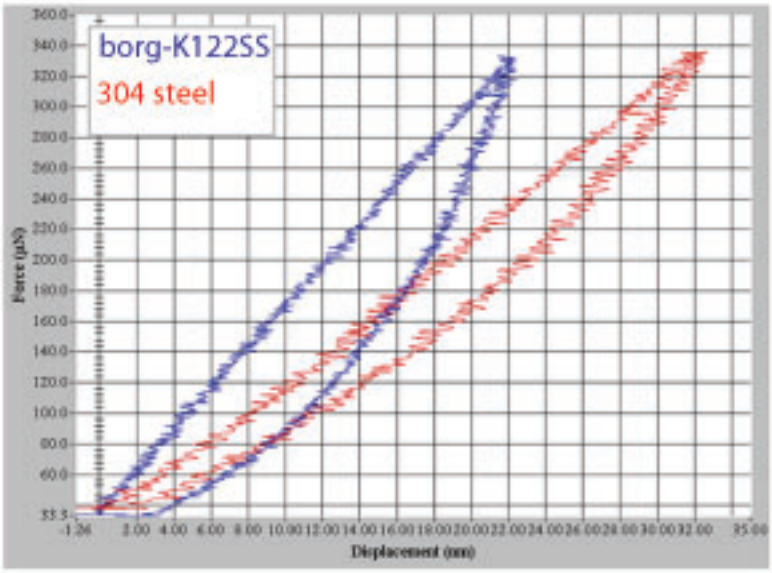

B

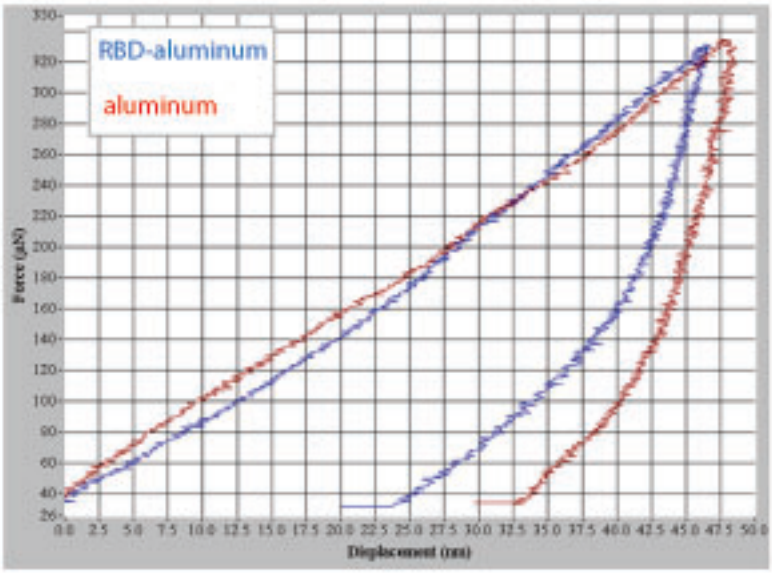

Figure 4-3. Force-displacement plots and high load nanoindentation of borg-PAKSS. Nanoindentation force-displacement plots of **A.** borg-K122SS 304 stainless steel and **B.** RBD-aluminum and uncoated aluminum using a 300 μN load.

4. 2. 2. X-ray photoelectron spectroscopy analysis of borg-K122SS

The changes in the materials properties of the steel suggested that there was a chemical interaction of the peptide with the steel surface and that the peptide was not simply binding to the surface of the steel. We had previously confirmed that the peptide was not simply bound to the surface, could not be displaced by exogenous peptide, and that the bound peptide was not in dynamic equilibrium (**Fig. 3-6**). We hypothesized that the peptide was chemically reacting with the surface electrons of steel to alter the properties of the steel surface by forming a novel form of chemical interaction. Such an interaction that generates a new material would result in changes in the electronic state of the surface, with measurable changes in the electron orbitals of the metal. To further characterize the chemical properties of borg-K122SS, as well as to determine whether a novel state of matter was created and to identify which elements were involved in the interaction, X-ray photoelectron spectroscopy (XPS) analysis was used to examine the electronic state of the elements on the surface of borg-K122SS in comparison to 304 steel. Spectra analysis revealed that the iron and chromium 2p 1/2 and 3/2 orbitals **(Fig. 4-4 A and B)** did not appear to play an important role in bond formation and electron stabilization as no shifts were observed in the borg-K122SS spectra when compared to 304 steel. Similarly, no significant changes were observed in the spectra of the nitrogen 1S orbital and the carbon 1S orbital (**Fig. 4-4 C and D**). An increase in the peak of the oxygen 1S orbital of borg-K122SS was observed compared to 304 steel (**Fig 4-5 A**), with the borg-K122SS O1S peak peaking at 50 counts per second (CPS) compared to 40 CPS for 304 steel, suggesting a role for oxygen in bond formation. 304 steel contains negligible amounts of sulfur and no classical sulfur electron orbitals were detected by XPS (**Fig. 4-5 B**). However, the peptide contains two sulfur atoms within the disulfide loop that would be visible by XPS. A significant peak was observed near the location of unbonded sulfur 1S orbital (**Fig. 4-5 B**) for borg-K122SS. This peak did not match any known shifts in sulfur peaks and could not be positively identified as sulfur based on XPS data alone. However, since sulfur must be present and was not identified anywhere else, this peak strongly suggests involvement of sulfur in this novel bonding event which has not been previously described. Electrons can flow through disulfide bonds, making it feasible that the disulfide bond could interact with and stabilize surface electrons by chemically binding with them. Further examination of the XPS spectra revealed the presence of a strong peak near the location of the iron 3S orbital (**Fig. 4-5 C**) in borg-K122SS that was absent from the spectra of 304 stainless steel. The differences between the electronic states of oxygen, iron, and sulfur on the surface of borg-K122SS and 304 steel confirm that borg-K122SS is a novel material that is chemically

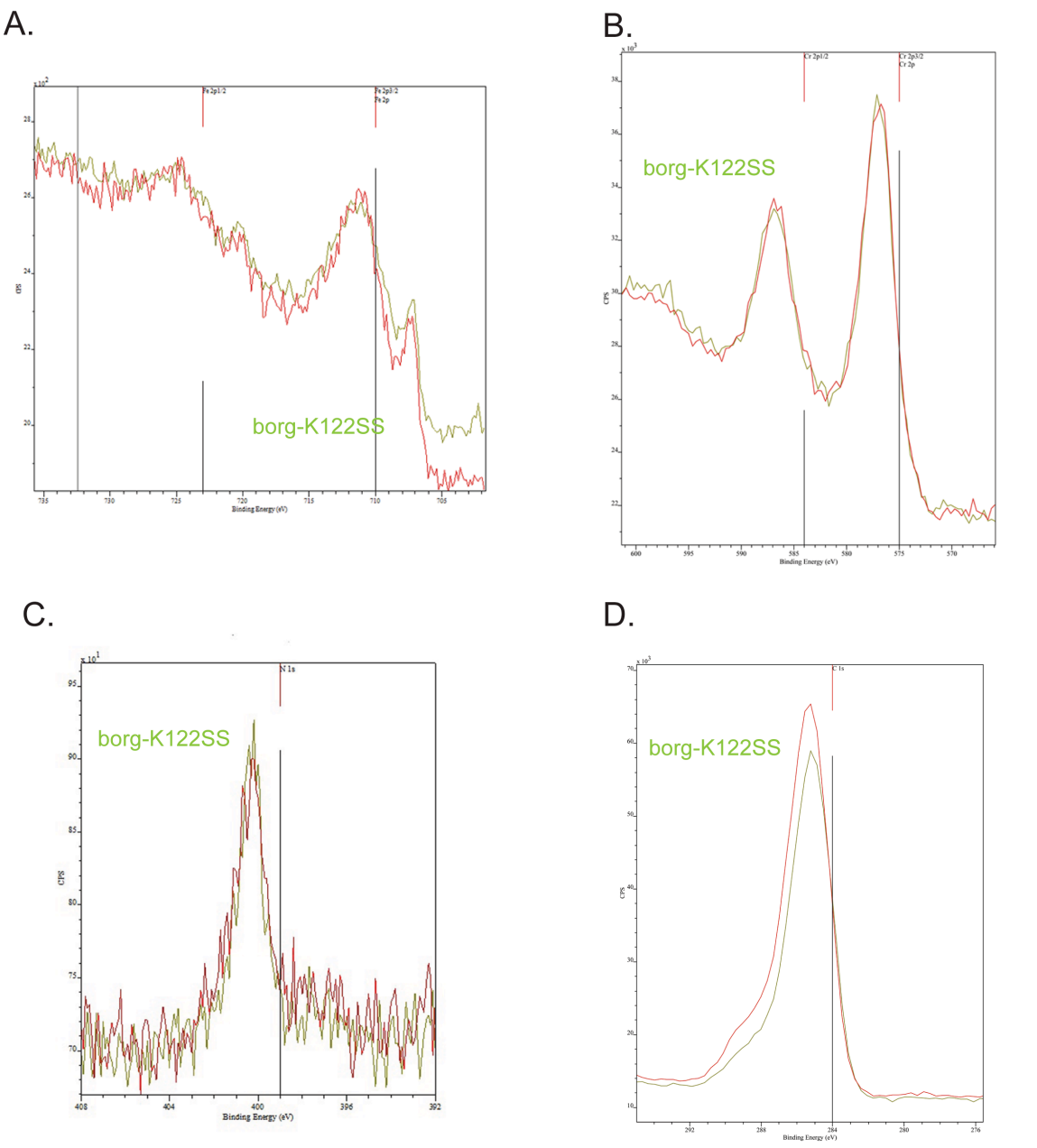

Figure 4-4. Analysis of XPS spectra of the elemental composition of borg-K122SS and 304 stainless steel. Overlays of borg-K122SS and 304 steel XPS spectra of **A)** complete scan, **B)** chromium 2p orbital region, **C)** nitrogen 1S orbital region, and **D)** carbon 1s orbital region. XPS spectra of borg-K122SS is plotted in green while the XPS spectra of 304 stainless steel is plotted in red.

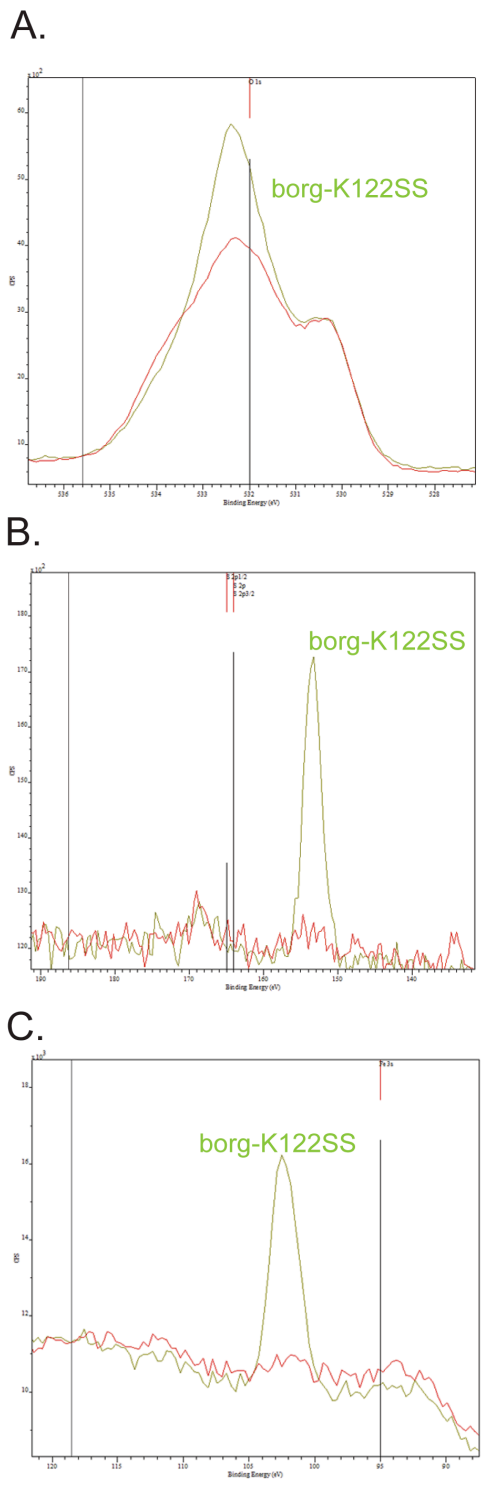

Figure 4-5. XPS spectra analysis of elemental composition of borg-K122SS and 304 stainless steel. Overlays of borg-K122SS and 304 steel XPS spectra of **A)** O 1s orbitals, **B)** sulfur 1S orbital region with an unidentified peak associated with the borg-K122SS surface, and **C)** iron 3s orbital region with an unidentified peak associated with the borg-K122SS surface. The XPS spectra of borg-K122SS is plotted in green while the XPS spectra of 304 stainless steel is plotted in red.

different from 304 steel. The XPS spectra data support the involvement of several elements in the formation of borg-K122SS.

4. 2. 3. Auger scanning electron microscopy of borg-K122SS

To supplement the XPS data, Auger scanning electron microscopy (SEM) scans of the surface of borg-K122SS were independently performed to look at the surface distribution of the elements nitrogen, oxygen, sulfur and carbon by determining the number and source of origin of back scattered secondary electrons of the appropriate energy levels for the specific elements on the borg-K122SS surface. Carbon, and oxygen were distributed across the surface in a mostly homogenous pattern, with a few areas of higher element concentration. Given the high concentration of carbon and oxygen in stainless steel, the lack of any specific distribution pattern was anticipated and no nanostructural pattern of distribution was observed for either carbon or oxygen (**Fig 4-6 A and B**). Nitrogen and sulfur (which are not normally components of steel surfaces and the presence of these elements is due to presence of the peptide) were clearly seen to be distributed across the surface in discrete nanostructures (see arrowheads in **Fig. 4-6 C and D**) which suggests that the peptide-steel interface was in fact imaged. These nanostructures were not discernable in a standard SEM surface scan and one would not anticipate imaging the peptide given that this was an uncoated specimen and that the accelerating potential used was 10.0 KeV (**Fig. 4-6 E**). The auger-SEM energy spectra of the back scattered electrons indicated the presence of low amounts of sulfur on the surface (**Fig. 4-6 F**). These results suggest that at least one of the unidentified electron orbitals observed in the XPS spectra of borg-K122SS is likely a far red shifted-sulfur electron orbital, perhaps suggesting a conjugated electron. It is likely that electrons are delocalized throughout the disulfide loop of the peptide and shared through multiple contact points with the steel surface. This hypothesis is supported by the observation that trypsin treatment of borg-K122SS releases the peptide from the steel surface (the RBD has two lysine residues, see **Table 1**) with a resulting change in the surface EWF (**Fig. 4-7 A and B**). It is worth noting that a formed disulfide bridge has previously been noted as a requirement for RBD functionality (Wong *et al*., 1995).

4. 3. Conclusions

The high strength of the RBD-stainless steel interaction, which anchors the pilus to the surface and enables the progressive movement of the cell along that surface when the pilus retracts, appears reasonable given the formation of a novel chemical interaction with the surface. The extremely high apparent affinity of the RBD for the steel surface is also reasonable given that

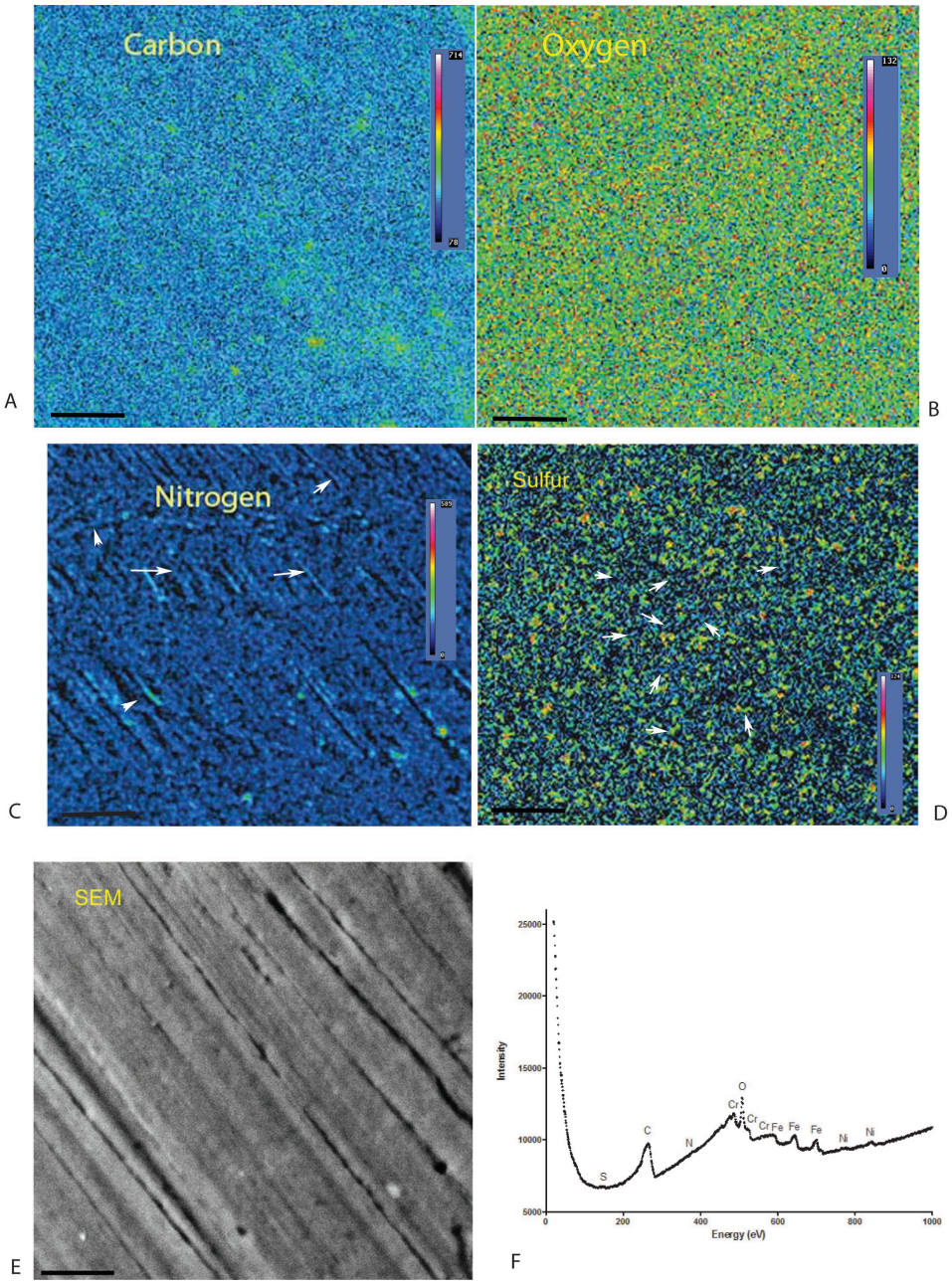

Figure 4-6. Auger SEM scan of distribution of elements on the surface of borg-K122SS. Elemental scan of **A)** carbon, **B)** oxygen, **C)** nitrogen, note the presence of nanostructed material (see arrowheads) and **D)** sulfur, note the presence of nanostructured material (see arrowheads). **E.** Topographical scan of the surface of borg-K122SS. **F.** Analysis of the backscattered electrons obtained from the borg-K122SS surface plotted as the frequency of electrons at a given energy (in eV) and labeled as to the element generating electrons of that energy value. Note the S and N peaks (originating solely from the peptide) are low but the energies of the backscattered electrons are observed at previously reported energy levels for these elements. Scale bar is 1 μm.

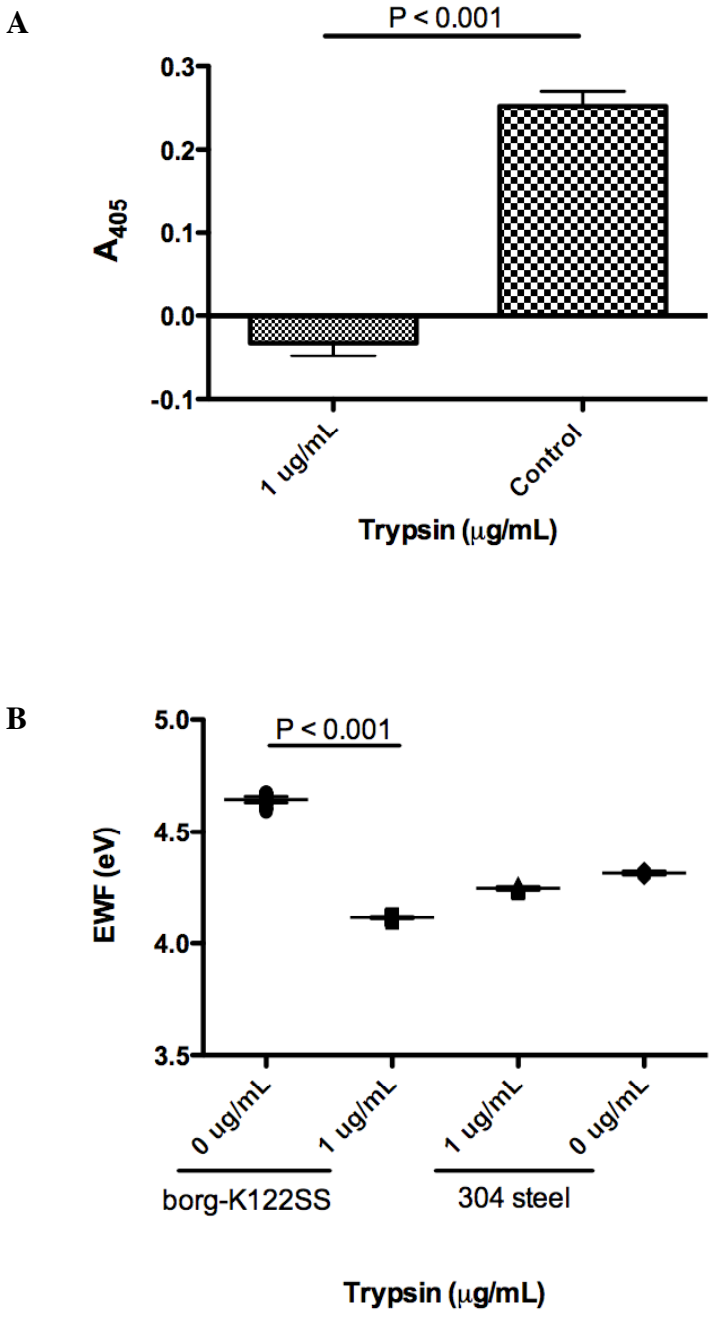

Figure 4-7. Borg-K122SS is sensitive to trypsinization. **A.** Tryspin sensitivity of biotinylated K122-4(128-144)ox peptide on the surface of 304 stainless steel. **B.** Trypsin sensitivity of borg-K122SS as determined by measuring the EWF.

a novel state of matter is formed. The observation that the strength of the RBD-steel interaction varies as a function of the surface electron activity of stainless steel (Yu *et al*., 2010) suggests that the novel state of matter formed with the RBD requires surface electrons that can be delocalized through the peptide. The PA RBD has been demonstrated to interact with a wide range of surfaces and metals including titanium (aluminum being an interesting case where the RBD does not appear to interact with the metal) suggesting that the nature of the surface electrons may be more important for binding than the elemental or material composition.

In summary, we have characterized a novel material, which we have termed borg-K122SS, which is readily and spontaneously formed from stainless steel with exposure to a synthetic peptide that is the functional adhesin of the T4P. Borg-K122SS has significantly different physical and chemical properties compared with regular 304 stainless steel. Borg-K122SS had a higher EWF and was less adhesive than unmodified 304 steel. Borg-K122SS surfaces were significantly harder and corroded significantly more slowly than the parental 304 steel. XPS spectra data of borg-K122SS suggests that multiple contact points exist between the peptide and the steel, with two currently unassigned electron orbitals (one likely due to a far red-shifted sulfur electron binding energy) which supports the formation of novel chemical interaction, possibly with extensive electron de-localization, that results in chemical and physical stabilization of the surface. The observation that the RBD reacts with stainless steel to form a previously unreported material that has novel physical/chemical attributes has significant implications for the facile design, modification and engineering of a common, widely used industrial material based on a "natural process" and our understanding of twitching motility and T4P structure and function.

Chapter 5

The *Pseudomonas aeruginosa* Type IV Pilus is a High Current Conducting Nanowire Which Can Function as a Variable Resistance Sensor

A version of this chapter was prepared as a manuscript and submitted to *PLOS One* for publication.

Davis, EM., Giltner, CL, van Schaik, EJ., Panmanee, W., Hassett., DJ., Li, DY., and RT Irvin

5. 1. Brief Introduction

The *P. aeruginosa* RBD interacts with 304 stainless steel to form a novel organo-metallic state of matter with reactive steel surface electrons, resulting in the formation of a new material with differing physicochemical surface properties compared to unaltered steel (Chapter 4) (Davis *et al*., 2011). In essence, the RBD is forming an electrical connection through the sharing of electrons between the peptide and the steel surface. Given the structural similarities between the T4P of *P. aeruginosa* and the conductive T4P of *G. sulfurreduscens* and *S. oneidensis* (**Fig. 1-8**), it was hypothesized that purified full-length T4P could function as external nanowires and conduct electrons to and from the bacterial surface. Conductivity of other T4P was demonstrated using conductive AFM although Reguera *et al*. (Reguera *et al*., 2005) were unable to demonstrate electrical conductivity of *P. aeruginosa* T4P. However, it is possible that the C-terminal globular domains of the T4P act as an insulating outer layer, thus preventing the use of conductive AFM to measure conductivity. Conductivity is measured by applying a voltage across the surface pilus to measure current flow and an insulating layer could account for the lack of conductivity of *P. aeruginosa* T4P. To circumvent the possibility of an insulated pilus, alternate physical methods were used to measure surface electron reactivity and pilus conductivity. If the T4P were functioning as a nanowire, then bound T4P should facilitate the removal of electrons from metal surfaces and, as a result, would alter some of the physicochemical surface properties of the surface and result in measurable changes in these properties. 304 stainless steel surfaces were reacted with synthetic RBD peptide PAK(128-144)ox of *P. aeruginosa* strain PAK, purified pili fibers obtained from PAK, and a monomeric form of pilin derived from strain PAK. The monomeric pilin is a truncated version of the PilA protein where amino acid residues 1-28 have been deleted (Audette & Hazes, 2007). The monomers can with exposure to hydrophobic compounds self-assemble in a multi-start helical manner to generate hollow nanotubes. The nanotubes are longer than classical full-length T4P but differ substantially from native pili.

5. 2. Results

5. 2. 1. Physical properties of steel modified with RBD, T4P, and pilin monomer

First, the activity of 304 stainless steel surface electrons in the presence of PAK(128-144)ox peptide, monomeric pilin, full-length T4P from PAK, and unaltered steel was determined using a Kelvin probe. As demonstrated previously with the K122-4(128-144)ox peptide, 304 stainless steel also reacted with the PAK(128-144)ox peptide to form a more stable, less reactive surface, termed borg-PAKSS. Borg-PAKSS possesses a significantly higher EWF of 4.97 eV compared to 4.11 eV for unaltered steel (**P<0.001**)(**Fig. 5-1 A**), indicating that the presence of the

PAK peptide bound on the steel surface stabilizes surface electrons. When full-length purified T4P was reacted with steel, the EWF decreased significantly, from 4.66 eV for unaltered steel compared to 4.02 eV when T4P were bound to the surface (**P<0.001**)(**Fig. 5-1 B**), indicating that bound T4P on the surface facilitates surface electron removal. Reacting a monomeric pilin with 304 stainless steel yielded a surface that was slightly but significantly (**P<0.001**) more reactive compared to unaltered steel, with the presence of PAK pilin monomer creating a surface with a EWF of 4.18 eV compared to 4.21 eV. This slight decrease in EWF suggests that despite the truncation PAK monomeric pilin can facilitate electron removal from stainless steel, but to a much lesser extent than native PAK pilin assembled into a pilus fiber. The decrease in electron conductivity by the monomeric pilin suggests that the quaternary structure of the pilus fiber, which is lacking for the monomer, significantly enhances electron release from the surface.

5. 2. 2. Electrochemical behavior of modified stainless steel

Electrochemical testing was employed to assess the bulk reactivity of stainless steel in the presence of bound PAK RBD peptide and full-length T4P. The corrosion rate of stainless steel samples that were untreated or had been modified with PAK RBD or T4P was determined by a classical corrosion test. Areas of higher electron activity (where the EWF is low), such as grain boundaries, are more susceptible to corrosion. Borg-PAKSS had a significantly lower corrosion rate (**P<0.01**) compared to unaltered steel, with a corrosion rate of $58.9e^{-3}$ ± $29.5e^{-3}$ mpy compared to a rate of $184.8e^{-3}$ ± $9.3e^{-3}$ mpy for unaltered steel (**Fig. 5-2 A**). These results mirror those for borg-K1224SS, where the presence of the RBD decreased the corrosion rate by over 40% (Davis *et al*., 2011) and strongly suggest that, in accordance with the EWF (**Fig. 5-1 A**), the presence of the RBD on the steel surface stabilizes surface electrons and acts as an insulator. Stainless steel reacted with T4P corroded at a rate of $174.2e^{-3}$ ± $104.7e^{-3}$ mpy whereas the unaltered stainless sample corroded at a significantly slower rate of $52.0e^{-3}$ ± $27.1e^{-3}$ mpy (**P<0.05**)(**Fig. 5-2 B**), further suggesting that the presence of the intact pilus facilitates electron removal from the surface resulting in a 320% increase in the corrosion rate of the stainless steel.

5. 2. 3. Surface-bound *P. aeruginosa* enhances corrosion of steel

The EWF (**Fig. 5-1 B**) and corrosion data (**Fig. 5-2 B**) strongly suggest that electrons can flow up through the pilus. Additional corrosion testing was performed to confirm that current flow was not limited to purified T4P but could also occur in intact T4P anchored to the surface of

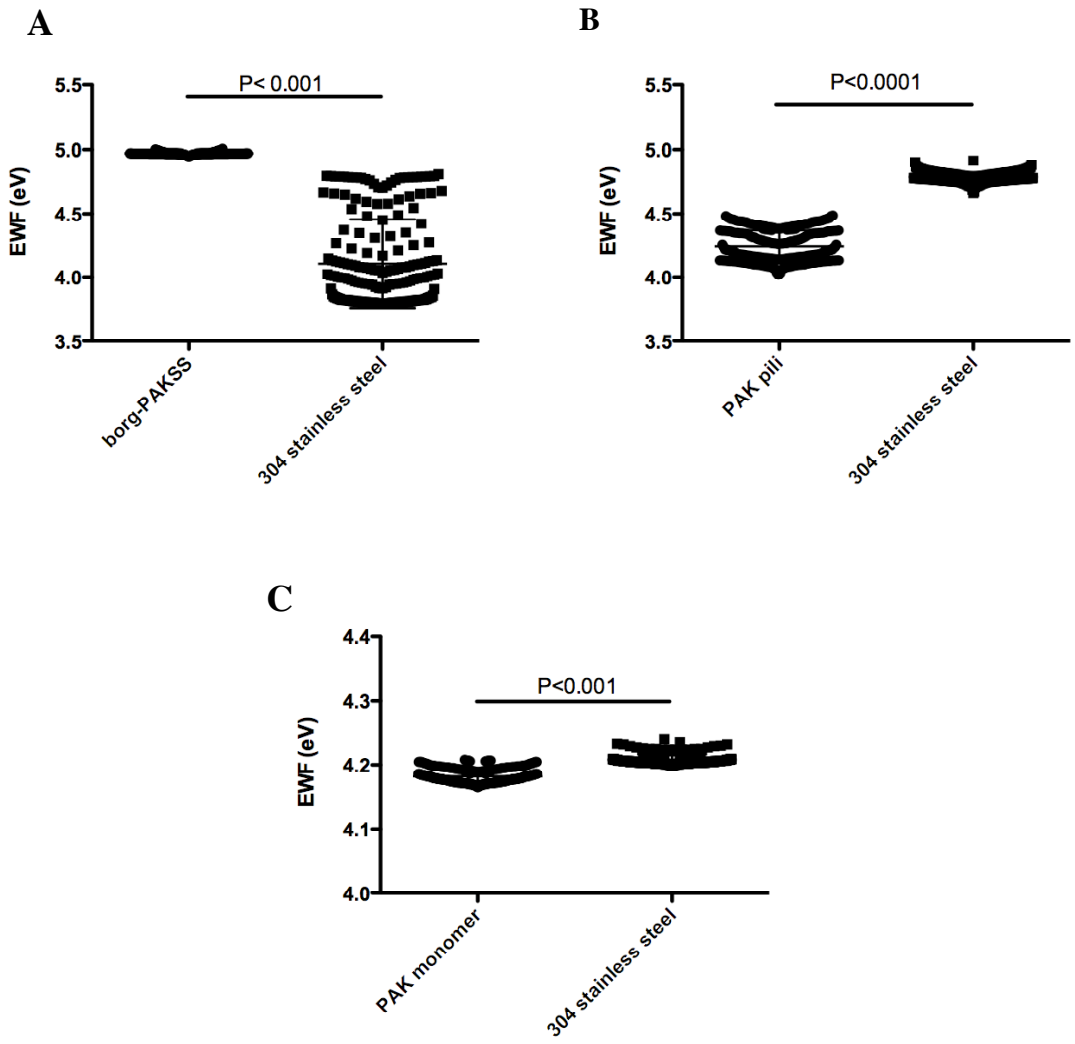

Figure 5-1. Electron work function of 304 stainless steel reacted with PAK(128-144)ox peptide, full-length PAK T4P, and monomeric PAK pilin. Electron work function measurements of (A) borg-PAKSS, (B) PAK pili, and (C) PAK monomer performed using a Kelvin probe. An area of 2 μm by 2 μm was scanned per sample. A total of 400 measurements were taken and means were plotted.

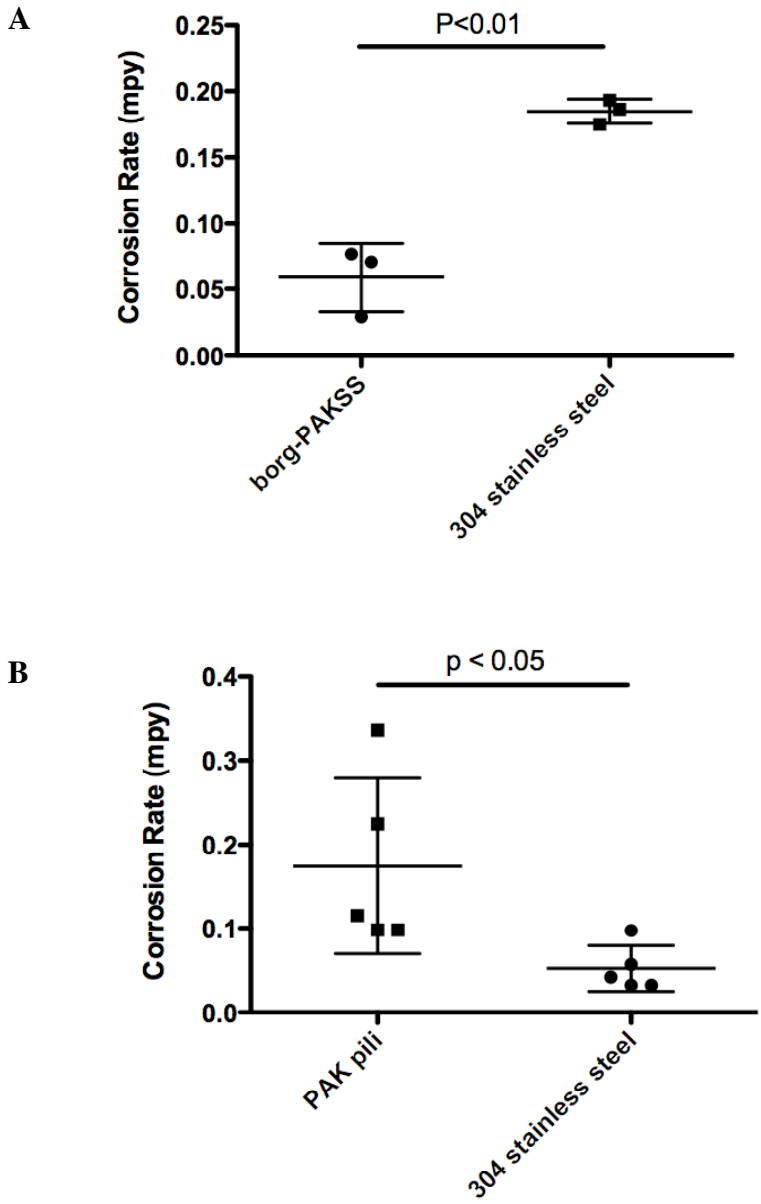

Figure 5-2. Electrochemical behaviour of borg-PAKss and stainless steel bound with T4P. **A.** Corrosion rates of borg-PAKSS and 304 stainless steel. **B.** Corrosion rates of steel in the presence of bound full-length PAK pili and unaltered 304 stainless steel. A minimum of three individual Tafel and linear polarization resistance experiments were performed to obtain corrosion rates. Corrosion rates were calculated using the Stern-Geary equation.

viable *P. aeruginosa*. Wild-type strain PAK readily binds to stainless steel using their T4P and, over time, will release from steel (**Chapter 3**, **Fig. 3-1 A and 3-2).** To ensure that bacteria remained bound to the stainless steel surface for the duration of the electrochemical tests, strain PAK R364 was used. PAK R364 is a strain with a transposon insertion that has inactivated the *pilT* gene to create a mutant PAK PilT$^-$ (*pilT*$^-$ through a transposon insertion) strain that is unable to retract pili. This strain displays a negative twitching phenotype and is hyper-piliated. Unlike its wild-type counterpart, the PAK *pilT*$^-$ mutant is unable to release from the surface once attached (**Chapter 3, Fig. 3-1 B and 3-2**)(Whitchurch *et al*., 2002), ensuring that bacterial cells remain bound to the steel surface during corrosion testing. Following one hour of binding, electrochemical corrosion testing was performed on PAK *pilT*$^-$ coated and unaltered stainless steel. Although counter intuitive, stainless steel with bacteria bound on the surface had a significantly (**P<0.05**) decreased corrosion rate (44.7± 8.0e^{-3} mpy) compared to unaltered steel (94.6±15.1e^{-3} mpy)(**Fig. 5-3**). Although it appears that the presence of bacteria decreased the corrosion rate, these results represent the limitations of the experimental setup, where electron release is facilitated in the presence of whole bacteria but where these electrons are captured by the bacteria (the system is fully aerobic and O_2 is being reduced by the cells during the course of the study) and are not detected by the counter electrode, resulting in a perceived decrease in corrosion (which is actually measured by the current flow in solution from the steel surface through a salt bridge to the platinum counter electrode). While our experimental design measures electron flow from the metal surface, alternative studies employing a *pilT*$^-$ strain utilizing appropriate growth conditions has demonstrated that electrons are readily transferred from the bacteria in a Δ*pilT* derivative of *P. aeruginosa* strain PAO to a metal surface (Mukherjee *et al*., 2012).

5. 2. 4. T4P can conduct microamps of current

Potentiostatic measurements, where a constant voltage is applied across a sample and current flow emanating from the system is measured over time, were employed as a more direct method of determining differences in surface conductance of steel reacted with PAK RBD, monomeric pilin, full-length PAK T4P, and unaltered steel. A physiologically relevant potential of +150 mV was continuously applied to the stainless steel and current flow was measured over 30 minutes. Initially the current flow through the samples reacted with RBD, monomeric pilin, and full-length pili was similar to that of unaltered steel (**Fig. 5-4**). However, at the end of the experiment, a current of 9.1 μA flowed through borg-PAKSS compared to 14.5 μA measured for

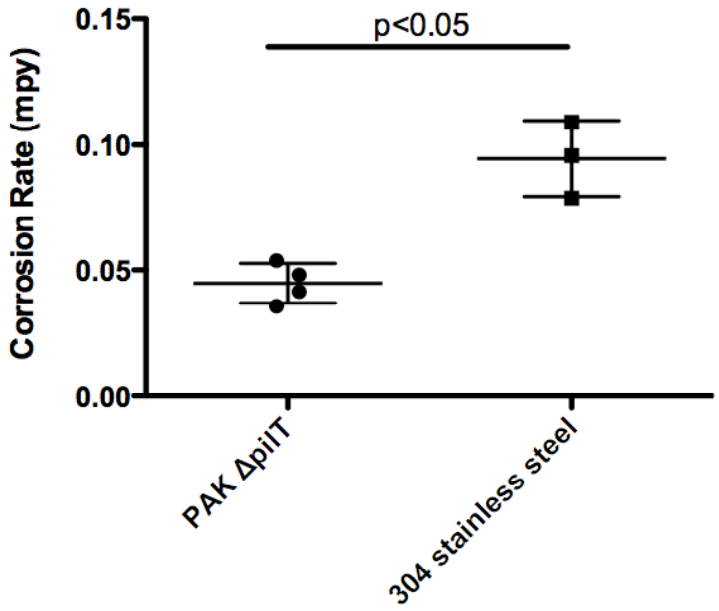

Figure 5-3. *P. aeruginosa* increases the corrosion rate of steel. The corrosion rates of stainless steel colonized by *P. aeruginosa* PAK Δ*pilT*, a retraction deficient mutant unable to release from the steel surface, and unaltered 304 were calculated using a minimum of three individual Tafel and linear polarization resistance experiments. Corrosion rates were calculated using the Stern-Geary equation. The perceived decreased corrosion rate of PAK Δ*pilT* reflects experimental conditions where the electron released from the steel surface flow up the pilus and are taken up by the bacterium. As a result the electrons are not detected by the counter electrode, resulting in a perceived decrease in corrosion rate.

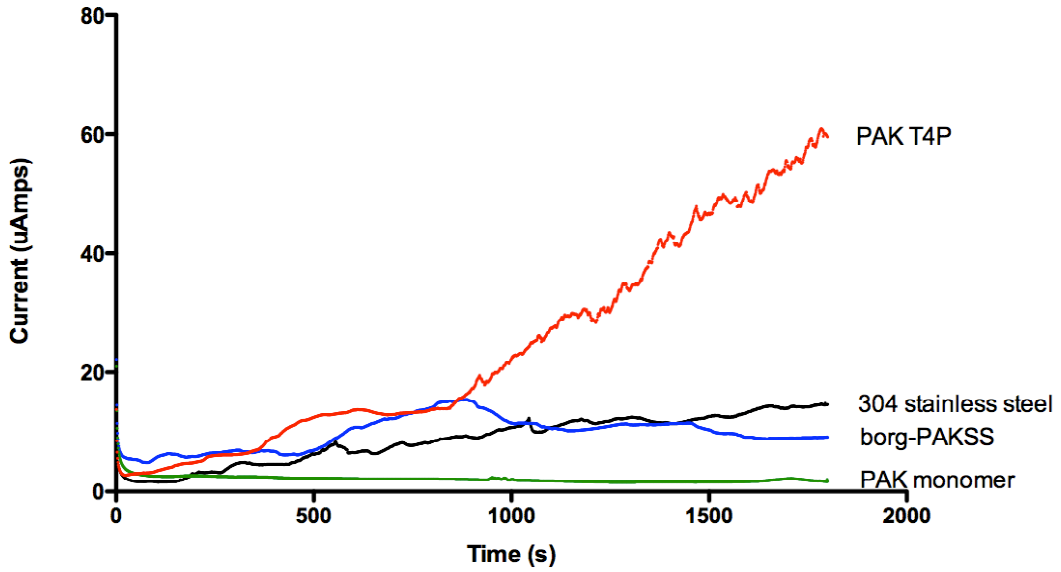

Figure 5-4. The T4P of *P. aeruginosa* conducts microamps of current. Potentiostatic measurements were performed to measure the amount of current flowing from steel reacted with RBD peptide for form borg-PAKss (blue), PAK T4P (red), PAK monomer (green), and 304 stainless steel (back) using an applied potential of +150 mV. The potential was continuously applied for 1800s and the current was measured over time.

unaltered steel (over time the current flow decreases the thickness of the insulating oxide surface of the steel surface, thus allowing enhanced current flow over time), further demonstrating that the RBD stabilizes the steel surface and functions as an insulator, to reduce the current flow from the metal surface. The presence of full-length T4P on the surface steadily increased current flow displaying a final current of 60 μA, 4 times as much current compared to unaltered steel. The presence of monomeric pilin did not increase current flow and final current measurement of 1.7 μA was observed (**Fig. 5-4**).

5. 2. 5. *Pseudomonas* autoinducers interact with T4P

T4P are multifunctional and, in addition to mediating binding events and powering twitching motility, play a role in quorum sensing in *P. aeruginosa* (Barken *et al*., 2008; Yeung *et al*., 2012). Quorum sensing is a form of inter-cellular signaling that is population density-dependent, where small molecules termed ***P****seudomonas* **a**uto**i**nducers (PAIs) are secreted into the extracellular environment and sensed by nearby bacteria. Sensing of autoinducers and their extracellular concentrations results in both positive and negative control of gene clusters involved in but not limited to motility, virulence, and metabolism (Schuster *et al*., 2003; Wagner *et al*., 2003). *P. aeruginosa* produces two acyl-homoserine lactone autoinducers, *N*-3-oxododecanoyl-homoserine lactone (PAI-1) and *N*-butryl-homoserine lactone (PAI-2) that have been shown to influence T4P expression, binding, and twitching motility (Glessner *et al*., 1999). When whole-cell WT PAK were incubated in the presence of PAI-2, bacteria were observed to bind to steel in significantly greater numbers compared to bacteria incubated in buffer alone (**Fig. A-1**). Increasing the concentration of autoinducer resulted in increased number of bacteria binding to steel, with nearly a 100% increase in binding observed when physiological concentrations (3.8 μM) of PAI-2 were used (**Fig. A2 i**). Interestingly, when purified full-length T4P were incubated with varying concentrations of PAI-2, a dose-dependent increase in T4P binding to steel was observed (**Fig. A2 ii**) with the highest increase in binding observed when a physiological concentration of 3.8 μM of PAI-2 was used. A similar concentration-dependent binding was observed with T4P binding to asialo-GM1, buccal epithelial cells (BECs), and DNA (**Fig. A3 i, ii, iii**). Stock autoinducer (mM range) was solubilized in 95% EtOH and pili were exposed to the equivalent concentrations of ethanol also showed a dose-dependent increase in binding, although significantly lower than the response observed with exposure to PAI-2 and EtOH. These data suggest that autoinducer can directly interact with T4P to modulate binding to a variety of surfaces and that the presence of ethanol can similarly increase binding.

We hypothesized that PAI-2 and ethanol directly interacted with T4P to induce conformational changes within the pilus structure and that these changes aside from modulating binding activities could affect pilus conductivity. Stainless steel coupled with purified PAK T4P fibers was incubated in the presence of 3.8 μM PAI-2 or equivalent diluted volumes of 95% ethanol, washed to remove excess unbound PAI-2 or ethanol, and a voltage of +150 mV was applied for 50 minutes. Current was measured continuously, and the presence of T4P fibers increased the current flow by ~140%, from 67.7 μA for unaltered steel to 160.4 μA (**Fig. 5-5**). The additional of PAI-2 reduced current flow in the T4P, decreasing it from 160.4 μA to 85.7 μA whereas the presence of ethanol alone had the opposite effect and increased the current flow from 160.4 μA to 217.5 μA, indicating that PAI-2 and ethanol induce different conformational changes in the T4P and that the pilus can sense changes in the environment and respond accordingly by modulating current flow through the pilus fiber (from Ohm's law of V=I/R and given that the voltage is fixed in the experimental design, this change in current reflects a change in the resistance of the system). Exposure of 304 stainless steel to ethanol and PAI-2 resulted in increased current flow through the steel, with a current of 75.5 μA and 113.9 μA compared to 67.7 μA, suggesting that ethanol and PAI-2 interact with the unaltered steel surface to reduce the oxide surface thickness and thus increase current flow by decreasing the resistance of the surface is decreased.

5. 2. 6. T4P modulate current flow in response to environmental stimuli

Finally, to confirm that T4P can sense environmental changes, stainless steel reacted with PAK T4P was exposed to ultraviolet (UV) light during the course of the potentiostatic measurements. PilA contains two Trp residues that strongly absorb UV and the effect of UV on the current flow when T4P are present was measured when a potential of +500 mV was applied to the system. At the higher voltage bias, large amounts of current (1.2 mA) were recorded flowing through the T4P, demonstrating that the pilus is a very effective nanowire that can accommodate high current transfers (**Fig. 5-6**). When continuously exposed to UV light, current flow through the T4P was dramatically reduced, decreasing to minimal levels that were lower than normal current flow observed through steel (400 μA) when a potential of +500 mV was applied. When unaltered steel was exposed to UV light, the current increased to ~1.7 mA compared to 400 μA, but this increase in current, a result of UV exposure, was negated in the presence of T4P. This suggested that the pilus reacts to the environment and can effectively counteract and shut down the increase in current that normally occurs when steel is exposed to UV (essentially increasing

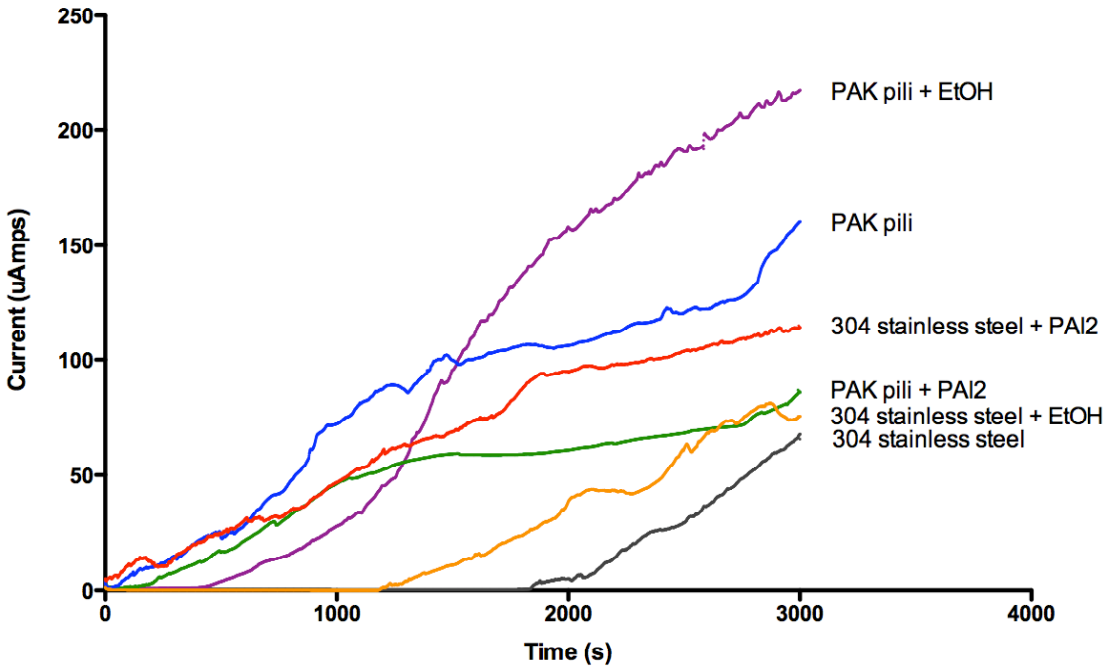

Figure 5-5. PAI-2 interacts with PAK pili to modulate current flow through the pilus. Potentiostatic measurements were performed to measure the amount of current flowing from steel reacted with PAK T4P (blue) and 304 stainless steel (back). The effects of PAI-2 and 95% ethanol on current flow were evaluated by incubating the stainless steel or stainless steel reacted with T4P with PAI-2 or 95% ethanol for one hour prior to running the potentiostatic measurements. An applied potential of +500 mV was used. The potential was continuously applied for 3000s and the change in current was measured over time.

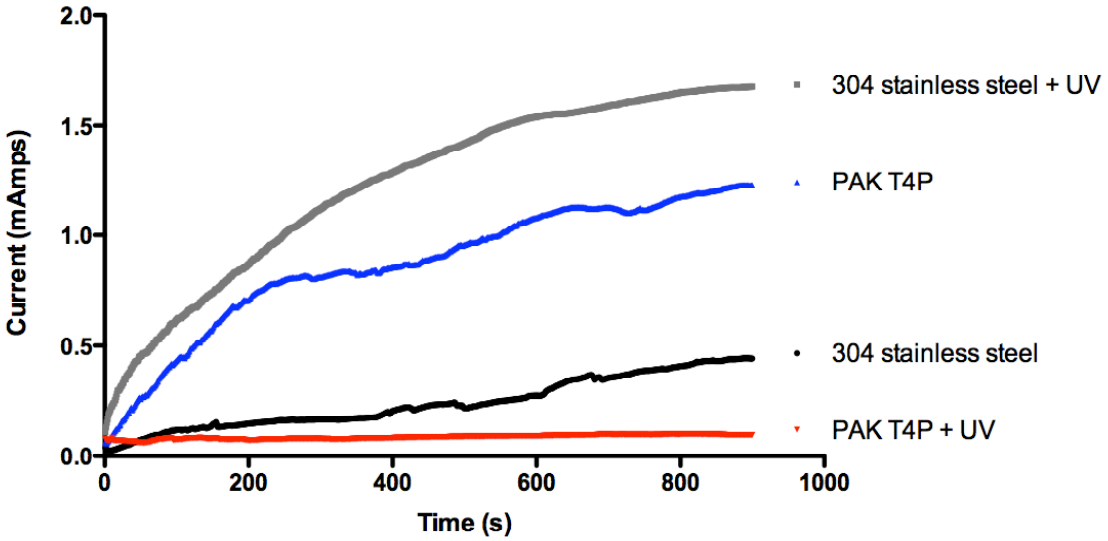

Figure 5-6. The T4P modulates current flow in response to UV light. Potentiostatic measurements were performed to measure the amount of current flowing from steel reacted with PAK T4P (blue) and 304 stainless steel (back). The effects of UV light on current flow were evaluated by exposing the T4P and stainless steel to UV light while simultaneously applying a potential of +500 mV and measuring current flow. The potential was continuously applied for 3000s and the change in current was measured over time. The UV light remained on for the duration of the experiment.

the resistance of the surface). When taken together with the PAI-2 and ethanol effects on current flow, these results demonstrate that the T4P of *P. aeruginosa* is an effective nanowire that can respond to environmental stimuli to increase or decrease current flow through the pilus fiber by modulating the resistance value of the nanowire.

5. 3. Conclusions

The T4P of *P. aeruginosa* can function as a bacterial nanowire. The presence of bound T4P on the surface of stainless steel facilitates the removal of electrons from the surface (**Fig. 5-1 B**) and increases the corrosion rate by 320 % (**Fig. 5-2 B**). The T4P is capable of sustaining currents of up to several milliamps over a period of time (**Fig. 5-4**) and through conformational changes in response to changes in the environment, such as the presence of *Pseudomonas* autoinducers and UV light, the pilus can alter its electrical resistance to an "on" state allowing high current transfer or to an "off" state where current transfer is low (**Fig. 5-5, 5-6**). A monomeric form of the pilin also facilitates the removal of electrons from the surface (**Fig. 5-1 C**) but to a lesser extent compared to T4P, suggesting that the truncation within the pilin monomer is involved in electron flow in the T4P fiber and removal of amino acids in positions 1-28 from the N-terminus of PilA impairs current flow (**Fig. 5-4**). The quaternary structure found in the T4P but is missing in the monomeric pilin may also contribute to ability of the proteins to facilitate electron flow.

Chapter 6

Stereospecific modification of physicochemical surface properties of stainless steel: Evidence that bacterial adherence mechanisms exploit unanticipated chiral structural complexity for surface colonization

A version of this chapter was published in *Acta Biomaterialia*

Davis, EM., Li, DY., Shahrooei, M., Yu., B., Muruve, D., and RT Irvin. (2012). Evidence of extensive diversity in bacterial adherence mechanisms that exploit unanticipated stainless steel surface structural complexity for biofilm formation. *Acta Biomaterialia* http://dx.doi.org/10.1016/j.actbio.2012.11.026

Figure 6-7 was generated by Dr. Daniel Muruve

6. 1. Brief introduction

In Chapters 4 and 5, we demonstrated that the K122-4(128-144)ox peptide of the RBD of *P. aerugniosa* changed the physicochemical surface properties of stainless steel to create borg-K122SS, a new bio-organic material, that decreased surface reactivity and adhesiveness, increased corrosion resistance, and increased hardness. The altered borg-K122SS surface suggested that bacteria, proteins, and other materials would be less likely to interact with and adhere to borg-K122SS due to the decrease in surface reactivity and stickiness. Studies have demonstrated that biofilm formation depends on the deposition of a conditioning layer which adsorbs onto the surface (Pringle, 1986; Renner, 2011) and the ability to modulate conditioning film formation and/or bacterial binding to adsorbed organic material by altering the properties of the surface can be used to control biofilm formation (Renner, 2011). However, bacteria produce a number of extracellular protease and the native RBD, composed of L-amino acids, that is used to create borg-K122SS is degraded by proteases, severely limiting the potential of borg-K122SS to control biofilms.

To overcome protease sensitivity we generated two protease resistant versions of the native RBD peptide. The first was a synthetic D-K122-4(128-144)ox peptide that is an enantiomeric (or chiral) form of the native peptide (Hung *et al*., 1999; Mandal *et al*., 2009). The second was a retro-inverso D-K122-4(128-144)ox peptide. The retro-inverso peptide is composed of D-amino acids but the sequence is reversed. Inverting the sequence positions the amino acid side chains in the correct relative positions that would be found in the native L-amino peptide (Goodman & Chorev, 1979; Li *et al*., 2010; Taylor *et al*., 2010). These two peptides have identical compositions and vary only in their 3 dimensional (3-D) structures (**Fig. 6-1**). The D-amino peptide is a mirror image of the L-amino K122-4 native RBD whereas the structure of the retro-inverso peptide is similar to but not identical to the native peptide. Peptides composed of D-enantiomeric amino acid residues are not recognized by proteases and are protease resistant. We hypothesized that these forms of the RBD should increase the potential utility of these novel peptides.

6. 2. Results

6. 2. 1. Physical properties of modified 304 stainless steel

We first examined the ability of the D-amino and retro-inverso D-amino peptides to alter the surface properties of 304 stainless steel. We also examined a stainless steel surface modified with a combination of the D-amino and retro-inverso (D+RI) peptides. The all D- and the retro-inverso forms of the RBD interacted with the steel surface to generate new materials that were termed D-

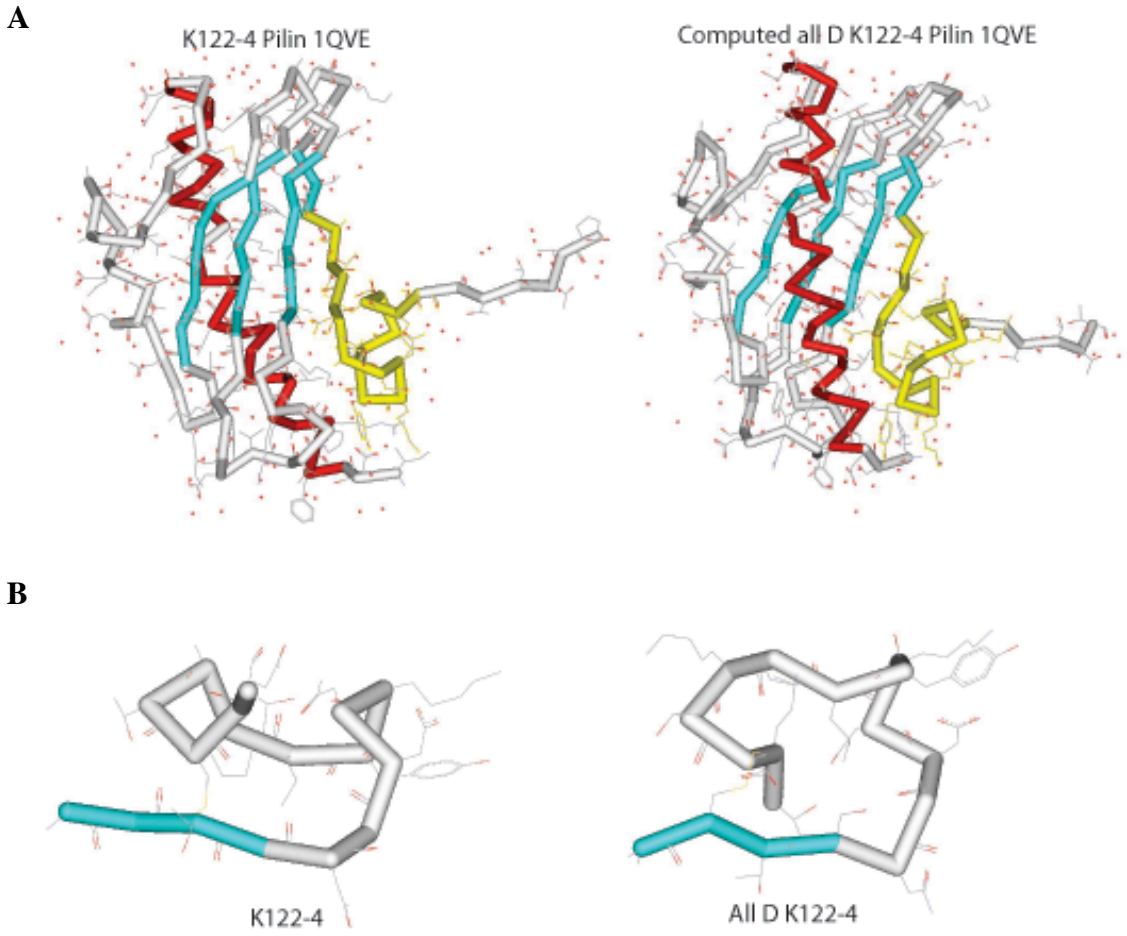

Figure 6-1. Structure of native pilin protein and structure of RBD within cognate protein. **A.** A stick representation of the X-ray crystal structure of *Pseudomonas aeruginosa* truncated PilA protein (the first 28 residues of native PilA have been truncated in this recombinant PilA protein construct) with the receptor binding domain (RBD) highlighted in yellow. The structure is identified in the Protein Data Bank as structure 1QVE (Audette *et al*., 2004). As protein structures of synthesized proteins consisting of only D-amino acid residues have been established to be the mirror image of the native protein structure which consists of only L-amino acid residues (Hung, 1999) the structure of D-form of 1QVE was calculated and is displayed as the stick representation with the RBD highlighted in yellow. **B.** Stick representation of the RBD employed in this study, with the structure being taken from the 1QVE data file and the all D-RBD taken from the computed structure, while the synthetic RBD is flexible *P. aeruginosa* RBDs have a conserved overall structure in aqueous solution at room temperature characterized by two β-turns and a hydrophobic core (Campbell *et al*., 1997) (*3*).

borgSS and RI-borgSS, respectively. The new surface generated by reacting steel with both the all D- and the retro-inverso peptides was termed D+RI-borgSS. Although the D-amino and retro-inverso peptides have identical chemical compositions and differ only in their 3-dimentional (3-D) structures, the peptides reacted with stainless steel to create surfaces with different EWFs. The D-borgSS, RI-borgSS, and D+RI-borgSS surfaces all had significantly increased EWF compared to the unaltered steel surface (**P<0.0001**) although modification with the D-amino peptide yielded a surface EWF that was significantly lower (**P<0.0001**) than that observed with the RI-K122-4 or D+RI modification (**Fig. 6-2 A**).

All surfaces were less adhesive, as measured by contact AFM using a silicon nitride tip, compared to untreated steel (**P<0.01**)(**Fig. 6-2 B**). Steel reacted with the retro-inverso peptide to form RI-borgSS was significantly harder (**P>0.01**) than untreated stainless steel and mirrored the improvement in hardness observed with the L-amino peptide on the borg-K122SS surface (**Fig. 6-2 C**). D-borgSS, RI-borgSS, and D+RI-borgSS were all significantly harder than untreated 304 stainless steel (**P<0.01**)(**Fig. 6-2 C**), although modification of the surface with the D-amino peptide resulted in a surface that had reduced hardness compared to borg-K122SS and surfaces modified with the retro-inverso and D+RI peptides (**P<0.01**). There was no significant difference between the RI-borgSS and D+RI-borgSS surfaces, suggesting that combining both peptides does not improve surface hardness.

The load limit of the nanoindenter is 1 mN and the bio-organic stainless steel surfaces tested showed improved hardness up to the limit of the equipment. To test whether improvements in surface hardness could be observed at higher force loads, samples were tested using a microindenter. At loads of 20 mN, no significant improvements in hardness were observed for any of the peptide-treated steel surfaces (**Fig. 6-2 D**), suggesting that the increased hardness is limited to the surface of the material, given that at higher loads the underlying structure of the material collapses under the load and no improvements in hardness are observed for the bulk of the material. As expected, both D-borgSS and RI-borgSS were protease resistant (**Fig. 6-3**) as demonstrated by the absence of change in the EWF. Whereas treatment of the K122-borgSS surface abolished the increase in EWF, trypsin digestion of RI-borgSS had no effect on the EWF, confirming that the retro-inverso peptide is resistant to protease treatment.

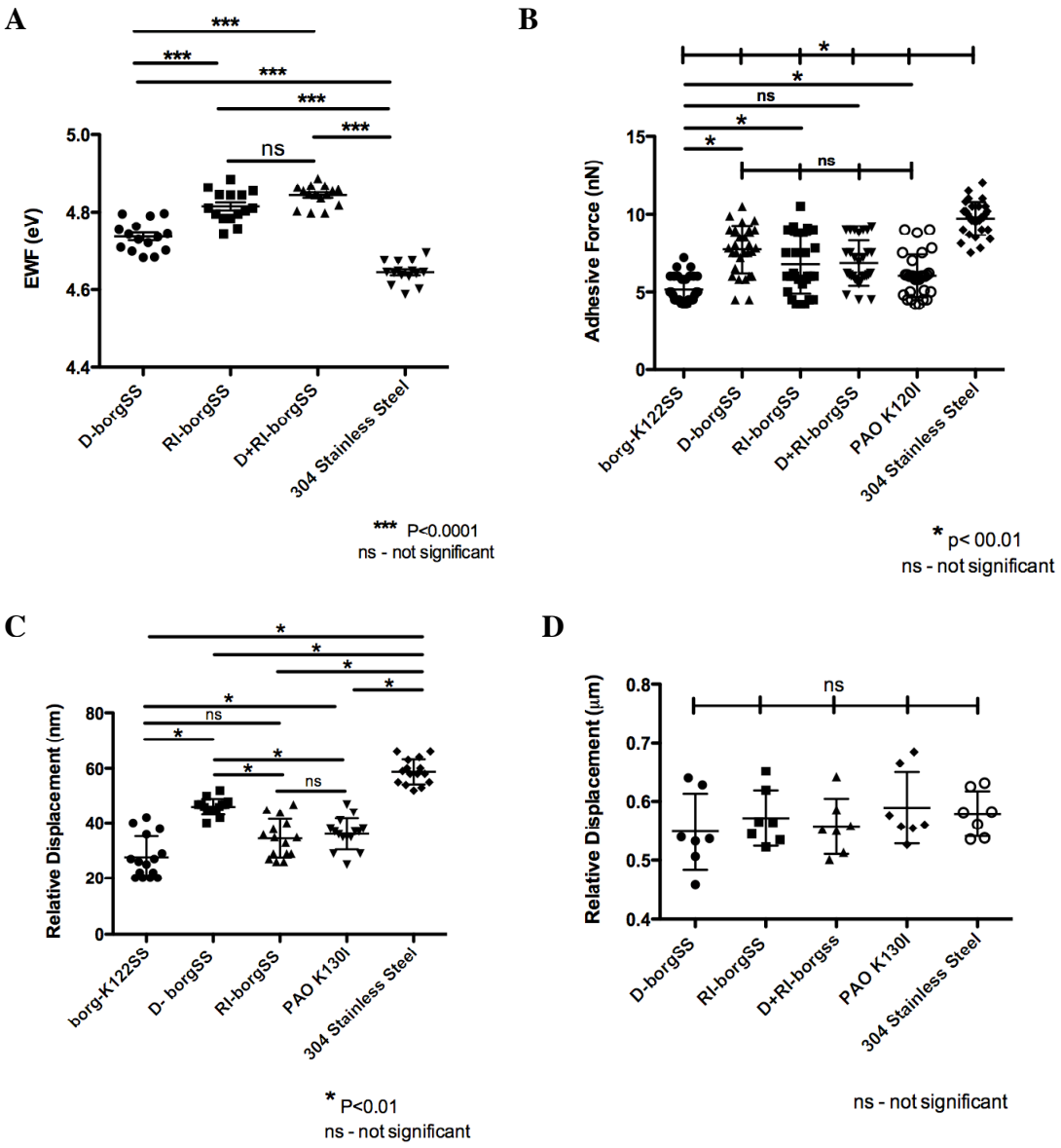

Figure 6-2. Physical characterization of peptide-modified steel surfaces. A. Electron work function measurements of D-borgSS, RI-borgSS, D+RI-borgSS, and 304 stainless steel performed using a Kelvin probe. Adhesive force (**B**) and nanoindentation measurements (**C**) of K122-borgSS, D-borgSS, RI-borgSS, D+RI-borgSS, steel reacted with PAO K130I peptide, and 304 stainless steel. Adhesive force measurements were performed with an AFM equipped with a non-conductive silicon nitride tip. An area of 1 µm x 1µm was scanned. A total of 25 measurements were obtained and means were plotted. Nanoindentation measurements were performed with a triboscope controlled by an AFM. A total of 15 load-displacement plots were obtained and relative total displacement was determined using the built in analysis software. **D.** Macroindentation measurements of D-borgSS, RI-borgSS, D+RI-borgSS, steel reacted with PAO K130I peptide, and 304 stainless steel were obtained using a microindenter. A total of 7 load-displacement plots were obtained per sample and relative displacement was calculated using the built in software.

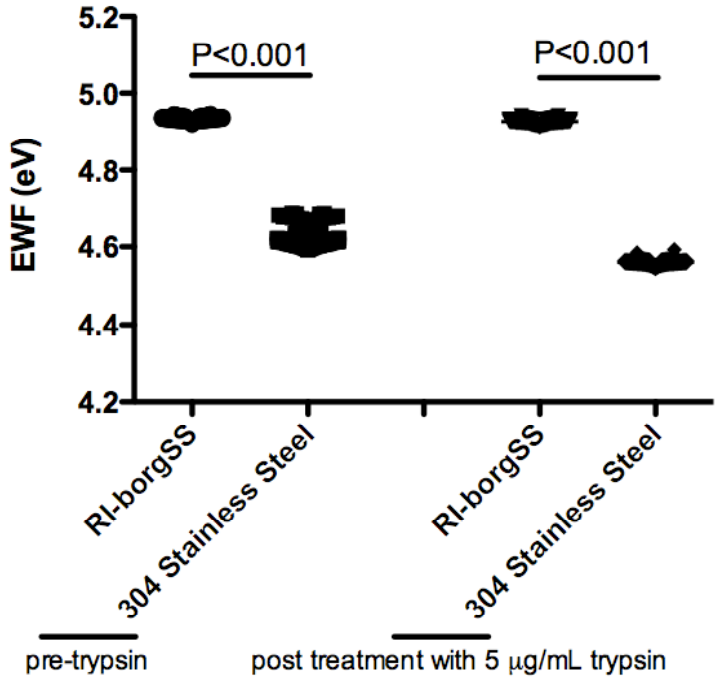

Figure 6-3. RI-borgSS is resistance to protease treatment. The EWF of RI-borgSS was analyzed before and after treatment with 5 μg/mL of trypsin for 4 hours at 37C. Digestion with trypsin has no effect on the EWF of RI-borgSS and the increase in EWF is retained.

6. 2. 2. Electrochemical behaviour

The EWF is a measure of the energy level of the surface electrons and the ability of those electrons to react with other materials and a high EWF generally reflects good resistance to corrosion. The high EWF of the RI-borgSS, D-borgSS, and D+RI-borgSS surfaces suggested that their corrosion rate would be lower compared to unaltered 304 stainless steel. RI-borgSS was significantly more corrosion resistant than regular stainless steel, having a corrosion rate ~50% of unaltered steel whereas a large variation in corrosion rate was observed for D-borgSS (**Fig. 6-4**). This variation was eliminated when stainless steel was bound with both the D-amino and retro-inverso peptides and corrosion rates for D+RI-borgSS were similar to those observed when only retro-inverso was present on the surface, suggesting that the retro-inverso peptide can counteract the effects of the D-amino peptide on corrosion.

6. 2. 3. Resistance to surface colonization

The major limitation of the original borg-K122SS surface was the sensitivity of the L-amino RBD peptide to proteases. D-borgSS, RI-borgSS, and D+RI-borgSS were tested to determine whether the altered surface properties of the materials could decrease the potential of the surface to be colonized by various bacteria. Work by Gilter *et al*. (2006)(Giltner *et al*., 2006) had already confirmed that reacting stainless steel with the native RBD generates a surface (borg-K122SS) that is less susceptible to colonization by *P. aeruginosa*. The RBD has not been tested to determine if it can inhibit the binding of other bacterial species to stainless steel. In *P. aeruginosa*, binding to stainless steel is mediated by the T4P but other metal colonizers use different mechanisms to adhere to steel. To determine whether D-borgSS, RI-borgSS, and D+RI-borgSS were less susceptible to colonization by bacteria that use adherence mechanisms other that the T4P we examined the adherence of a number of Gram-positive bacteria which do not produce type IV pili and that have been noted to form biofilms on stainless steel, namely *Listeria monocytogenes* (3 strains), *Listeria innocua* (1 environmental strain), *Staphylococcus aureus* (3 strains), and *Staphylococcus epidermidis* (1 strain). We observed that the D-borgSS surface was significantly less effectively colonized (<50% of the observed binding, $P<0.0001$) by all 3 strains of *Listeria monocystogenes* relative to the unmodified 304 stainless steel surface (**Fig. 6-5 A,B,C**). Interestingly, for *L. monocytogenes* strains H8 and J10 D-borgSS was significantly less colonized than was RI-borg-SS (**$P< 0.001$**) while with strain I9 there was no significant difference between the D versus RI treatment (**Fig. 6-5 A,B,C**) . The D+RI-borgSS varied considerably in its colonization potential with *L. monocyotogenes*. *L. monocytogenes* strain H8 colonization was enhanced relative to unmodified steel (Figure 2a), strain J10 was

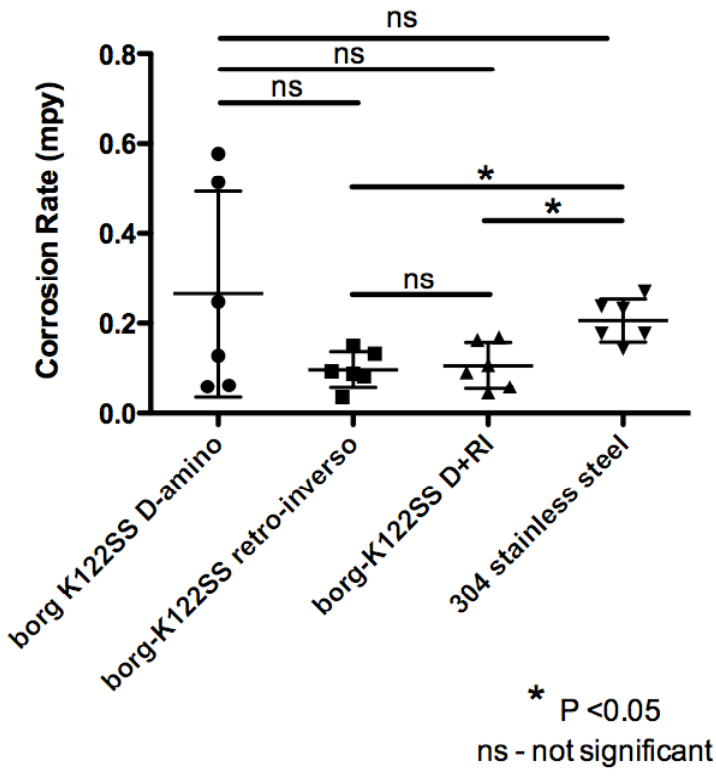

Figure 6-4. Electrochemical behaviour of 304 stainless steel modified with synthetic peptides. Potentiodymanic polarization curves (**A**) and corrosion rates (**B**) of 304 stainless steel and steel reacted with the synthetic peptides D-amino, retro-inverso D-amino, and a combination of D-amino and retro-inverso to generate D-borgSS, RI-borgSS, and D+RI-borgSS.

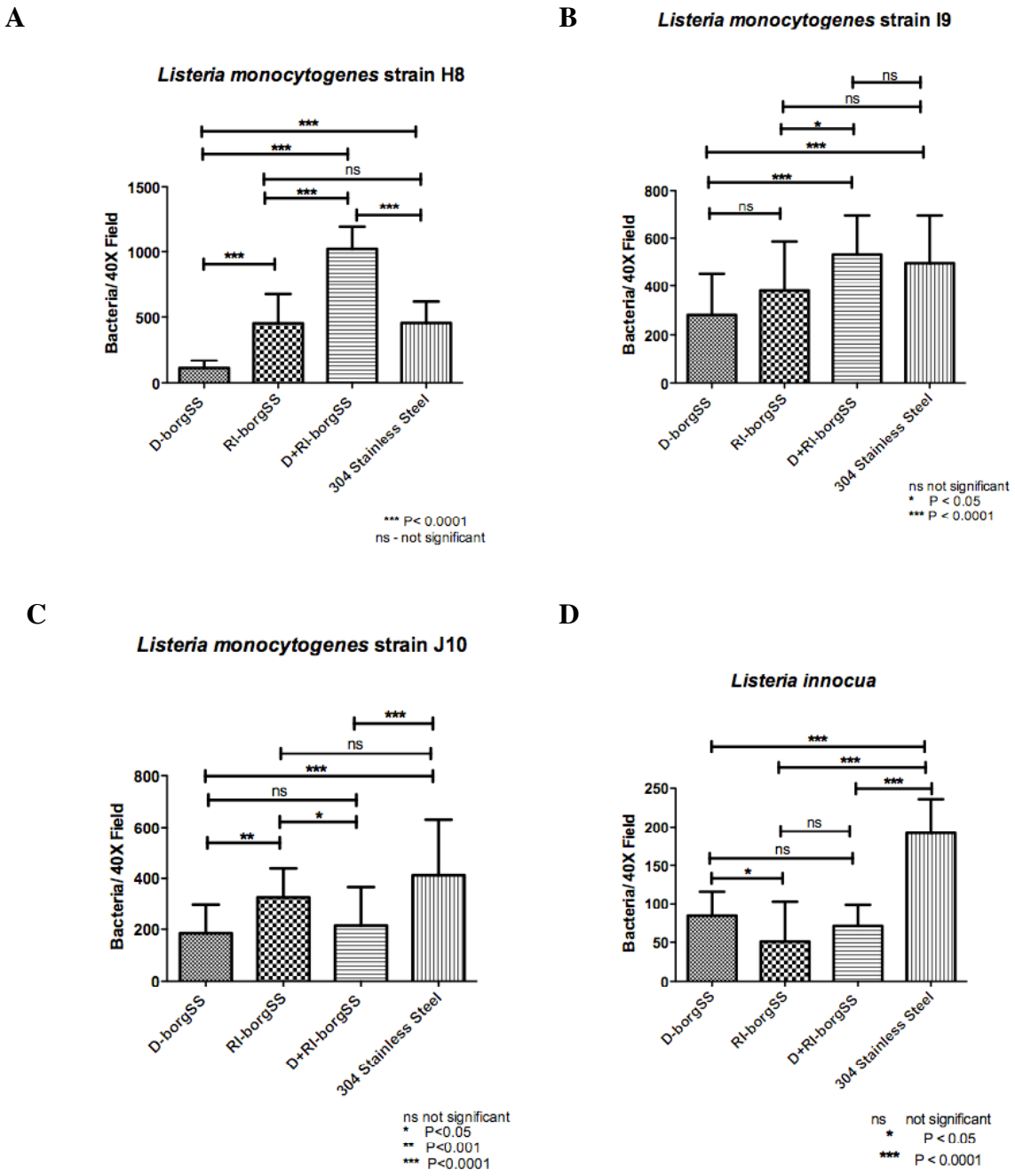

Figure 6-5. Adherence of *Listeria monocytogenes* and *Listeria innocua* to 304 stainless steel modified with D-amino, retro-inverso D-amino, and both D-amino and retro-inverso peptides relative to unmodified stainless steel. Effect on adherence of *L. monocytogenes* strain H8 (**A**), *L. monocytogenes* strain I9 (**B**), *L. monocytogenes* strain J10 (**C**) and an environmental isolate of *L. innocua* (**D**) to the D-borgSS, RI-borgSS, D+RI-borgSS, and 304 stainless steel surfaces.

significantly inhibited relative to unmodified steel but not significantly greater than what was observed for D-borgSS (**Fig. 6-5 C**), and strain I9 colonization of D+RI borg-SS was not significantly different from unmodified steel (**Fig. 6-5 B**).

The closely related species *Listeria innocua*, which is frequently isolated in identical environments and in food processing plants, was less able to colonize RI-borgSS compared to D-borgSS (**P<0.05**) and unmodified steel (73% less binding, **P<0.0001**) (**Fig. 6-5 D**). The D-borgSS was somewhat more colonized with *L. innocua* compared to the D+RI treated surface, and colonization of D-borgSS was decreased by 56% relative to unmodified steel (**Fig. 6-5 D**). The D-borgSS was significantly (**P<0.0001**) less colonized by all 3 strains of *Staphylococcus aureus* compared to that observed with unmodified stainless steel. Initial adherence was reduced by 47% for strain 25923, 49% for strain D4, and 78% for strain RN F6 (**Fig. 6-6 A, B, C**). Strikingly, RI-borgSS did not inhibit colonization for strain 25923 (**Fig. 6-6 A**), but significantly (**P<0.0001**) inhibited colonization of strains D4 and RN F6 (63% and 48% respectively)(**Fig. 6-6 B, C**) relative to unmodified stainless steel. The D+RI treated surface was either ineffective in inhibiting binding (strain 25923, **Fig. 6-6 A**) or slightly inhibited colonization (17% for strain D4 and 23% for strain RN F6, **P<0.0001**)(**Fig. 6-6 B,C**) relative to unmodified stainless steel. *Staphylococcus aureus* has not been widely associated with biofilm formation on metal surfaces but readily forms biofilms on medical devices, whereas *Staphylococcus epidermidis* has historically been associated with biofilm formation on most abiotic surfaces. Thus we examined whether *S. epidermidis* colonization could be altered by peptide treatment. The D-borgSS was quite effective at inhibiting binding (77% inhibition relative to unmodified stainless steel, **P<0.0001**) (**Fig. 6-6 D**) of the *Staphylococcus epidermidis* strain and significantly (**P<0.0001**) more effective than the RI-K122-4 borg-SS surface in minimizing bacterial binding. The D+RI treated surface did not differ significantly from the D-borgSS surface in terms of minimizing *S. epidermidis* colonization (**Fig. 6-6 D**).

Previous studies had established an inverse relationship between the observed surface EWF and adherence of *P. aeruginosa* bacterial binding to stainless steel (Yu *et al*., 2008). In contrast, consistently lower bacterial adherence to a surface with a lower EWF, the D-K122-4 modified surface (**Fig. 6-5, 6-6**), was observed. Treatment of the stainless steel surface with both the D-K122-4 and RI-K122-4 peptides resulted in a surface EWF that did not differ significantly from the RI-K122-4 surface (**Fig. 6-2 A**) and yet bacterial colonization of the steel treated with both the D-K122-4 and RI-K122-4 peptides was not more effective in restricting bacterial adherence. In a number of cases the D+RI treated steel was much less effective in minimizing

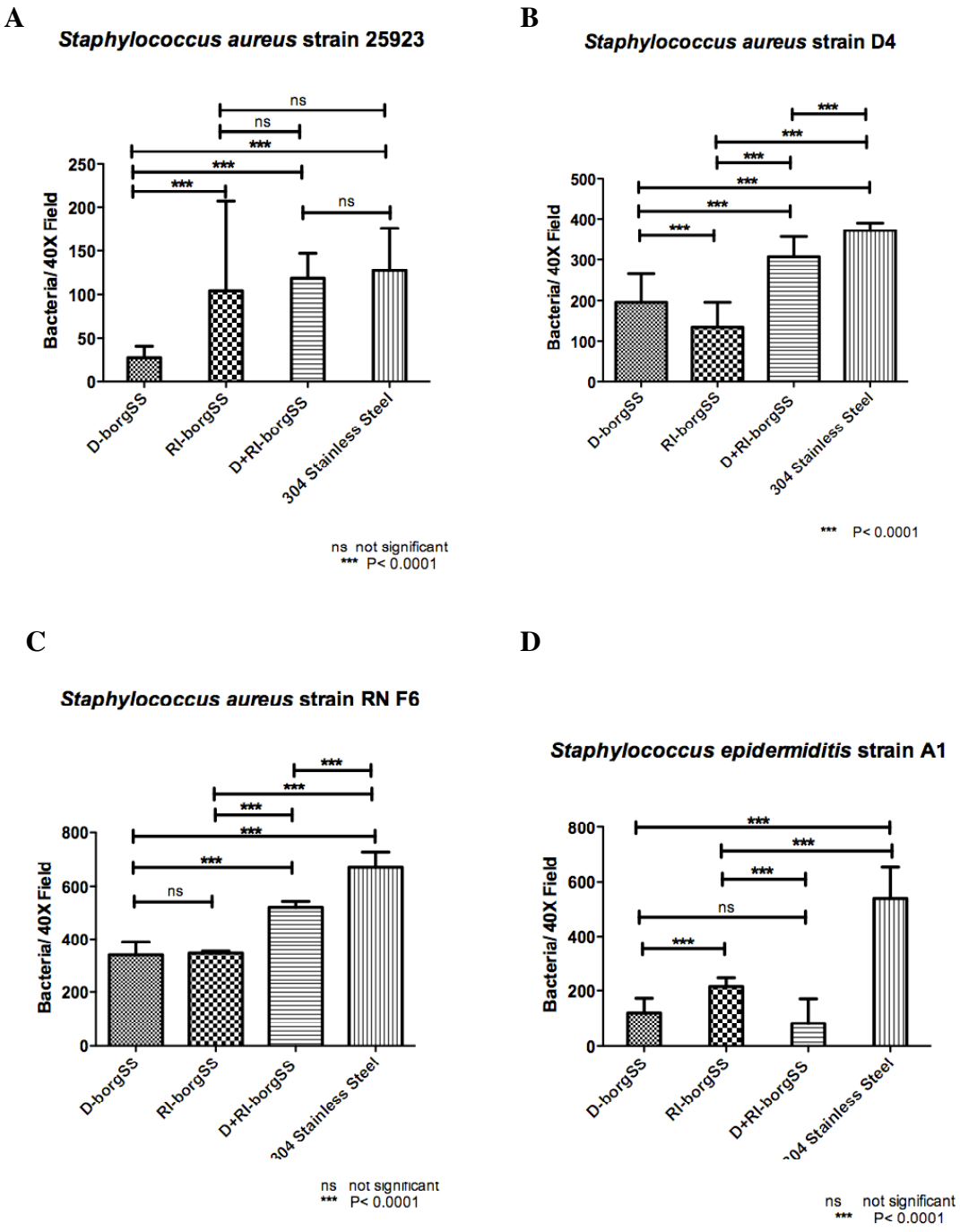

Figure 6-6. Adherence of Staphylococcus aureus and Staphylococcus epidermidis to 304 stainless steel modified D-amino, retro-inverso D-amino, and both D-amino and retro-inverso peptides relative to unmodified stainless steel. Effect on adherence of *S. aureus* strain 25923 (**A**), *S. aureus* strain D4 (**B**), *S. aureus* strain RN F6 (**C**) and *S. epidermidis* (**D**) to the D-borgSS, RI-borgSS, D+RI-borgSS, and 304 stainless steel surfaces.

bacterial adherence (**Fig. 6-5, 6-6**). All peptide-treated surfaces possessed a significantly (**P<0.0001**) reduced surface adhesive force compared to unmodified stainless steel but significant difference in the surface adhesive force between the peptide-modified surfaces was observed (**Fig. 6-2 B**). As a result, no correlation could be established between reduced surface adhesive force and bacterial adherence as the D-borgSS surface did not differ significantly from the RI-borgSS or the D+RI-borgSS surface despite bacterial adherence to the three surfaces differing considerably (**Fig. 6-5, 6-6),** with the greatest reduction of bound bacteria observed for D-borgSS.

6. 2. 4. Evidence of stereospecific interactions of chiral peptides on steel surfaces

Bacterial adherence to the D-borgSS and RI-borgSS surfaces clearly differ (**Fig. 6-5, 6-6**) and yet the chemical compositions of the two peptides utilized to create these surfaces are identical with the only differences lying in their 3 dimensional structures, generating results that are difficult to interpret unless there is unanticipated structural complexity in the 304 stainless steel surface that influences the reaction in a manner that yields different products with each chiral peptide, constituting evidence for chiral features on the steel surface. To determine whether the interaction of the native L-K122-4 peptide, D-K122-4 peptide and RI-K122-4 peptide yielded chiral specific localization patterns biotinylated forms of the peptides were reacted with steel and visualized by epifluorescent microscopy. The localization of biotinylated L-K122-4, D-K122-4 and RI-K122-4 peptides were not equivalent (**Fig. 6-7**) as both the amount of peptide detected on the surface and the macroscopic pattern of surface peptide differed appreciably. The D-K122-4 peptide appeared to interact slightly more extensively and in a more contagious distribution relative to the native L-K122-4 or RI-K122-4 peptides. These results indicate that the D and L enantiomers of the PilA RBD interact differently with the 304 stainless steel surface, indicating that there are region on the steel surface that display chiral specificity.

Given that the L-amino, D-amino and retro-inverso forms of the K122-4 RBD peptide all interacted with 304 stainless steel to generate surfaces with different physiochemical properties, we suspected that previous studies involving a mutant of the PAO PilA RBD (**Table 1**) (Giltner *et al*., 2006; Yu *et al*., 2007) which demonstrated that a synthetic peptide where the lysine at position 130 was substituted with an isoleucine did not inhibit the binding of PAK RBD, pili, or whole cell binding to steel surfaces might have incorrectly concluded that the mutant peptide did not bind to the steel surface. These results were originally interpreted as indicating that the altered sequence did not bind to stainless steel, but an alternative explanation that also accounts for the lack of inhibition of binding is that the K130I mutant of the RBD reacts with a distinct site

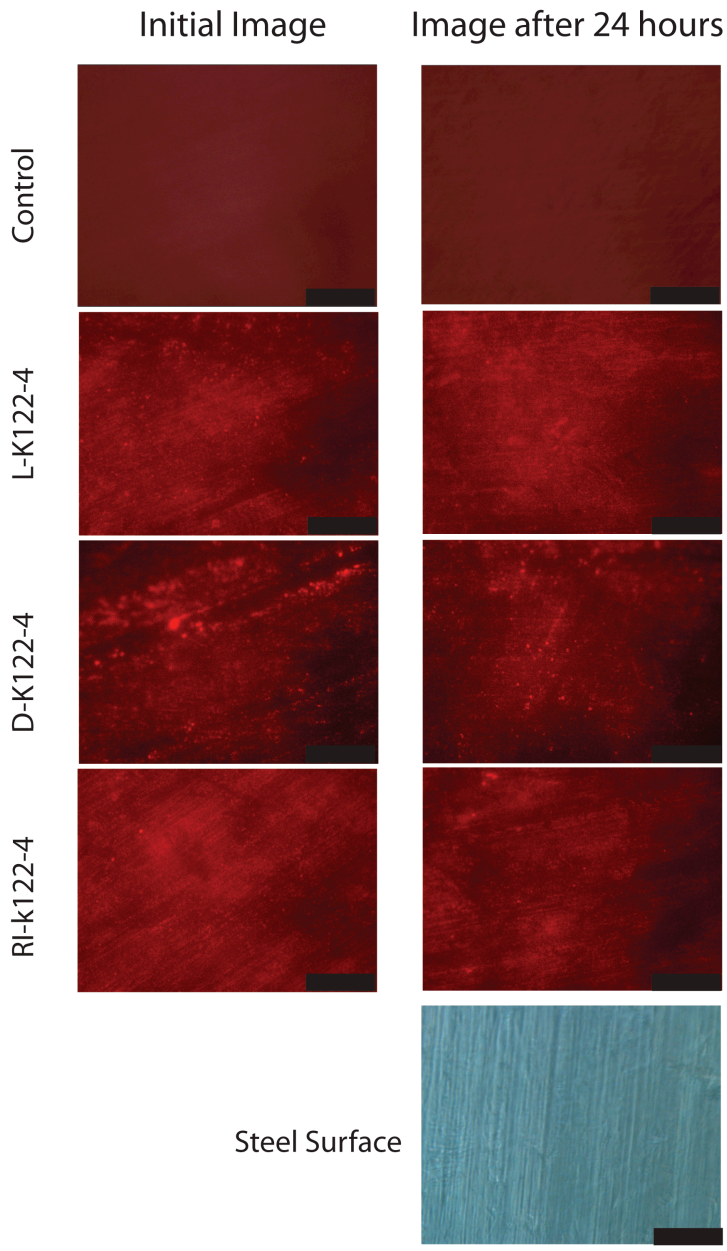

Figure 6-7. Distribution of biotinylated RBD peptides on 304 stainless steel surfaces. Images were collected either immediately after reaction of the peptides (either the native L-K122-4, the D-ennantiomer form D-K122-4, and the retro-inverso form RI-K122-4) with the 304 stainless steel or after 24 hours. Peptides localization patterns were determined by utilizing a cy3 fluochrome coupled to avidin to visualize the peptide distribution which bound to biotin that was coupled to the N-termini of the peptides during the synthesis of these peptides. Samples were examined by epifluorescence microscopy. The surface of the 304 stainless steel was also imaged with standard illumination to demonstrate sample topology. Note the bar in micrographs represents 50 μm.

or domain on the steel surface that the native RBD does not recognize. To determine if the peptide might actually recognize a different structural region on the steel surface not recognized by the PAK RBD, the hardness of 304 stainless steel treated with the PAO-K130I mutant RBD via nanoindentation was measured. The PAO-K130I mutant RBD significantly increased the hardness of the 304 stainless steel surface (**P<0.0001**) to the same degree as was observed for the L-K122-4 peptide (**Fig. 6-2 C**). It was previously assumed that the PAO-K130I peptide could not inhibit *P. aeruginosa* bacterial binding because it did not interact with the surface (Giltner *et al*., 2006; Yu *et al*., 2007) yet the nanoindentation hardness data (**Fig. 6-2 C**) indicates that the PAO-K130I peptide does interact with the steel surface, but clearly this interaction occurs at a different site which is not recognized by the native PAK RBD or the K122-4 RBD, and thus is not a inhibitor PilA RBD mediated adherence to steel.

6. 3. Conclusions

The differential effects of the L-amino, D-amino, retro-inverso, and PAO K130I peptides on the surface properties of stainless steel suggest that chirality of the peptides influences peptide binding to stainless steel and that peptides will differentially recognize unanticipated chiral features, such a topographical features generated by the polycrystalline nature of steel that display some degree of chirality, on the steel surface. The data also suggests that bacteria are either capable of recognizing and binding to separate and distinct surface regions or that the chiral specific products have different properties that differentially affect bacterial surface interactions. The differential effects of the surface treatments on bacterial colonization indicates that different bacterial species and even strains of the same species can exploit several surface niches to initiate biofilm formation. The relative ineffectiveness of the D+RI-borgSS modified surface suggests that bacterial colonization of the hydrated modified surfaces is significantly impacted by surface hydrophobicity and charge patterns, classical features that are critical for biologically based molecular interactions, in addition to the classic surface physiochemical properties of a material.

Chapter 7

Surface modification of metals: Improvements in hardness, friction, and resistance to bacterial colonization

A version of this chapter was submitted to *Acta Biomaterialia*.
Davis, EM., Hodges, RS., Li, DY., and RT Irvin.

7. 1 Brief introduction

Given the successful modification of steel surfaces properties (**Chapter 4 and 6**) using variants of the RBD of *P. aeruginosa* (**Table 1**), we then sought to expand the potential versatility of the RBD by investigating whether the RBD could interact with other metal surfaces and modify their physicochemical properties. We hypothesized that the ability of the RBD peptide to interact with and form a novel state of matter with surface electrons was not limited to 304 stainless steel but could occur with other metal surfaces.

7. 2. Results

7. 2. 1. Surface modification and physical changes of peptide-modified titanium

Titanium is the preferred choice for prosthetic devices, including periodontal implants, artificial heart pumps, pacemaker cases, and hip-joint replacements. The high failure rate of titanium devices as a result of corrosion (Adya *et al*., 2005), stress fractures (Tagger Green *et al*., 2002), and biofilm formation (Subramani *et al*., 2005) highlights the need for the development of improved titanium implants.

7. 2. 1. 1. The RBD-titanium interaction leads to stabilization of surface electrons

We investigated whether the RBD could interact with the titanium surface electrons and result in stabilization of surface electrons in a manner similar to the peptide-steel interaction. Titanium (99.5% purity) was reacted with the D-amino, D-amino retro-inverso, and a combination of both the D-amino and retro-inverso K122-4(128-144)ox RBD peptides (**Table 1**) to generate new materials, termed D-borgTi, RI-borgTi, and D+RI-borgTi respectively, that were tested for changes in their surface properties compared to unaltered titanium. All three peptide treatments significantly increased the EWF of titanium (**P<0.001**)(**Fig. 7-1 A**). The greatest increase in EWF was observed for D-borgTi, with an EWF of 5.104±0.001 eV compared to 4.916±0.002 eV for unaltered titanium. The increase in EWF for RI-borgTI and D+RI-borgTi was not as great as that observed for D-borgTI, with EWFs of 4.976 eV and 5.035 compared to 4.916 for unaltered titanium. These results suggest that the presence of bound RBD of *P. aeruginosa* on the titanium surface can stabilize surface electrons and that formation of a novel organo-metallic state of matter between the RBD and the metal surface is not restricted to stainless steel but will occur when the RBD is bound on other metals. The EWF of D- borgTi and RI-borgTi differed significantly (**P<0.001**)(**Fig. 7-1 A**), suggesting that the titanium surface may also have chiral elements that are differentially recognized by the D-amino and retro-inverso peptides.

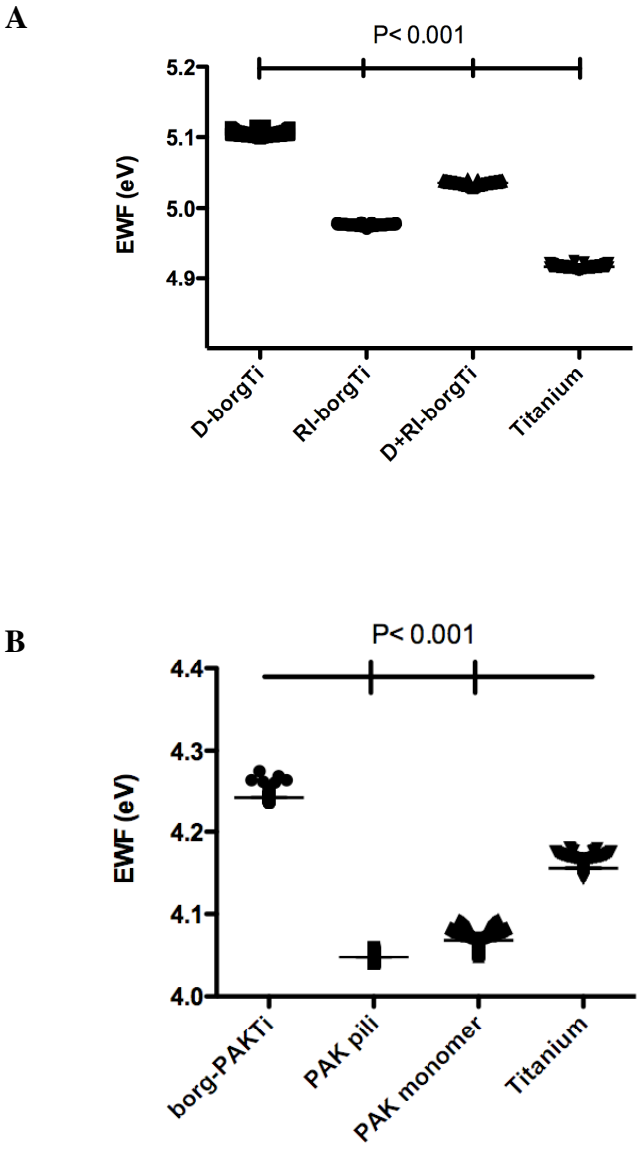

Figure 7-1. Electron work function measurements of modified titanium surfaces. A. Electron work function measurements of D-borgTi, RI-borgTi, and D+RI-borgTi surfaces. **B.** Electron work function measurements of titanium reacted with PAK(128-144)ox peptide, PAK pili, and PAK monomer as compared to unaltered titanium. All measurements were performed using a Kelvin probe. An area of 2μm x 2μm was tested and 400 measurements were taken per sample.

We also investigated whether T4P could facilitate the removal of electrons from the titanium surface. The activity of titanium surface electrons in the presence of PAK(128-144)ox peptide, monomeric pilin, full-length T4P from PAK, and unaltered titanium was detetermined. Titanium reacted with the PAK(128-144)ox peptide to form a more stable, less reactive surface termed borg-PAKTi. Borg-PAKTi possessed a significantly higher EWF of 4.243 eV compared to 4.156 eV for unaltered steel (**P<0.001**)(**Fig. 7-1 B**) and mirrored results obtained when characterizing stainless steel reacted with PAK(128-144)ox (**Fig. 5-1 A**). When full-length purified T4P was reacted with steel, the EWF decreased significantly, from 4.156 eV for unaltered steel compared to 4.043 eV when T4P were bound to the surface (**P<0.001**)(**Fig. 7-1 B**), indicating that bound T4P on the surface facilitates surface electron removal. Reacting a monomeric pilin with titanium yielded a surface that was significantly (**P<0.001**) more reactive compared to unaltered titanium, with the presence of PAK pilin monomer creating a surface with a EWF of 4.069 eV compared to 4.156 eV. These results are in agreement with the effects of the T4P and PAK monomeric pilin on stainless steel (**Fig. 5-1**) and indicate that the T4P and PAK monomer interact in a similar manner with stainless steel and titanium.

7. 2. 1. 2. Surface hardness of D-borgTi, RI-borgTi, and D+RI-borgTi

Nanoscale surface hardness measurement of D-borgTI, RI-borgTi, and D+RI-borgTi were obtained load-displacement plots using an AFM equipped triboscope. At a load of 1 mN all three surface were found to be significantly harder and less displacement into the surface was observed when compared to unaltered titanium (**P<0.001**)(**Fig. 7-2 A**). In the presence of peptides, total displacement into the surface of D-borgTi, RI-borgTi, and D+RI-borgTi were measured to be 3.21±0.43, 2.88±4.28, and 2.73±0.94 nm as compared to 9.92±1.44 nm for unaltered titanium. The D-amino and retro-inverso peptides bound to the surface significantly increased material hardness at the nanoscale. Surface treatment with a combination of both peptides to generate D+RI-borgTi did not improve surface hardness beyond what was obtained for D-borgTi and RI-borgTi. To determine whether improvements in hardness were limited to the surface of the material macroindentation testing of D-borgTi, RI-borgTi, D+RI-borg, and titanium was performed. When total displacement into the surface was calculated from load-displacement plots obtained using a load of 20 mN no significant difference was observed between D-borgTi, RI-borgTi, and unaltered titanium (**Fig. 7-2 B**). Modification of the titanium with D-amino, retro-inverso, and a combination of both peptides significantly increases hardness but this modification only alters the surface structure of the metals.

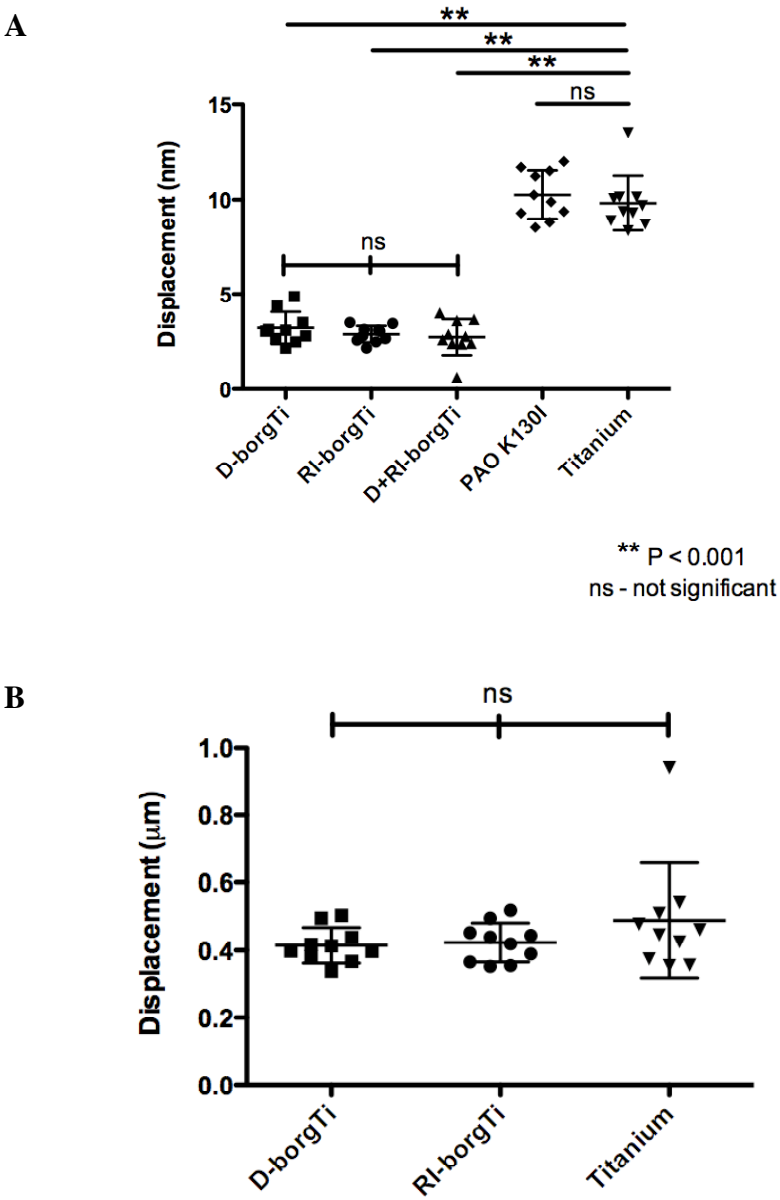

Figure 7-2. Nanoindentation characteristics of modified titanium surfaces. A. Total displacement into the surface of D-borgTi, R-borgTi, D+RI-borgTi and unaltered titanium was measured by nanoindentation using an AFM equipped with a triboscope. A load of 1 mN was applied and the displacement was obtained from the load-displacement plots. Ten measurements were obtained per sample. **B.** Total displacement into the surface of D-borgTi, RI-borgTi, and titanium was measured using a microindenter. A load of 20 mN was applied and 10 load-displacement plots were obtained per sample.

7. 2. 1. 3. Surface coefficient of friction of modified titanium surfaces

Friction occurs when two surface, that are moving in opposite directions, come into contact with each other and resist further movement. Decreasing the surface roughness, by smoothing out additional points of contact between the surfaces to facilitate movement, lowers friction (Porgess & Wilman, 1959). The surface coefficient of friction (COF) was measured by nanoscratch testing on lightly polished titanium surfaces bound with D-amino peptide, retro-inverso peptide, and a combination of both peptides. When a 500 μN load was applied to the surface, a small but noticeable decrease in the COF and a smoothing out of the surface of D-borgTi, RI-borgTi, and D+RI-borgTi was observed as compared to unaltered titanium (**Fig. 7-3**). In the presence of D-amino peptide a COF of approximately 0.2 was observed whereas in the absence of peptide the COF varied greatly, ranging from 0 to 0.5. Similarly, the surfaces of RI-borgTi and D+RI-borgTi had an average COF of 0.2 as compared to a COF of 0-0.5 for unaltered titanium, suggesting that unaltered titanium had a much rougher surface and that the surface was smoothed out when peptide was bound to the metal surface. Surfaces with higher electron reactivity will interact more readily with the nanoscratch tip to generate a higher COF. D-borgTi, RI-borgTi, and D+RI-borgTi all have surface electrons that are less reactive, as reflected by higher EWF values, as compared to unaltered titanium (**Fig. 7-1**) and a decreased COF could reflect a surface with stabilized surface electrons.

7. 2. 1. 4. Modified titanium is less susceptible to colonization by *P. aeruginosa*

Finally, we tested the ability of the D-amino and retro-inverso peptides to reduce initial surface colonization by *P. aeruginosa*. D-borgTi and RI-borgTi were exposed to bacteria for an hour and then imaged to compare the overall bacterial binding pattern in the presence and absence of peptide. A significant decrease in overall binding of *P. aeruginosa* to D-borgTi and RI-borgTi was observed compared to titanium (**P<0.001**) (**Fig. 7-4**) but no significant difference was observed in total number of bacteria binding to D-borgTi as compared to RI-borgTi, suggesting that D-borgTi and RI-borgTi are equally resistant to bacterial colonization by *P. aeruginosa* compared to an unaltered metal surface.

7. 2. 2 PEG-ylation of steel, titanium, and aluminum alloy surfaces for biofilm control

As discussed in the introduction (section 1.2.3), many options exist for modifying the physicochemical properties of surfaces. The major drawback of the described methods is that they are multi-step processes and in many cases are limited in their widespread use by having a

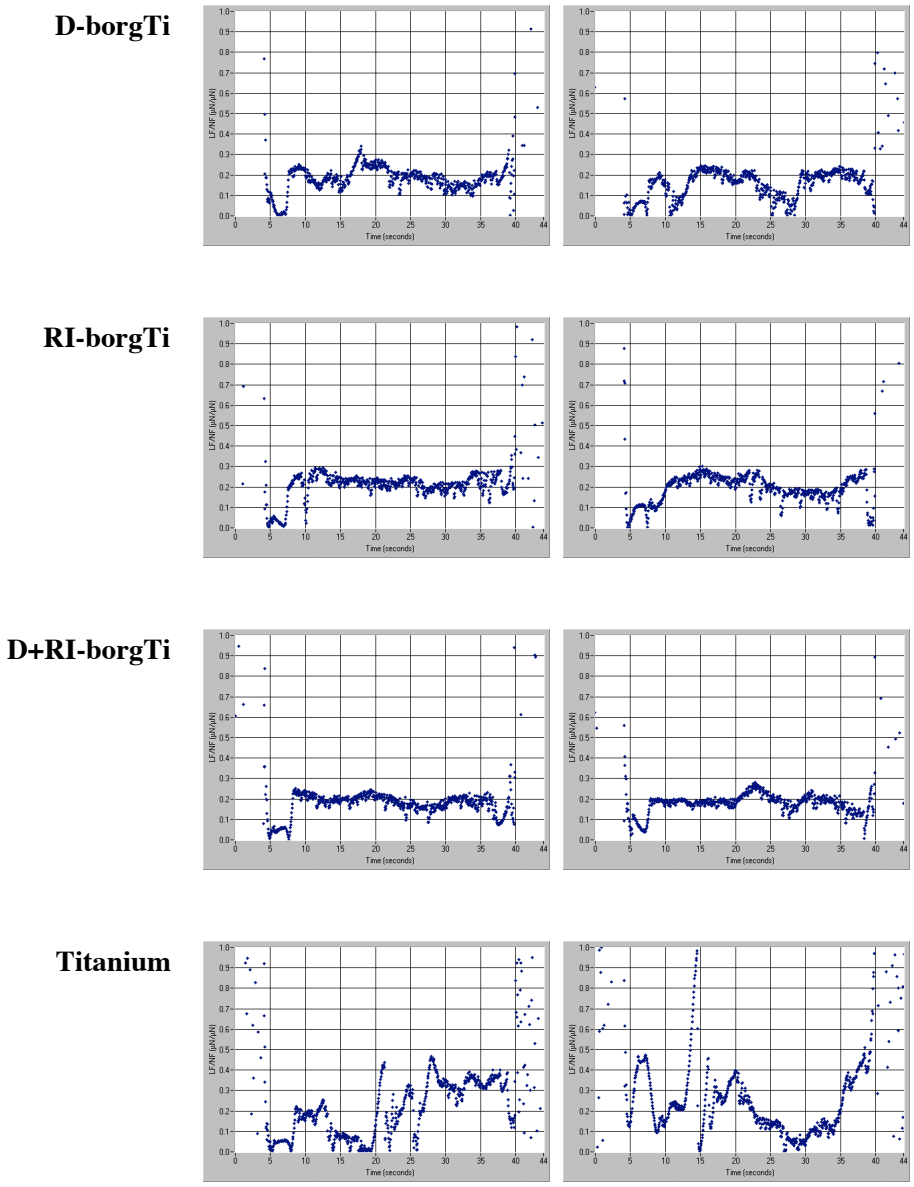

Figure 7-3. Coefficient of friction of modified titanium surfaces. Coefficient of friction over time measured during a 5 second scratch under a 500 μN load for D-borgTi, RI-borgTi, D+RI-borgTi, and titanium.

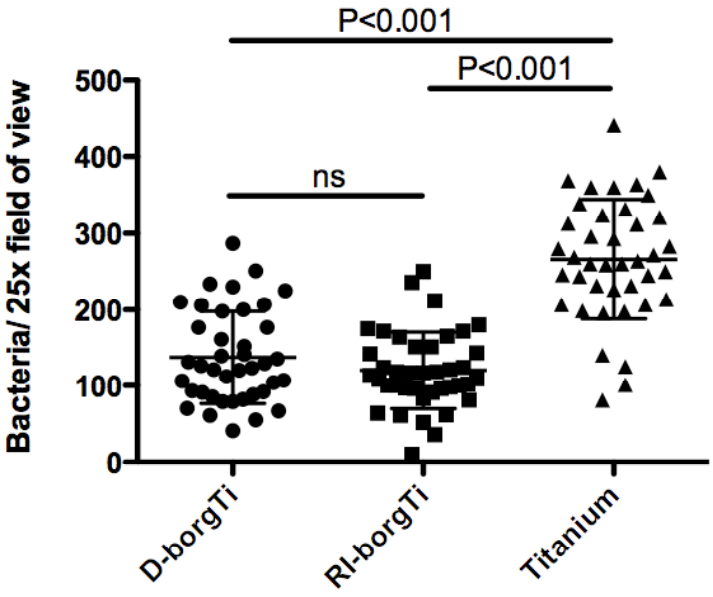

Figure 7-4. D-borgTi and RI-borgTi are less susceptible to colonization by *P. aeruginosa*. D-borgTi and RI-borgTi were colonized with PAK WT for one hour. The surfaces were stained with acridine orange and viewed by epifluorescent microscopy using the 25x objective. Twenty images were taken per sample and the total number of bound bacteria were enumerated per field of view.

specific function, thus requiring the development of individual modifications and coatings for the desired function and material to be modified. Versatile surface coatings present an attractive economical and efficient option to generate materials that can serve multiple functions. A single-step long-lasting multi-functional modification that reduces corrosion, friction, and bacterial colonization while increasing hardness fills an empty niche in the current market. Given the success of modifying the physicochemical properties of the surfaces of stainless steel and titanium, we sought to further alter the physicochemical surface of metals and increase the versatility of the RBD peptide variants.

A single-chain PEG molecule was covalently coupled via a linker to the N-terminus of the K122-4 D-amino peptide (**Table 1**). The D-amino RBD is an enantiomer, or mirror image, of the native RBD structure, and is protease resistant, but D-amino-borgSS displays similar increases in hardness and decreases in adhesive force as K122-borgSS created with the native L-amino peptide. The PEG molecule selected was monodisperse in terms of its molecular weight. PEG molecules have been extensively used to reduce the propensity of a surface for biofilm formation (section **1.2.3.3** of introduction).

We hypothesized that the PEG-D-amino peptide would retain the native peptide's properties by continuing to increase hardness and reduce corrosion but that the presence of the PEG molecule would also reduce friction and the surface propensity for bacterial colonization. Both pure metals and alloys, namely 304 stainless steel, titanium, and a plate of industrial A2024 aircraft aluminum were tested. The widespread use of 304 stainless steel and titanium in industry and the medical field have been previously discussed. A2024 aluminum is the predominant alloy used in applications where a high strength to weight ratio is required and is primarily used in aircraft, including the fuselage, wings, and blades of airplanes and helicopters. Aluminum A2024 has poor corrosion resistance and is often coated with aluminum-zinc to improve corrosion resistance, although surface coating can compromise the strength of the material and lead to increased fracturing (Polmear, 1995).

7. 2. 2. 1. Surface hardness of PEG-D-borg metal surfaces

We first confirmed that the initial properties of improved hardness and corrosion were still retained when a PEG molecule was added to the RBD and the PEG-D-amino peptide was reacted with metal surfaces. Hardness was measured by nanoindentation using a triboscope, composed of a pyramidal diamond nanoindenter probe attached to an AFM. Load-displacement plots were obtained for loads of 1mN and the hardness (H) and reduced Young's (or elasticity) modulus (E_r) were evaluated from the load-displacement plots using the built-in analysis

software. When 304 stainless steel was reacted with PEG-D-amino, the resulting material, which we termed PEG-D-borgSS, was significantly harder than unaltered steel. In the presence of the peptide surface hardness increased 2.77 fold, from 1311±446.6 GPa to 4945±1711 GPa (**P<0.0001**)(**Fig. 7-5 A**). Similar results were observed when titanium and A2024 aircraft aluminum were reacted with PEG-D-amino. These new materials were termed PEG-D-borgTi and PEG-D-borgAl respectively. Hardness in the presence of bound peptide was increased 9.6 fold, 6093±3716 GPa for PEG-D-borgTi compared to 575.5±275.3 GPa for unaltered titanium (**P<0.0001**)(**Fig. 7-5 C**) and by 101%, 2923±2082 GPa for PEG-D-borgAl compared to 1451±882.3 for unaltered aluminum (**P<0.05**)(**Fig. 7-5 E**). The presence of PEG-D-amino peptide bound to the surface significantly increased the relative hardness of all three metals significantly.

The reduced Young's modulus (E) of PEG-D-amino-reacted samples was also compared to those of unaltered metal surfaces as a second measure of relative hardness and material stiffness. When PEG-D was present on the surface of 304 stainless steel, Er was calculated, based on the indentation force-depth curve, to be 6540±1687 GPa for PEG-D-borgSS as compared to 2515±742.4 GPa for unaltered steel, an increase of 160% (**P<0.0001**)(**Fig. 7-5 B**). Similar results were observed for titanium, with the presence of PEG-D increasing the calculated Er by ~50%, from 144120±8331 GPa for unaltered titanium to 268416±29378 GPa for PEG-D-borgTi (**P<0.0001**)(**Fig. 7-5 D**). PEG-D modification of the surface of 2024 aluminum also significantly increased the overall material stiffness by 73%, with an Er of 26198±8240 GPa for PEG-D-borgAl as compared to an Er of 15097±2598 GPa for unaltered aluminum (**P<0.0001**)(**Fig. 7-5 E**).

These results suggest that the presence of the bulky PEG molecule on the surface does not impair the ability of the RBD peptide to significantly increase the overall hardness of the material. The peptide increased the material hardness and stiffness by a minimum of 50% for 304 stainless steel, titanium, and 2024 aluminum, with the greatest increase observed for 304 stainless steel. The PEG-D-amino peptide bound to the surface significantly increases material hardness at the nanoscale but this modification only alters the surface structure of the metals. The macroscale structural properties of the materials are unchanged as the bulk material defines the macroscale structural properties.

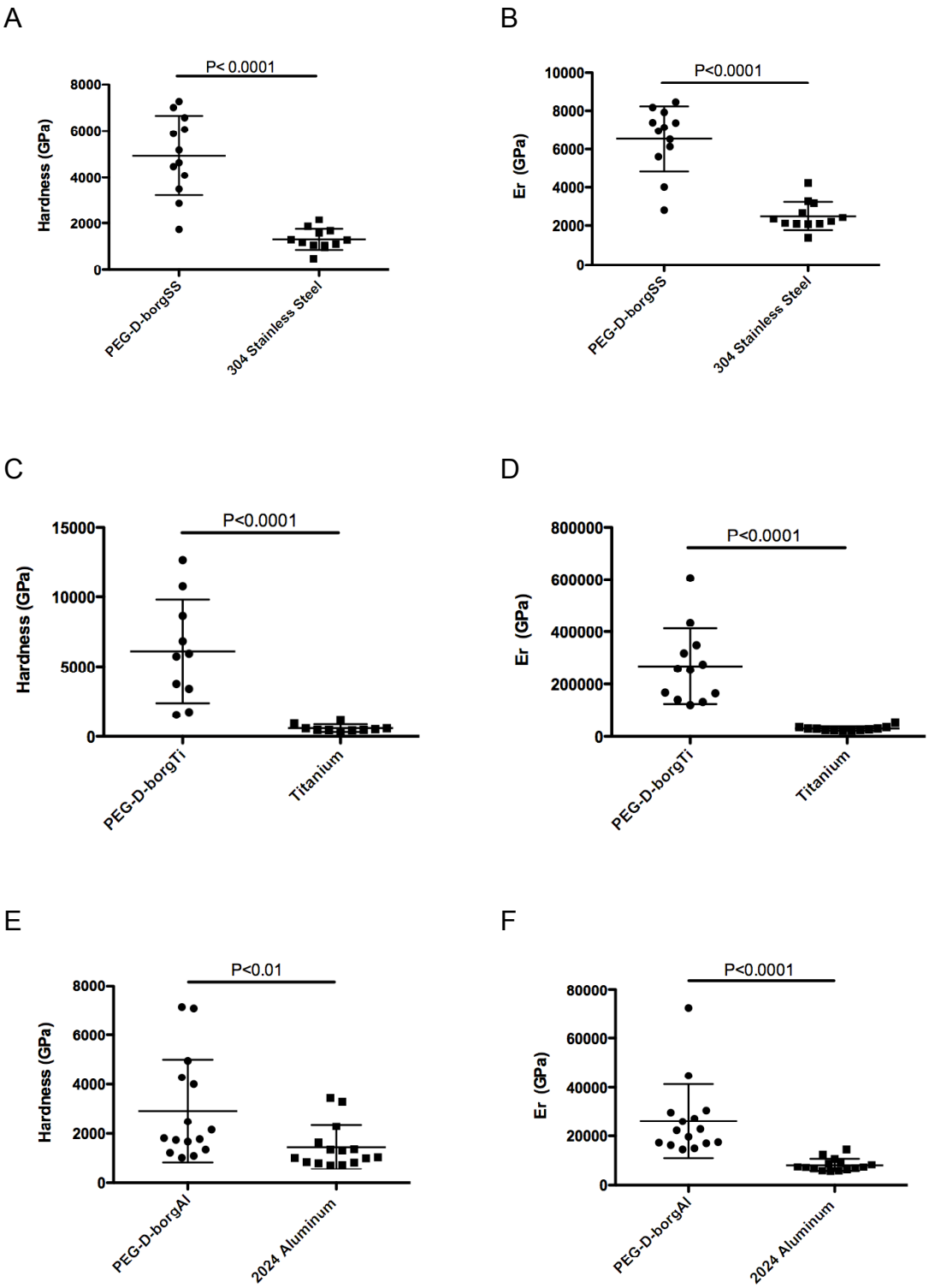

Figure 7-5. Nanoindentation characteristics of PEG-D-amino-modified surfaces of 304 stainless steel, titanium, and 2024 aluminum compared to unaltered surfaces. Overall hardness (**A, C, and E**) and the reduced Young's modulus (**B, D, and F**) were obtained based on 10 or 12 nanoindentation measurements under 1 mN load per sample.

7. 2. 2. 2. Electrochemical behaviour of PEG-D-borgSS and PEG-D-borgTi

Modifying the sample surface, from altering the element concentration of the alloy to coating the surface, alters the overall electrochemical behaviour of the sample and can be used to improve corrosion resistance. To determine whether the presence of the PEG-D-amino RBD modification improved the overall corrosion resistance of metals the polarization behaviour of metals reacted with the PEG-D-amino peptide was evaluated. Experiments were performed at room temperature in a 15 mM NaCl solution with neutral pH (7.4). Potentiodynamic polarization curves revealed that PEG-D modified PEG-D-borgSS and PEG-D-borgTi had higher corrosion potentials compared to their unaltered counterparts (**Fig. 7-6 A** and **7-7 A**). The corrosion rate of 304 stainless steel decreased by nearly 75% with PEG-D-amino modification of the steel surface, with a corrosion rate of 0.1621±0.1943 mpy for PEG-D-borgSS compared to a rate of 0.6559±0.3854 mpy for unaltered steel (**P<0.01**)(**Fig. 7-7 B**). A more moderate but still significant decrease of ~35% in corrosion rate was observed when titanium was modified with PEG-D-amino, with PEG-D-borgTi corroding at a rate of 0.02332±0.01036 mpy as compared to a rate of 0.03641±0.01616 mpy for unaltered titanium (**P<0.05**)(**Fig. 7-7 B**). These results strongly suggest that the PEG-D-amino peptide could function as a coating for metals to improve their corrosion resistance. It is worth noting that the PEG-D modified surfaces, where the PEG-D-amino peptide is covalently coupled to the metals, is considerably harder than the original unmodified surfaces. The increased hardness leads to a high resistance to mechanical attacks such as scratching. Stainless steel and titanium spontaneously form protective oxide layers that develop over time on their surface and breaks in the oxide layer have greater susceptibility to corrosion. Increasing the overall surface hardness of materials minimizes the potential for breaks in the oxide layer and provides a greater capability to protect metal surfaces from not only pure corrosion but also those involving synergistic attack of corrosion and mechanical actions.

7. 2. 2. 3. Surface coefficient of friction of PEG-D-borg surfaces

The presence of a bulky PEG molecule on the surface of metals should decrease the COF of the surface by essentially smoothing out the surface. The surface coefficient of friction was measured on lightly polished metal surfaces by nanoscratch testing. When a 500 μN load was applied to the surface, a noticeable decrease in the coefficient of friction of PEG-D-borgSS was observed as compared to unaltered steel (**Fig. 7-8 A**). In the presence of peptide a COF of approximately 0.1 was observed whereas in the absence of peptide the COF varied greatly, ranging from 0 to 0.6, suggesting that unaltered steel had a much rougher surface that could be smoothed out when peptide was bound to the metal surface. Similarly, the surface of unaltered

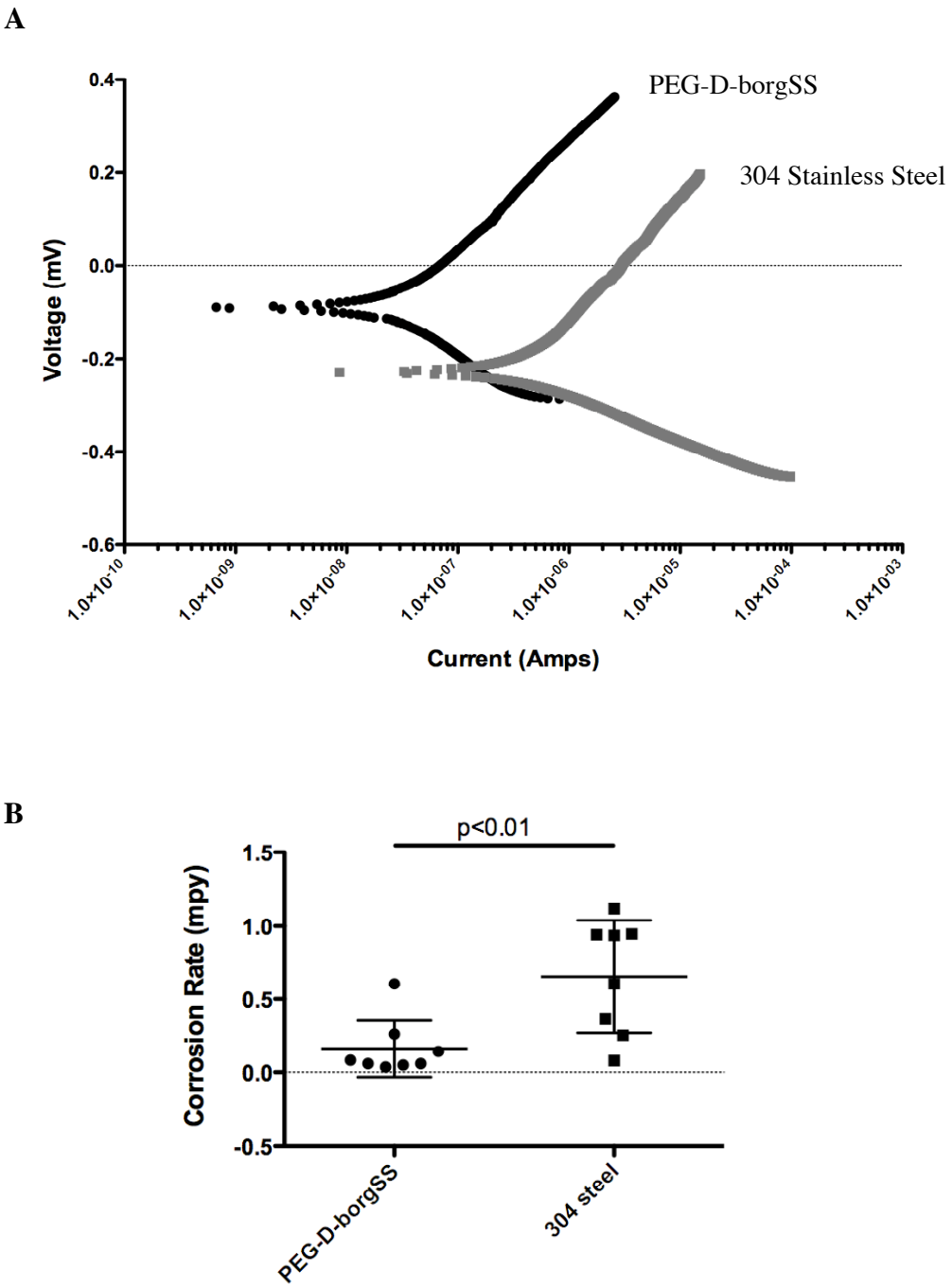

Figure 7-6. Electrochemical behaviour of 304 stainless steel reacted with PEG-D-amino. (**A**) Potentiodymanic polarization curves and (**B**) corrosion rates of PEG-D-borgSS and unaltered stainless steel surfaces. Representative potentiodynamic plots for PEG-D-borgSS (black) and 304 stainless steel (grey) were selected.

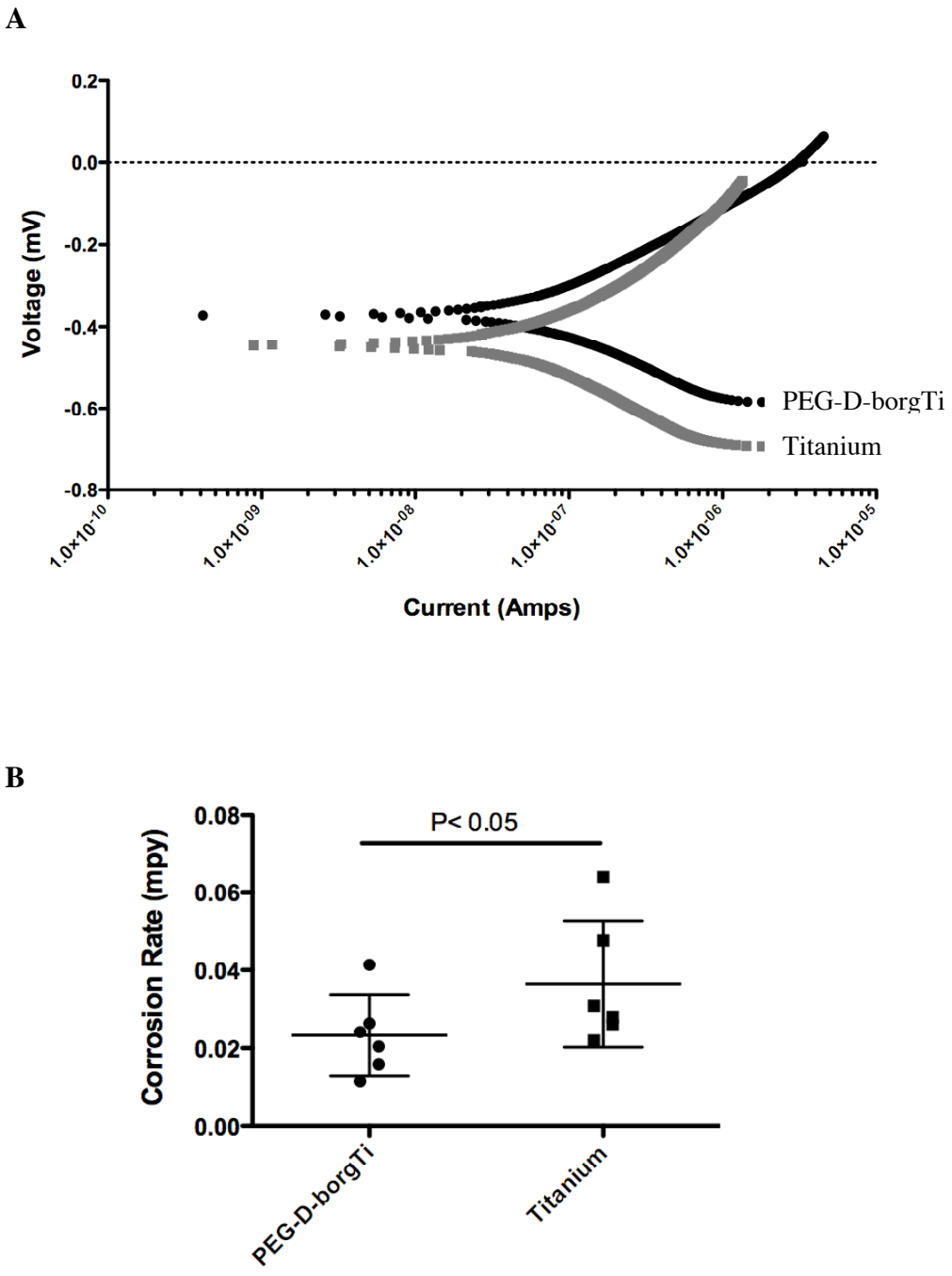

Figure 7-7. Electrochemical behaviour of titanium reacted with PEG-D-amino. (**A**) Potentiodymanic polarization curves and (**B**) corrosion rates of PEG-D-borgTi and unaltered titanium surfaces. Representative potentiodynamic plots for PEG-D-borgTi (black) and titanium (grey) were selected.

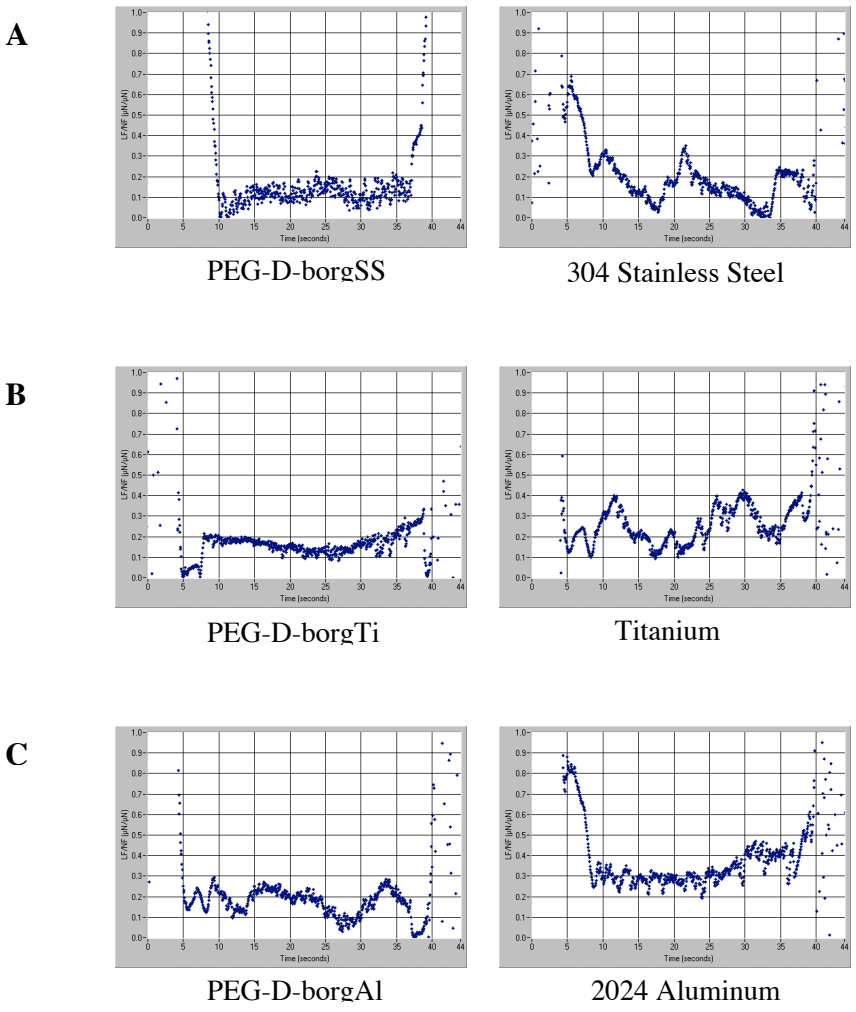

Figure 7-8. Coefficient of friction of PED-D-amino-modified surfaces. Coefficient of friction over time measured during a 5 second scratch under a 500 μN load for (**A**) 304 stainless steel, (**B**) titanium, and (**C**) 2024 aluminum.

titanium appeared much rougher, with a greater COF ranging from 0.1 to 0.4, compared to PEG-D-borgTi which had a COF averaging near 0.2 (**Fig. 7-8 B**). The PEG-D-borgAl surface did not appear smoother than unaltered aluminum but had a noticeably lower COF, appearing to average around 0.2, whereas the COF for unaltered 2024 aluminum averaged around 0.3 (**Fig. 7-8 C**). An important factor to consider is that when performing measurements on the nanoscale, the adhesive force of a material can lead to interactions between the nanoscratch tip and the surface and can become a significant and predominant force in influencing friction (Li & Li, 2004). When measured, there was no significant difference in the adhesive force between PEG-D-borgTi and unaltered titanium (**Fig. 7-9**), suggesting that differences in COF between surfaces are not the result of changes in the adhesive force but rather that the presence of the PEG molecule on the surface of the metal can reduce surface friction by smoothing out the surface. The PEG molecule is very flexible despite being tethered at one end to the metal surface end and can flow or move to effect surface smoothing. The increased surface hardness also helps to decrease friction by reducing the penetration of the nanoscratch tip, thereby helping to lower the resistance to lateral tip movement.

7. 2. 2. 4. Resistance to bacterial adhesion

PEG-ylation of surfaces is a well-documented method for reducing bacterial adherence and biofilm formation (Amiji & Park, 1993; Bearinger *et al*., 2003; Elbert & Hubbell, 1998; Lee *et al*., 1989; Liu *et al*., 2002; Llanos & Sefton, 1993; Prime & Whitesides, 1991; Prime & Whitesides, 1993). Traditional methods of PEG-ylating surfaces to develop very thin coatings involve attaching the polymer chains through one or several anchor points on the surface by either adsorption or chemical coupling the PEG to the surface. To covalently modify the surface, a multi-step process is required to graft the PEG molecule to the surface via a preformed functional group on the polymer or using *in situ* polymerization using an initiator immobilized on the surface (Pyun *et al*., 2003; Sirard *et al*., 2003). We tested the ability of the PEG-D modification of the metal surfaces to reduce initial surface colonization by *P. aeruginosa* and *S. aureus*. Titanium and 304 stainless steel surfaces were manually patterned with 1μL dots of 10μg/mL PEG-D. Following air drying, the surfaces were exposed to bacteria for an hour and then imaged to compare the overall bacterial binding pattern in the presence and absence of peptide. When the surface was modified by the addition of PEG-D to the surface, a noticeable and drastic decrease in overall binding of *P. aeruginosa* and *S. aureus* was noted relative to adjacent surface regions of unaltered stainless steel and titanium (**Fig. 7-10**).

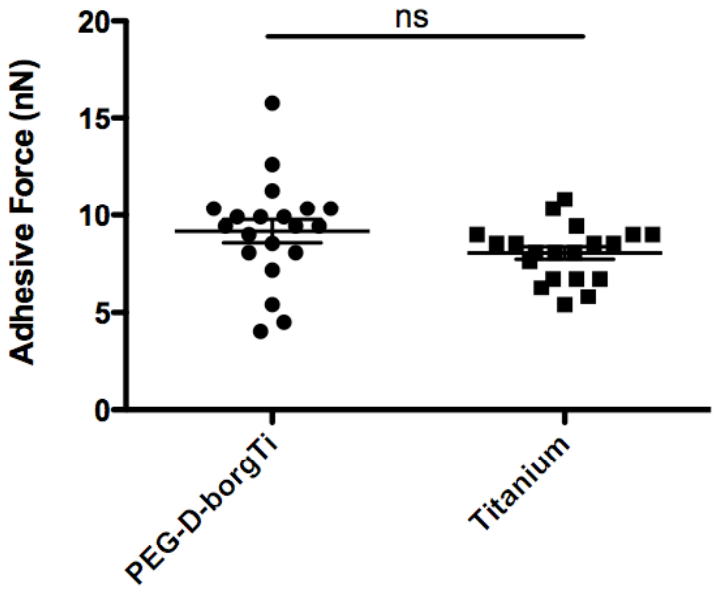

Figure 7-9. Adhesive force of titanium with PEG-D-amino bound to the surface. The adhesive force of PEG-D-borgTi and titanium was measured using an AFM in contact mode and equipped with a silicon nitride tip. Fifteen adhesive for measurements were obtained per sample and means were plotted.

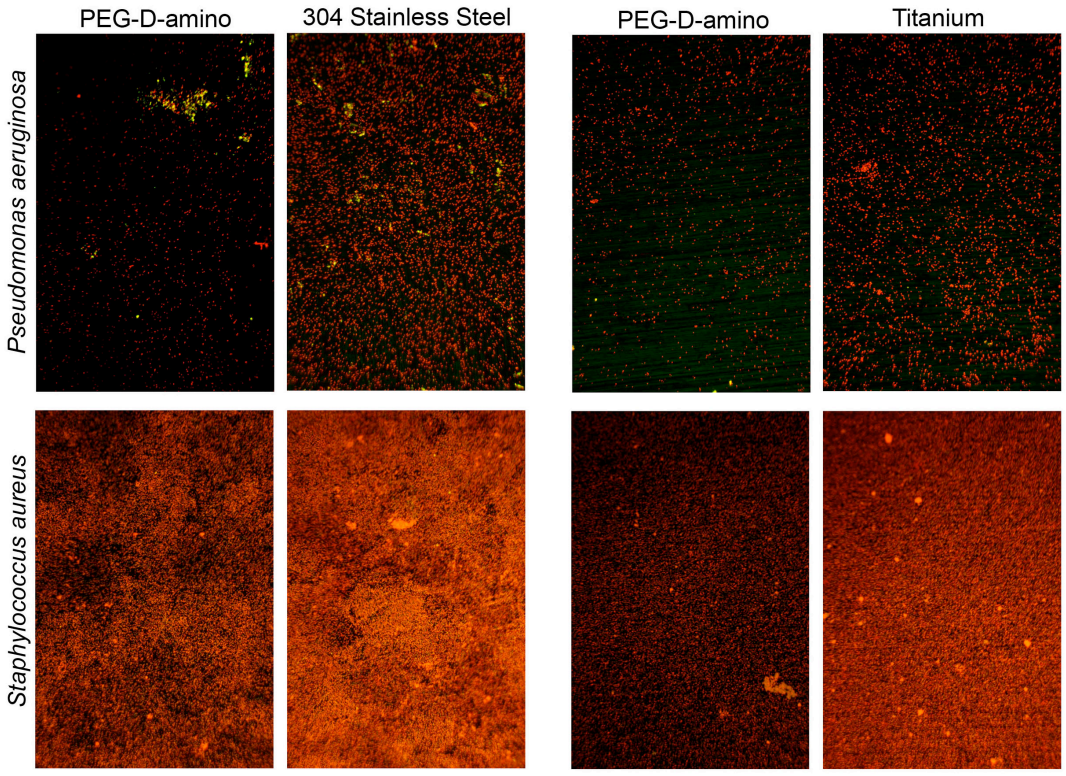

Figure 7-10. Adherence of *Pseudomonas aeruginosa* and *Staphyloccus aureus* to 304 stainless steel and titanium surfaces modified with PEG-D-amino. The surface of stainless steel was manually patterned with 1μL dots of PEG-D-amino peptide, allowed to air dry, and was colonized for one hour with *P. aeruginosa* or *S. aureus*. The sample were stained with acridine orange and viewed by epifluorescent microscopy using the 25x objective. Images were taken of bacterial colonization on the PEG-D-amino peptide dots and in regions immediately adjacent to the dots. Representative images are shown.

Kingshott *et al* (Kingshott *et al*., 2003) have previously demonstrated that for efficient bacterial reduction, covalent attachment of PEG to the surface is required and the data in Fig. 7-6 suggests that using the RBD of *P. aeruginosa* to covalently immobilize a PEG molecule to the surface of 304 stainless steel and titanium results in a surface that is more resistance to bacterial colonization by *P. aeruginosa* and *S. aureus* compared to an unaltered metal surface.

7. 3. Conclusions

The ability of the D-amino acid and retro-invero D-amino acid peptides of the RBD of *P. aeruginosa* were investigated to determine if reacting the peptides with the surface of metals other than stainless steel to generate novel bio-organic materials. Both peptides significantly modified the surface properties, generating surfaces that were less reactive, as observed by an increase in the EWF, had increased hardness, reduced friction, and were less susceptible to colonization by *P. aeruginosa*. These results indicate that the RBD can interact and form organo-metallic states of matter with the surface electrons of metals and that formation of novel peptide-metal states of matter is not restricted to stainless steel.

Additionally, a PEG-D-amino peptide, composed of the D-amino acid enantiomer and linked to a single-chain PEG molecule was investigated to test its versatility as a coating for modifying multiple surface properties of 304 stainless steel, titanium, and 2024 aircraft aluminum surfaces. Reacting PEG-D-amino with all three of these surfaces resulted in surfaces with improved surface properties, including an over 50% increase in hardness at the nanoscale, significant reduction in corrosion rates, and decreased friction for all surfaces. PEG-D surface modification also decreased colonization on 304 stainless steel and titanium. This surface modification method is a rapid, facile single-step reaction that generates a new metallo-organic material that substantially alters the surface properties of metals.

Chapter 8

Discussion

8. 1. The T4P catches and releases from stainless steel surfaces

The ability of *P. aeruginosa* to rapidly colonize and form complex, enduring biofilms on metal surfaces has significant implications for human disease and in environmental and industrial settings (Blenkinsopp *et al*., 1992; Hirsch & Rades-Rohkohl, 1990; Johansen *et al*., 1997; Leake *et al*., 1982; Stanley, 1983; Vanhaecke *et al*., 1990). Grade 304 stainless steel is widely used in surgical implants, hydrotherapy tubs in burn units, water storage and distribution, milk distribution pipelines, and power plant condenser tubes (Costerton *et al*., 1987; Gordon, 1987; Lewis & Gilmour, 1987; MacMillan, 1980; Mayer & Zinner, 1985; Passerini *et al*., 1992; Tredget *et al*., 1992). The colonization of these surfaces, combined with high intrinsic resistance of this pathogen to antimicrobials makes eradication of *P. aeruginosa* a continuous challenge in medical and industrial communities (Costerton *et al*., 1987; Costerton *et al*., 1999).

During the initial stages of biofilm formation, twitching motility plays an important role in the colonization of steel and other surfaces (O'Toole & Kolter, 1998). *P. aeruginosa* efficiently attaches to steel, moves along the surface, and then detaches (Merz *et al*., 2000; Sauer *et al*., 2007). During this energetically expensive and highly regulated process, the PilB and PilT ATPases control pilus extension and retraction through the polymerization and depolymerization of T4P PilA subunits at a rate of ~1000 subunits per second under laboratory conditions (Mattick, 2002). To move efficiently and smoothly, the pilus must be capable of attaching to, and releasing from the surface in a coordinated manner. Still, little is known of the mechanism underlying *P. aeruginosa* release from the surface once it has bound (Mattick, 2002; Turner *et al*., 1993; Whitchurch *et al*., 1991b; Whitchurch & Mattick, 1994).

In this study, we investigated the dynamics of *P. aeruginosa* colonization of steel surfaces and the requirements needed for efficient release from steel surfaces. More specifically, we examined the requirements of the *P. aeruginosa* strains PAK, and strains R364 and PAK S34 that have transposon insertions in the gene encoding the PilT and PilU ATPases in initial surface colonization and release from steel coupons.

8. 1. 1. *P. aeruginosa* release from steel is coupled to pilus retraction

The initial binding and colonization studies demonstrate that retraction associated ATPase motor is not required to mediated *Pseudomonas* attachment to surfaces. Wild-type PAK, as well as the retraction deficient PAK R364 and PAK S34 mutants, all efficiently colonized stainless steel (**Fig. 3-3 and 3-4**). While it may appear that the PAK R364 mutation enhances the overall rate of adherence compared to wild-type or the PAK S34 mutant because of the noticeably higher number of PAK R364 bacteria bound to steel (700 bacteria/FOV compared to 25-40

bacteria/FOV after 30 minutes of colonization) (**Fig. 3-3**), this is likely not the case but is rather a reflection of a post-binding event. Release and adhesion studies demonstrated that wild-type *P. aeruginosa* do not remain bound to steel but rather quickly detaches from the surface (**Fig. 3-4**). PAK WT and the PAK S34 mutant first bind to and then within 30 minutes following initial adherence have essentially completely dissociated or detached from the steel surface, presumably a reflection of a dynamic equilibrium (**Fig. 3-1 A and B**), making it difficult to determine how many binding and release events have occurred during a given incubation time. The T4P is estimated to extend and retract at a rate of 0.5 μm per second and can extend to a length of 5-10 μm (Skerker & Berg, 2001). Assuming that every extension and retraction cycle is coupled with a release from the surface, bacteria could be binding to the surface and releasing once every 30 seconds, allowing for numerous binding and release events during an hour incubation. It is reasonable to assume that PAK WT and PAK S34 bacteria, once bound to steel, may dissociate quickly from the surface in search of a more favorable or nutrient-rich environment instead of engaging in twitching motility, whereas PAK R364, once bound, will be unable to release. As a result, while it may appear that the absence of the PilT motor in the PAK R364 mutant enhances adherence to steel, the pilus retraction powered by the PilT ATPase is a necessary component for mediating the release from the surface, and in the absence of pilus retraction, steel colonization appears more efficient simply because no bacteria are releasing from the surface. Alternatively, apparent decrease in binding of PAK WT and PAK S34 could reflect that once the surface has been washed and fresh buffer is added the probability of binding is decreased as a result of the lower bacterial cell concentration in the new buffer volume. The possibility does exist that the increase in PAK R364 binding is the result of hyperpiliation but, given that once bound PAK R364 cannot release from the surface, the presence of multiple pili would only serve to more firmly anchor the bacterium to the surface and would not increase the total amount of bacterium bound since the initial binding event determines the fate of the bacterium. The absence of the PilU ATPase in the PAK S34 mutant does not appear to affect colonization or release of the bacteria from the steel coupons and may not play an important role in detachment of the pili from a surface.

8. 1. 2. Proteases are not required for the complete release of T4P from the surface

Pilus extension and retraction have been well described and visualized but the process through which the T4P releases from the surface following retraction remains unknown (Skerker & Berg, 2001). *P. aeruginosa* binds with strong affinity to steel (Giltner *et al*., 2006; Stanley, 1983). Given that the $Ki_{apparent}$ of the RBD for binding human epithelial cells is 120 μM, the

affinity for stainless steel surfaces, exemplified by a $Ki_{apparent}$ of 0.2 nM (a 600,000 fold difference in apparent affinities, not accounting for the multi-valency of the pilus fiber), is significantly and surprisingly greater than for eukaryotic surfaces. This high affinity for steel, including the high entropic penalty associated with the binding of a flexible peptide to a surface, makes it energetically expensive for the bacterium to undergo numerous rounds of binding and release during twitching motility. To circumvent the energy expenses required for breaking the interaction of the RBD with the steel, *P. aeruginosa* may release by shedding or proteolytically degrading the bound pilus but this method would also require energy as replacement pili must be generated to mediate future colonization events. To investigate whether *P. aeruginosa* releases from steel by shedding or through the use of proteases, surfaces colonized by WT bacteria were challenged with PAK R364 bacteria. PAK R364 bacteria bound in equivalent levels to steel surfaces that were previously exposed to PAK WT compared to naïve surfaces that had not been previously exposed, suggesting that *P. aeruginosa* releases cleanly from steel and does not leave behind a portion of the pilus bound to the surface (**Fig. 3-5 A**), since the presence of bound pili or synthetic RBD peptide would inhibit future surface colonization by the bacterium (Giltner *et al.*, 2006). To confirm that the pilus releases cleanly and that remaining bound pili are not removed by proteases, and that release is not mediated by proteolysis of the pilus, PAK WT bacteria were incubated in the presence of protease inhibitors. If release requires a proteolytic step, then WT bacteria should be unable to release or will have reduced release kinetics in the presence of protease inhibitors. Lower amounts of total bound bacteria should be observed following PAK R364 colonization (employed in these studies in order to assess only the binding phase of the interaction of the bacterium and the surface) on samples where wild-type bacteria were exposed to the protease inhibitors. Similarly, if the pilus does not dissociate cleanly from steel, then the addition of inhibitors would prevent proteolysis of any bound T4P remaining on the steel coupons and lower amounts of PAK R364 would be observed binding. However, the binding of the PAK R364 mutant was not affected by the presence of protease inhibitors and no PAK WT bacteria were left on the surface, suggesting that during release no portion of the T4P remains bound to the steel and is left behind. Thus, bacterial release from steel surfaces appears to be a complete dissociation of the T4P from the surface that is protease-independent and no portion of the pilus remains bound to the surface following release.

8. 1. 3. T4P release from steel requires viable bacteria

One possibility that cannot be entirely discounted is that a dynamic equilibrium exists between the T4P and the steel, where pili bind and dissociate freely. However, the very high

affinity and strength of interaction between the RBD and steel surface strongly suggests that the dissociation rate would be very low and would in fact cause the organism to remain stuck in place. Even if there was a rapid enough dissociation from the surface, this would imply that release is not an event that is controlled by *P. aeruginosa*. Thus, the bacterium could release randomly from the surface during twitching motility, thereby decreasing motility efficiency. When steel was coated with PAK(128-144)ox peptide or pili, neither the peptide nor the pilus released from the surface over time and could not be displaced from the surface in the presence of exogenous peptide (**Fig. 3-6 A, C, and D**), suggesting that binding and release are not the result of a rapid dynamic equilibrium between the surface and the pilus. Large, excessive amounts of unbound pili with a much higher apparent affinity for the steel due to their increased avidity could only partially displace bound PAK(128-144)ox peptide from the steel surface (**Fig. 3-6 B**). This could be due to the valency of the pilus, as three receptor binding domains (RBD) are exposed at the T4P tip, as compared to one RBD encoded in the peptide, and the 3:1 ratio of binding domains promotes the displacement of the peptide in the presence of the pilus. However, when equivalent numbers of RBDs are present, such as when pili are added in the presence of bound pili, displacement does not occur and any bound pili remain attached to the steel surface. Our results suggest that release must be mediated by the bacterium, as purified pili will not release from the surface, and is not the result of a rapid dynamic equilibrium existing between the pilus and the steel.

We have demonstrated that PAK R364 strain did not desorb from the steel surface due to the lack of a functional PilT ATPase while the lack of a functional PilU ATPase does not appear to impair bacterial release. The mechanism of pilus release from the surface is unclear and could involve a number of factors that could allow the pilus to exist in various states or conformations, with one state capable of binding to steel and one incapable of binding. The T4P system is complex in that it not only generates substantial forces, generating up to 150 pN of force during retraction (Clausen *et al*., 2009), but includes a force sensor where retraction is shifted to pilus extension if the force on the pilus increases beyond the normal levels (Maier *et al*., 2004).

In summary, our observations strongly suggest that T4P release from surfaces is an active process that is tightly controlled by the bacterium. Productive twitching motility coordinates pilus extension, binding, retraction, and release to generate very effective and rapid movement along solid surfaces. The release of the pilus from steel does not leave behind a residual portion of the T4P. Purified pili and synthetic RBD does not readily dissociate from the steel surface, implying that pilus release is affected by means of an active cellular process that alters the state or conformation of the pilus fiber.

8. 2. The RBD of *P. aeruginosa* forms a novel peptide-steel state of matter with metal surface electrons

Given the high affinity of the RBD for stainless steel surface and our observations that (i) T4P dissociate completely from the steel surface, (ii) T4P do not passively dissociated from the surface, and (iii) release appears to be an active cellular process controlled by *P. aeruginosa*, we hypothesized that the RBD was interacting with the steel surface using a novel mechanism. Traditional biological receptor-ligand interactions are mediated by hydrophobic interactions, where the exclusion of water molecules and other bulk solvents provides the energy required for binding (Li & Logan, 2004; Morra & Cassinelli, 1997; Pereni *et al*., 2006) and yet the RBD binds directly to the steel surface in the absence of a conditioning film and with enough strength to withstand the forces generated by the retracting pilus (Yu *et al*., 2008). In metallic surfaces bonding between metal atoms occurs when valence electrons become delocalized and form an electron cloud around the positive ion cores (**Fig. 1-7**). The surface electrons are mobile and interact with their environment. The reactivity of surface electrons is directly described by the EWF which also influences other important physicochemical properties of the metal surface, including the adhesive force, surface hardness, surface friction, and corrosion propensity (Ashcroft & Mernim, 1976; Guan *et al*., 2005; Hua & Li, 2012; Li & Li, 2002; Li & Li, 2005). Some areas in the metal grains structure, such as the grain boundary, have a decreased EWF, reflecting the increase in electron reactivity. AFM adhesive force studies using an RBD-derived silicon nitride tip demonstrated that the RBD-steel interaction is strongest in regions of low EFW and high electron activity, such as the grain boundary, suggesting that the strength of the RBD-steel interaction is directly proportional to the surface electron activity (Yu *et al*., 2010). We hypothesized that the RBD could interact with the delocalized electrons of the steel surface and that electron sharing formed a novel organo-metallic state of matter between the RBD and the delocalized electrons on the steel surface. We investigated the molecular basis of the RBD-steel interaction by examining changes in the physicochemical surface properties of steel reacted with the synthetic peptide K122-4(128-144)ox, synthetic native RBD peptide, hypothesizing that electron sharing between the RBD and steel would result in measurable changes in the reactivity of surface electrons and would alter the chemical composition of the metal surface.

8. 2. 1. Physicochemical characterization of borg-K122SS

Stainless steel was reacted with the K122-4(128-144)ox peptide to generate a new material that was termed borg-K122SS. We hypothesized that sharing of electrons between the RBD and steel surface would results in measurable changes in the reactivity of steel surface

electrons. The EWF of borg-K122SS and stainless steel was measured by Kelvin probe. Borg-K122SS had a significantly increased EWF (**P<0.001**)(**Fig. 4-1 A**) as compared to stainless steel, with the EWF of steel increasing from 4.79±0.07 eV to 4.9±0.05 eV in the presence of bound RBD, suggesting that the presence of the RBD stabilizes surface electrons. We sought to confirm these results by indirectly assessing electron reactivity by measuring the adhesive force and hardness of borg-K122SS and stainless steel. The adhesive force is an indirect measurement of EWF, with "sticky" surfaces possessing more reactive surface electrons. The adhesive forces of borg-K122SS and stainless steel were 19.4±8.8 nN and 56.7±10.5 nN respectively, confirming that bound RBD on the stainless steel surface significantly increased the adhesive force (**P<0.001**) (**Fig. 4-1 C**). Nanoindentation measurements were obtained using loads from 50 to 400 μN. Even at the highest load of 400 μN a significant decrease (**P<0.0001**) in the indentation displacement of borg-K122SS relative to the steel surface was observed (**Fig. 4-1 E**) and at all loads borg-K122SS was ~40% harder than unaltered steel. The EWF, adhesive force, and nanoindentation data all strongly suggest that surface electrons are stabilized when the RBD is bound to the stainless steel surface.

Interestingly, when K122-4(128-144)ox was reacted with a pure aluminum surface to generate RBD-aluminum, no significant differences in the EWF, adhesive forces, and hardness were observed between unaltered aluminum and aluminum treated with peptide (**Fig. 4-1 B, D, and F**). Unaltered aluminum is more reactive than stainless steel, with an average EWF of 3.9 eV compared to 4.7 eV, and if the only important criteria for electron sharing between the RBD and a metal surface is the presence of reactive surface electrons then the RBD should readily interact with the aluminum surface. The RDB-aluminum data suggests that other factors in the metal surface are important for electron sharing and matter of state formation.

8. 2. 2. Borg-K122SS is a chemically distinct material

To confirm that a novel organo-metallic state of matter was created during the RBD-steel interaction we examined the chemical and electronic state of borg-K122SS. Electron sharing alters the position of electron within the electron orbitals of metal atoms in stainless steel. Analysis of XPS spectra of the borg-K122SS and stainless steel surfaces confirmed that both materials are chemically distinct. No shifts in the spectra of the iron and chromium 2p 1/2 and 3/2 orbitals, carbon 1S orbital, and nitrogen 1S orbital were observed, suggesting that these orbitals do not have an important role in bond formation (**Fig. 4-4**). A noticeable peak in the oxygen 1S orbital spectra of borg-K122SS, with an increase to 60 CPS as compared to 40 CPS (**Fig. 4-5 A**), indicates that oxygen may have a role in bond formation. Alternatively, the amino

acids of the peptide contains oxygen atoms and the increase in oxygen 1S orbitals in borg-K122SS could reflect the increase in oxygen atoms present on the metal surfaces when peptide is present. The peptide is composed of 24% oxygen and when reacted with steel using saturating concentrations of 10 μg/mL, generates borg-K122SS where the peptide is observed on ~50% of the metal surface (**Fig. 4-6**), most likely accounting for the ~50% increase, from 40 CPS to 60 CPS, of oxygen 1S orbitals observed in borg-K122SS. Stainless steel contains negligible amounts of sulfur and as expected no sulfur was detected on the surface but the RBD contains two sulfur atoms that are involved in disulfide bond formation. No classical sulfur peak was detected in the borg-K122SS sample, but a peak near the sulfur 1S was identified (**Fig. 4-5 B**). This peak could not be positively identified as it did not match any known sulfur peaks. Given that borg-K122SS should have detectible amounts of sulfur on the surface we suspected that this peak could represent a far red-shifted sulfur electron binding energy and that the classical sulfur peak was shifted due to the involvement of the sulfur in bond formation. A second unidentified peak near the iron 3s orbital was also identified on the borg-K122SS surface but this peak was absent in spectra obtained from the stainless steel surface (**Fig. 4-5 C**). The changes in the spectra of oxygen, sulfur, and iron on the surface of borg-K122SS indicate that these elements may play significant roles in bond formation and also conform that borg-K122SS is a new material that is chemically unique from 304 stainless steel.

Direct visualization of the RBD on steel by AFM in contact mode was unsuccessful and Auger-SEM analysis was employed to examine the surface distribution of nitrogen, oxygen, sulfur, and carbon to confirm the presence of the RBD on the surface of borg-K122SS. Steel contains large amounts of carbon and oxygen and both element were homogenously distributed across the surface of borg-K122SS (**Fig. 4-6 A and B**). Nitrogen and sulfur are not typically found on steel and their presence on the borg-K122SS surface indicates the presence of bound RBD. Nitrogen and sulfur localized as discrete nanostructures across the surface that could not be visualized by standard SEM (**Fig. 4-6 E**) and localization resulting in ~50% coverage of the steel surface, suggesting that the RBD peptide is binding at unique sites on the metal surface and coverage of the surface is not complete but discrete.

This discrete binding pattern also serves to confirm that we are in fact characterizing the surface properties of borg-K122SS (ie. the RBD-steel interface) and not the properties of the RBD alone. If our characterization techniques (EWF, adhesive force, hardness), were only measuring the peptide, then we would expect to see two distinct populations of data when examining a steel surface reacted with RBD, one representing the characterization of the steel surface (which would be identical to our unaltered steel control) and one for the peptide, given

that the surface is only covered by ~50% of the peptide. However, our data strongly suggests that we are in fact characterizing the organo-metallic interface between the RBD and steel, and that a new material, which has altered surface properties from unaltered stainless steel, is generated at this interface.

8. 2. 3. Formation of borg-K122SS requires disulfide bond cyclized RBD

We suspected that the stabilization of surface electrons through the RBD was partially dependent on the delocalization of the electrons in the disulfide loop present in the RBD and that electrons were shared between multiple contact points between the RBD and the steel. To test this hypothesis, borg-K122SS was incubated with the trypsin, an endoprotease that recognizes lysine residues, and the EWF of the surface was measured before and after treatment. Treatment of borg-K122SS with protease released the RBD from the surface and abolished the increase in EWF observed for borg-K122SS. Biotinylated K122-4(128-144)ox peptide could no longer be detected following trypsinization (**Fig. 4-7 A**), and there was no significant different between the EWFs borg-K122SS treated with trypsin and stainless steel (**Fig., 4-7 B**), demonstrating that the RBD must cyclized in order that electrons from the steel are delocalized to create a novel organo-metallic state of matter as a result of the RBD-steel interaction.

In summary, we have characterized a novel material that is readily formed when stainless steel is exposed to a synthetic peptide that constitutes the *Pseudomonas aeruginosa* PilA RBD, which functions as the functional adhesin for the T4P of *P. aeruginosa*. This new material was termed borg-K122SS and possesses significantly different physical and chemical properties compared to unmodified 304 stainless steel. The surface of borg-K122SS is less reactive than stainless steel, as demonstrated by a higher EWF and a lower adhesive force. Borg-K122SS is significantly harder than stainless steel. XPS spectra data of borg-K122SS suggests that multiple contact points may exist between the peptide and the steel, with two currently unassigned electron orbitals, one likely due to a far red-shifted sulfur electron binding energy, which supports the formation of novel chemical interaction. This novel state of matter is most likely formed by electron de-localization through the disulfide loop of the RBD and multiple contact points between the RBD and the steel assist in electron de-localization. State of matter formation results in chemical and physical stabilization of the surface. Given these results, the high apparent affinity of the RBD for the steel surface and the strength of the RBD-stainless steel interaction, which anchors the pilus to the surface and enables the progressive movement of the cell along that surface when the pilus retracts, appears reasonable given the formation of a novel chemical interaction with the surface.

8. 3. The T4P of *P. aeruginosa* is a variable resistance nanowire

Proteins and peptides are important mediators of electron transfer in biological systems (Cretich *et al*., 2006; Dawson *et al*., 2006; Ligler & Erickson, 2006) and recently T4P functioning as "bacterial nanowires"(Reguera *et al*., 2005) have been characterized in environmental metal reducing bacteria such as *S. oneidensis* and *G. sulfurreducens*. The N-terminal region of PilA of *P. aerugniosa* shared sequence similarity with the pilin protein of *G. sulfurreducens* (**Fig. 1-9**). Given that the RBD of PilA shares electrons with metal surfaces and forms what can essentially be considered an electrical connection between the metal surface and the T4P, there is both experimental evidence and theoretical models to strongly suggest that the T4P of *PA* may be an insulated molecular nanowire, with the N-terminal region acting as a central conducting core and the C-terminal region creating an insulating protein cover.

To confirm our hypothesis that the T4P of *P. aeruginosa* can function as a nanowire we employed various materials engineering and electrochemical tests to demonstrate electron flow through the pilus.

8. 3. 1. The T4P facilitates electron removal from the steel surface

As shown previously, EWF measurements revealed that reacting the steel surface with a synthetic peptide of the RBD generates a new material. The PAK(128-144)ox peptide reacted similarly to what was observed when K122-4(128-144)ox was reacted with steel and formed borg-PAKSS. Borg-PAKSS had stabilized surface electrons and possessed a significantly higher EWF compared to unaltered steel (**P<0.001**)(**Fig. 5-1 A**) and a significantly lower corrosion rate (**P<0.01**)(**Fig. 5-2 A**). Potentiostatic studies support electron stabilization and demonstrate that, when applied to steel surfaces, the RBD functions as an insulator by decreasing current flow from 14.5 μA to 9.1 μA (**Fig. 5-4**) when a constant physiologically relevant potential of +150 mV is applied to the metal surface.

The RBD functions as a surface electron stabilizer and surface insulator whereas the presence of full-length PAK T4P pilin monomers in the form of intact pilus fibers appeared to facilitate the removal of surface electrons. The EWF of stainless steel decreased significantly (P<0.0001) from 4.7 to 4.3 eV (**Fig. 5-1 B**) when T4P were bound to the steel surface and the corrosion rate significantly increased (**P<0.05**)(**Fig. 5-2 B**). These data suggest that a more reactive and conductive surface is generated in the presence of T4P. Potentiostatic measurements of current flow through the T4P further support the conclusion that the T4P of *P. aeruginosa* functions as a conductive nanowire. When a +150 mV potential was applied constantly to a steel surface the current flow greatly increased from 14.5 μA for unaltered steel to 60 μA in the

presence of bound T4P (**Fig. 5-4**). The nanowire function is retained when the pili are anchored to the bacterial surface, as demonstrated by electrochemical testing of stainless steel surfaces colonized by *P. aeruginosa*. In the presence of bacteria, the corrosion rate was observed to decrease by 50% (from 0.1 mpy to 0.05 mpy) (**Fig. 5-3**), reflecting the uptake of the electrons up the pilus fiber and into the bacterium instead of being detected by the counter-electrode.

8. 3. 3. The T4P is a sensor that modulates current flow in response to extracellular stimuli

A novel finding of this study is the ability of the T4P to function as a variable resistance nanowire capable of sensing environmental stimuli and increasing or decreasing the current flow accordingly. Modulating current flow is most likely the result of conformational changes in the T4P fiber that alter the distance between electron or hole residence sites in the pilus fiber. This would effectively alter the electron transfer rates/probability and directly alter the resistance of the wire. In the presence of the quorum-sensing molecule PAI-2, wild-type *P. aeruginosa* bound in greater numbers to stainless steel (**Fig. A1, A2 i**). Incubating full-length pili with PAI-2 increased the amount of pili that bound to stainless steel, with a maximal increase of 100% when using physiological concentrations of 3.8 μM of PAI-2 (**Fig. A2 ii**). Similar results were observed for binding to asialo-GM1, BECs, and DNA (**Fig. A3 i, ii, and iii**), suggesting that autoinducer can interact directly with T4P to affect its binding properties, an alteration in the conformation of the T4P. Ethanol (95%), at very low concentrations, in the absence of PAI-2 also increased T4P binding to stainless steel but the increase in binding was significantly less compared to when PAI-2 was present (**P<0.0001**)(**Fig. A2 ii**). When T4P immobilized on the steel surface were pre-treated with PAI-2 prior to being exposed to a constant +500 mV voltage, the current flow through T4P exposed to PAI-2 was decreased compared to untreated T4P, whereas pre-treatment with ethanol increased current flow (**Fig. 5-5**). This differential effect of PAI-2 and ethanol suggests that the pili respond differently to ever-changing environmental stimuli. PAI-2 and ethanol interacted with unaltered stainless steel to increase to current flow from 67.6 μA to 113.9 μA and 75.7 μA, respectively (**Fig. 5-5**). Ethanol had similar effects on T4P and unaltered steel, increasing the current flow by 11% for steel and by 35% in the presence of T4P, suggesting that the greater increase in current flow in the presence of the T4P is the result of the T4P responding to the presence of ethanol (**Fig. 5-5**). If the ethanol had no effect on the pilus, the increase in current flow would have been the same regardless of the presence of the T4P on the steel surface but an additional 20% increase was observed when T4P were present, strongly suggesting that the ethanol does affect current flow through the T4P. In contrast, pre-treatment with PAI-2 resulted in a 68% increase in current in unaltered steel, but a 47% decrease

in current when T4P were bound to the surface, strongly suggesting that PAI-2 interacts directly with T4P, that this result decreased current flow through the pilus fiber by increasing the resistance in the T4P, and that the change in the T4P is sufficient to counteract the observed increase in current flow that occurs when steel is exposed to PAI-2 in the absence of T4P.. A possible explanation for the large difference in current flow in the presence and absence of PAI-2 and ethanol is that the interaction of external stimuli with the T4P results in conformational changes in PilA that directly affect the resistance of the T4P. Studies examining structural fluctuations in α-helical polypeptides demonstrated that electron transfer rate is highly sensitive to structural changes and minor changes in the spacing of resting sites had significant effects on the final transfer rate (Daizadeh *et al*., 1997; Wolfgang *et al*., 1997). Given that the length of the T4P is relatively constant and that all T4P are exposed to constant voltages, then the functional resistance of the nanowire must be changed in order to observe changes in the current flow. Changing the conformation of the pilin subunits, thereby altering the distance between the resting sites within the T4P necessary for electron transfer throughout the length of the pilus, could result in a controllable way to change the overall electrical resistance of the T4P and account for the observed variations in the current.

To acquire further evidence that the T4P senses and reacts to external stimuli, a constant voltage was applied to T4P exposed to UV light for the duration of the experiment. When exposed to UV light, current flow through the T4P decreased by ~90%, effectively shutting down current flow, whereas exposure of unaltered steel to UV light resulted in a ~300% increase in current flow (**Fig. 5-6**). These data further suggest that the T4P senses external stimuli and responds by altering current flow through the pilus fiber. In this case, exposure to UV light primes the T4P to switch to an "off" conformation, preventing current flow through the pilus to such an extent that the effect of UV light on stainless steel, a large increase in current flow, can be counteracted and prevented by the T4P. The ability of the T4P to regulate current flow through conformational changes is reflected in the corrosion rate measurements. The wide variability in the corrosion rate of PAK T4P may be explained as a fluctuation between conformations, resulting in a range of corrosion rates (**Fig. 5-2 B**). These fluctuations are minimized when the T4P is anchored to the bacterium (**Fig. 5-3**), possibly because the conformational changes are regulated by the bacterium and, in the absence of bacteria, the T4P is in a state of dynamic equilibrium between various conformational states in aqueous solution. Similar fluctuations in the corrosion rate were observed when monomeric pili were used to coat stainless steel instead of T4P (**Fig. 5-6**)

8. 3. 4. Proposed model for electron transfer in T4P

Many models have been put forward describing electron transfer through peptides and proteins. Current models propose that electrons traveling over a range of short distances (10-25 A) between redox centres move by single-step electron tunneling (Crane *et al*., 2001; Gray & Winkler, 2003; Langen *et al*., 1995; Skov *et al*., 1998). Compared to other models of electron transfer through peptides, T4P are significantly larger and longer (~2500 nm), and electrons must travel much longer distances through the protein. Travel over large distances (> 30 A) requires a multi-step tunneling or hopping process where the electron travels through the protein by hopping between energetically accessible discrete resting sites in the protein (Frey, 1990; Stubbe & van der Donk, 1998). Resting sites can include passing through covalent and hydrogen bonds and amino acids capable of accommodating charges, such as arginines, tyrosines, and tryptophans (Long *et al*., 2005). Lysine and arginine have a net positive charge at a neutral pH and could theoretically accommodate an electron. The transfer of electrons at high potentials requires the involvement of the side chains of redox active amino acids, such as those in tyrosine, phenylalanine, and tryptophan (Gray & Winkler, 2003; Gray & Winkler, 2005) and strongly influenced transfer rates in cytochrome c and b_5 (Liang *et al*., 1987; Yao *et al*., 1997). Disulfide loops can also stably accommodate electrons and transfer electrons between amino acid side chains and between proteins (Banci *et al*., 2012).

The RBD of *P. aeruginosa* contains several amino acids that could serve as resting sites for tunneling electrons. A positively charged lysine is conserved at position 140 (**Fig. 1-4**) and several strains of *P. aeruginosa* have arginine residues present in the RBD, including PAK at position 144 and KB7 at position 138. The highly conserved disulfide loop, as well as additional arginine residues in the N-terminal helix and two tryptophan residues found in PilA, particularly a strictly conserved tryptophan located just outside the RBD at residue 127, could also accommodate an electron. The disulfide loop was shown to be necessary for state of matter formation between the RBD and steel and this new state of matter was abolished when the disulfide loop cyclized structure was degraded by proteases (**Fig. 4-7**) and novel state of matter formation between the metal and the T4P is likely the first step in electron transfer. Once the RBD-steel interaction is established electrons can begin flowing up the T4P, hopping between resting sites until they reach the bacterium and *P. aeruginosa* can extract many electrons from the metal surface by removing electrons from the electron cloud.

In order for transfer to occur, the resting sites must be properly spaced and based on model of T4P assembly any amino acid in the RBD would be placed approximately 30A from a matching residue in an adjacent RBD. This is a reasonable distance for multi-step electron

tunneling. Secondary structure can also influence electron transfer within a protein and both helical and beta-sheet secondary structures, such as those of the N-terminus and C-terminus of PilA and other pilin proteins, can facilitate electron transfer (Sek *et al*., 2006). Assembly of the T4P so that the N-terminal hydrophobic domain of PilA is located in the internal core of the pilus whereas the C-terminal domain surrounds the internal core (Craig *et al*., 2006) provides a structure where electrons could theoretically hop between RBDs or a combination of resting sites within the α-helices and β-sheets and suggests that the C-terminal globular domains are insulating conductive core.

Furthermore, as previously hypothesized, the EWF data of the monomeric pilin suggests that the central hydrophobic core may play an important role in electron conductance. Monomeric PAK pilin is composed of a truncated version of the PilA pilin monomer, where truncation of the first 28 residues of PilA, which are highly hydrophobic yields a soluble pilin monomer that still retains the receptor binding properties of the full-length pilus (Hazes *et al*., 2000; Keizer *et al*., 2001). The truncated portion of the N terminal helical domain constitutes ~48% of the equivalent *Shewanella* pilin protein that assembles to form nanowires. During assembly, residues 1-28 of the N-terminus remain exposed whereas residues 29-54 are predicted to pack onto the C-terminal globular head. Truncation of residues 1-28 resulted in a slight but significant decrease in EWF compared to unaltered steel (4.18 eV compared to 4.21 eV, **Fig. 5-1 C**), suggesting that monomeric pilin can somehow still facilitate electrons removal from metal surfaces but removal is significantly impaired as a result of the truncation. Results from potentiostatic measurements further support the importance of the central core for current transfer across the pilus. When a constant voltage of +150 mV was applied to steel reacted with monomeric pili, very little current was recorded (**Fig. 5-4**).

It is possible that the decrease in EWF (**Fig. 5-1 A**) and increase in corrosion rate (**Fig. 5-2 B**) and current flow (**Fig. 5-4**) in the presence of bound full-length pili are reflecting changes in the steel surface, as a result of pili binding, and are not evidence of electron transfer through the pilus. However, if only the presence of bound pili was required to facilitate electron removal, then the monomeric pilin should have a similar effect on current measured, as it would similarly affect the steel surface. The lack of current flow through the monomeric pilin (**Fig. 5-4**) strongly suggests that the quaternary structure of the pilus plays an important role in electron transfer. Additionally, the effect of PAI2 on current flow through the pilus strongly suggests that the current is channeled through the pilus. PAI2 has been shown to bind to and affect T4P binding, most likely through conformational changes in the T4P, not only to steel but also to asialo-GM_1, DNA, and buccal epithelial cells. If current was not flowing through the pilus then the quaternary

structure and structural conformational changes in the pilus, as a result of PAI2 interacting with the T4P, would have no effect on the current measured and similar currents to those measured for steel in the presence of PAI2 would be observed for steel in the presence of T4P and PAI2, yet a clear difference was observed (**Fig. 5-5**). These data all suggest that the T4P can facilitate electron transfer and conduct current.

We present experimental evidence, supported by theory, demonstrating that the T4P of *P. aeruginosa* may function as a bacterial nanowire that is capable of sustaining currents of up to several mA over a period of time. In addition, through conformational changes in response to changes in the environment, our data suggests that the pilus alters its electrical resistance through a dynamic range of conformational states that switch between allowing higher or lower rates of current transfer.

8. 4. Evidence of chiral features in metals

Bacterial adherence to abiotic surfaces is the crucial first step for successful surface colonization and biofilm formation. Limiting or completely abolishing initial adherence of bacteria to surfaces is an attractive method for preventing the financial and health issues that emerge as a result of biofouling. Preventing material corrosion (Lechevallier *et al*., 1993), contamination of food and food processing equipment (Costerton, 1984), and nosocomial infections from contaminated implants and medical equipment (Passerini *et al*., 1992) is economically advantageous and would extend the longevity of materials that would otherwise need to be replaced as a result of contamination by bacterial colonization.

In order to successfully develop surface treatments that abolish biofilm formation one must understand the fundamental basis governing bacterial adherence to surfaces. Unfortunately, despite decades of investigation and a large amount of information, the molecular mechanism for baterial attachment to abiotic surfaces has yet to be fully described.

In Chapter 4 we sought to describe the actual molecular basis for *P. aeruginosa* attachment to stainless steel and established that binding was mediated by the direct interaction of the RBD with steel in the absence of a conditioning layer and that formation of a novel organo-metallic state of matter between the RBD and the surface electrons of stainless steel occurred in the absence of hydrophobic interactions. This is the first description of the molecular basis governing the binding of a bacterial adhesin to an abiotic surface and it is likely that this mechanism would only be observed in bacteria that possess a type IV pilus and which utilize pilus retraction to power twitching motility or utilize an adhesin that displays extensive homology with the type IV pilus RBD.

We hypothesized that bio-organic surfaces generated using the PilA RBD would have a decreased propensity for bacterial adherence and biofilm formation based on the observations that borg-K122SS had a surface with a lower adhesive force (**Fig, 4-1 C**). We predicted that a less "sticky" surface would limit the adsorption of bacteria, proteins, and other materials that traditionally form the conditioning layer exploited by bacteria for surface colonization. The original borg-K122SS surface is generated by reacting stainless steel with a synthetic peptide of the native RBD composed of L-amino acids and as a result borg-K122SS is protease sensitive. Sensitivity to proteases greatly limits the potential applications of borg-K122SS because bacteria naturally produce a number of proteases that would degrade the RBD.

8. 4. 1. Enantiomers of the RBD have differential effects on surface properties

To overcome the issue of protease sensitivity we generated two variants of the native RBD, a D-enantomeric isomer and a retro-inverso D-amino acid residue containing peptide of the RBD. Both peptides are predicted to have a 3-D structure similar to that of the native RBD (Hung *et al*., 1999; Mandal *et al*., 2009), with the D-amino enantiomer being a mirror image of the native structure and the retro-inverso peptide having a structure similar to the L-amino acid RBD (**Fig. 6-1**). Peptides composed entirely of D-amino acids are protease resistant and as predicted the D-amino and retro-inverso variants were not susceptible to trypsinization (**Fig. 6-3**). The D-amino and retro-inverso RBD peptides reacted with the steel to generate two novel protease resistant bioorganic metals that were termed D-borgSS and RI-borgSS. A third borg steel surface was generated by reacting the surface with a combination of both peptides to generate the D+RI-borgSS surface. These borg steel variants both displayed a decreased surface adhesive force (**Fig. 6-2 B**) and increased hardness (**Fig. 6-2 C**) but displayed different surface electron properties as exemplified by different EWFs (**Fig. 6-2 A**). D-borgSS and RI-borgSS also varied in their corrosion rates, with RI-borgSS having a significantly reduced corrosion rate compared to stainless steel (**$P<0.05$**)(**Fig. 6-4**) whereas D-borgSS had a variable corrosion rate (**Fig. 6-4**). The differences in EWF and corrosion rate between D-borgSS and RI-borgSS were unexpected given that the D-amino and retro-inverso peptides have the same chemical composition and have identical net hydrophobic/charge properties (**Fig. 6-1**) and suggests that the stereochemistry of the RBD influences the stabilization of electrons during bond formation since the D-amino and retro-inverso peptides differ only in their 3-dimentional structure. This most likely reflects a chiral specific reaction of the peptides with the steel surface.

8. 4. 2. Bacteria employ different adherence mechanism to colonize different sites on steel surfaces

We employed a number of bacterial isolates to investigate the importance of surface adhesive force, electron activity (in terms of the EWF), and stereochemistry on the propensity of surfaces to allow for biofilm formation. We observed that decreasing the average adhesive force of a surface, which has been generally attributed to van der Waals forces (Renner & Weibel, 2011), does not directly reduce the surface's propensity for biofilm formation as the retro-inverso peptide interaction with 304 stainless steel was generally able to reduce the adherence of several bacterial species and strains to RI-borgSS, but the RI peptide did not significantly inhibit binding of *Listeria monocytogenes* strains I9 and J10 or *Staphylococcus aureus* strain 25923 (**Fig. 6-5 B and C, 6-6 A**). However, the D-amino peptide interaction with 304 stainless steel did inhibit binding of all strains tested (**Fig. 6-5, 6-6**) and yet the adhesive force properties of the D-borgSS did not differ from that of RI-borgSS (**Fig. 6-2 B**). Modifying stainless steel with both the D-amino and retro-inverso peptides was largely ineffective in reducing the surface propensity for biofilm formation, and D+RI-borgSS surfaces displayed enhanced adherence of *Listeria monocytogenes* strain H8 (**Fig. 6-5 A**), had no effect on adherence of *L. monocytogenes* strain I9 (**Fig. 6-5 B**) or *S. aureus* strain 2593 (**Fig. 6-6 A**) or inhibited bacterial binding but not significantly better than observed for steel modified by the D-K122-4 alone (**Fig. 6-5, 6-6**). These observations suggest that alteration of the surface electron activity, as described by the observed surface EWF, does not directly correlate to a surface's propensity for biofilm colonization as the EWF of D-borgSS was lower than those observed for RI-borgSS and D+RI-borgSS surface and yet D-borgSS showed the lowest propensity for bacterial colonization. Previous studies had demonstrated that a low surface electron activity was associated with a higher propensity for biofilm formation (Yu *et al*., 2007; Yu *et al*., 2008), but these studies only utilized *P. aeruginosa*. *P. aeruginosa* utilizes the PilA RBD to directly interact with the surface, whereas *L. monocytogenes, L. innocua, S. aureus*, and *S. epidermidis* do not possess T4P and use other mechanisms to colonize steel surfaces.

8. 4. 3. The RBD displays stereospecific interaction with steel surfaces

We had originally hypothesized that the D-amino and retro-inverso peptides would equivalently interact with the steel surface yet the differential effects of the D-borgSS and RI-borgSS surfaces on bacterial colonization suggest that the hydrophobicity and charge of the surfaces may differ despite having identical chemical compositions. The surface localization of

the peptides was explored using biotinylated versions of the peptides to determine whether the interaction of the peptides with stainless steel surfaces was equivalent. D-amino and D-amino retro-inverso K122-4 peptides were synthetized with a biotin molecule attaches to the N-terminus via a Gly-Gly-Gly linker.

The localization pattern of the peptides on the 304 steel surface was found to differ significantly with the localization pattern of the retro-inverso peptide appearing very similar to that observed with the native K122-4 RBD while the D-amino binding was observed to be much more punctuated in nature with more intensely labeled regions (**Fig. 6-7**). The differential localization of the peptides on the steel surface suggests that peptide chirality influences binding and that the enantiomers may be interacting with chiral features on the steel surface.

Adsorption of chiral molecules onto metal surfaces has been extensively studied. Chirality can be introduced onto simple intrinsically achiral surfaces by adsorbing chiral molecules onto the surface in what has been termed chiral modification. Alanine, the simplest of chiral amino acids, adsorbed onto single crystal Cu(110) to form adlayers characterized by regions completely covered by alanine alternating with empty regions (channels)(Jones *et al*., 2006; Rankin & Sholl, 2005; Sayago *et al*., 2005). At low concentrations, below what would be necessary to form dense adlayers, D-cysteine molecules formed dimers with a characteristic shape that could be distinguished from L-cysteine dimers and demonstrated stereospecific adsorption patterns on the surface. Dimers composed of one D- and one L-cysteine were never observed (Kuhnle *et al*., 2002; Kuhnle *et al*., 2004).

Although chirality is most commonly associated with organic and biological molecules, more complex solid surfaces, including pure metals and alloys, possess intrinsic chirality that arises when the symmetry of the crystal structure is broken and misalignments are introduced in the metal surface (McFadden *et al*., 1996; Sholl, 1998). When adsorbing onto chiral surfaces, chiral molecules display enantiospecific adsorption patterns that have been demonstrated using electrochemical (Ahmadi *et al*., 1999; Attard, 2001) and vaccuum experiments (Horvath & Gellman, 2001; Horvath *et al*., 2004).

While there does not appear to be a chemical basis for chiral centers in stainless steel, such as those observed in biological molecules, we suspect that the polycrystalline nature of the material generate topographical features that may display some degree of chirality and thus interact preferentially with one or the other of the D-amino and retro-inverso enantiomers of the PilA RBD. The enantiomeric specificity of the steel surface is reflected in the differential localization of the peptides on steel (**Fig. 6-7**).

Further evidence for chiral-specific binding sites on stainless steel were obtained by observing interaction of a mutant of the *P. aeruginosa* PilA RBD from strain PAO1 with stainless steel. It was previously believed that the PAO K130I RBD could not bind to stainless steel based on evidence that it did not inhibit *P. aeruginosa* strain K binding to stainless steel (Giltner *et al*., 2006). In light of the possibility that stainless steel possessed multiple binding sites, we hypothesized that PAO K130I might in fact interact with the 304 stainless steel surface but at a different site.

Surprisingly, we observed that the synthetic peptide PAO(128-144)oxK130I peptide we had used in previous studies (Yu *et al*., 2007; Yu *et al*., 2008) did interact with 304 stainless steel to reduce the adhesive force of the surface and increased the surface hardness (**Fig. 6-2 B and C**), strongly suggesting that the L-amino PAO K130I peptide interacts with a region of the 304 steel surface that is not recognized by the native PilA RBDs, thus explaining why it did not inhibit binding of *P. aeruginosa* on steel.

Collectively our results indicate that the surface of 304 stainless steel is considerably more complex than previously hypothesized. The differential interaction of the D and L-enantiomers and the D-amino retro-inverso variant of the K122-4 RBD suggests that there are chiral features on the steel surface that are recognized by the pepides. The differential interaction of the L-PAO K130I RBD and the PAK RBD indicates that there is further structural complexity present on the steel surface that the *P. aeruginosa* RBD variants readily discern. The differential effects of the D-amino and retro-inverso peptide modification of the steel surface and the differential features of these surfaces for their propensities for biofilm formation are significant as they indicate that bacteria utilize a range of surface structures to initiate biofilm formation and that individual species and even different strains have long evolved in association with surfaces and have evolved or adapted to very specific environmental niches for biofilm formation

Unfortunately, although a significant decrease in biofilm formation was observed for the D-borgSS surface bacterial adherence was not completely inhibited, Reacting the steel surface with both the D-amino and retro-inverso pepties had unexpected detrimental effects and in some cases increased the propensity of the surface for biofilm formation. The localization of the peptides on D+RI-borgSS may have generated novel hydrophobic/charge patterns on the surface and that some strains could exploit these regions for enhanced biofilm formation. These results demonstrate that there is a complex interplay of factors, including surface complexity, that influence bacterial adherence. Furthermore, additional improvements are necessary to decrease the propensity of the surface for biofilm formation while avoiding modifications with detrimental effects that unexpectedly facilitate bacterial adherence.

8. 5. Modifications of metal surfaces for improved performance

8. 5. 1. RBD stabilizes surface electrons of titanium to generate new materials

Stainless steel surface properties were successfully modified using the synthetic peptides K122-4(128-144)ox of the RBD and the D-amino and D-amino-retro-inverso variants of the peptide. Reacting the peptides with the steel surface generated new materials and the formation of a peptide-steel state of matter via the sharing of delocalized surface electrons. All metal surfaces are composed of grains and metal atoms are bonded together when valence electrons become delocalized and form an electron cloud. We hypothesized that the RBD would be able to interact with other metals and form peptide-metal states of matter with the surface.

Reacting 99.5% pure titanium with the D-amino and retro-inverso peptides and a combination of both peptides generated three new titanium surfaces, termed D-borgTI, RI-borgTi, and D+RI-borgTi. The electrons on all three surfaces were significantly more stabilized and the surfaces were harder compared to an unaltered titanium surface (**P<0.001**)(**Fig. 7-1 A, Fig. 7-2 A**). A similar increase in EWF was obtained when PAK(128-144)ox was reacted with titanium (**P<0.001**)(**Fig. 7-1 B**), strongly suggesting that the RBD interacts with the titanium and forms an organo-metallic state of matter that stabilizes the surface. PAK T4P or PAK monomeric pili bound to the titanium surface decreased the EWF of the surface (**P<0.001**)(**Fig. 7-1 B**), providing further evidence that the RBD interacts with titanium surface electrons and that the presence of T4P can facilitate electron removal from the surface in a manner similar to that observed for T4P bound to stainless steel (**Fig. 5-1 B**). The surfaces of D-borgTi, RI-borgTi, and D+RI-borgTi were noticeably smoother than the unaltered titanium surface and had lower COFs (**Fig. 7-3**) and D-borgTi and RI-borgTi were less susceptible to colonization by *P. aeruginosa* (**Fig. 7-4**). Titanium surface properties can therefore easily be modified by the RBD.

Interestingly, titanium reacted with PAO K130I, a single point mutant of the native PAO RBD, did not show improved hardness of titanium (**Fig. 7-2 A**). PAO K130I increased the hardness of stainless steel (**Fig. 6-2 C**) and decreased the adhesive force of the surface (**Fig. 6-3 C**) despite being unable to inhibit *P. aeruginosa* colonization of stainless steel (Giltner *et al*., 2006; Yu *et al*., 2007). On stainless steel PAO K130I appears to recognize a binding site that is distinct from the sites recognized by the native RBD and its enantiomers whereas PAO K130I does not appear to bind to titanium surfaces and does not improve surface hardness. One possibility is that the titanium and stainless steel surfaces do not possess the same topographical features recognized by the peptides. 304 stainless steel is an alloy and contains iron, chromium, nickel and manganese. The surface is heterogeneous and the joining of different metal atoms may create more structural complexity than what is observed on pure titanium, essentially

creating more distinct binding sites that can be recognized by the RBD. Metal surfaces appear to possess more structural complexity than previously anticipated.

8. 5. 2. PEG-ylation of metal surfaces improves physical properties of the surface

Stainless steel surfaces modified with the D-amino and retro-inverso-D-amino variants of the RBD displayed different propensities for biofilm formation and were differentially colonized by strains of *L. monocytogenes*, *L, innocua*, *S. aureus*, and *S. epidermidis* and in some cases the presence of the peptides had detrimental effects and increased bacterial adherence to the surface (**Fig. 6-5**, **6-6**).

We hypothesized that we would be able to improve our surface modification approach and further decrease a surface's propensity for biofilm formation if the resulting material surface did not display significant charge or hydrophobic regions, by incorporation or linking a PEG molecule to the surface. PEG surface modifications have previously been shown to be somewhat effective in reducing biofilm formation propensity (Khoo *et al*., 2010; Tanaka *et al*., 2010).

The ability of a PEG-D-amino peptide, composed of the RBD of the Type IV pilus of *P. aeruginosa* and linked to a single-chain PEG molecule was investigated to tests its versatility as a coating for modifying multiple surface properties, including hardness, corrosion resistance, friction, and resistance to bacterial colonization, of 304 stainless steel, titanium, and 2024 aircraft aluminum surfaces. Reacting PEG-D-amino with stainless steel, titanium and aluminum surfaces generated three new materials that were termed PEG-D-borgSS, PEG-D-borgTi, and PEG-D-borgAl respectively (**Table 1**). All three surfaces displayed a 50% increase in hardness at the nanoscale (**Fig. 7-5**), significant reduction in corrosion rates for PEG-D-borgTi and PEG-RI-borgSS, and decreased friction for all surfaces (**Fig. 7-3**). We suspect that covalent coupling of the PEG to metal surfaces and resulting decrease in corrosion rates may in part be due to the dielectric properties or insulating properties of the PEG. PEG-D surface modification also decreased colonization of *P. aeruginosa* and *S. aureus* on 304 stainless steel and titanium (**Fig. 7-10**), consistent with previous studies that have demonstrated that covalent coupling of PEG to surfaces decreases biofilm formation on those surfaces (Kingshott *et al*., 2003). Our surface modification method represents a very rapid single step reaction, involving non-toxic materials, which creates a single molecule thick layer of organometallic material that substantially alters the surface properties of metals.

8. 5. Future applications

We have demonstrated that metal surfaces can easily and rapidly be modified by the RBD of *P. aeruginosa* and that surfaces with different physicochemical surface properties can be generated. Stainless steel, titanium, and aircraft aluminum surfaces modified with RBD have stabilized surface electrons, decreased adhesive force, increased hardness, decreased friction, and decreased corrosion rates.

The PEG-D-amino peptide shows that additional molecules can be successfully linked to the RBD without compromising the ability of the RBD to form the peptide-metal state of matter with the surface and to modify the properties of the surface. These findings provide many possible future applications in both industry and medicine.

Biomaterial engineering focuses on improving the performance, compatibility, and longevity of biomaterials while still preserving the bulk properties of the material. Surface modification using RBDs presents an attractive option. Current methods of surface modification, including physical and chemical treatments of the surface, are complex, multi-step, and often involve toxic reagents, whereas we present a non-toxic alternative to irreversibly modify surfaces. The RBD also binds irreversibly to the surface and the use of protease-resistant variants ensures the longevity of the modifications. Possible future uses include linking the RBD with Arginine-Glycine-Asparatate (RGD) sequences. Tissue scaffolds are often coated with RGD sequences to improve cell adhesion and tissue regeneration (Wang *et al*., 2006). Stents and artificial cardiovascular grafts could be coated with RBD-RGB, RBD-fibronectin, or RBD-YIGSR peptides to reduce thrombogenicity and improve endothelial cell attachment (Shin *et al*., 2003a). The stereospecific binding of the peptides can be exploited to pattern molecules such as growth factors and antimicrobial molecules and immobilize multiple molecules onto the surface.

Modifying surfaces for industrial applications would also be advantageous as current methods of surface modification are multi-step and complex (see section **1. 2. 3.** of introduction). The RBD could be used to increase the resistance to wear and corrosion in equipment used the oil sands industry, in slurry pumping systems, in mining, and in milling industries (Jones & Llewellyn, 2009). In theory an RBD-coated pipe used to transport slurry, water, or oil would have an increased flow rate as a result of decreased friction and would improve productivity by increasing the amount of liquid transported through the pipes.

There is considerable interested in developing renewable biomass-based means of producing fuels and chemicals to replace the use of fossil fuels as the main source of energy. Microbial fuel cells (MFCs) offer the ability of converting chemical energy from organic waste into electrical energy by utilizing electrogenic bacteria. During the oxidization of organic

materials these bacteria generate electrons that the bacteria can transfer to external electrodes, thereby generating electrical energy that can be harvested for future use (Du *et al*., 2007; Mansfeld, 2007; Rachinski *et al*., 2010; Sharma & Kundu, 2010). *Shewanella oneidensis* and *Geobacter sulfurreducens* are the model organisms for MFC development but the ability of the T4P of *P. aeruginosa* to sustain milliamps of current suggests that it could be exploited for MFC development.

T4P and the RBD also have potential applications in bioelectronics. The conductive nature of T4P could be used to develop biosensor arrays for diagnostic purposes and in bionanoelectronics to generate interfaces between biological molecules and electronics (Noy, 2011). The RBD acts as an insulator (**Fig. 5-4**) and could perform as a biological insulator on electronic devices.

In the scope of this thesis we have demonstrated that Type IV pili release from the stainless steel surfaces is a reversible process that is controlled by *P. aeruginosa*. The T4P binds to metals via the formation of a novel organo-metallic state of matter between the receptor binding domain of type IV pilus and the surface electrons of the metal surface. The pilus functions as a variable resistance molecular wire that can conduct milliamps of current through the pilus. In addition, *P. aeruginosa* uses its pilus to sense environmental stimuli and varies current flow to the pilus in response to the presence of autoinducers and ultra-violet light. Finally, the physicochemical properties of metal surfaces are readily modified using peptides of the receptor binding domain and the peptides display stereospecific binding patterns on stainless steel that suggest that stainless steel displays chiral features recognized by enantiomers of the receptor binding domain.

Bibliography

Ahmadi, A., Attard, G., Feliu, J. & Rodes, A. (1999). Surface reactivity at "chiral" platinum surfaces. *Langmuir* **15**, 2420-2424.

Alm, R. A. & Mattick, J. S. (1995). Identification of a gene, pilV, required for type 4 fimbrial biogenesis in Pseudomonas aeruginosa, whose product possesses a pre-pilin-like leader sequence. *Molecular microbiology* **16**, 485-496.

Alm, R. A., Bodero, A. J., Free, P. D. & Mattick, J. S. (1996). Identification of a novel gene, pilZ, essential for type 4 fimbrial biogenesis in Pseudomonas aeruginosa. *Journal of bacteriology* **178**, 46-53.

Amiji, M. & Park, K. (1993). Surface Modification of Polymeric Biomaterials with Poly(Ethylene Oxide), Albumin, and Heparin for Reduced Thrombogenicity. *Journal of Biomaterials Science-Polymer Edition* **4**, 217-234.

Amiji, M. & Park, K. (1994). Surface Modification of Polymeric Biomaterials with Poly(Ethylene Oxide) - a Steric Repulsion Approach. *Polymers of Biological and Biomedical Significance* **540**, 135-146.

Antonello, S., Formaggio, F., Moretto, A., Toniolo, C. & Maran, F. (2003). Anomalous distance dependence of electron transfer across peptide bridges. *Journal of the American Chemical Society* **125**, 2874-2875.

Arnold, J. W., Boothe, D. H., Suzuki, O. & Bailey, G. W. (2004). Multiple imaging techniques demonstrate the manipulation of surfaces to reduce bacterial contamination and corrosion. *Journal of microscopy* **216**, 215-221.

Ashcroft, N. W. & Mernim, N. D. (1976). Solid State Phyiscs. **Saunders College Publishing, Philadelphia**.

Attard, G. A. (2001). Electrochemical studies of enantioselectivity at chiral metal surfaces. *Journal of Physical Chemistry B* **105**, 3158-3167.

Audette, G. F., Irvin, R. T. & Hazes, B. (2004). Crystallographic analysis of the Pseudomonas aeruginosa strain K122-4 monomeric pilin reveals a conserved receptor-binding architecture. *Biochemistry* **43**, 11427-11435.

Audette, G. F. & Hazes, B. (2007). Development of protein nanotubes from a multi-purpose biological structure. *Journal of nanoscience and nanotechnology* **7**, 2222-2229.

Azghani, A. O., Idell, S., Bains, M. & Hancock, R. E. (2002). Pseudomonas aeruginosa outer membrane protein F is an adhesin in bacterial binding to lung epithelial cells in culture. *Microbial pathogenesis* **33**, 109-114.

Bagshaw, S. M. & Laupland, K. B. (2006). Epidemiology of intensive care unit-acquired urinary tract infections. *Current Opinion in Infectious Diseases* **19**, 67-71.

Baikie, P. J. (1998). Estrup, Low cost PC based scanning Kelvin probe. *Review Scientific Instruments* **69**.

Baker, N. R., Minor, V., Deal, C., Shahrabadi, M. S., Simpson, D. A. & Woods, D. E. (1991). Pseudomonas aeruginosa exoenzyme S is an adhesion. *Infection and immunity* **59**, 2859-2863.

Banci, L., Bertini, I., Calderone, V., Cefaro, C., Ciofi-Baffoni, S., Gallo, A. & Tokatlidis, K. (2012). An Electron-Transfer Path through an Extended Disulfide Relay System: The Case of the Redox Protein ALR. *Journal of the American Chemical Society* **134**, 1442-1445.

Barken, K. B., Pamp, S. J., Yang, L. & other authors (2008). Roles of type IV pili, flagellum-mediated motility and extracellular DNA in the formation of mature multicellular structures in Pseudomonas aeruginosa biofilms. *Environmental microbiology* **10**, 2331-2343.

Baumgart, F. (2000). Stiffness - an unknown world of mechanical science? *Injury-International Journal of the Care of the Injured* **31**, 14-23.

Beachey, E. H. (1981). Bacterial adherence: adhesin-receptor interactions mediating the attachment of bacteria to mucosal surface. *The Journal of infectious diseases* **143**, 325-345.

Bearinger, J. P., Terrettaz, S., Michel, R., Tirelli, N., Vogel, H., Textor, M. & Hubbell, J. A. (2003). Chemisorbed poly(propylene sulphide)-based copolymers resist biomolecular interactions. *Nature Materials* **2**, 259-264.

Beatson, S. A., Whitchurch, C. B., Sargent, J. L., Levesque, R. C. & Mattick, J. S. (2002a). Differential regulation of twitching motility and elastase production by Vfr in Pseudomonas aeruginosa. *Journal of bacteriology* **184**, 3605-3613.

Beatson, S. A., Whitchurch, C. B., Sargent, J. L., Levesque, R. C. & Mattick, J. S. (2002b). Differential regulation of twitching motility and elastase production by Vfr in Pseudomonas aeruginosa. *Journal of bacteriology* **184**, 3605-3613.

Bendall, D. (1996). Protein Electron Transfer. *BIOS Scientific Publishers*.

Bhushan, B. & ViGoldade, A. (2000). *Applied Surface Science* **157**.

Blenkinsopp, S. A., Khoury, A. E. & Costerton, J. W. (1992). Electrical enhancement of biocide efficacy against Pseudomonas aeruginosa biofilms. *Applied and environmental microbiology* **58**, 3770-3773.

Bodey, G. P., Bolivar, R., Fainstein, V. & Jadeja, L. (1983). Infections caused by Pseudomonas aeruginosa. *Reviews of infectious diseases* **5**, 279-313.

Bradley, D. E. (1972). Shortening of Pseudomonas aeruginosa pili after RNA-phage adsorption. *Journal of general microbiology* **72**, 303-319.

Bradley, D. E. (1980). A function of Pseudomonas aeruginosa PAO polar pili: twitching motility. *Canadian journal of microbiology* **26**, 146-154.

Burrows, L. L. (2005). Weapons of mass retraction. *Molecular microbiology* **57**, 878-888.

Campbell, A. P., McInnes, C., Hodges, R. S. & Sykes, B. D. (1995). Comparison of NMR solution structures of the receptor binding domains of Pseudomonas aeruginosa pili strains PAO, KB7, and PAK: implications for receptor binding and synthetic vaccine design. *Biochemistry* **34**, 16255-16268.

Campbell, A. P., Wong, W. Y., Houston, M., Jr., Schweizer, F., Cachia, P. J., Irvin, R. T., Hindsgaul, O., Hodges, R. S. & Sykes, B. D. (1997). Interaction of the receptor binding domains of Pseudomonas aeruginosa pili strains PAK, PAO, KB7 and P1 to a cross-reactive antibody and receptor analog: implications for synthetic vaccine design. *Journal of molecular biology* **267**, 382-402.

Campbell, A. P., Wong, W. Y., Irvin, R. T. & Sykes, B. D. (2000). Interaction of a bacterially expressed peptide from the receptor binding domain of Pseudomonas aeruginosa pili strain PAK with a cross-reactive antibody: conformation of the bound peptide. *Biochemistry* **39**, 14847-14864.

Campbell, A. P., Spyracopoulos, L., Wong, W. Y., Irvin, R. T. & Sykes, B. D. (2003). Interaction of a peptide from the receptor-binding domain of Pseudomonas aeruginosa pili strain PAK with a cross-reactive antibody: changes in backbone dynamics induced by binding. *Biochemistry* **42**, 11334-11346.

Castric, P. (1995). pilO, a gene required for glycosylation of Pseudomonas aeruginosa 1244 pilin. *Microbiology (Reading, England)* **141 (Pt 5)**, 1247-1254.

Characklis, W. G. & James, D. B. I. B. (2009). Bioengineering Report. Fouling biofilm development: a process analysis. Biotechnol Bioeng., Vol. XXIII, Pp. 1923-60 (1981). *Biotechnology and bioengineering* **102**, 309, 310-347.

Chastre, J. & Fagon, J. Y. (2002). Ventilator-associated pneumonia. *American journal of respiratory and critical care medicine* **165**, 867-903.

Chawick, G. & Smith, D. (1979). Grain boundary structure and properties. **Academic Press, London**.

Chen, C., Li, D. Y. & Shang, C. J. (2009a). Nanocrystallization of aluminized surface of carbon steel for enhanced resistances to corrosion and corrosive wear. *Electrochimica Acta* **55**, 118-124.

Chen, C., Shang, C. J. & Li, D. Y. (2009b). A combination of Al diffusion and surface nanocrystallization of carbon steel for enhanced corrosion resistance. *Philosophical Magazine Letters* **89**, 231-240.

Chen, C., Shang, C. J. & Li, D. Y. (2009c). Surface nanocrystallization of Al-plated steel for application in the exhaust system of vehicles. *Wear* **267**, 345-349.

Chiang, P. & Burrows, L. L. (2003). Biofilm formation by hyperpiliated mutants of Pseudomonas aeruginosa. *Journal of bacteriology* **185**, 2374-2378.

Chiang, P., Habash, M. & Burrows, L. L. (2005). Disparate subcellular localization patterns of Pseudomonas aeruginosa Type IV pilus ATPases involved in twitching motility. *Journal of bacteriology* **187**, 829-839.

Chiang, P., Sampaleanu, L. M., Ayers, M., Pahuta, M., Howell, P. L. & Burrows, L. L. (2008). Functional role of conserved residues in the characteristic secretion NTPase motifs of the Pseudomonas aeruginosa type IV pilus motor proteins PilB, PilT and PilU. *Microbiology (Reading, England)* **154**, 114-126.

Clausen, M., Jakovljevic, V., Sogaard-Andersen, L. & Maier, B. (2009). High-force generation is a conserved property of type IV pilus systems. *Journal of bacteriology* **191**, 4633-4638.

Collinge, C. A., Goll, G., Seligson, D. & Easley, K. J. (1994). Pin Tract Infections - Silver Vs Uncoated Pins. *Orthopedics* **17**, 445-448.

Comolli, J. C., Hauser, A. R., Waite, L., Whitchurch, C. B., Mattick, J. S. & Engel, J. N. (1999). Pseudomonas aeruginosa gene products PilT and PilU are required for cytotoxicity in vitro and virulence in a mouse model of acute pneumonia. *Infection and immunity* **67**, 3625-3630.

Costerton, J. W. (1984). The etiology and persistence of cryptic bacterial infections: a hypothesis. *Reviews of infectious diseases* **6 Suppl 3**, S608-616.

Costerton, J. W., Cheng, K. J., Geesey, G. G., Ladd, T. I., Nickel, J. C., Dasgupta, M. & Marrie, T. J. (1987). Bacterial biofilms in nature and disease. *Annual review of microbiology* **41**, 435-464.

Costerton, J. W., Stewart, P. S. & Greenberg, E. P. (1999). Bacterial biofilms: a common cause of persistent infections. *Science (New York, NY* **284**, 1318-1322.

Craig, L., Taylor, R. K., Pique, M. E. & other authors (2003). Type IV pilin structure and assembly: X-ray and EM analyses of Vibrio cholerae toxin-coregulated pilus and Pseudomonas aeruginosa PAK pilin. *Molecular cell* **11**, 1139-1150.

Craig, L., Pique, M. E. & Tainer, J. A. (2004). Type IV pilus structure and bacterial pathogenicity. *Nature reviews* **2**, 363-378.

Craig, L., Volkmann, N., Arvai, A. S., Pique, M. E., Yeager, M., Egelman, E. H. & Tainer, J. A. (2006). Type IV pilus structure by cryo-electron microscopy and crystallography: implications for pilus assembly and functions. *Molecular cell* **23**, 651-662.

Crane, B. R., Di Bilio, A. J., Winkler, J. R. & Gray, H. B. (2001). Electron tunneling in single crystals of Pseudomonas aeruginosa azurins. *Journal of the American Chemical Society* **123**, 11623-11631.

Cretich, M., Damin, F., Pirri, G. & Chiari, M. (2006). Protein and peptide arrays: recent trends and new directions. *Biomolecular engineering* **23**, 77-88.

Crowther, L. J., Anantha, R. P. & Donnenberg, M. S. (2004). The inner membrane subassembly of the enteropathogenic Escherichia coli bundle-forming pilus machine. *Molecular microbiology* **52**, 67-79.

D'argenio, D. A., Gallagher, L. A., Berg, C. A. & Manoil, C. (2001). Drosophila as a model host for Pseudomonas aeruginosa infection. *Journal of bacteriology* **183**, 1466-1471.

Daizadeh, I., Medvedev, E. S. & Stuchebrukhov, A. A. (1997). Effect of protein dynamics on biological electron transfer. *Proceedings of the National Academy of Sciences of the United States of America* **94**, 3703-3708.

Davis, E. M., Li, D. Y. & Irvin, R. T. (2011). A peptide-stainless steel reaction that yields a new bioorganic-metal state of matter. *Biomaterials* **32**, 5311-5319.

Dawson, E. D., Moore, C. L., Smagala, J. A. & other authors (2006). MChip: a tool for influenza surveillance. *Analytical chemistry* **78**, 7610-7615.

Devicente, A., Borrego, J. J., Arrabal, F. & Romero, P. (1986). Comparative-Study of Selective Media for Enumeration of Pseudomonas-Aeruginosa from Water by Membrane Filtration. *Applied and environmental microbiology* **51**, 832-840.

DiBilio, A. J., Hill, M. G., Bonander, N., Karlsson, B. G., Villahermosa, R. M., Malmstrom, B. G., Winkler, J. R. & Gray, H. B. (1997). Reorganization energy of blue copper: Effects of temperature and driving force on the rates of electron transfer in ruthenium- and osmium-modified azurins. *Journal of the American Chemical Society* **119**, 9921-9922.

Doig, P., Smith, N. R., Todd, T. & Irvin, R. T. (1987). Characterization of the binding of Pseudomonas aeruginosa alginate to human epithelial cells. *Infection and immunity* **55**, 1517-1522.

Doig, P., Todd, T., Sastry, P. A., Lee, K. K., Hodges, R. S., Paranchych, W. & Irvin, R. T. (1988). Role of pili in adhesion of Pseudomonas aeruginosa to human respiratory epithelial cells. *Infection and immunity* **56**, 1641-1646.

Du, Z. W., Li, H. R. & Gu, T. Y. (2007). A state of the art review on microbial fuel cells: A promising technology for wastewater treatment and bioenergy. *Biotechnology Advances* **25**, 464-482.

Dunsmore, D. G. (1983). The Incidence and Implications of Residues of Detergents and Sanitizers in Dairy-Products. *Residue Reviews* **86**, 1-63.

El-Naggar, M. Y., Wanger, G., Leung, K. M., Yuzvinsky, T. D., Southam, G., Yang, J., Lau, W. M., Nealson, K. H. & Gorby, Y. A. (2010). Electrical transport along bacterial nanowires from Shewanella oneidensis MR-1. *Proceedings of the National Academy of Sciences of the United States of America* **107**, 18127-18131.

Elbert, D. L. & Hubbell, J. A. (1998). Reduction of fibrous adhesion formation by a copolymer possessing an affinity for anionic surfaces. *Journal of Biomedical Materials Research* **42**, 55-65.

Engelhart, S., Krizek, L., Glasmacher, A., Fischnaller, E., Marklein, G. & Exner, M. (2002). Pseudomonas aeruginosa outbreak in a haematology-oncology unit associated with contaminated surface cleaning equipment. *Journal of Hospital Infection* **52**, 93-98.

Erb, U. (1995). Electrodeposited nanocrystals: Synthesis, properties and industrial applications. *Nanostructured Materials* **6**, 533-538.

Falkow, S., Isberg, R. R. & Portnoy, D. A. (1992). The interaction of bacteria with mammalian cells. *Annual review of cell biology* **8**, 333-363.

Feldman, M., Bryan, R., Rajan, S., Scheffler, L., Brunnert, S., Tang, H. & Prince, A. (1998). Role of flagella in pathogenesis of Pseudomonas aeruginosa pulmonary infection. *Infection and immunity* **66**, 43-51.

Ferroni, A., Nguyen, L., Pron, B., Quesne, G., Brusset, M. C. & Berche, P. (1998). Outbreak of nosocomial urinary tract infections due to Pseudomonas aeruginosa in a paediatric surgical unit associated with tap-water contamination. *Journal of Hospital Infection* **39**, 301-307.

Fionova, L. & Artemyev, A. (1993). Grain boundaries in metals and seminconductors. *Editions de Physique, Les Ulis* **66**.

Fleiszig, S. M. & Evans, D. J. (2002). The pathogenesis of bacterial keratitis: studies with Pseudomonas aeruginosa. *Clin Exp Optom* **85**, 271-278.

Fletcher, M. & Loeb, G. I. (1979). Influence of Substratum Characteristics on the Attachment of a Marine Pseudomonad to Solid-Surfaces. *Applied and Environmental Microbiology* **37**, 67-72.

Fletcher, M. & Marshall, K. C. (1982). Bubble Contact-Angle Method for Evaluating Substratum Interfacial Characteristics and Its Relevance to Bacterial Attachment. *Applied and Environmental Microbiology* **44**, 184-192.

Fletcher, M. (1994). Bacterial biofilms and biofouling. *Current opinion in biotechnology* **5**, 302-306.

Folkhard, W., Marvin, D. A., Watts, T. H. & Paranchych, W. (1981). Structure of polar pili from Pseudomonas aeruginosa strains K and O. *Journal of molecular biology* **149**, 79-93.

Frey, P. A. (1990). Importance of Organic Radicals in Enzymatic Cleavage of Unactivated C-H Bonds. *Chemical Reviews* **90**, 1343-1357.

Fussenegger, M., Rudel, T., Barten, R., Ryll, R. & Meyer, T. F. (1997). Transformation competence and type-4 pilus biogenesis in Neisseria gonorrhoeae--a review. *Gene* **192**, 125-134.

Giltner, C. L., van Schaik, E. J., Audette, G. F., Kao, D., Hodges, R. S., Hassett, D. J. & Irvin, R. T. (2006). The Pseudomonas aeruginosa type IV pilin receptor binding domain functions as an adhesin for both biotic and abiotic surfaces. *Molecular microbiology* **59**, 1083-1096.

Gleiter, H. (1989). Nanocrystalline Materials. *Progress in Materials Science* **33**, 223-315.

Glessner, A., Smith, R. S., Iglewski, B. H. & Robinson, J. B. (1999). Roles of Pseudomonas aeruginosa las and rhl quorum-sensing systems in control of twitching motility. *Journal of bacteriology* **181**, 1623-1629.

Goodman, M. & Chorev, M. (1979). Concept of Linear Modified Retro-Peptide Structures. *Accounts of Chemical Research* **12**, 1-7.

Gorby, Y. A., Yanina, S., McLean, J. S. & other authors (2006). Electrically conductive bacterial nanowires produced by Shewanella oneidensis strain MR-1 and other microorganisms. *Proceedings of the National Academy of Sciences of the United States of America* **103**, 11358-11363.

Gordon, A. S. (1987). Influence of Alginate on Attachment of Vibrio spp. to Stainless Steel Surfaces in Seawater. *Applied and environmental microbiology* **53**, 1175-1177.

Gray, H. (1997). Journal of Electroanalytical Chemistry. *Journal Electroanalytical Chemistry* **438**, 1-176.

Gray, H. B. & Winkler, J. R. (1996). Electron transfer in proteins. *Annual Review of Biochemistry* **65**, 537-561.

Gray, H. B. & Winkler, J. R. (2003). Electron tunneling through proteins. *Quarterly Reviews of Biophysics* **36**, 341-372.

Gray, H. B. & Winkler, J. R. (2005). Long-range electron transfer. *Proceedings of the National Academy of Sciences of the United States of America* **102**, 3534-3539.

Green, S. K., Schroth, M. N., Cho, J. J., Kominos, S. D. & Vitanzajack, V. B. (1974). Agricultural Plants and Soil as a Reservoir for Pseudomonas-Aeruginosa. *Applied Microbiology* **28**, 987-991.

Gristina, A. G. (1987). Biomaterial-Centered Infection - Microbial Adhesion Versus Tissue Integration. *Science (New York, NY* **237**, 1588-1595.

Guan, X. S., Dong, Z. F. & Li, D. Y. (2005). Surface nanocrystallization by sandblasting and annealing for improved mechanical and tribological properties. *Nanotechnology* **16**, 2963-2971.

Guo, B., Tong, Y. X., Chen, F., Zheng, Y. F., Li, L. & Chung, C. Y. (2012). Effect of Sn addition on the corrosion behavior of Ti-Ta alloy. *Materials and Corrosion-Werkstoffe Und Korrosion* **63**, 259-263.

Gupta, S. K., Berk, R. S., Masinick, S. & Hazlett, L. D. (1994). Pili and lipopolysaccharide of Pseudomonas aeruginosa bind to the glycolipid asialo GM1. *Infection and immunity* **62**, 4572-4579.

Gustafson, T. L., Band, J. D., Hutcheson, R. H., Jr. & Schaffner, W. (1983). Pseudomonas folliculitis: an outbreak and review. *Reviews of infectious diseases* **5**, 1-8.

Hall-Stoodley, L., Costerton, J. W. & Stoodley, P. (2004). Bacterial biofilms: from the natural environment to infectious diseases. *Nature reviews* **2**, 95-108.

Harden, V. P. & Harris, J. O. (1953). The Isoelectric Point of Bacterial Cells. *Journal of Bacteriology* **65**, 198-202.

Hauser, A. R. & Engel, J. N. (1999). Pseudomonas aeruginosa induces type-III-secretion-mediated apoptosis of macrophages and epithelial cells. *Infection and immunity* **67**, 5530-5537.

Hazes, B., Sastry, P. A., Hayakawa, K., Read, R. J. & Irvin, R. T. (2000). Crystal structure of Pseudomonas aeruginosa PAK pilin suggests a main-chain-dominated mode of receptor binding. *Journal of molecular biology* **299**, 1005-1017.

Hirsch, P. & Rades-Rohkohl, E. (1990). Microbial colonization of aquifer sediment exposed in a groundwater well in northern Germany. *Applied and environmental microbiology* **56**, 2963-2966.

Hoiby, N., Frederiksen, B. & Pressler, T. (2005). Eradication of early Pseudomonas aeruginosa infection. *J Cyst Fibros* **4 Suppl 2**, 49-54.

Holm, R. & Solomon, E. (1996). Chemical Reviews. *Chemical Reviews* **66**, 2237-3042.

Horiuchi, T. & Komano, T. (1998). Mutational analysis of plasmid R64 thin pilus prepilin: the entire prepilin sequence is required for processing by type IV prepilin peptidase. *Journal of bacteriology* **180**, 4613-4620.

Horvath, J. D. & Gellman, A. J. (2001). Enantiospecific desorption of R- and S-propylene oxide from a chiral Cu(643) surface. *Journal of the American Chemical Society* **123**, 7953-7954.

Horvath, J. D., Koritnik, A., Kamakoti, P., Sholl, D. S. & Gellman, A. J. (2004). Enantioselective separation on a naturally chiral surface. *Journal of the American Chemical Society* **126**, 14988-14994.

Howie, H. L., Glogauer, M. & So, M. (2005). The N. gonorrhoeae type IV pilus stimulates mechanosensitive pathways and cytoprotection through a pilT-dependent mechanism. *PLoS biology* **3**, e100.

Hua, G. M. & Li, D. Y. (2012). The correlation between the electron work function and yield strength of metals. *Physica Status Solidi B-Basic Solid State Physics* **249**, 1517-1520.

Hung, L. W., Kohmura, M., Ariyoshi, Y. & Kim, S. H. (1999). Structural differences in D and L-monellin in the crystals of racemic mixture. *Journal of molecular biology* **285**, 311-321.

Hung, L. W., Kohmura, M., Ariyoshi, Y., and Kim, S.H. (1999). Structural Differences in D and L-monellin in the crystals of racemic mixture. *Journal of Molecular Biology* **285**, 311-321.

Ista, L. K., Fan, H. Y., Baca, O. & Lopez, G. P. (1996). Attachment of bacteria to model solid surfaces: Oligo(ethylene glycol) surfaces inhibit bacterial attachment. *Fems Microbiology Letters* **142**, 59-63.

Iwahashi, Y., Horita, Z., Nemoto, M. & Langdon, T. G. (1998). The process of grain refinement in equal-channel angular pressing. *Acta Materialia* **46**, 3317-3331.

Johansen, C., Falholt, P. & Gram, L. (1997). Enzymatic removal and disinfection of bacterial biofilms. *Applied and environmental microbiology* **63**, 3724-3728.

Jones, G., Jones, L. B., Thibault-Starzyk, F., Seddon, E. A., Raval, R., Jenkins, S. J. & Held, G. (2006). The local adsorption geometry and electronic structure of alanine on Cu{110}. *Surface Science* **600**, 1924-1935.

Jones, M. & Llewellyn, R. J. (2009). Erosion-corrosion assessment of materials for use in the resources industry. *Wear* **267**, 2003-2009.

Kallstrom, H., Islam, M. S., Berggren, P. O. & Jonsson, A. B. (1998). Cell signaling by the type IV pili of pathogenic Neisseria. *The Journal of biological chemistry* **273**, 21777-21782.

Kang, P. J., Hauser, A. R., Apodaca, G., Fleiszig, S. M., Wiener-Kronish, J., Mostov, K. & Engel, J. N. (1997). Identification of Pseudomonas aeruginosa genes required for epithelial cell injury. *Molecular microbiology* **24**, 1249-1262.

Kao, D. J., Churchill, M. E., Irvin, R. T. & Hodges, R. S. (2007). Animal protection and structural studies of a consensus sequence vaccine targeting the receptor binding domain of the type IV pilus of Pseudomonas aeruginosa. *Journal of molecular biology* **374**, 426-442.

Kearns, D. B., Robinson, J. & Shimkets, L. J. (2001). Pseudomonas aeruginosa exhibits directed twitching motility up phosphatidylethanolamine gradients. *Journal of bacteriology* **183**, 763-767.

Keizer, D. W., Slupsky, C. M., Kalisiak, M., Campbell, A. P., Crump, M. P., Sastry, P. A., Hazes, B., Irvin, R. T. & Sykes, B. D. (2001). Structure of a pilin monomer from Pseudomonas aeruginosa - Implications for the assembly of pili. *Journal of Biological Chemistry* **276**, 24186-24193.

Khoo, X., O'Toole, G. A., Nair, S. A., Snyder, B. D., Kenan, D. J. & Grinstaff, M. W. (2010). Staphylococcus aureus resistance on titanium coated with multivalent PEGylated-peptides. *Biomaterials* **31**, 9285-9292.

Kingshott, P. & Griesser, H. J. (1999). Surfaces that resist bioadhesion. *Current Opinion in Solid State & Materials Science* **4**, 403-412.

Kingshott, P., Wei, J., Bagge-Ravn, D., Gadegaard, N. & Gram, L. (2003). Covalent attachment of poly(ethylene glycol) to surfaces, critical for reducing bacterial adhesion. *Langmuir* **19**, 6912-6921.

Kirn, T. J., Lafferty, M. J., Sandoe, C. M. & Taylor, R. K. (2000). Delineation of pilin domains required for bacterial association into microcolonies and intestinal colonization by Vibrio cholerae. *Molecular microbiology* **35**, 896-910.

Klausen, M., Heydorn, A., Ragas, P., Lambertsen, L., Aaes-Jorgensen, A., Molin, S. & Tolker-Nielsen, T. (2003). Biofilm formation by Pseudomonas aeruginosa wild type, flagella and type IV pili mutants. *Molecular microbiology* **48**, 1511-1524.

Koch, C. C., Pathak, D. & Yamada, K. (1993). Effect of Milling Temperature on the Structure of Some Intermetallic Compounds after Mechanical Milling. *Mechanical Alloying for Structural Applications*, 205-212.

Kraatz, H. B., Bediako-Amoa, I., Gyepi-Garbrah, S. H. & Sutherland, T. C. (2004). Electron transfer through H-bonded peptide assemblies. *Journal of Physical Chemistry B* **108**, 20164-20172.

Kuhnle, A., Linderoth, T. R., Hammer, B. & Besenbacher, F. (2002). Chiral recognition in dimerization of adsorbed cysteine observed by scanning tunnelling microscopy. *Nature* **415**, 891-893.

Kuhnle, A., Molina, L. M., Linderoth, T. R., Hammer, B. & Besenbacher, F. (2004). Growth of unidirectional molecular rows of cysteine on Au(110)-(1x2) driven by adsorbate-induced surface rearrangements. *Physical review letters* **93**.

Kus, J. V., Tullis, E., Cvitkovitch, D. G. & Burrows, L. L. (2004). Significant differences in type IV pilin allele distribution among Pseudomonas aeruginosa isolates from cystic fibrosis (CF) versus non-CF patients. *Microbiology (Reading, England)* **150**, 1315-1326.

Langen, R., Chang, I. J., Germanas, J. P., Richards, J. H., Winkler, J. R. & Gray, H. B. (1995). Electron-Tunneling in Proteins - Coupling through a Beta-Strand. *Science (New York, NY* **268**, 1733-1735.

Leake, E. S., Gristina, A. G. & Wright, M. J. (1982). Use of chemotaxis chambers for studying in vitro bacterial colonization of biomaterials. *Journal of clinical microbiology* **15**, 320-323.

LeChevallier, M. W., Cawthon, C. D. & Lee, R. G. (1988). Inactivation of biofilm bacteria. *Appl Environ Microbiol* **54**, 2492-2499.

Lechevallier, M. W., Lowry, C. D., Lee, R. G. & Gibbon, D. L. (1993). Examining the Relationship between Iron Corrosion and the Disinfection of Biofilm Bacteria. *Journal American Water Works Association* **85**, 111-123.

Lee, J. H., Kopecek, J. & Andrade, J. D. (1989). Protein-Resistant Surfaces Prepared by Peo-Containing Block Copolymer Surfactants. *Journal of Biomedical Materials Research* **23**, 351-368.

Lee, J. H., Lee, H. B. & Andrade, J. D. (1995). Blood Compatibility of Polyethylene Oxide Surfaces. *Progress in Polymer Science* **20**, 1043-1079.

Lee, K. K., Sheth, H. B., Wong, W. Y., Sherburne, R., Paranchych, W., Hodges, R. S., Lingwood, C. A., Krivan, H. & Irvin, R. T. (1994). The binding of Pseudomonas aeruginosa pili to glycosphingolipids is a tip-associated event involving the C-terminal region of the structural pilin subunit. *Molecular microbiology* **11**, 705-713.

Leung, J. W. C., Lau, G. T. C., Sung, J. J. Y. & Costerton, J. W. (1992). Decreased Bacterial Adherence to Silver-Coated Stent Material - an in Vitro Study. *Gastrointestinal Endoscopy* **38**, 338-340.

Lewis, D. A., Leaper, D. J. & Speller, D. C. E. (1984). Prevention of Bacterial-Colonization of Wounds at Operation - Comparison of Iodine-Impregnated (Ioban) Drapes with Conventional Methods. *Journal of Hospital Infection* **5**, 431-437.

Lewis, S. J. & Gilmour, A. (1987). Microflora associated with the internal surfaces of rubber and stainless steel milk transfer pipeline. *The Journal of applied bacteriology* **62**, 327-333.

Li, C., Pazgier, M., Li, J. & other authors (2010). Limitations of Peptide Retro-inverso Isomerization in Molecular Mimicry. *Journal of Biological Chemistry* **285**, 19572-19581.

Li, W. & Li, D. Y. (2002). Effects of dislocation on electron work function of metal surface. *Materials Science and Technology* **18**, 1057-1060.

Li, X. & Logan, B. E. (2004). Analysis of bacterial adhesion using a gradient force analysis method and colloid probe atomic force microscopy. *Langmuir* **20**, 8817-8822.

Li, Y. & Li, D. (2005). Eletron work function, adhesion, and friction between 3d transition metals under ligt loads. *Wear* **259**.

Li, Y. P. & Li, D. Y. (2004). Experimental studies on relationships between the electron work function, adhesion, and friction for 3d transition metals. *Journal of Applied Physics* **95**, 7961-7965.

Liang, N., Pielak, G. J., Mauk, A. G., Smith, M. & Hoffman, B. M. (1987). Yeast Cytochrome-C with Phenylalanine or Tyrosine at Position-87 Transfers Electrons to (Zinc Cytochrome-C Peroxidase)+ at a Rate 10000 Times That of the Serine-87 or Glycine-87 Variants. *Proceedings of the National Academy of Sciences of the United States of America* **84**, 1249-1252.

Ligler, F. S. & Erickson, J. S. (2006). Bioengineering: diagnosis on disc. *Nature* **440**, 159-160.

Liu, F. C., Liang, W., Li, X. R., Zhao, X. G., Zhang, Y. & Wang, H. X. (2008). Improvement of corrosion resistance of pure magnesium via vacuum pack treatment. *Journal of Alloys and Compounds* **461**, 399-403.

Liu, V. A., Jastromb, W. E. & Bhatia, S. N. (2002). Engineering protein and cell adhesivity using PEO-terminated triblock polymers. *Journal of Biomedical Materials Research* **60**, 126-134.

Llanos, G. R. & Sefton, M. V. (1993). Does Polyethylene Oxide Possess a Low Thrombogenicity. *Journal of Biomaterials Science-Polymer Edition* **4**, 381-400.

Llewellyn, R. J., Yick, S. K. & Dolman, K. F. (2004). Scouring erosion resistance of metallic materials used in slurry pump service. *Wear* **256**, 592-599.

Lomander, A., Schreuders, P., Russek-Cohen, E. & Ali, L. (2004). Evaluation of chlorines' impact on biofilms on scratched stainless steel surfaces. *Bioresource technology* **94**, 275-283.

Long, Y. T., Abu-Irhayem, E. & Kraatz, H. B. (2005). Peptide electron transfer: more questions than answers. *Chemistry (Weinheim an der Bergstrasse, Germany)* **11**, 5186-5194.

Louthan, M. J. (1987). Metals: A History. *ASM International*.

Lovley, D. R. & Phillips, E. J. (1988). Novel mode of microbial energy metabolism: organic carbon oxidation coupled to dissimilatory reduction of iron or manganese. *Applied and environmental microbiology* **54**, 1472-1480.

Lu, K. (1996). Nanocrystalline metals crystallized from amorphous solids: Nanocrystallization, structure, and properties. *Materials Science & Engineering R-Reports* **16**, 161-221.

Lyczak, J. B., Cannon, C. L. & Pier, G. B. (2000). Establishment of Pseudomonas aeruginosa infection: lessons from a versatile opportunist. *Microbes and infection / Institut Pasteur* **2**, 1051-1060.

MacMillan, B. G. (1980). Infections following burn injury. *The Surgical clinics of North America* **60**, 185-196.

Maier, B., Potter, L., So, M., Long, C. D., Seifert, H. S. & Sheetz, M. P. (2002). Single pilus motor forces exceed 100 pN. *Proceedings of the National Academy of Sciences of the United States of America* **99**, 16012-16017.

Maier, B., Koomey, M. & Sheetz, M. P. (2004). A force-dependent switch reverses type IV pilus retraction. *Proceedings of the National Academy of Sciences of the United States of America* **101**, 10961-10966.

Malak, R. A., Gao, Z. N., Wishart, J. F. & Isied, S. S. (2004). Long-range electron transfer across peptide bridges: The transition from electron superexchange to hopping. *Journal of the American Chemical Society* **126**, 13888-13889.

Malvankar, N. S., Vargas, M., Nevin, K. P. & other authors (2011). Tunable metallic-like conductivity in microbial nanowire networks. *Nature nanotechnology* **6**, 573-579.

Mandal, K., Pentelute, B. L., Tereshko, V., Thammavongsa, V., Schneewind, O., Kossiakoff, A. A. & Kent, S. B. H. (2009). Racemic crystallography of synthetic protein enantiomers used to determine the X-ray structure of plectasin by direct methods. *Protein Science* **18**, 1146-1154.

Mansfeld, F. (2007). The interaction of bacteria and metal surfaces. *Electrochimica Acta* **52**, 7670-7680.

Mao, X. Y., Li, D. Y., Fang, F., Tan, R. S. & Jiang, J. Q. (2010). A simple technique of nanocrystallizing metallic surfaces for enhanced resistances to mechanical and electrochemical attacks. *Materials Science and Engineering a-Structural Materials Properties Microstructure and Processing* **527**, 2875-2880.

Mattick, J. S. (2002). Type IV pili and twitching motility. *Annual review of microbiology* **56**, 289-314.

Mayer, K. H. & Zinner, S. H. (1985). Bacterial pathogens of increasing significance in hospital-acquired infections. *Reviews of infectious diseases* **7 Suppl 3**, S371-379.

McCabe, C. & Bauer, C. (1964). Metals, Atoms, and Alloys. *National Science Teachers Association, Inc* **McGraw-Hill**.

McFadden, C. F., Cremer, P. S. & Gellman, A. J. (1996). Adsorption of chiral alcohols on "chiral" metal surfaces. *Langmuir* **12**, 2483-2487.

McInnes, C., Sonnichsen, F. D., Kay, C. M., Hodges, R. S. & Sykes, B. D. (1993). NMR solution structure and flexibility of a peptide antigen representing the receptor binding domain of Pseudomonas aeruginosa. *Biochemistry* **32**, 13432-13440.

McInnes, C., Kay, C. M., Hodges, R. S. & Sykes, B. D. (1994). Conformational differences between cis and trans proline isomers of a peptide antigen representing the receptor binding domain of Pseudomonas aeruginosa as studied by 1H-NMR. *Biopolymers* **34**, 1221-1230.

McLean, D. (1957). Grain boundaries in metals. **Clarendon Press, London**.

Merz, A. J., Enns, C. A. & So, M. (1999). Type IV pili of pathogenic Neisseriae elicit cortical plaque formation in epithelial cells. *Molecular microbiology* **32**, 1316-1332.

Merz, A. J., So, M. & Sheetz, M. P. (2000). Pilus retraction powers bacterial twitching motility. *Nature* **407**, 98-102.

Merz, A. J. & Forest, K. T. (2002). Bacterial surface motility: slime trails, grappling hooks and nozzles. *Curr Biol* **12**, R297-303.

Moller, P. C., Evans, M. J., Fader, R. C., Henson, L. C., Rogers, B. & Heggers, J. P. (1994). The effect of anti-exotoxin A on the adherence of Pseudomonas aeruginosa to hamster tracheal epithelial cells in vitro. *Tissue & cell* **26**, 181-188.

Morand, P. C., Bille, E., Morelle, S., Eugene, E., Beretti, J. L., Wolfgang, M., Meyer, T. F., Koomey, M. & Nassif, X. (2004). Type IV pilus retraction in pathogenic Neisseria is regulated by the PilC proteins. *Embo Journal* **23**, 2009-2017.

Morra, M. & Cassinelli, C. (1997). Bacterial adhesion to polymer surfaces: a critical review of surface thermodynamic approaches. *Journal of biomaterials science* **9**, 55-74.

Mukherjee, S., Su, S., Panmanee, W., Irvin, R. T., Hassett, D. J. & Choi, S. (2012). A microliter-scale microbial fuel cell array for bacterial electrogenic screening. *Sensors and Actuators A: Physical*, http://dx.doi.org/10.1016/j.sna.2012.1010.1025.

Myers, C. R. & Nealson, K. H. (1988). Bacterial manganese reduction and growth with manganese oxide as the sole electron acceptor. *Science (New York, NY* **240**, 1319-1321.

Noy, A. (2011). Bionanoelectronics. *Advanced Materials* **23**, 807-820.

Nunn, D. N. & Lory, S. (1991). Product of the Pseudomonas aeruginosa gene pilD is a prepilin leader peptidase. *Proceedings of the National Academy of Sciences of the United States of America* **88**, 3281-3285.

O'Toole, G. A. & Kolter, R. (1998). Flagellar and twitching motility are necessary for Pseudomonas aeruginosa biofilm development. *Molecular microbiology* **30**, 295-304.

O'Toole, G. A., Pratt, L. A., Watnick, P. I., Newman, D. K., Weaver, V. B. & Kolter, R. (1999). Genetic approaches to study of biofilms. *Methods in enzymology* **310**, 91-109.

Obritsch, M. D., Fish, D. N., MacLaren, R. & Jung, R. (2005). Nosocomial infections due to multidrug-resistant Pseudomonas aeruginosa: epidemiology and treatment options. *Pharmacotherapy* **25**, 1353-1364.

Paranchych, W., Sastry, P. A., Frost, L. S., Carpenter, M., Armstrong, G. D. & Watts, T. H. (1979). Biochemical studies on pili isolated from Pseudomonas aeruginosa strain PAO. *Canadian journal of microbiology* **25**, 1175-1181.

Paranchych, W., Sastry, P. A., Volpel, K., Loh, B. A. & Speert, D. P. (1986). Fimbriae (pili): molecular basis of Pseudomonas aeruginosa adherence. *Clinical and investigative medicine* **9**, 113-118.

Parge, H. E., Forest, K. T., Hickey, M. J., Christensen, D. A., Getzoff, E. D. & Tainer, J. A. (1995). Structure of the fibre-forming protein pilin at 2.6 A resolution. *Nature* **378**, 32-38.

Pasloske, B. L., Scraba, D. G. & Paranchych, W. (1989). Assembly of mutant pilins in Pseudomonas aeruginosa: formation of pili composed of heterologous subunits. *Journal of bacteriology* **171**, 2142-2147.

Passerini, L., Lam, K., Costerton, J. W. & King, E. G. (1992). Biofilms on indwelling vascular catheters. *Critical care medicine* **20**, 665-673.

Pellett, S., Bigley, D. V. & Grimes, D. J. (1983). Distribution of Pseudomonas-Aeruginosa in a Riverine Ecosystem. *Applied and environmental microbiology* **45**, 328-332.

Pereni, C. I., Zhao, Q., Liu, Y. & Abel, E. (2006). Surface free energy effect on bacterial retention. *Colloids and surfaces* **48**, 143-147.

Petrov, E. G. & Hanggi, P. (2001). Nonlinear electron current through a short molecular wire. *Physical review letters* **86**, 2862-2865.

Petrov, E. G., Teslenko, V. I. & May, V. (2003). Two-electron transfer reactions in proteins: bridge-mediated and proton-assisted processes. *Physical review* **68**, 061916.

Plotnikova, J. M., Rahme, L. G. & Ausubel, F. M. (2000). Pathogenesis of the human opportunistic pathogen Pseudomonas aeruginosa PA14 in Arabidopsis. *Plant Physiology* **124**, 1766-1774.

Polizzi, N. F., Skourtis, S. S. & Beratan, D. N. (2011). Physical constraints on charge transport through bacterial nanowires. *Faraday discussions* **155**, 43-62; discussion 103-114.

Polmear, I. (1995). Light Alloys. *Arnold*.

Polo, F., Antonello, S., Formaggio, F., Toniolo, C. & Maran, F. (2005). Evidence against the hopping mechanism as an important electron transfer pathway for conformationally constrained oligopeptides. *Journal of the American Chemical Society* **127**, 492-493.

Porgess, P. V. K. & Wilman, H. (1959). The Dependence of Friction on Surface Roughness. *Proceedings of the Royal Society of London Series a-Mathematical and Physical Sciences* **252**, 35-&.

Prime, K. L. & Whitesides, G. M. (1991). Self-Assembled Organic Monolayers - Model Systems for Studying Adsorption of Proteins at Surfaces. *Science* **252**, 1164-1167.

Prime, K. L. & Whitesides, G. M. (1993). Adsorption of Proteins onto Surfaces Containing End-Attached Oligo(Ethylene Oxide) - a Model System Using Self-Assembled Monolayers. *Journal of the American Chemical Society* **115**, 10714-10721.

Pringle, J. H. & Fletcher, M. (1986). Influence of Substratum Hydration and Adsorbed Macromolecules on Bacterial Attachment to Surfaces. *Applied and Environmental Microbiology* **51**, 1321-1325.

Pringle, J. H., and M. Fletcher (1986). Influence of Substratum Hydration and Adsorbed Macromolecules
on Bacterial Attachment to Surfaces. *Appl Environ Microbiol* **51**, 1321-1325.

Pruitt, B. A., McManus, A. T., Kim, S. H. & Goodwin, C. W. (1998). Burn wound infections: Current status. *World Journal of Surgery* **22**, 135-145.

Pyun, J., Kowalewski, T. & Matyjaszewski, K. (2003). Synthesis of polymer brushes using atom transfer radical polymerization. *Macromolecular Rapid Communications* **24**, 1043-1059.

Rachinski, S., Carubelli, A., Mangoni, A. P. & Mangrich, A. S. (2010). Microbial Fuel Cells Used in the Production of Electricity from Organic Waste: A Perspective of Future. *Quimica Nova* **33**, 1773-1778.

Rankin, R. B. & Sholl, D. S. (2005). Structure of enantiopure and racemic alanine adlayers on Cu(110). *Surface Science* **574**, L1-L8.

Reguera, G., McCarthy, K. D., Mehta, T., Nicoll, J. S., Tuominen, M. T. & Lovley, D. R. (2005). Extracellular electron transfer via microbial nanowires. *Nature* **435**, 1098-1101.

Reguera, G., Nevin, K. P., Nicoll, J. S., Covalla, S. F., Woodard, T. L. & Lovley, D. R. (2006). Biofilm and nanowire production leads to increased current in Geobacter sulfurreducens fuel cells. *Applied and environmental microbiology* **72**, 7345-7348.

Renner, L. D. & Weibel, D. B. (2011). Physicochemical regulation of biofilm formation. *Mrs Bulletin* **36**, 347-355.

Renner, L. D., and D.B. Weibel (2011). Physicochemical regulation of biofilm formation. *MRS Bull* **36**, 347–355.

Riley, D. M., Classen, D. C., Stevens, L. E. & Burke, J. P. (1995). A Large Randomized Clinical-Trial of a Silver-Impregnated Urinary Catheter - Lack of Efficacy and Staphylococcal Superinfection. *American Journal of Medicine* **98**, 349-356.

Robertson, J. (1992). Properties of Diamond-Like Carbon. *Surface & Coatings Technology* **50**, 185-203.

Roncero, C., Darzins, A. & Casadaban, M. J. (1990). Pseudomonas aeruginosa transposable bacteriophages D3112 and B3 require pili and surface growth for adsorption. *Journal of bacteriology* **172**, 1899-1904.

Russell, M. A. & Darzins, A. (1994). The pilE gene product of Pseudomonas aeruginosa, required for pilus biogenesis, shares amino acid sequence identity with the N-termini of type 4 prepilin proteins. *Molecular microbiology* **13**, 973-985.

Sadikot, R. T., Blackwell, T. S., Christman, J. W. & Prince, A. S. (2005). Pathogen-host interactions in Pseudomonas aeruginosa pneumonia. *American journal of respiratory and critical care medicine* **171**, 1209-1223.

Saiman, L., Ishimoto, K., Lory, S. & Prince, A. (1990). The effect of piliation and exoproduct expression on the adherence of Pseudomonas aeruginosa to respiratory epithelial monolayers. *The Journal of infectious diseases* **161**, 541-548.

Sandoz-Rosado, E. J., Tertuliano, O. A. & Terrell, E. J. (2012). An atomistic study of the abrasive wear and failure of graphene sheets when used as a solid lubricant and a comparison to diamond-like-carbon coatings. *Carbon* **50**, 4078-4084.

Sasaki, H., Makino, M., Sisido, M., Smith, T. A. & Ghiggino, K. P. (2001). Photoinduced electron transfer on beta-sheet cyclic peptides. *Journal of Physical Chemistry B* **105**, 10416-10423.

Sauer, K., Rickard, A. H. & Davies, D. G. (2007). Biofilms and Biocomplexity. *Microbe* **2**, 7.

Sayago, D. I., Polcik, M., Nisbet, G., Lamont, C. L. A. & Woodruff, D. P. (2005). Local structure determination of a chiral adsorbate: Alanine on Cu(110). *Surface Science* **590**, 76-87.

Schuster, M., Lostroh, C. P., Ogi, T. & Greenberg, E. P. (2003). Identification, timing, and signal specificity of Pseudomonas aeruginosa quorum-controlled genes: a transcriptome analysis. *Journal of bacteriology* **185**, 2066-2079.

Schweizer, H. P. & Po, C. (1996). Regulation of glycerol metabolism in Pseudomonas aeruginosa: characterization of the glpR repressor gene. *Journal of bacteriology* **178**, 5215-5221.

Scott, R. E. (1997). Journal of BIology and Inorganic Chemistry. *Journal Biology and Inorganic Chemistry* **2**, 372-404.

Sedlak-Weinstein, E., Cripps, A. W., Kyd, J. M. & Foxwell, A. R. (2005). Pseudomonas aeruginosa: the potential to immunise against infection. *Expert Opinion on Biological Therapy* **5**, 967-982.

Sek, S., Tolak, A., Misicka, A., Palys, B. & Bilewicz, R. (2005). Asymmetry of electron transmission through monolayers of helical polyalanine adsorbed on gold surfaces. *Journal of Physical Chemistry B* **109**, 18433-18438.

Sek, S., Misicka, A., Swiatek, K. & Maicka, E. (2006). Conductance of alpha-helical peptides trapped within molecular junctions. *The journal of physical chemistry* **110**, 19671-19677.

Sharma, V. & Kundu, P. P. (2010). Biocatalysts in microbial fuel cells. *Enzyme and Microbial Technology* **47**, 179-188.

Sheth, H. B., Lee, K. K., Wong, W. Y., Srivastava, G., Hindsgaul, O., Hodges, R. S., Paranchych, W. & Irvin, R. T. (1994). The pili of Pseudomonas aeruginosa strains PAK and PAO bind specifically to the carbohydrate sequence beta GalNAc(1-4)beta Gal found in glycosphingolipids asialo-GM1 and asialo-GM2. *Molecular microbiology* **11**, 715-723.

Sheth, H. B., Glasier, L. M., Ellert, N. W., Cachia, P., Kohn, W., Lee, K. K., Paranchych, W., Hodges, R. S. & Irvin, R. T. (1995). Development of an anti-adhesive vaccine for Pseudomonas aeruginosa targeting the C-terminal region of the pilin structural protein. *Biomed Pept Proteins Nucleic Acids* **1**, 141-148.

Sheu, S. Y. & Yang, D. Y. (2001). Dynamic scaling theory for a tethered membrane in solution. *Physical review* **63**, 061207.

Shin, H., Jo, S. & Mikos, A. G. (2003a). Biomimetic materials for tissue engineering. *Biomaterials* **24**, 4353-4364.

Shin, Y. G. K., Newton, M. D. & Isied, S. S. (2003b). Distance dependence of electron transfer across peptides with different secondary structures: The role of peptide energetics and electronic coupling. *Journal of the American Chemical Society* **125**, 3722-3732.

Sholl, D. S. (1998). Adsorption of chiral hydrocarbons on chiral platinum surfaces. *Langmuir* **14**, 862-867.

Sirard, S. M., Gupta, R. R., Russell, T. P., Watkins, J. J., Green, P. F. & Johnston, K. P. (2003). Structure of end-grafted polymer brushes in liquid and supercritical carbon dioxide: A neutron reflectivity study. *Macromolecules* **36**, 3365-3373.

Sisido, M., Hoshino, S., Kusano, H., Kuragaki, M., Makino, M., Sasaki, H., Smith, T. A. & Ghiggino, K. P. (2001). Distance dependence of photoinduced electron transfer along alpha-helical polypeptides. *Journal of Physical Chemistry B* **105**, 10407-10415.

Skerker, J. M. & Berg, H. C. (2001). Direct observation of extension and retraction of type IV pili. *Proceedings of the National Academy of Sciences of the United States of America* **98**, 6901-6904.

Skov, L. K., Pascher, T., Winkler, J. R. & Gray, H. B. (1998). Rates of intramolecular electron transfer in Ru(bpy)(2)(im)(His83)-modified azurin increase below 220 K. *Journal of the American Chemical Society* **120**, 1102-1103.

Song, S. (1990). in situ High resolution eletronc microscopy of grain-boundary migration through ledge motion in an Al-Mg alloy. *Phil Mag Letters* **79**.

Stanley, P. M. (1983). Factors affecting the irreversible attachment of Pseudomonas aeruginosa to stainless steel. *Canadian journal of microbiology* **29**, 1493-1499.

Stickler, D. J., Morris, N. S. & Williams, T. J. (1996). An assessment of the ability of a silver-releasing device to prevent bacterial contamination of urethral catheter drainage systems. *British Journal of Urology* **78**, 579-588.

Stover, C. K., Pham, X. Q., Erwin, A. L. & other authors (2000). Complete genome sequence of Pseudomonas aeruginosa PAO1, an opportunistic pathogen. *Nature* **406**, 959-964.

Strom, M. S., Nunn, D. N. & Lory, S. (1993). A single bifunctional enzyme, PilD, catalyzes cleavage and N-methylation of proteins belonging to the type IV pilin family. *Proceedings of the National Academy of Sciences of the United States of America* **90**, 2404-2408.

Stubbe, J. & van der Donk, W. A. (1998). Protein radicals in enzyme catalysis. *Chemical Reviews* **98**, 705-762.

Su, C. W., Lee, J. W., Wang, C. S., Chao, C. G. & Liu, T. F. (2008). The effect of hot-dipped aluminum coatings on Fe-8Al-30Mn-0.8C alloy. *Surface & Coatings Technology* **202**, 1847-1852.

Suh, J. Y., Spyracopoulos, L., Keizer, D. W., Irvin, R. T. & Sykes, B. D. (2001). Backbone dynamics of receptor binding and antigenic regions of a Pseudomonas aeruginosa pilin monomer. *Biochemistry* **40**, 3985-3995.

Sumner, D. R., Turner, T. M., Igloria, R., Urban, R. M. & Galante, J. O. (1998). Functional adaptation and ingrowth of bone vary as a function of hip implant stiffness. *Journal of Biomechanics* **31**, 909-917.

Swanson, J. (1973). Studies on gonococcus infection. IV. Pili: their role in attachment of gonococci to tissue culture cells. *The Journal of experimental medicine* **137**, 571-589.

Tanaka, Y., Matin, K., Gyo, M., Okada, A., Tsutsumi, Y., Doi, H., Nomura, N., Tagami, J. & Hanawa, T. (2010). Effects of electrodeposited poly(ethylene glycol) on biofilm adherence to titanium. *Journal of Biomedical Materials Research Part A* **95A**, 1105-1113.

Tang, X. H., Chung, R., Pang, C. J., Li, D. Y., Hinckley, B. & Dolman, K. (2011). Microstructure of high (45 wt.%) chromium cast irons and their resistances to wear and corrosion. *Wear* **271**, 1426-1431.

Tao, S. & Li, D. Y. (2008a). Nanocrystallization effect on the surface electron work function of copper and its corrosion behaviour. *Philosophical Magazine Letters* **88**, 137-144.

Tao, S. & Li, D. Y. (2008b). Nanocrystallization effect on the surface electron work function of copper and its corrosion behaviour. *Phil Mag Letters* **88**.

Taylor, M., Moore, S., Mayes, J., Parkin, E., Beeg, M., Canovi, M., Gobbi, M., Mann, D. M. A. & Allsop, D. (2010). Development of a Proteolytically Stable Retro-Inverso Peptide Inhibitor of beta-Amyloid Oligomerization as a Potential Novel Treatment for Alzheimer's Disease. *Biochemistry* **49**, 3261-3272.

Taylor, R. K., Miller, V. L., Furlong, D. B. & Mekalanos, J. J. (1987). Use of phoA gene fusions to identify a pilus colonization factor coordinately regulated with cholera toxin. *Proceedings of the National Academy of Sciences of the United States of America* **84**, 2833-2837.

Tian, H. H., Addie, G. R. & Visintainer, R. J. (2009). Erosion-corrosion performance of high-Cr cast iron alloys in flowing liquid-solid slurries. *Wear* **267**, 2039-2047.

Touhami, A., Jericho, M. H., Boyd, J. M. & Beveridge, T. J. (2006). Nanoscale characterization and determination of adhesion forces of Pseudomonas aeruginosa Pili by using atomic force microscopy. *Journal of bacteriology* **188**, 370-377.

Tredget, E. E., Shankowsky, H. A., Joffe, A. M., Inkson, T. I., Volpel, K., Paranchych, W., Kibsey, P. C., Alton, J. D. & Burke, J. F. (1992). Epidemiology of infections with Pseudomonas aeruginosa in burn patients: the role of hydrotherapy. *Clin Infect Dis* **15**, 941-949.

Turner, L. R., Lara, J. C., Nunn, D. N. & Lory, S. (1993). Mutations in the consensus ATP-binding sites of XcpR and PilB eliminate extracellular protein secretion and pilus biogenesis in Pseudomonas aeruginosa. *Journal of bacteriology* **175**, 4962-4969.

Valiev, R. Z., Korznikov, A. V. & Mulyukov, R. R. (1993). Structure and Properties of Ultrafine-Grained Materials Produced by Severe Plastic-Deformation. *Materials Science and Engineering a-Structural Materials Properties Microstructure and Processing* **168**, 141-148.

van Loosdrecht, M. C., Lyklema, J., Norde, W., Schraa, G. & Zehnder, A. J. (1987). The role of bacterial cell wall hydrophobicity in adhesion. *Applied and environmental microbiology* **53**, 1893-1897.

van Schaik, E. J., Giltner, C. L., Audette, G. F., Keizer, D. W., Bautista, D. L., Slupsky, C. M., Sykes, B. D. & Irvin, R. T. (2005). DNA binding: a novel function of Pseudomonas aeruginosa type IV pili. *Journal of bacteriology* **187**, 1455-1464.

Vanhaecke, E., Remon, J. P., Moors, M., Raes, F., De Rudder, D. & Van Peteghem, A. (1990). Kinetics of Pseudomonas aeruginosa adhesion to 304 and 316-L stainless steel: role of cell surface hydrophobicity. *Applied and environmental microbiology* **56**, 788-795.

Wagner, V. E., Bushnell, D., Passador, L., Brooks, A. I. & Iglewski, B. H. (2003). Microarray analysis of Pseudomonas aeruginosa quorum-sensing regulons: effects of growth phase and environment. *Journal of bacteriology* **185**, 2080-2095.

Wang, Y. J., Lu, L., Zheng, Y. D. & Chen, X. F. (2006). Improvement in hydrophilicity of PHBV films by plasma treatment. *Journal of Biomedical Materials Research Part A* **76A**, 589-595.

Wassall, M. A., Santin, M., Isalberti, C., Cannas, M. & Denyer, S. P. (1997). Adhesion of bacteria to stainless steel and silver-coated orthopedic external fixation pins. *Journal of Biomedical Materials Research* **36**, 325-330.

Watanabe, J., Morita, T. & Kimura, S. (2005). Effects of dipole moment, linkers, and chromophores at side chains on long-range electron transfer through helical peptides. *Journal of Physical Chemistry B* **109**, 14416-14425.

Weiss, R. L. (1971). The structure and occurrence of pili (fimbriae) on Pseudomonas aeruginosa. *Journal of general microbiology* **67**, 135-143.

Wetscher, F., Vorhauer, A. & Pippan, R. (2005). Strain hardening during high pressure torsion deformation. *Materials Science and Engineering a-Structural Materials Properties Microstructure and Processing* **410**, 213-216.

Whitchurch, C. B., Hobbs, M., Livingston, S. P., Krishnapillai, V. & Mattick, J. S. (1991a). Characterization of a Pseudomonas-Aeruginosa Twitching Motility Gene and Evidence for a Specialized Protein Export System Widespread in Eubacteria. *Gene* **101**, 33-44.

Whitchurch, C. B., Hobbs, M., Livingston, S. P., Krishnapillai, V. & Mattick, J. S. (1991b). Characterisation of a Pseudomonas aeruginosa twitching motility gene and evidence for a specialised protein export system widespread in eubacteria. *Gene* **101**, 33-44.

Whitchurch, C. B. & Mattick, J. S. (1994). Characterization of a gene, pilU, required for twitching motility but not phage sensitivity in Pseudomonas aeruginosa. *Molecular microbiology* **13**, 1079-1091.

Whitchurch, C. B., Erova, T. E., Emery, J. A., Sargent, J. L., Harris, J. M., Semmler, A. B., Young, M. D., Mattick, J. S. & Wozniak, D. J. (2002). Phosphorylation of the Pseudomonas aeruginosa response regulator AlgR is essential for type IV fimbria-mediated twitching motility. *Journal of bacteriology* **184**, 4544-4554.

Winther-Larsen, H. C., Wolfgang, M., Dunham, S., van Putten, J. P., Dorward, D., Lovold, C., Aas, F. E. & Koomey, M. (2005). A conserved set of pilin-like molecules controls type IV pilus dynamics and organelle-associated functions in Neisseria gonorrhoeae. *Molecular microbiology* **56**, 903-917.

Wolfgang, J., Risser, S. M., Priyadarshy, S. & Beratan, D. N. (1997). Secondary structure conformations and long range electronic interactions in oligopeptides. *Journal of Physical Chemistry B* **101**, 2986-2991.

Wong, W. Y., Irvin, R. T., Paranchych, W. & Hodges, R. S. (1992). Antigen-antibody interactions: elucidation of the epitope and strain-specificity of a monoclonal antibody directed against the pilin protein adherence binding domain of Pseudomonas aeruginosa strain K. *Protein Sci* **1**, 1308-1318.

Wong, W. Y., Campbell, A. P., McInnes, C., Sykes, B. D., Paranchych, W., Irvin, R. T. & Hodges, R. S. (1995). Structure-function analysis of the adherence-binding domain on the pilin of Pseudomonas aeruginosa strains PAK and KB7. *Biochemistry* **34**, 12963-12972.

Yang, X. H., Zhu, W. L., Lin, Z. & Huo, J. J. (2005). Aerodynamic evaluation of an internal epoxy coating in nature gas pipeline. *Progress in Organic Coatings* **54**, 73-77.

Yao, P., Xie, Y., Wang, Y. H., Sun, Y. L., Huang, Z. X., Xiao, G. T. & Wang, S. D. (1997). Importance of a conserved phenylalanine-35 of cytochrome b(5) to the protein's stability and redox potential. *Protein Engineering* **10**, 575-581.

Yeung, A. T., Parayno, A. & Hancock, R. E. (2012). Mucin promotes rapid surface motility in Pseudomonas aeruginosa. *mBio* **3**.

Yu, B., Giltner, C. L., van Schaik, E. J., Bautista, D. L., Hodges, R. S., Audette, G. F., Li, D. Y. & Irvin, R. T. (2007). A Novel Biometallic Interface: High Affinity Tip-Associated Binding by Pilin-Derived Protein Nanotubes. *Journal of Bionanoscience* **1**, 11.

Yu, B., Davis, E. M., Hodges, R. S., Irvin, R. T. & Li, D. Y. (2008). Surface nanocrystallization of stainless steel for reduced biofilm adherence. *Nanotechnology* **19**, 8.

Yu, B., Lesiuk, A., Davis, E. M., Irvin, R. T. & Li, D. Y. (2010). Surface Nanocrystallization for bacterial control. *Langmuir* **26**.

Yu, B., Davis, E. M., Lesiuk, A. E., Irvin, R. T. & Li, D. Y. (2011). Nanocrystallization of Ag-incorporated stainless steel surface for enhanced resistance to corrosion and bacterial colonization. *Philosophical Magazine Letters* **91**, 697-704.

Yu, L., Lee, K. K., Paranchych, W., Hodges, R. S. & Irvin, R. T. (1996). Use of synthetic peptides to confirm that the Pseudomonas aeruginosa PAK pilus adhesin and the Candida albicans fimbrial adhesin possess a homologous receptor-binding domain. *Molecular microbiology* **19**, 1107-1116.

Zhang, Y., Liang, W., Wang, H. X., Liu, F. C., Li, X. R. & Zhao, X. G. (2008). Research on Microstructure and Properties of Aluminum Alloyed Coating on AZ91D Magnesium Alloy by Vacuum Solid Diffusion. *Rare Metal Materials and Engineering* **37**, 2023-2026.

Zhou, Y. L., Niinomi, M. & Akahori, T. (2004). Mechanical properties of binary Ti-Ta alloys for biomedical applications. *Designing, Processing and Properties of Advanced Engineering Materials, Pts 1 and 2* **449-4**, 1089-1092.

Zisman, W. (1964). Relationship of equilibrium contact angle to liquid and solid constitution. *Contact angle, wettability, and adhesion, advances in chemical series* **43**, 1.

Zuo, R., Ornek, D. & Wood, T. K. (2005). Aluminum- and mild steel-binding peptides from phage display. *Applied microbiology and biotechnology* **68**, 505-509.

Appendix A

Supplemental data for Chapter 5

Experiments were performed by Carmen Giltner and Erin van Schaik

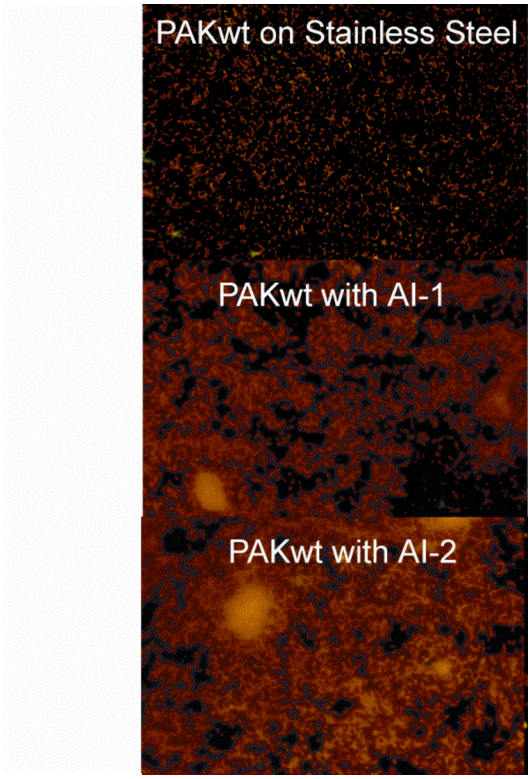

Figure A-1. Autoinducer promotes *P. aeruginosa* colonization of stainless steel. Wtil-type *P. aerugniosa* strain K (PAK) was incubated in the presence or absence of PAI-1 or PAI-2 for 1 hour with stainless steel coupons. Bound bacteria were stained with acridine orange and visualized by epifluorescent microscopy. Representative images are shown.

i

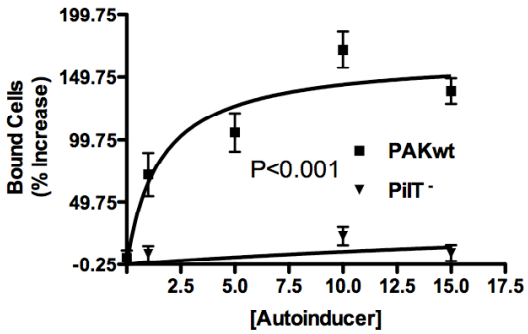

ii

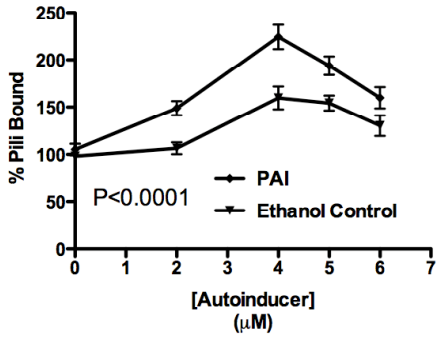

Figure A-2. ***P. aeruginosa*** **and pili binding to stainless steel is influenced by PAI-2 concentration. i.** concentration-dependent increase of WT PAK and PAK Δ*pilT* binding to stainless steel in the presence of increasing concentrations of PAI-2. **ii.** Concentration-dependent increase of PAK pili binding to stainless steel in the presence of increasing concentrations of PAI-2 and 95% ethanol.

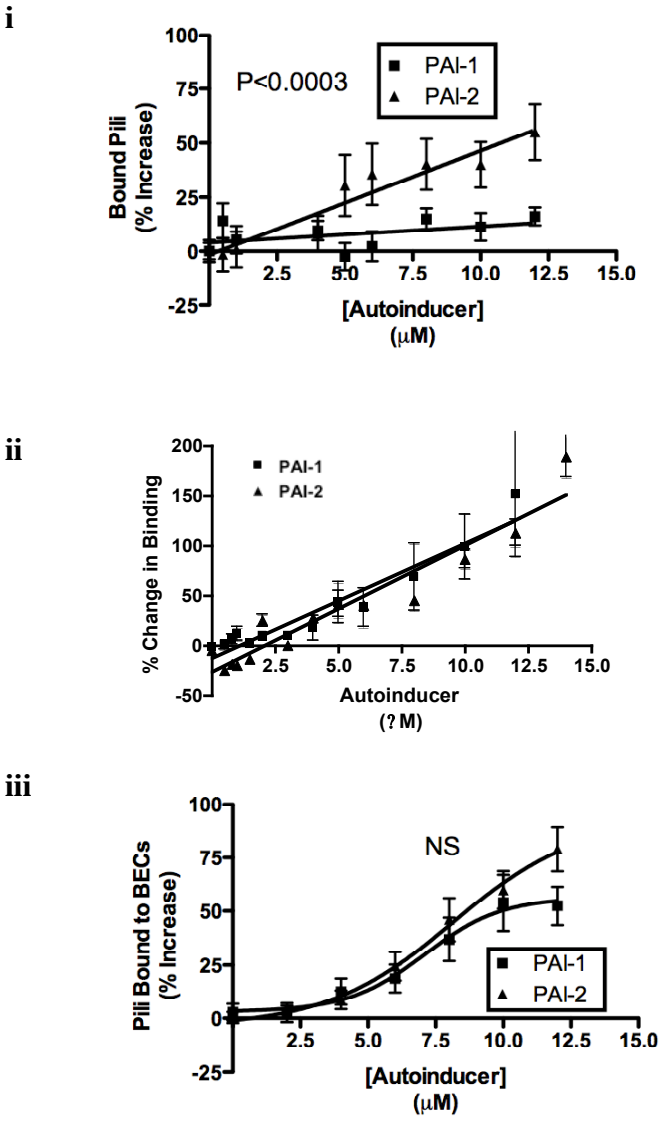

Figure A-3. PAI-1 and PAI-2 concentrations influence binding of pili.
Concentration-dependent increase of pili binding to (**i**) asialo-GM_1, (**ii**) sperm DNA, and (**iii**) buccal epithelial cells (BECs) in the presence of increasing concentrations of PAI-1 and PAI-2.